

Universität
Rostock



Traditio et Innovatio

Synthesis of Functionalized Heterocycles via Palladium
Catalyzed Cross-Coupling Reactions

Dissertation

zur

Erlangung des akademischen Grades

doctor rerum naturalium (Dr. rer. nat.)

der Mathematisch-Naturwissenschaftlichen Fakultät

der Universität Rostock

vorgelegt von Huy Hoang Do, geb. am 31.07.1987 in Hanoi, Vietnam

Rostock, 04.05.2017

Die vorliegende Arbeit wurde in der Zeit von April 2012 bis May 2017 am Institut für Chemie der Universität Rostock am Lehrstuhl für Organische Chemie in der Arbeitsgruppe von Prof. Dr. Peter Langer angefertigt.

1. Gutachter: Prof. Dr. Peter Langer

Universität Rostock, Institut für Chemie

2. Gutachter: Prof. Dr. Jens Christoffers

Universität Oldenburg, Institut für Chemie

Datum der Einreichung: 03.07.2017

Datum der Verteidigung: 14.11.2017

ERKLÄRUNG

Ich versichere hiermit an Eides statt, dass ich die vorliegende Arbeit selbstständig angefertigt und ohne fremde Hilfe verfasst habe. Dazu habe ich keine außer den von mir angegebenen Hilfsmitteln und Quellen verwendet und die den benutzten Werken inhaltlich und wörtlich entnommenen Stellen habe ich als solche kenntlich gemacht.

Rostock, 04.05.2017

.....

Huy Hoang Do

Acknowledgements

First of all, I would like to gratefully and sincerely thank Prof. Peter Langer (Department of Organic Chemistry, Institute of Chemistry, University of Rostock) who provided me the opportunity to join his research group and for the continuous support of my PhD studies, for his patience and motivation. I am grateful to Dr. Tran Quang Hung who supported me with many advices from the beginning of my work. Beside my supervisor, I would like to thank Dr. Peter Ehlers for sharing his experience and insights which are valuable for my researching process. I would also like to say special thanks for their supports, Dr. Alexander Villinger for X-ray diffraction, Prof Stefan Lochbrunner, Mr. Wolfgang Breitsprecher for fluorescence measurement, Dr Annette Enrica Surkus for Cyclic voltammetry measurement, Dr. Jamshed Iqbal and his students, Sundas Sarwar, Syeda Abida Ejaz, Syeda Mahwish Bakht, for the biological studies, Dr. Dirk Michalik for NMR measurements and valuable discussion, Dr. Holger Feist and Dr. Martin Hein for their support and advice, as well as Anne Hallman, Claudia Hahn, Carmen Esser, and all other members of analytical and technical staffs of the Department of Chemistry, University of Rostock and LIKAT (Leibniz-Institut für Katalyse).

Furthermore, I thank to all my Vietnamese PhD friends in Rostock and my colleagues in Prof. Langer group for all their encouragement, companionship and support during my work in the laboratory. Last but not least, I would like to thank my family, my parents for spiritually supporting me throughout doing this thesis and my development path in general. Again, sincere thanks to all my teachers, colleagues, friends and family who have given me love and support throughout my professional life.

This work has been supported by the Landesgraduiertenförderung program, which is gratefully acknowledged.

Zusammenfassung

Abstract

This present thesis is dedicated to the design and the synthesis of novel biologically active and fluorescent heterocycles from common starting materials, such as naphthoquinones, furans, benzofurans, pyridines and quinoxalines. Based on Palladium(0) catalyzed cross-coupling reactions, a series of new ethynylated naphthalenes, ethynylated naphthaleneindoles, benzo[*b*]carbazoliones, indolo[2,3-*b*]quinoxalines, 5,7-dihydropyrido[3,2-*b*,5,6-*b'*]diindoles, benzofuroindoles and furodiindoles were synthesized with high yield. Synthesized compounds show interesting fluorescence properties with high quantum yields (19-78%). The benzocarbazoliones were tested for biological activity and are suggested to be used as selective inhibitors against nucleotide pyrophosphatase,

Die vorliegende Dissertation widmet sich der Synthese von neuen, biologisch aktiven bzw. fluoreszierenden Heterozyklen, ausgehend von leicht zugänglichen Ausgangsstoffen, wie z.B. Naphthochinonen, Furanen, Pyridinen und Chinoxalinen. Durch Anwendung von Palladium(0) katalysierten Kupplungsreaktionen wurden verschiedene, zum Teil bisher unbekannte, alkynylierte Naphthalenindole und Benzocarbazoldione sowie Indolochinoxaline, Diindolopyridine und verschiedene Furoindole in vorwiegend guten Ausbeuten hergestellt. Die synthetisierten Verbindungen zeigen interessante Fluoreszenzeigenschaften wie z.B. hohe Quantenausbeuten (19-78%). Außerdem wurden die hergestellten Benzocarbazoldione bezüglich ihrer Aktivität gegen verschiedene Nukleotid Pyrophosphatasen untersucht und zeigen zum Teil eine hohe Selektivität gegenüber bestimmten Pyrophosphatasen und gleichzeitig eine hohe inhibitorische Wirkung.

List of abbreviations

Abs.	Absorption	NMR	Nuclear Magnetic Resonance
Ar	Aryl	m/z	mass to charge ratio
ca.	Approximately	NPPs	Nucleotide pyrophosphatases
conc.	Concentration	OLED	Organic light-emitting diode
CV	Cyclic Voltammetry	Ph	Phenyl
DFT	Density functional theory (DFT)	ppm	Parts per million
DNA	Deoxyribonucleic Acid	Ref.	Reference
DPV	Differential Pulse Voltammetry	Temp.	Temperature
em	Emission	UV	Ultraviolet
equiv.	Equivalent	UV-Vis	Ultraviolet–visible
ESI	Electrospray ionization	V	Volume
HRMS	High Resolution Mass Spectrometry	vol. %	Volume percent
e.g.	For example	TOF-MS	Time-of-flight mass spectrometry
M.p.	Melting point	vs.	versus
Me	Methyl	XRD	X–ray diffraction
MS	Mass Spectrometry	wt%	Weight percent

Table of Contents

List of abbreviations	vi
1. Introduction	1
1.1. The importance of organic synthesis for new materials and drugs synthesis	1
1.2. Cross-coupling reactions as a versatile tool in fine chemical productions	3
1.2.1. Suzuki-Miyaura reaction.....	5
1.2.2. Sonogashira cross-coupling reaction	7
1.2.3. Buchwald–Hartwig amination.....	8
1.2.4. CH arylation reaction.....	10
1.3. Objectives of this thesis	11
2. Palladium-Catalyzed Synthesis of Multiple Ethynylated Compounds.....	12
2.1. Synthesis of Ethynylated Benzoindoles.....	12
2.1.1. Introduction.....	12
2.1.2. Results and Discussion	13
2.1.3. Absorption and fluorescence properties.....	21
2.1.4. Electrochemical studies	23
2.1.5. Density functional theory (DFT) calculations.....	26
2.2. Multiple Ethynylated Naphthalene.....	29
2.2.1. Introduction.....	29
2.2.2. Results and Discussion	30
2.2.3. Absorption and fluorescence properties.....	35
2.3. Conclusion	38
3. One-Pot Palladium-Catalyzed Synthesis of Benzo[<i>b</i>]carbazolediones	39
3.1. Introduction.....	39
3.3. Results and Discussion	40
3.3.1. One-pot synthesis of benzo[<i>b</i>]carbazolediones	40
3.3.2. Domino Synthesis of benzo[<i>b</i>]carbazolediones	43
3.4. Nucleotide Pyrophosphatase Activity	48
3.5. Conclusion	50
4. Palladium-Catalyzed Two-fold Buchwald-Hartwig Amination	51
4.1. Synthesis and Optical Properties of Indolo[2,3- <i>b</i>]quinoxalines and 5,7-dihydropyrido[3,2- <i>b</i> ,5,6- <i>b'</i>]diindoles	51
4.1.1. Introduction.....	51
4.1.2. Synthesis of Indolo[2,3- <i>b</i>]quinoxalines	52
4.1.3. Synthesis of 5,7-dihydropyrido[3,2- <i>b</i> ,5,6- <i>b'</i>]diindoles	55
4.1.4. Absorption and Fluorescence Properties.....	57

4.1.5. Electrochemical properties.....	59
4.1.6. Conclusion	61
4.2. Palladium-Catalyzed Synthesis and Nucleotide Pyrophosphatase Activity of Benzo[4,5]-furo[3,2- <i>b</i>]indoles and Furo[3,2- <i>b</i> ,4,5- <i>b'</i>]diindoles	62
4.2.1. Introduction.....	62
4.2.2. Synthesis of benzo[4,5]-furo[3,2- <i>b</i>]indoles	63
4.2.3. Synthesis of furo[3,2- <i>b</i> ,4,5- <i>b'</i>]diindole	67
4.2.4. Absorption and fluorescence properties.....	72
4.2.5. Electrochemical studies	74
4.2.6. Nucleotide Pyrophosphatase Activity.....	77
4.2.7. Conclusion.	78
5. Summary	79
6. Reference	79
7. Appendix.....	90

List of Figure

Figure 1. Examples of commercial drugs	1
Figure 2. Examples of commercial organic light-emitting compounds	2
Figure 3. Examples of fluorescent and/or bioactive benzoindole derivatives.	12
Figure 4. ORTEPs of compound 3m . (The propability of ellipsoids: 45%).....	20
Figure 5. Absorption and corrected emission spectra of 3a , 3j and 3m	21
Figure 6. Absorption and corrected emission spectrum of 5a compared to 3a	21
Figure 7. CVs of 3a and 5a in DMF.....	24
Figure 8. DPVs of selected compounds 3 in DMF.....	24
Figure 9. DPVs of compounds 3a and 5a in DMF.....	25
Figure 10. Frontier orbital for HOMO (top) and LUMO (bottom) of compound 3a	26
Figure 11. Frontier orbital for HOMO (top) and LUMO (bottom) of compound 5a	27
Figure 12. Examples of alkynylated compounds	29
Figure 13. ORTEPs of compound 7b . (The propability of ellipsoids: 45%).....	35
Figure 14. Absorption and corrected emission spectra of 6a , 6b and 6d	36
Figure 15. Absorption and corrected emission spectra of 7a , 7c and 7f	36
Figure 16. Structures of carbazolequinone alkaloids	39
Figure 17. ORTEP of 10c (The propability of ellipsoids: 45%).....	47
Figure 18. ORTEP of 11h (The propability of ellipsoids: 45%).....	47
Figure 19. Selected examples of highly π -conjugated aza-carbazoles compounds	51
Figure 20. Absorption and emission spectra of selected compounds 15	58
Figure 21. Absorption and emission spectra of selected compound 19	58
Figure 22. Differential Pulse Voltammetry Plot of 15	60
Figure 23. Differential Pulse Voltammetry Plot of 19	60
Figure 24. Selected examples of furoindole derivatives.....	62
Figure 25. ORTEPs of 23c (The propability of ellipsoids: 45%).	70
Figure 26. ORTEPs of 27d (The propability of ellipsoids: 45%).....	71

Figure 27. Absorption and emission spectra of selected compounds 23	72
Figure 28. Absorption and emission spectra of selected compounds of 27	72
Figure 29. Cyclic Voltammetry plot of 23b and 27b in DMF.....	74
Figure 30. Differential Pulse Voltammetry plot of selected compounds 23	75
Figure 31. Differential Pulse Voltammetry plot of selected compounds 27	75

List of Schemes

Scheme 1. Classical total synthesis of murrayaquinone A ¹²	3
Scheme 2. Total synthesis of murrayaquinone A using a Palladium catalyst. ¹³	3
Scheme 3. General Mechanism of Palladium(0)-catalyzed Cross-Coupling Reactions.	5
Scheme 4. Applications of Suzuki-Miyaura coupling in the synthesis of D159687. ^{26g}	6
Scheme 5. Mechanism of the Suzuki-Miyaura reaction.	7
Scheme 6. Application of the Sonogashira reaction in the synthesis of Altinicline.	7
Scheme 7. Mechanism of the Sonogashira reaction.....	8
Scheme 8. Application of Buchwald-Hartwig amination in the synthesis of (-)-epi-Indolactam.....	9
Scheme 9. Mechanism of Buchwald-Hartwig amination.	9
Scheme 10. Mechanism of CH-arylation.....	10
Scheme 11. Proposed mechanism of the CH activation.	11
Scheme 12. Synthesis of brominated diarylethynyl naphthalene 2a-f	13
Scheme 13. The synthesis of 3f and byproduct 4f	17
Scheme 14. Two-fold cascade C-N cross-coupling and hydroamination.....	17
Scheme 15. Synthesis of tetraarylethynyl naphthalene 6a	30
Scheme 16. Synthesis of 2,3-diaryl-1,4-diethynyl naphthalene 7a	33
Scheme 17. The three-step one-pot synthesis of 10b	40
Scheme 18. The two-step domino synthesis of 10a	43
Scheme 19. The domino reaction with carbazole (A), methylindole (B), and indolinone (C).	46
Scheme 20. Synthesis of indolo[2,3- <i>b</i>]quinoxalines 15e	52
Scheme 21. Synthesis of indolo[2,3- <i>b</i>]quinoxalines 15d	54
Scheme 22. Synthesis of 2,3,5,6-Tetrabromopyridine 17	55
Scheme 23. Synthesis of 5,7-dihydropyrido[3,2- <i>b</i> ,5,6- <i>b'</i>]diindoles 19d	55
Scheme 24. Synthesis of 2,3-Dibromobenzofuran 21	63
Scheme 25. Synthesis of benzo[4,5]-furo[3,2- <i>b</i>]indoles 23a-j	63
Scheme 26. Synthesis of 2,3,4,5-Tetrabromofuran 25	67

Scheme 27. Synthesis of furo[3,2- <i>b</i> ,4,5- <i>b'</i>]diindole 27b	67
Scheme 28. The modification of naphthoquinone structure	79
Scheme 29. The combination of Suzuki-Miyaura and Buchwald-Hartwig cross-couplings.....	80

List of Tables

Table 1. Optimization of the synthesis of 3a	14
Table 2. Synthesis of ethynylbenzoindoles 3a-m	16
Table 3. Optimization for the Synthesis of 5a	18
Table 4. Cascade C-N cross-coupling and hydroamination from dibromodiethynyl compounds. ...	19
Table 5. The absorption and emission properties of 3 , 5	22
Table 6. Redox data of selected compounds 3 and 5a in DMF.	25
Table 7. Bandgraps of selected compounds 3 and 5a in DMF.	28
Table 8. Optimization of the synthesis of 6a	31
Table 9. Synthesis of tetraalkynynaphthalene 6a-l	32
Table 10. Optimization of the synthesis of 7a	33
Table 11. Synthesis of 2,3-diaryl-1,4-diarylethynynaphthalenes 7a-k	34
Table 12. The absorption and emission properties of 6 and 7	37
Table 13. Optimization of the one-pot synthesis of 11b	41
Table 14. One-pot synthesis of Benzo[<i>b</i>]carbazolediones 10a-v	42
Table 15. Optimization of the two-step domino synthesis of 10a	44
Table 16. Domino synthesis of benzo[<i>b</i>]carbazolediones (10 and 11).	45
Table 17. Inhibition activity of samples 9b , 10 , 11 , 12a against NPP-1 and NPP-3.*	49
Table 18. Optimization for the Synthesis of 15e	53
Table 19. Synthesis of 15a-f	54
Table 20. Optimization for the Synthesis of 19d	56
Table 21. Synthesis of 19a-f	57
Table 22. Absorption and emission spectroscopic data of 15 and 19	59
Table 23. Electrochemical properties of selected compounds of 15 and 18	61
Table 24. Optimization for the synthesis of 21b	64
Table 25. Optimization for the synthesis of 23h	64
Table 26. Synthesis of 23a-j	66

Table 27. Optimization for the synthesis of 27b	68
Table 28. Synthesis of 27a-h	69
Table 29. Absorption and emission properties of 23 and 27	73
Table 30. Redox data of 23 and 27 in DMF.....	76
Table 31. Biological activity of 23 and 27	77

1. Introduction

1.1. The importance of organic synthesis for new materials and drug synthesis

Organic synthesis is involved in most of the industries, in which consumer goods originate from oil, coal, and gas and possess a tremendous value in the global economy. The intensive development of new synthetic strategies has been noticed to produce new compounds with unique properties. They are central to the applications in almost all fields of daily life, such as pharmacy, biotechnology, and electronic industry. For example, the drug industry achieved a massive development in the 20th century. The discovery of penicillin in the 1930s¹ was the starting of the golden time for pharmaceutical research. After this eminent discovery, a lot of new pharmacological compounds were discovered, developed, improved and manufactured. Structural modifications of natural products by organic synthesis was particularly useful to improve the pharmacological activity against a chosen target and to reduce side effects.² For instance, morphine is a particular example as an addictive compound, found in opium from the unripe seedpods of the *Papaver somniferum* poppy³ and is used as a pain reliever. At the end of 19th century, the modification of morphine has been intensively studied with more than 200 derivatives such as heroin, codeine. By a small modification of functional groups, the compound etorphine possesses its opiate agonist potency 1443 times more than morphine.⁵ Hence, the organic synthesis is one of the most powerful tools for drug discovery.

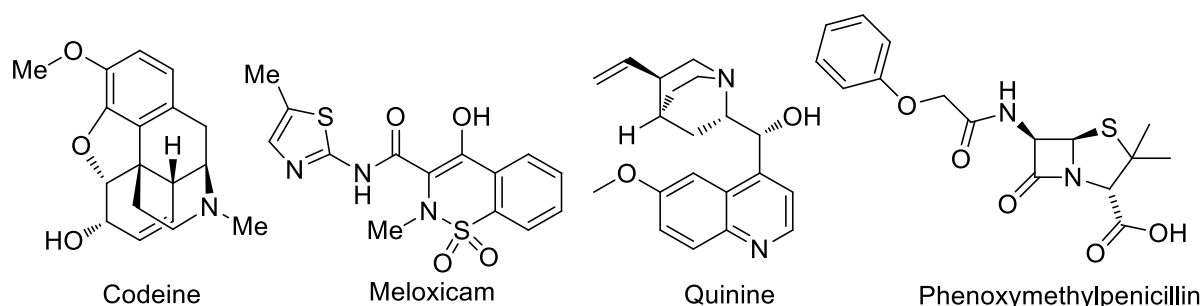


Figure 1. Examples of commercial drugs

Furthermore, the development of organic electronic technologies is a noticeable achievement in the 21st century. The word Organic Light – Emitting Diodes, OLEDs is more and more popular and appearing everywhere in human life. The OLED display technologies have been globally commercialized in high-end smart watches, mobile devices, laptops, and television. Therefore, the new organic light-emitting compounds with a π -conjugated aromatic

heterocyclic systems have been intensively studied to apply in the field of electronic technologies.⁶ For example, pentacene is the particular choice of a highly conjugated organic semiconductor generating light under ultra-violet- and visible light. The compound is very sensitive to the oxidation and unstable when exposed to air and light. Synthetic modification of pentacene by introducing heteroatoms or functional groups resulted in derivatives with improved thermal stability, charge mobility, and molecular packing. In particular, new pentacene analogs such as 5,12-dimethyl-quinolino[2,3-*b*]acridine-7,14(5*H*,12*H*)-dione (DMQA), bis(triisopropylsilylethynyl)pentacenes, perfluoropentacene are potential candidates for the development of organic field effect transistors.⁸ Consequently, organic semiconductors such as pentacene derivatives and other polyarylated compounds like 2,5,8,11-tetra-*tert*-butylperylene (TBP), rubrene have replaced silicon based diodes in a lot of electronic devices.⁹

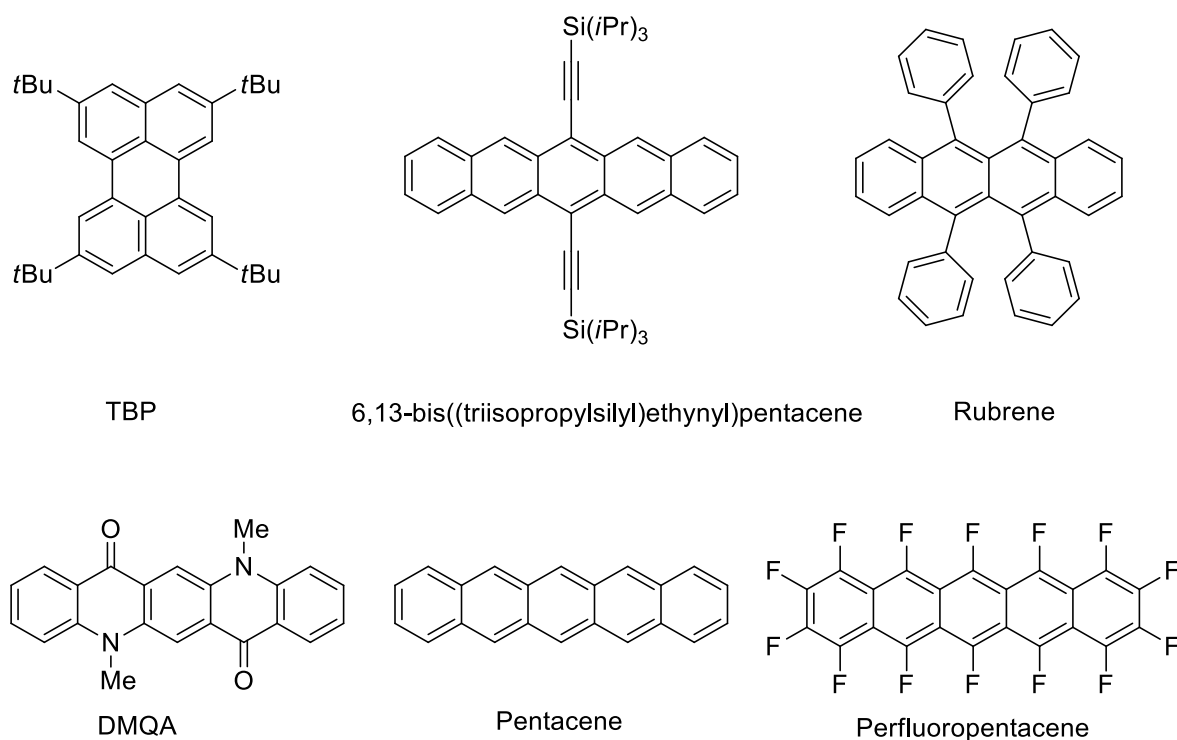


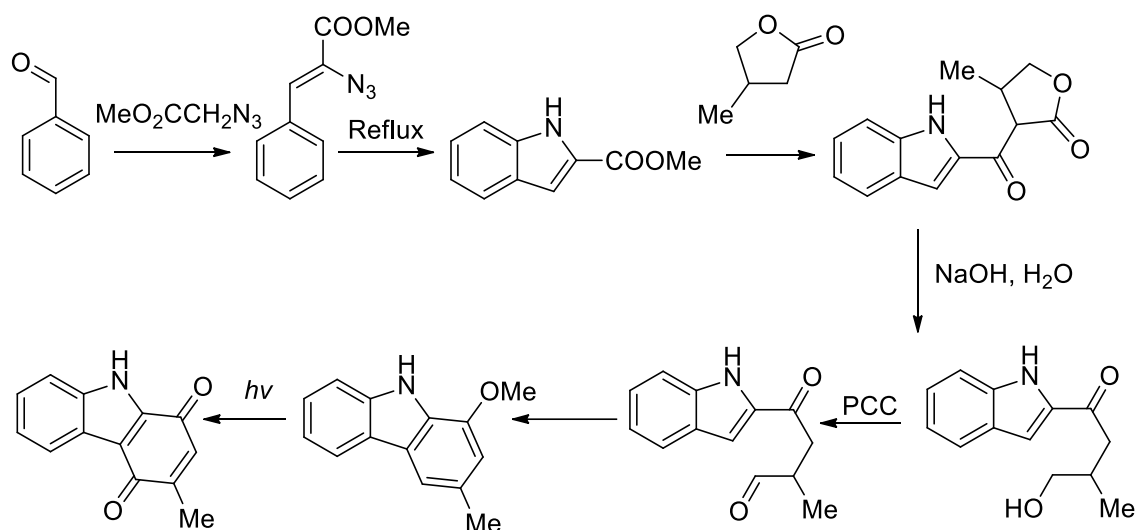
Figure 2. Examples of commercial organic semiconductors

Due to the increasing demand of chemicals for drug- and organic electronic materials development, many efforts have been made for developing new synthetic approaches. In recent years catalysis has emerged as powerful tool of organic chemists, as it opens new avenues for new bond formations and reaction outcomes. Moreover it reduces required energy for production processes by decreasing the activation barrier of certain processes or avoids the

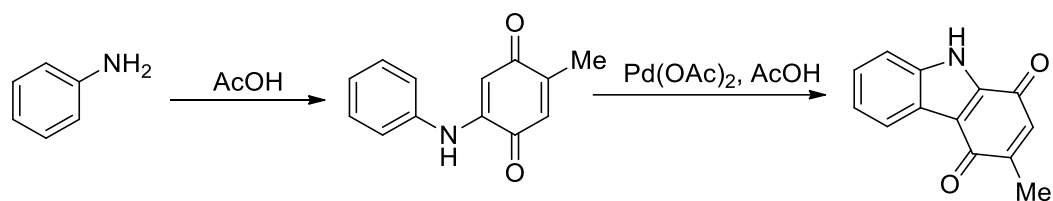
application of stoichiometric reagents. The huge impact of catalysis on chemistry and consequently on society has been acknowledged by 15 Nobel Prizes from 1901 until 2016 in the field of catalysis.¹⁰ Catalysis is also important in the environmental technology to solve the problem of pollution, energy waste. In the aspect of economy, the catalyst business makes approximately \$15 billion as the annual turnover. The full value of the products under the catalysis processes has a remarkable contribution to the planetary GDP.¹¹

1.2. Cross-coupling reactions as a versatile tool in fine chemical productions

At the beginning of the 20th century, few commercial drugs such as aspirin, codeine, and insulin were manufactured with a high price and limited quantity due to the limitation of the organic synthesis. Most of the methodologies for drug synthesis underwent several steps with often harsh reaction conditions. For examples, carbazole alkaloid murrayaquinone A have been totally synthesized by a 6-step procedure with very low yield (Scheme 1).¹²



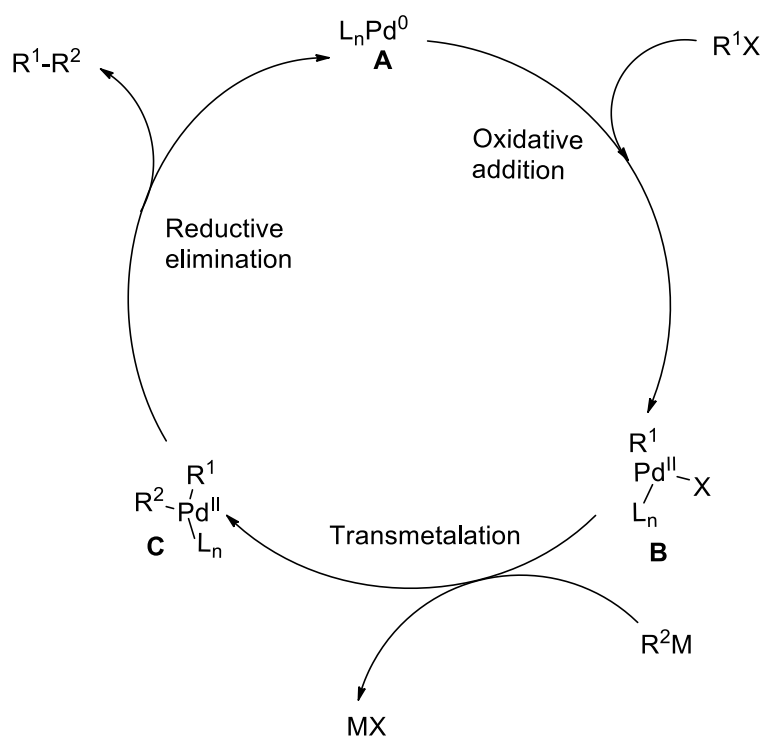
Scheme 1. Classical total synthesis of murrayaquinone A¹²



Scheme 2. Total synthesis of murrayaquinone A using a Palladium catalyst.¹³

With the development of metal-catalyzed cross-coupling reactions, organic compounds are easier synthetically accessible comparing to classical synthesis. For instance, natural product murrayaquinone A can be synthesized by a two-step route from aniline with high yield (Scheme 2), representing an impressive example of the important contribution of metal catalyzed organic synthesis in organic chemistry.¹³ Cross-coupling reactions in the presence of organometallic Mg, Li, Zr, Ni, Cu compounds have been used for innumerable organic synthesis.^{14,15} These methodologies are essential tools for the synthesis of complicated natural products, biologically relevant compounds, functional materials, pharmaceuticals and agrochemicals. Thus, Palladium catalyzed cross-coupling reactions are one of the well-known approaches due to the wide-ranging reactivity and high selectivity of Palladium catalysts.¹⁷

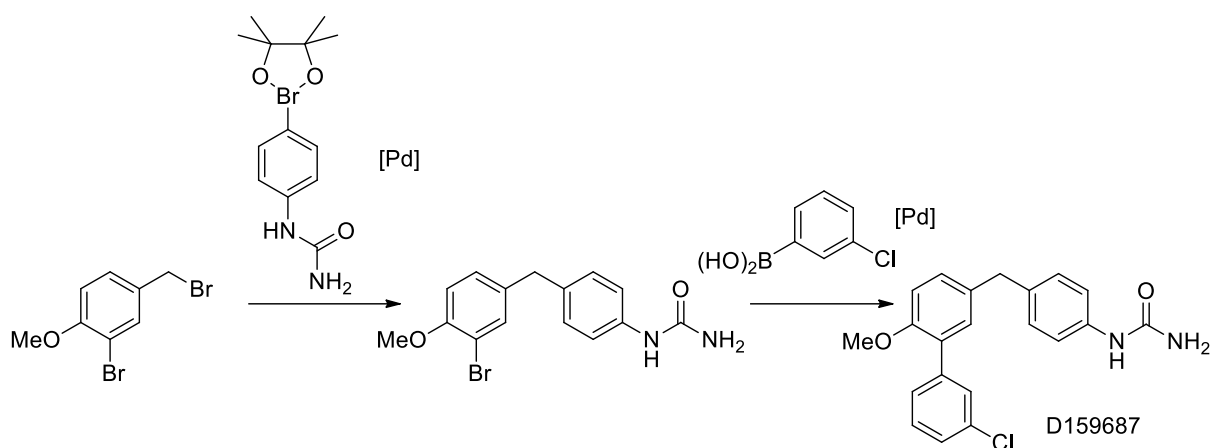
Palladium catalyzed cross-coupling reactions are certainly useful in the transformation of aryl (pseudo)halides with manifold nucleophiles such as organometallic reagents (Suzuki-Miyaura-, Sonogashira-, Stille-, Neghishi-reaction), amines (Buchwald-Hartwig-reaction) or alkenes (Heck-reaction), to name just a few.¹⁸ Using individually each cross-coupling reaction or a combination of two reactions makes the organic synthesis of drugs and functional materials convenient and flexible.¹⁹ The mechanism in Scheme 3 describes the three-step catalytic cycle in which the oxidative addition and reductive elimination is part of all Palladium(0) catalyzed cross-coupling reactions. The active Pd(0) complex **A** undergoes oxidative addition with an aryl (pseudo)halide R¹X to produce the oxidized Palladium(II) complex **B**. The strength of carbon-halidebond decides about the reactivity of the substrates in the order C-I>C-Br>C-Cl>C-F. Organofluoride is the least reactive substance. Active bromo and iodo compounds are widely used in cross-coupling reactions. After oxidative addition, complex **B** is electrophilic and takes part in the next step with a nucleophilic reactant to produce complex **C**. The step can follow different processes: ligand substitution, transmetalation or migratory insertion, which depends on the character of the nucleophiles. In detail, ligand substitution often occurs in Buchwald-Hartwig reaction²⁰ while transmetalation takes place for organometallic nucleophiles in Suzuki-Miyaura cross-coupling or Sonogashira cross-coupling²¹ and migratory insertion for Heck-type reaction.²² The last step is the reductive elimination of Pd(II) complex **C** to form the desired product with the regeneration of Pd(0) species which can enter a new catalytic cycle.



Scheme 3. General Mechanism of Palladium(0)-catalyzed cross-coupling reactions.

1.2.1. Suzuki-Miyaura reaction

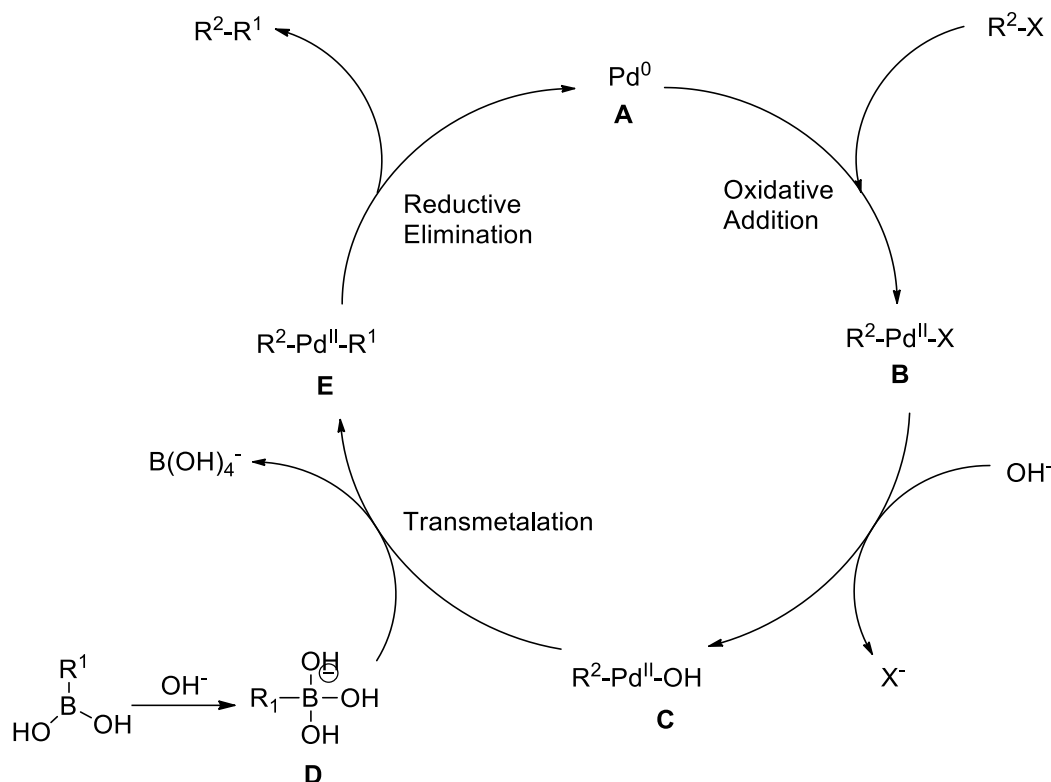
One of the most widely used catalytic organometallic methodologies in organic synthesis is the Suzuki-Miyaura cross-coupling reaction which was firstly reported in 1981 by Professor Akira Suzuki and Professor Norio Miyaura. Their discovery is based on the use of Palladium to catalyze the coupling of various organohalides or –pseudohalides with organoboron compounds.^{23,24} For Akira Suzuki's valuable contributions in organic synthesis, he, Richard F. Heck and Ei-ichi Negishi won the Nobel Prize in Chemistry in 2010.¹¹ The reaction has expressed its excellent utility to prepare many kinds of organic compounds through a lot of applications related to synthetic chemistry.²⁵ In particular, the Suzuki-Miyaura reactions are often used to synthesize intermediates for the pharmaceutical industry such as anticancer Crizotinib,^{26a} Yuehchukene,^{26b} anti HIV Michellamine B,^{26c} bioactive compound Ribisins A, B and D,^{26d} Diazonamide A,^{26e} Vitamin A^{26f} and D159687.^{26g} Furthermore, the antihypertensive drug Valsartan for the treatment of heart problems is a commercial example from Novartis, and BASF.²⁷ In addition, highly- π conjugated compounds are prepared via Suzuki-Miyaura cross-coupling in the metric-ton scale by Sigma-Aldrich for organic light-emitting diodes.²⁷



Scheme 4. Applications of Suzuki-Miyaura cross-coupling in the synthesis of D159687.^{26g}

The mechanism of Suzuki-Miyaura reaction has been investigated intensively. Similar to the mechanism of other cross-coupling reactions,²⁸ the first step is the oxidative addition to form complex **B** (Scheme 5). Then, complex **B** reacts with the base to form complex **C**. The second step is the transmetalation of the, base activated, organoboron species **D** to form **E**. The direct formation of complex **E** from **B** by the reaction with the tetracoordinated organoboron species is discussed in literature as well. The transmetalation involves the transfer of ligands from **D** to **C** with no change of the oxidation state of Palladium. The final step is the reductive elimination of Palladium(II) complex **E** and the regeneration of the Palladium(0) catalyst **A**.

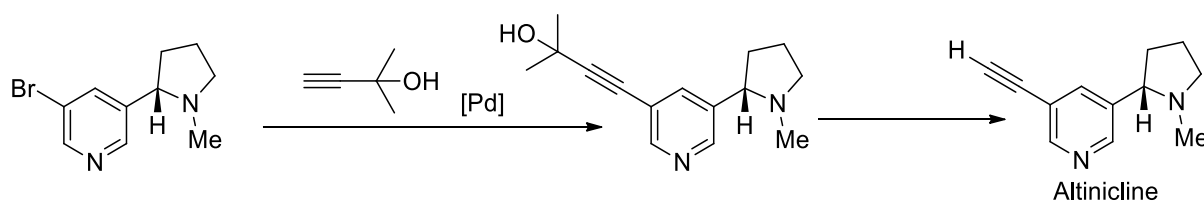
K_2CO_3 , K_3PO_4 , Na_2CO_3 , $NaOH$, $NaHCO_3$ are common bases for Suzuki-Miyaura cross-coupling reactions to conduct the reaction well and improve the yield.²⁹ The presence of a base increases the rate of the transmetalation step by activating the organoboron reagents and the intermediate **B**. The most common catalysts are $Pd(PPh_3)_4$, $PdCl_2$, $Pd(OAc)_2$, $Pd_2(dba)_3$ in combination with various phosphine ligands.³⁰ Biphasic solvent systems consisting of an organic solvent and water are often used because it disperses the organic substances, boron compounds, and inorganic salts to increase the selectivity and the yield of the cross-coupling reaction.³⁰



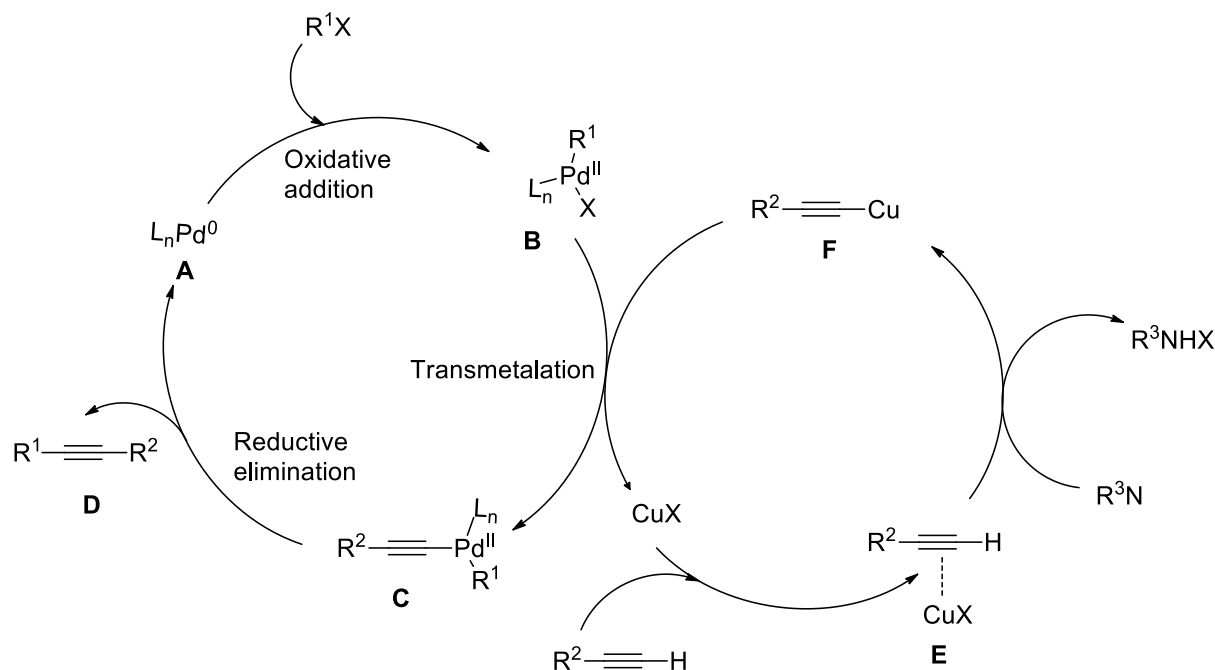
Scheme 5. Mechanism of the Suzuki-Miyaura reaction.

1.2.2. Sonogashira cross-coupling reaction

In 1975, Heck and Cassar independently reported a cross-coupling of terminal alkyne and aryl halides using Palladium catalysts.³⁵ However, the reaction conditions require high temperatures and gave low yield. Later, based on Stephens-Castro reaction, Kenkichi Sonogashira, Yasuo Tohda, and Nobue Hagihara developed a milder protocol for the reaction of terminal alkynes with aryl halides by adding CuI as a co-catalyst.³¹ The Sonogashira reaction is a powerful tool to synthesize aryl- and vinyl alkynes. Additionally, the reaction is applied in the synthesis of pharmaceuticals such as benzyloquinoline^{32a} or altinicline,^{32b} as well as natural products.³³ The Sonogashira reaction is currently the method of choice for the construction of a Csp-Csp² bond.



Scheme 6. Application of the Sonogashira cross-coupling in the synthesis of Altinicline.

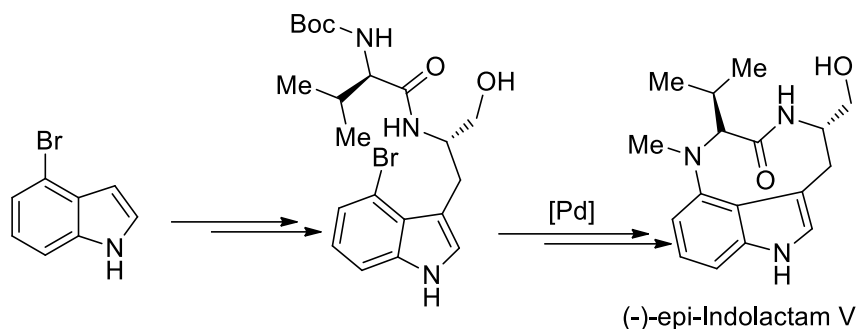


Scheme 7. Mechanism of the Sonogashira reaction

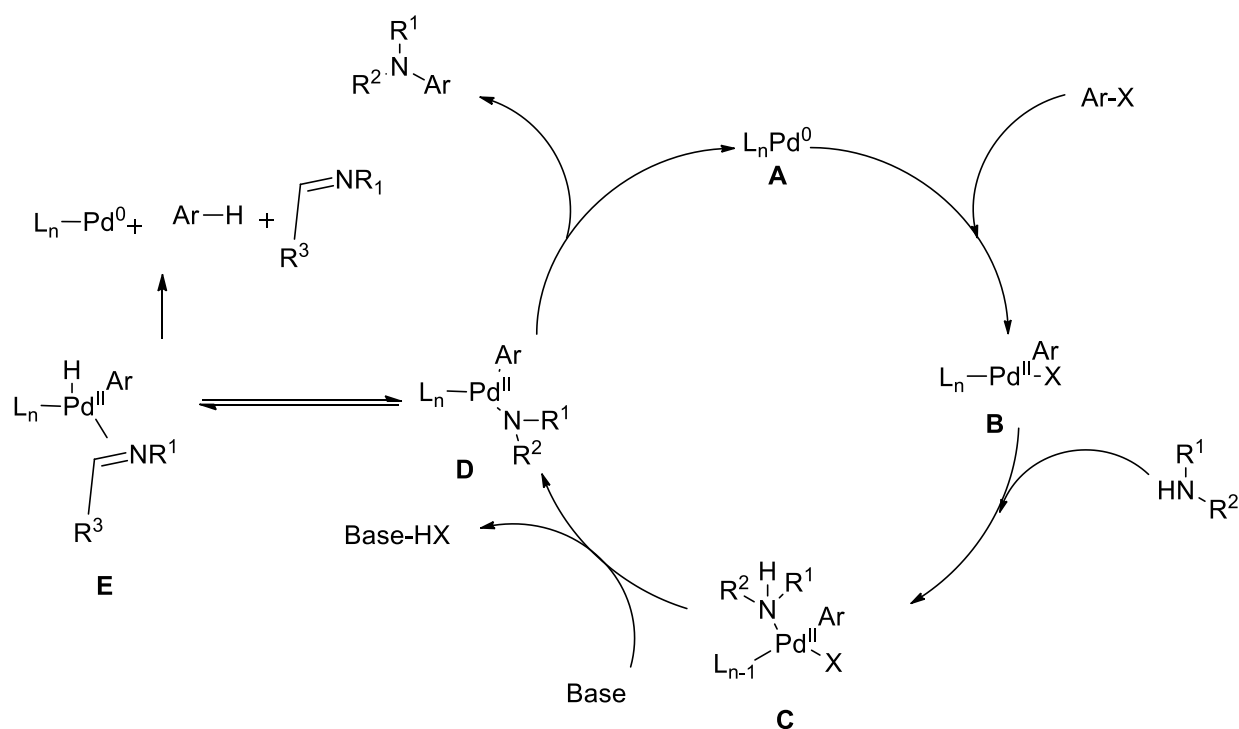
The Sonogashira reaction consists of two catalytic cycles. The Palladium cycle follows the general cross-coupling mechanism for the oxidative addition and reductive elimination steps. The organocopper compound is formed *in situ* by the reaction between the terminal alkyne and CuX in the presence of an amine as base. The integration of Pd cycle and Cu cycle is shown in Scheme 7.³⁴

1.2.3. Buchwald–Hartwig amination

Most pharmaceuticals and natural products comprise at least one nitrogen atom. Therefore, the $C(sp^2)$ -N cross-coupling reaction has gained wide use in synthetic organic chemistry with expanded substrate scope. The Buchwald-Hartwig reaction has been noticed for the replacement of the conventional amination such as the Goldberg reaction, Mannich reaction, reductive amination, etc.³⁷ Buchwald-Hartwig cross-coupling reaction are very useful in the synthesis of natural products, bioactive compounds and drugs such as imatinib, a tyrosine kinase inhibitor,^{40a} or (-)-epi-Indolactam V.^{40b}



Scheme 8. Application of Buchwald-Hartwig amination in the synthesis of (-)-epi-Indolactam.

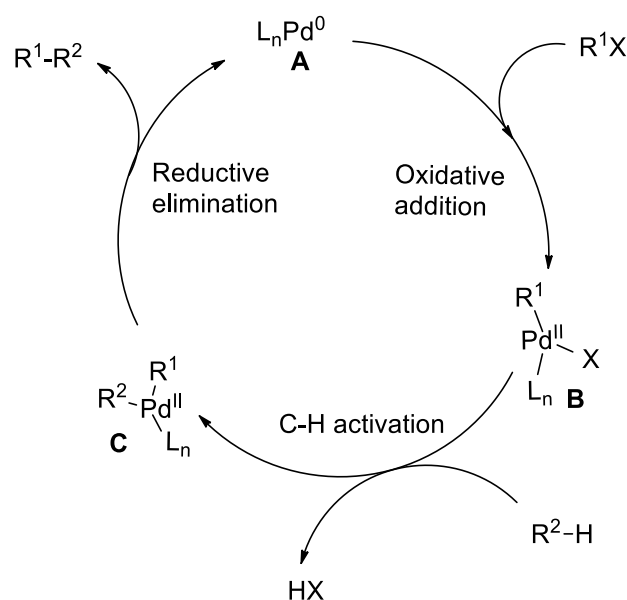


Scheme 9. Mechanism of the Buchwald-Hartwig amination.

Buchwald–Hartwig amination is to form C(sp²)-N bonds via a Pd-catalyzed process using either primary or secondary amines and aryl halides. Stephen L. Buchwald and John F. Hartwig developed the methodology independently between 1994 and the late 2000s.³⁶ The mechanism undergoes via steps like those known for Palladium catalyzed C-C cross-coupling reactions.³⁸ In particular, the Buchwald-Hartwig reaction involves the addition of an amine to form complex **C**, followed by deprotonation to form complex **D**. The amine addition is named as ligand exchange. β -H elimination might occur as a typical side reaction if alkyl- or benzylamines are applied. To some extent this side reaction can be suppressed by the application of bidentate ligands like Xantphos or BINAP.

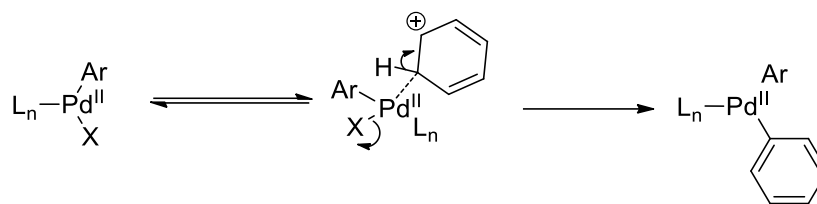
1.2.4. CH arylation reaction

C-X/C-H bond activations were firstly mentioned in 1955 to synthesize phenylisoindolin-1-one.^{41a} (E)-1,2-diphenylethene was prepared in 1969 via oxidative CH activation of benzene and styrene with the catalyst system of Pd(OAc)₂ and Cu(OAc)₂.^{41b} Avoiding the requirement of a stoichiometric organometallic coupling partner makes this reaction especially attractive to chemists and chemical manufactures due to the reduction of synthetically steps, waste and energy production. However, the strong C-H-bond and the typically high number of C-H bonds in organic molecules makes these reaction challenging with regard to turn-over and selectivity.



Scheme 10. Mechanism of CH-arylation.

The catalytic cycle proceeds similarly to the general mechanism of Palladium catalyzed cross-coupling reactions (scheme 10). After an oxidative addition step, a CH-activation step takes place, followed by the reductive elimination. Particularly, the mechanism of C-H bond activation is shown in Scheme 11. It can undergo via electrophilic substitution pathways.⁴³ Electrophilic substitution is the electrophilic aromatic substitution S_{EAr} . The interaction of C-H bond with Palladium undergoes a charge transfer from occupied $d\pi$ orbital of Palladium to the σ^* orbital of the C-H bond. The charge transfer can weaken and break the C-H bond for the next steps in the catalytic cycle.



Scheme 11. Proposed mechanism of the CH activation.

The interaction of the weak bonds between carbon, hydrogen, the ligands and the metal in the intermediate promotes the break of the CH bond of the arene. Studies have supported that the acidity of C-H bond of electron-deficient arenes decides the activity of that bond in C-H activation reaction. The C-H arylation have been especially noticed for the functionalisation of heterocycles such as pyrroles, indoles, carbazoles, quinazolines,^{44a} as well as biologically active compounds such as calothrixin A,¹³ Lithospermic acid,^{44b} kibdelone,^{44c} piperarborenine B and D.^{44d}

1.3. Objectives of this thesis

The possibility of introducing new C–C and C–N bonds via Palladium catalyzed methodologies is a highly attractive strategy for drug discovery and advanced materials as discussed above. Designing biologically active compounds based on natural products can be handled through modifying and combining different Palladium-catalyzed approaches. These methodologies are also useful to synthesize new organic materials, aromatic polyheterocyclic compounds. Motivated by the importance of aromatic heterocycles and Palladium-catalysis, this thesis is focused on the synthesis of important or new aromatic nitrogen-containing heterocycles from brominated starting materials of 1,4-naphthoquinone, furan, quinoxaline and pyridine. These carbo- and heterocycles have been chosen as they are prominent moieties in various biological active compounds which makes the development of new methodologies and the synthesis of new derivatives worthwhile. Moreover, a special emphasis of this thesis is devoted to the construction of π -conjugated, polyarylated compounds based on the aforementioned starting materials, due to their potential application in organic electronic materials such as organic semiconductors or fluorescent dyes.

2. Palladium-Catalyzed Synthesis of Multiple Ethynylated Compounds

2.1. Synthesis of Ethynylated Benzoindoles

2.1.1. Introduction

Highly π -conjugated compounds based on nitrogen heterocycles have been attractive targets for fluorescent applications such as light-emitting materials, fluorescent labeling and bio-sensors.⁴⁵ Particularly, the indole moiety is one of such natural sensitive fluorophores.⁴⁶ Comparing to the indole moiety, the more π conjugated structure of benzoindole, with an additional fused benzene ring, possesses a reduced bandgap.⁴⁷ Benzoindole moieties are considered as electronic donor substructures for new fluorescent ladder-type π conjugated compounds.⁴⁸ Besides, benzoindole derivatives show high biological activities such as antibacterial (with higher activity than indole compounds e.g. duocarmycin CC-1065),⁴⁹ antitumor (pyrolo[9,10-*b*]phenanthrene)⁵⁰ and potent antifouling properties for marine coatings (benzo[*g*]dipodazine).⁵¹ Therefore, various new synthetic approaches to benzoindole scaffolds are already available.⁵² To improve the π conjugation, the fluorescent ability as well as the stability, ethynylene moieties are useful to design the new structure.⁵³⁻⁵⁴

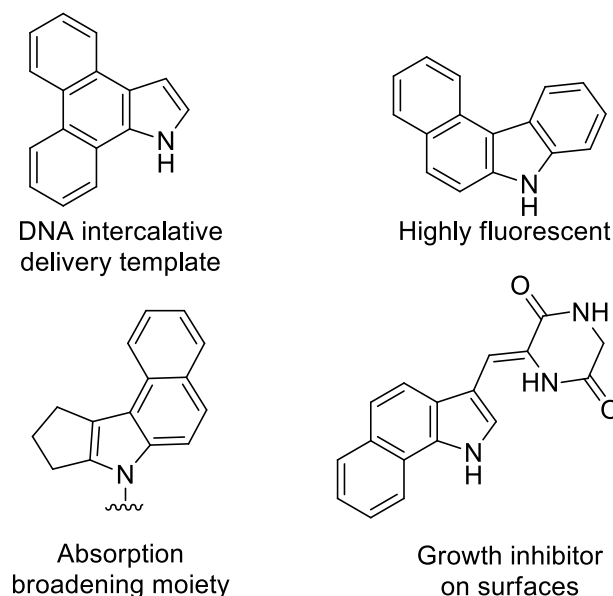
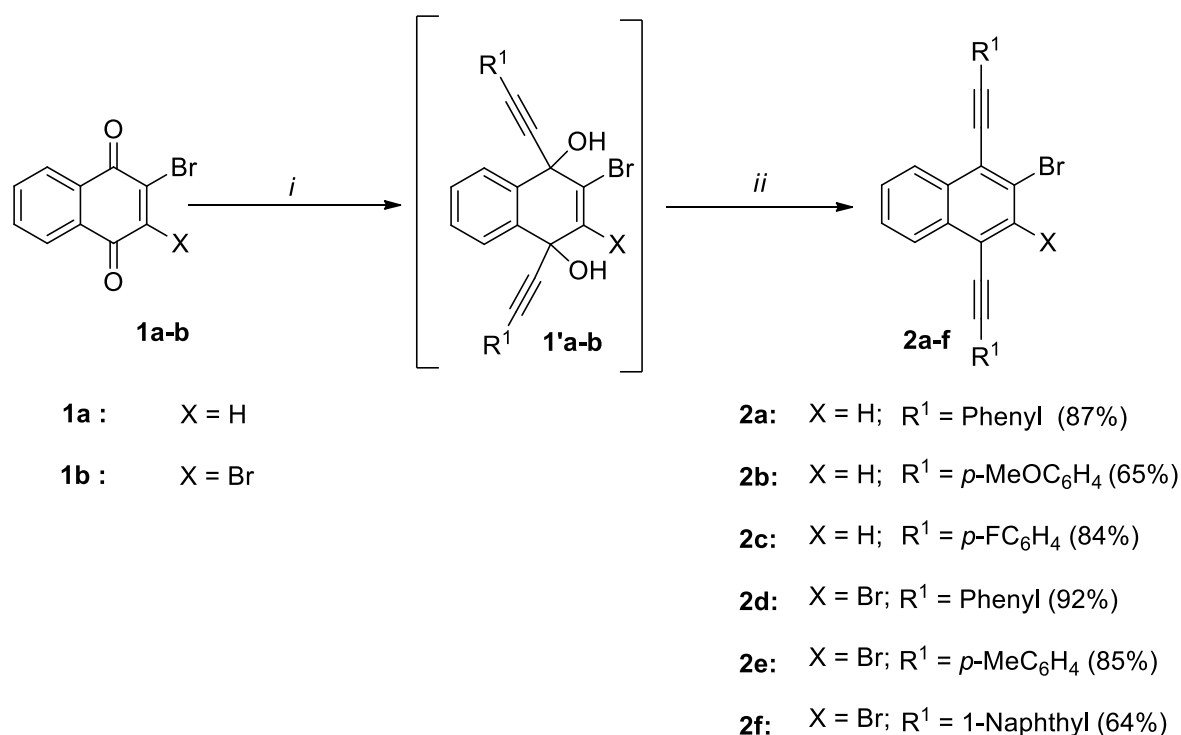


Figure 3. Examples of fluorescent and/or bioactive benzoindole derivatives.

In literature, alkylnylated structures are also found in some bioactive compounds so that numerous strategies have been developed for the synthesis of these compounds. In fact, most of the methodologies are based on alkynylation by the Sonogashira reaction.⁵⁵ Brachet *et. al.*

reported a mild and general C-H activation for a selective and efficient access to regioselectively alkynylated pyrroles, using various bromoalkynes as starting materials.⁵⁶ An efficient, convenient and high yielding procedure for the synthesis of tetra(alkynyl)pyridines and pentaalkynylpyridines via multiple Sonogashira reactions of penta- and tetrachloropyridines was mentioned in the literature.⁵⁷ The products are promising light emitting organic materials with high quantum yields. The synthesis of alkynylated benzo[*e*]indoles has not been mentioned in literature before, which encouraged me towards the synthesis of novel alkynylated benzo[*e*]indoles. I present here a new strategy to such compounds, applying nucleophilic addition of organolithium reagents to bromobenzoquinone followed by tin(II)-mediated reduction of resulting dioles. The last step is based on a Palladium-catalyzed cascade reaction, involving C-N cross-coupling and cyclization via hydroamination.

2.1.2. Results and Discussion



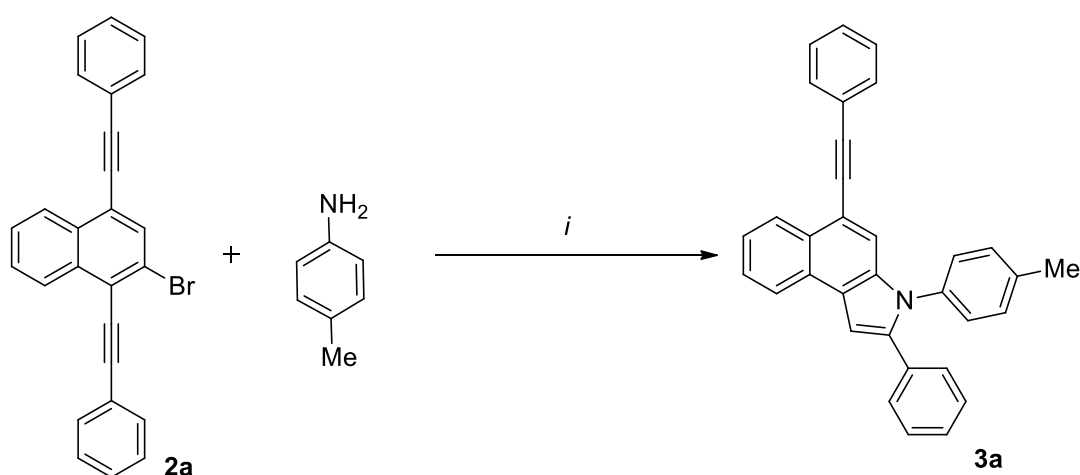
Scheme 12. Synthesis of brominated diarylethynyl naphthalene **2a - f**.

Condition, i, 2.2 equiv. *n*-BuLi, 2.2 equiv. aryl acetylene, THF, rt; *ii*, 2 equiv. SnCl₂, MeCN, H₂O, reflux.

The synthetic approach for the bromodiethynyl naphthalenes **2a - f** follows a publication of Tykwinsky and co-workers.⁵⁸ The precursors **2a - f** were prepared in good yields ranging from

64 – 92% yield (Scheme 12). I synthesized ethynylbenzoindoles **3** via a cascade consisting of a C-N cross-coupling reaction, followed by a ring-closing step by hydroamination using various amines (Table 1). For the first trial, the reaction of **2a** with *p*-toluidine I used Pd(OAc)₂/Xantphos as the catalytic system in DMF to produce target benzoindole **3a** with 38% yield. When increasing the reaction time to 48 h, the yield rose to 64% (entry 2, Table 1). Furthermore, I examined different reaction conditions by varying Palladium sources and ligands. The monodentate ligand SPhos gave 8% higher yield compared to Xantphos (entry 3). Unfortunately, the C-N bond formation in the presence of other ligands gave lower yields (see Table 1). The use of Pd₂(dba)₃ resulted in lower yields. To further optimize the procedure, the reaction was carried out at different temperatures (60 °C, 90 °C, 110 °C), various bases and with toluene instead of DMF. None of them gave improved results. The best reaction condition is Pd(OAc)₂ (5 mol%), SPhos (10 mol%), Cs₂CO₃ (0.9 mmol), DMF (10 mL), 90 °C, 48 h.

Table 1. Optimization of the synthesis of **3a**.



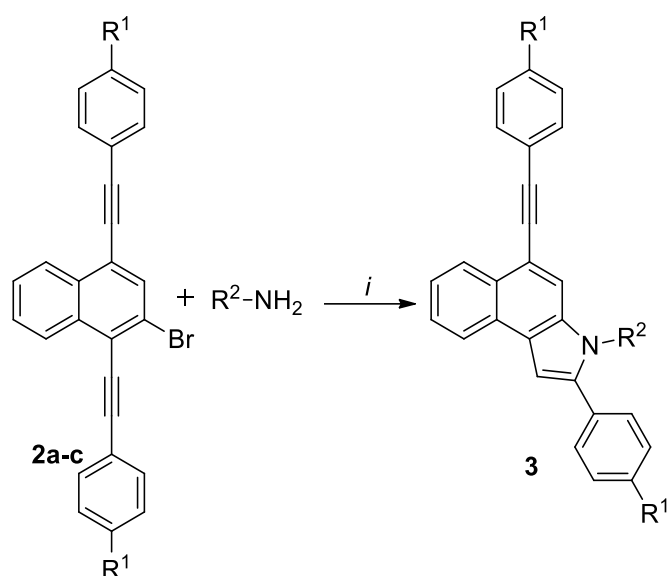
	Catalyst	Ligand	Solvent	Base	Temp (°C)	Yield (%) ^a
1 ^b	Pd(OAc) ₂	Xantphos	DMF	Cs ₂ CO ₃	110	38
2	Pd(OAc) ₂	Xantphos	DMF	Cs ₂ CO ₃	110	66
3	Pd(OAc) ₂	SPhos	DMF	Cs ₂ CO ₃	110	74
4	Pd(OAc) ₂	BINAP	DMF	Cs ₂ CO ₃	110	34
5	Pd(OAc) ₂	DPEPhos	DMF	Cs ₂ CO ₃	110	24
6	Pd(OAc) ₂	PtBu ₃ ·HBF ₄	DMF	Cs ₂ CO ₃	110	33

7	Pd(OAc) ₂	dppf	DMF	Cs ₂ CO ₃	110	-
8	Pd(OAc) ₂	dppe	DMF	Cs ₂ CO ₃	110	26
9	Pd(OAc) ₂	PCy ₃ ·HBF ₄	DMF	Cs ₂ CO ₃	110	54
10	Pd(OAc) ₂	SPhos	DMF	K ₃ PO ₄	110	23
11	Pd(OAc) ₂	SPhos	Toluene	Cs ₂ CO ₃	110	11
12	Pd(OAc) ₂	SPhos	DMF	NaOtBu	110	32
13	Pd(OAc) ₂	SPhos	DMF	Cs ₂ CO ₃	90	49
14	Pd(OAc) ₂	SPhos	DMF	Cs ₂ CO ₃	60	-
15	Pd ₂ (dba) ₃	SPhos	DMF	Cs ₂ CO ₃	110	17
16	Pd ₂ (dba) ₃	RuPhos	Toluene	Cs ₂ CO ₃	110	15

Reaction condition, *i*, **2a - d** (0.3 mmol), 1.0 equiv. amine, Palladium catalyst (5 mol%), ligand (10 mol%), 3.0 equiv base, solvent (10 mL), 90 °C, 48 h. ^a Yield of isolated products, ^b24h reaction time.

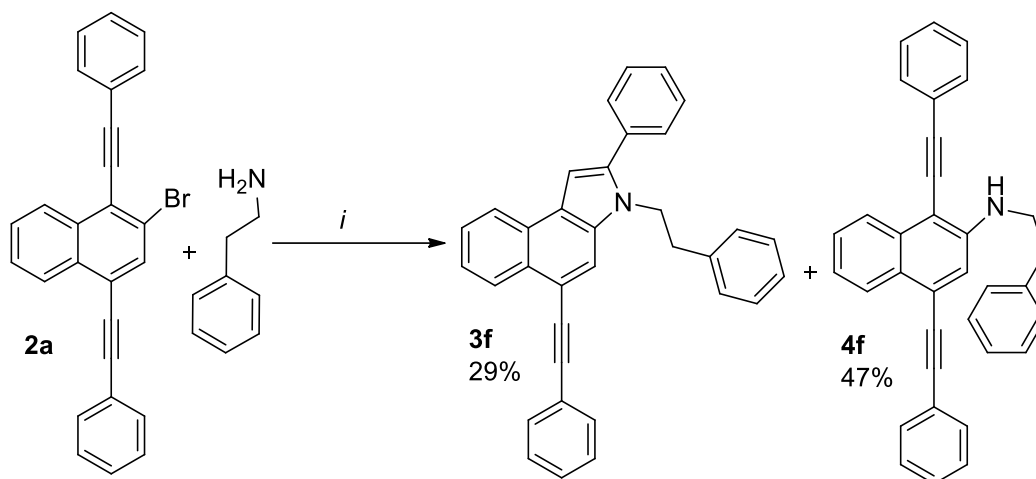
With optimized condition, the cascade of C-N cross-coupling and cyclizing hydroamination gave products **3a - m** in good to excellent yields (47-80%) (Table 2). Benzylamines (**3d** and **3e**) were successfully employed, but gave generally lower yields compared to arylamines. Moreover, using an aliphatic amine, **3f** was obtained in low 29% yield. The diminished yield might be explained by the low reactivity of the 2-phenylethanamine in the hydroamination step. Besides, I have isolated a debrominated side-product **4f** with 47% yield which has not cyclized to the product. However, intermediate **4f** hints that the Buchwald-Hartwig reaction might be the first step of the developed methodology (Scheme 13). No relationship of the substituent pattern of the amine and the yield of products have been detected. The highest yield of 80% was obtained when **2a** reacted with *p*-anisidine.

Table 2. Synthesis of ethynylbenzoindoles **3a - m**.



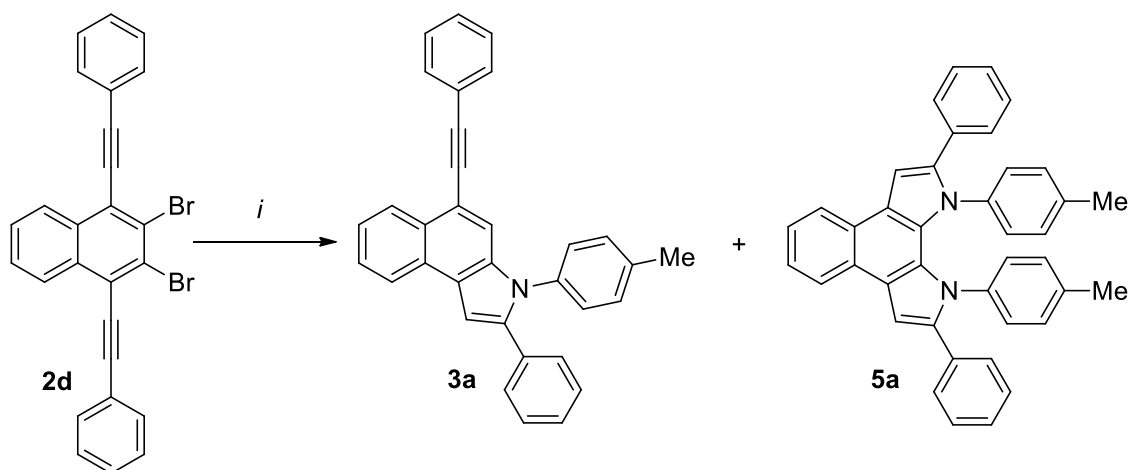
Compound	R ¹	R ²	Yield (%) ^a
3a	H	4-MeC ₆ H ₄	74
3b	H	4-FC ₆ H ₄	64
3c	H	4-MeO-C ₆ H ₄	80
3d	H	4-F-C ₆ H ₄ -CH ₂	53
3e	H	3-F ₃ C-C ₆ H ₄ -CH ₂	47
3f	H	Ph-CH ₂ CH ₂	29
3g	MeO	Ph	52
3h	MeO	3-F ₃ C-C ₆ H ₄	75
3i	MeO	4-MeO-C ₆ H ₄	65
3j	F	Ph	79
3k	F	3-F ₃ C-C ₆ H ₄	45
3l	F	4-MeO-C ₆ H ₄	66
3m	F	4-F-C ₆ H ₄	65

Reaction condition, *i*, **2a - d** (0.3 mmol), 1.0 equiv. amine, Pd(OAc)₂ (5 mol%), SPhos (10 mol%), 3.0 equiv. Cs₂CO₃, DMF (10 mL), 90 °C, 48 h. ^aYield of isolated products.



Scheme 13. The synthesis of **3f** and byproduct **4f**.

Reaction condition, *i*, **2d** (0.3 mmol), 1.0 equiv. amine, Pd(OAc)₂ (5 mol%), SPhos (10 mol%), 3.0 equiv. Cs₂CO₃, DMF (10 mL), 90 °C, 48 h. ^aYield of isolated products.



Scheme 14. Two-fold cascade C-N cross-coupling and hydroamination.

Reaction condition, *i*, **2d** (0.3 mmol), 2.0 equiv. amine, Pd(OAc)₂ (5 mol%), SPhos (10 mol%), 3.0 equiv. Cs₂CO₃, DMF (10 mL), 90 °C, 48 h. ^aYield of isolated products

As a next step, the reactions of symmetrical dibromodiethynylnaphthalenes **2d - e** with various amines was studied to obtain the pyrrolobenzoindoles **5** (Scheme 14). Unfortunately, previously developed conditions produced only one desired product **5a** with moderate 35% yield and **3a** as a major side-product with 47% yield. After optimizing the procedure by testing different ligands, solvents, changing reaction time and temperature (Table 3) no improved results were obtained for the synthesis of compound **5**.

Table 3. Optimization for the Synthesis of **5a**.

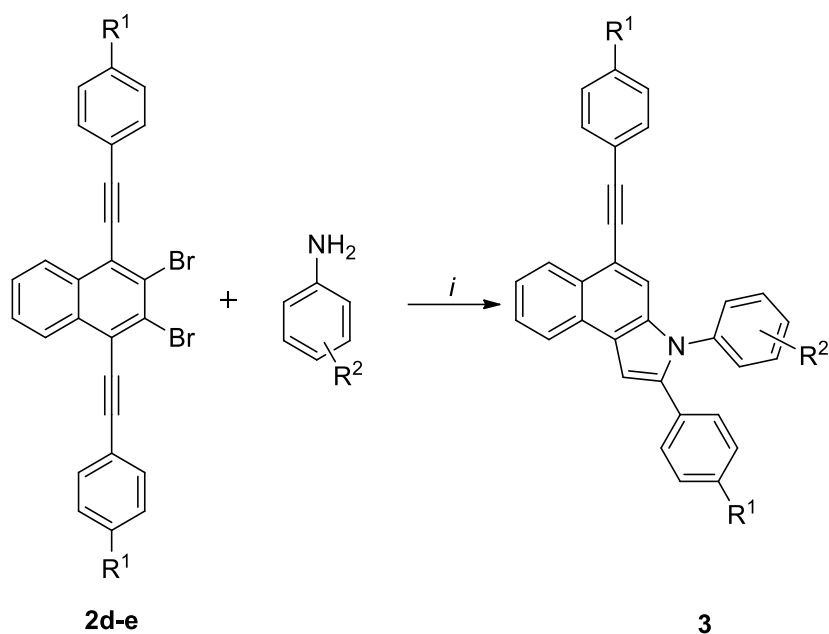
Entry	Pd precursor	Ligand	Base	Solvent	Yield (%) ^a
1	Pd(OAc) ₂	Xantphos	Cs ₂ CO ₃	DMF	28
2	Pd(OAc) ₂	SPhos	Cs ₂ CO ₃	DMF	35
3	Pd(OAc) ₂	Dppe	Cs ₂ CO ₃	DMF	-
4	Pd(OAc) ₂	Dppf	Cs ₂ CO ₃	DMF	-
5	Pd(OAc) ₂	BINAP	Cs ₂ CO ₃	DMF	12
6	Pd(OAc) ₂	PCy ₃ ·HBF ₄	Cs ₂ CO ₃	DMF	-
7	Pd(OAc) ₂	PtBu ₃ ·HBF ₄	Cs ₂ CO ₃	DMF	-
8	Pd(OAc) ₂	XPhos	Cs ₂ CO ₃	DMF	-
9	Pd ₂ (dba) ₃	Xantphos	Cs ₂ CO ₃	DMF	-
10	Pd ₂ (dba) ₃	SPhos	Cs ₂ CO ₃	DMF	-
11 ^b	Pd(OAc) ₂	Xantphos	Cs ₂ CO ₃	DMF	26
12	Pd(OAc) ₂	RuPhos	Cs ₂ CO ₃	DMF	-
13	Pd(OAc) ₂	-	Cs ₂ CO ₃	DMF	-
14	Pd(OAc) ₂	SPhos	Na ₂ CO ₃	DMF	28
15	Pd(OAc) ₂	SPhos	NaOtBu	DMF	-
16	Pd(OAc) ₂	SPhos	Cs ₂ CO ₃	Toluene	-

Reaction condition: **2a** (0.3 mmol), 2.0 equiv. amine, Pd(OAc)₂ (5 mol%), ligand (10 mol%), 3.0 equiv. base, solvent (10 mL), 90 °C, 48 h. ^a Yield of isolated products.

Although the optimization for the two-fold cascade reaction gave only low yield, the reactions of **2d** with different amines afforded coupling products **3a**, **3d**, **3e** and **3p** in moderate yield without corresponding products **5** as side products (Table 4). The starting material **2e** with *p*-

tolyl groups efficiently gave products **3n - o** in good yield (57-62%), which were higher than the yields of products from the precursor with phenyl groups.

Table 4. Cascade C-N cross-coupling and hydroamination from dibromodiethynyl compounds.



Compound	R ¹	R ²	Yield ^a (%)
3a	H	4-Me	47
3d	H	4-MeO	58
3e	H	4-F	46
3n	Me	4-Me	57
3o	Me	3-F ₃ C	62
3p	H	3,5-(Me) ₂	58

Reaction condition, *i*, **2d - e** (0.3 mmol), 2.0 equiv. amine, Pd(OAc)₂ (5 mol%), SPhos (10 mol%), 3.0 equiv. Cs₂CO₃, DMF (10 mL), 90 °C, 48 h. ^aYield of isolated products.

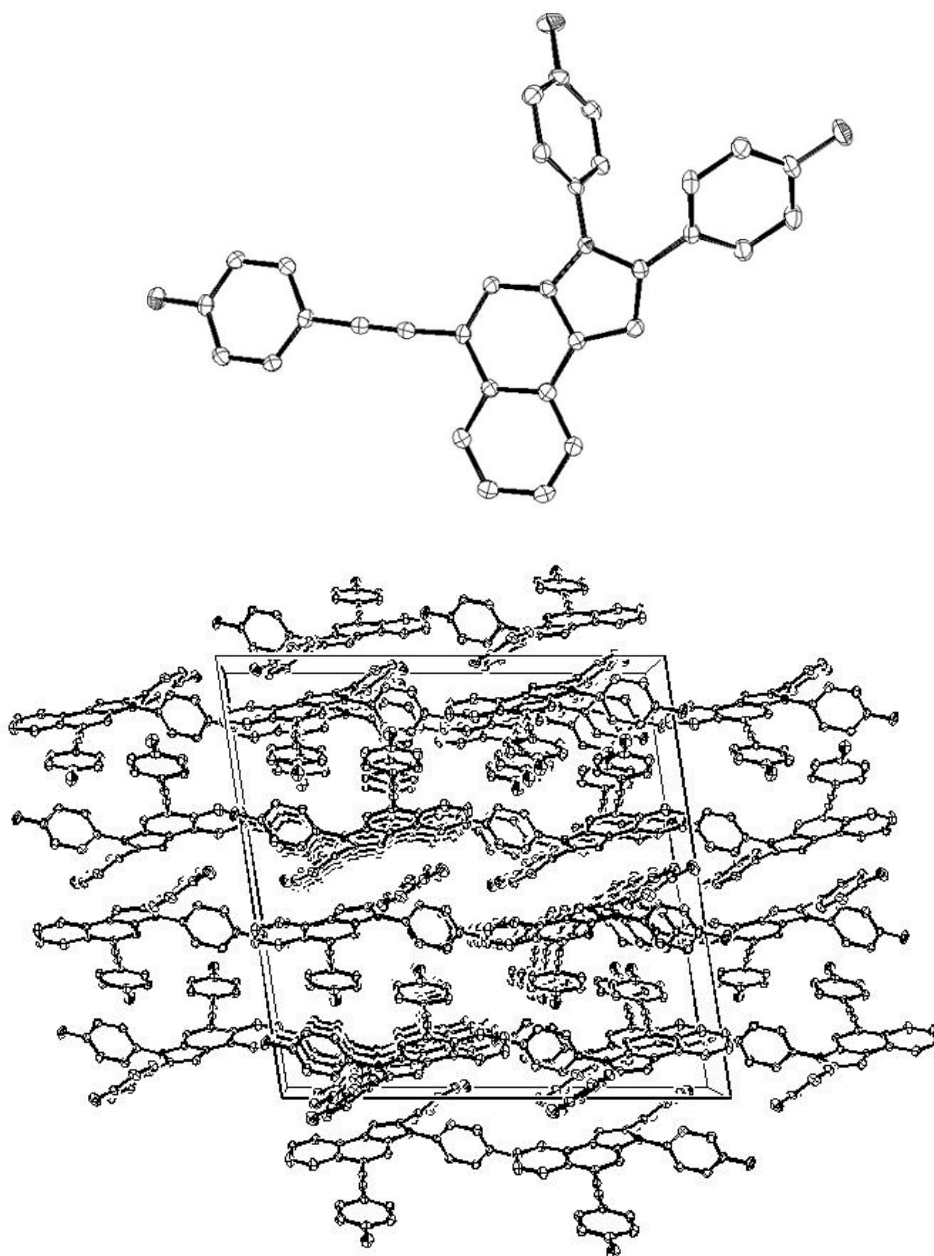


Figure 4. ORTEPs of compound **3m**. (The propability of ellipsoids: 45%)

X-ray crystal structure analysis proves the molecular structure of **3p** independently. Interestingly, the alkynyl moiety is almost in the same plane with the planar benzoindole core structure (the phenyl ring is twisted by 7°). The 4-FC₆H₄ group at the nitrogen atom of the benzoindole scaffold is twisted by 71.2° , while the second 4-FC₆H₄ group at position 2 is rotated only by 40.8° . In the solid state, the molecules are ordered parallelly in the crystal lattice with different direction between two layers (Figure 4).

2.1.3. Absorption and fluorescence properties.

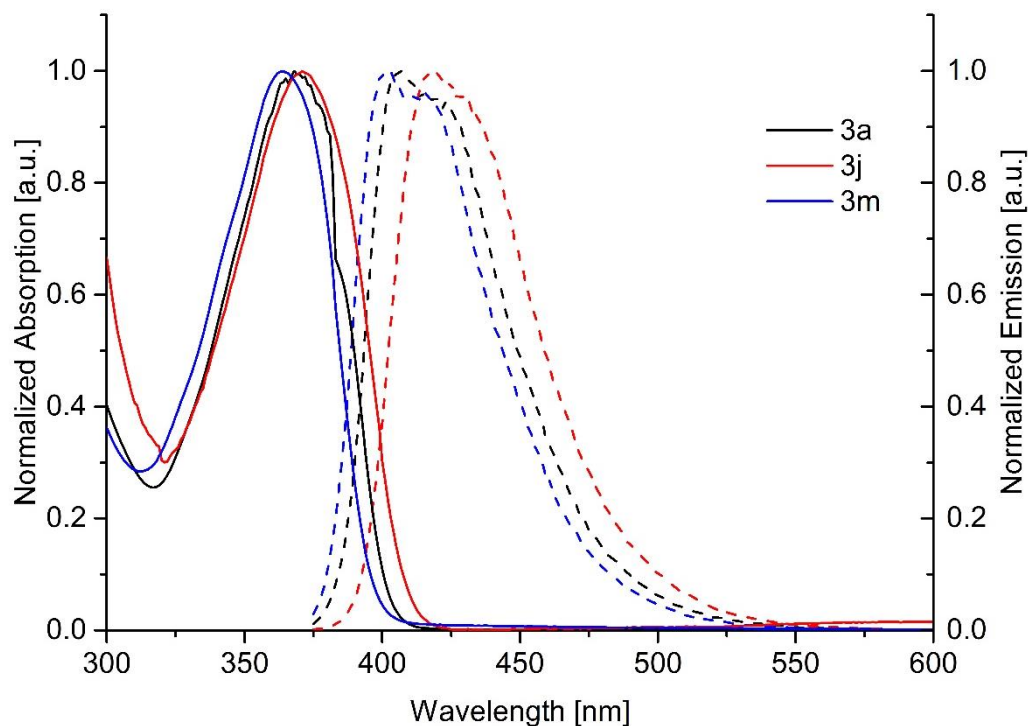


Figure 5. Absorption and corrected emission spectra of **3a**, **3j** and **3m**.

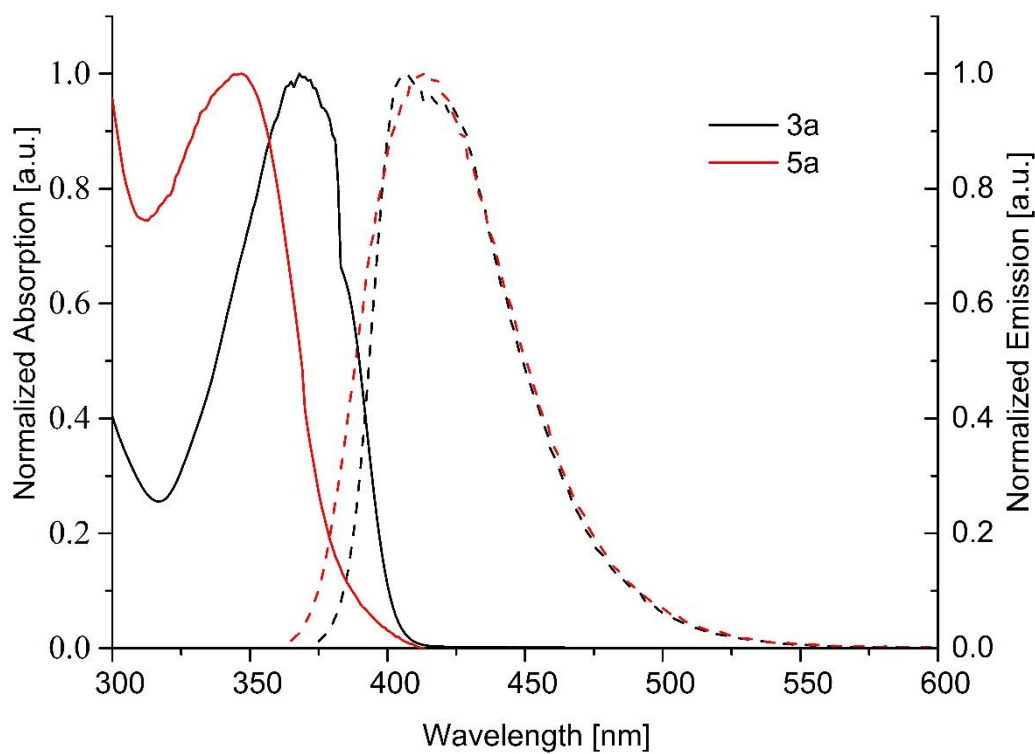


Figure 6. Absorption and corrected emission spectrum of **5a** compared to **3a**.

Table 5. Absorption and emission properties of **3**, **5**.

cp	λ_{abs1} (nm)	$\text{Log } \epsilon (\lambda_{\text{abs1}})$ ($\text{l}\cdot\text{mol}^{-1}\cdot\text{cm}^{-1}$)	λ_{abs2} (nm)	$\text{Log } \epsilon (\lambda_{\text{abs2}})$ ($\text{l}\cdot\text{mol}^{-1}\cdot\text{cm}^{-1}$)	λ_{em} (nm)	$\Phi_{\text{fluo}}^{\text{a}}$ (%)
3a	285	4.577	368	4.752	406	77
3b	276	5.144	365	5.300	404	74
3c	276	4.524	366	4.638	406	66
3d	278	5.094	364	5.038	404	78
3e	281	4.596	365	4.734	403	75
3f	282	4.579	367	4.714	405	75
3g	275	4.622	364	4.718	416	77
3h	285	5.026	370	5.085	414	65
3i	289	3.629	371	3.652	418	77
3j	275	4.394	364	4.519	405	71
3k	277	4.925	364	5.058	403	77
3l	277	4.525	364	4.598	401	74
3m	283	4.489	366	4.628	402	74
3n	286	4.658	369	4.789	408	72
3o	284	4.838	367	4.950	408	65
5a	268	4.936	346	4.598	411	70

^ausing quinine hemisulfate monohydrate in 0.05 M H₂SO₄, as standard for the determination of quantum yields ($\Phi = 51\%$)⁵⁹

I characterized each compound of **3** and **5** by UV-VIS absorption and fluorescence spectroscopy in acetonitrile at room temperature. Table 5 summarizes the results of these experiments (Figures 5 and 6; Table 5). Emission quantum yields were determined using a solution of quinine hemisulfate monohydrate in 0.05 M H₂SO₄ ($\phi = 51\%$) as a reference standard.⁵⁹ All compounds show strong purple fluorescence upon irradiation under UV light at 365 nm. The acquired absorption and emission spectra have a similar shape but the bands differ in intensity and position due to the influence of functional groups.

The UV/VIS spectra of all compounds **3** and **5** show strong absorption bands in the range of 250-300 nm and bands in the range of 300-400 nm (Figure 5-6). Emission spectra of the compounds were collected at the excitation wavelength of 360 nm. The emission maxima were detected in the range of 397 – 470 nm. The determined quantum yields were mainly high (19-78%) (Table 5).

For compounds **3**, derivatives substituted with electron donating methoxy groups, like **3g**, **3h** and **3i** show bathochromically shifted emission spectra while ones substituted with fluorine as electron accepting functional group (**3k**, **3l**, **3m**) are blue shifted. Comparing among compounds **3a** - **f**, there is a small effect from the amine substituent on the optical properties because the strongly twisted orientation of the substituents relative to the benzoindole chromophore is induced by steric constraints. The quantum yields of compounds **3** are only slightly affected by the substitution pattern on both the amine and acetylene moiety. Compound **5**, consisting of an additional pyrrol ring show a strongly blue shifted absorption maximum relative to compounds **3**, while the emission band is not affected compared to **3a**.

2.1.4. Electrochemical studies

To get first insights into the electronic properties of synthesized compounds cyclic voltammograms of **3a** and **5a** were measured (Figure 7). The oxidation event of **3a** and **5a** are ascribed to the oxidation of the indole parts. The earlier oxidation event of **5a** at 0.40 V comparing with that of **3a** at 0.69 V might be caused from the additional electron donating pyrrole moiety in compound **5a**. However, the reduction of compound **3a** is more complicated showing multiple peaks (Figure 7, 8) due to the complex conjugated π -system. Compound **5a** gives only one reduction event at 3.00 V vs. [Fc⁺/Fc]. Differential Pulse Voltammetry (DPV) for the determination of detailed electronic behaviors are shown in Figures 8, 9 and Table 6. There is a small effect of substituents binding to the nitrogen on the oxidation and reduction behaviors. Therefore the IP energy (HOMO) and EA energy (LUMO) differ only slightly among compounds **3**. Compound **3i** with a methoxy group binding to the arylethynyl moiety possesses a lower oxidation potential, resulting in a higher electrochemical bandgap compared to compound **3a**. Compound **5a** possesses a larger electrochemical bandgap by 0.31 eV, with lower oxidation and reduction potentials than compound **3a**. The electrochemical bandgaps are smaller than the optical bandgap. However, both determined bandgaps are affected likewise by the substitution pattern. The difference of these bandgaps can be explained by the interaction between the solvent and the substances on the electrode surface.

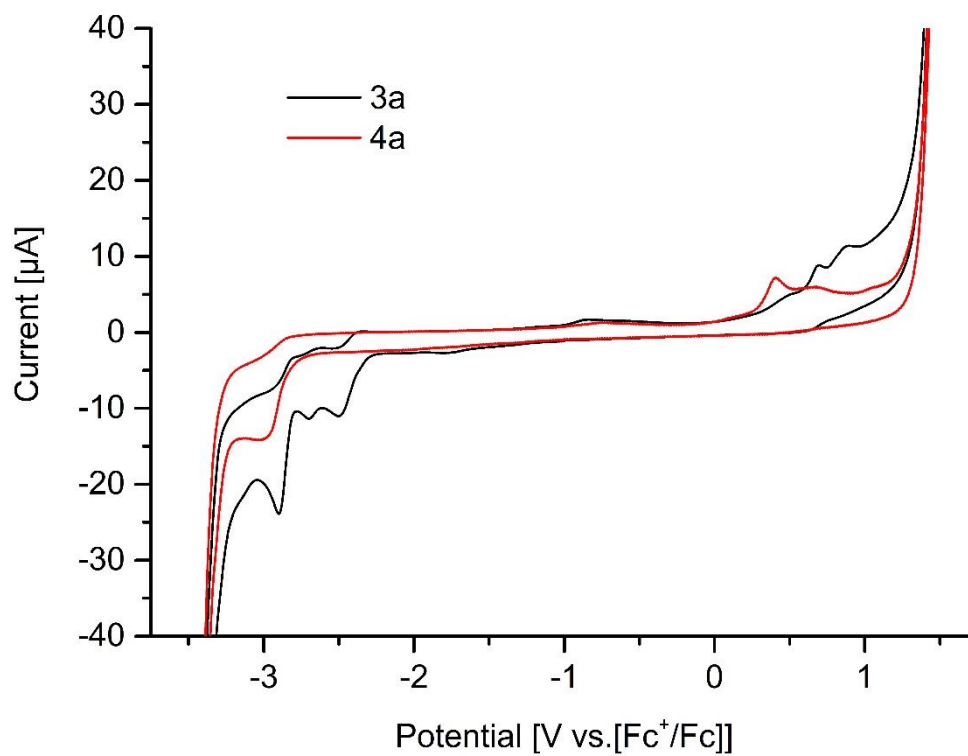


Figure 7. CVs of **3a** and **5a** in DMF.

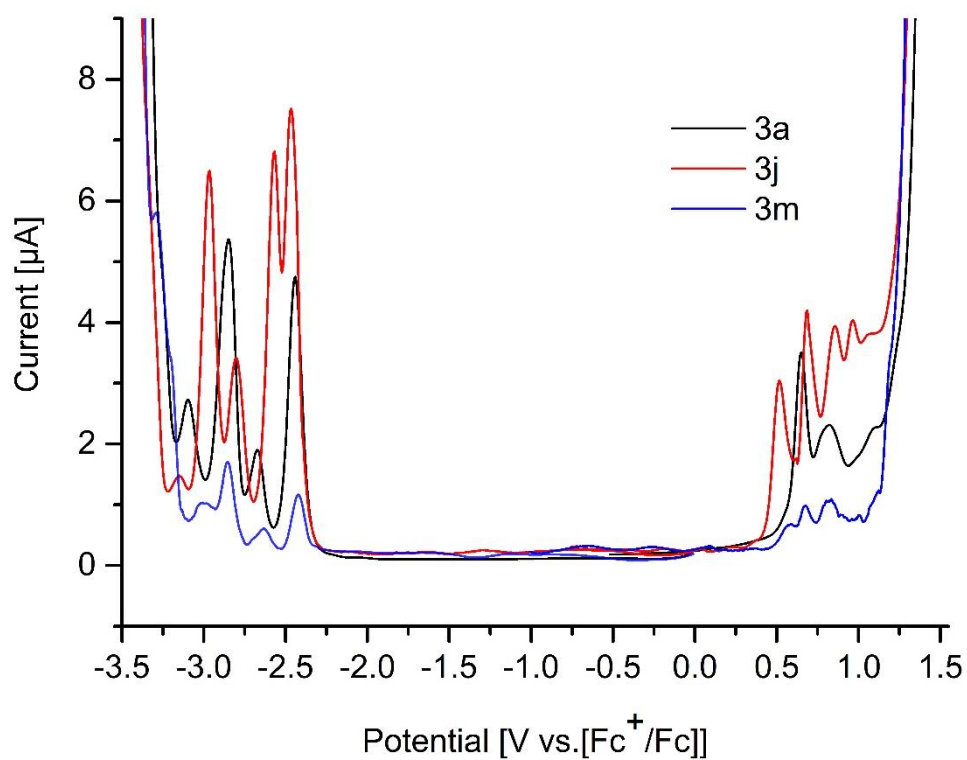


Figure 8. DPVs of selected compounds **3** in DMF.

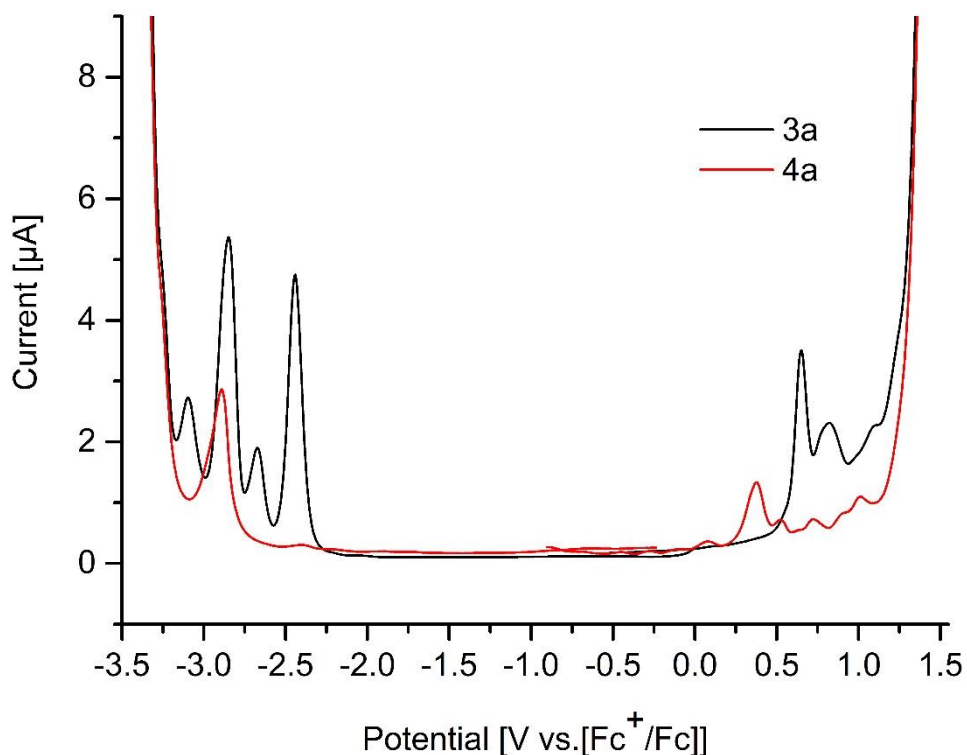


Figure 9. DPVs of compounds **3a** and **5a** in DMF

Table 6. Redox data of selected compounds **3** and **5a** in DMF.

Cp	E^{1-ox} (V vs. Fc ⁺ /Fc)	E^{1-ox} (V vs. NHE)	IP (eV)	E^{2-red} (V vs. Fc ⁺ /Fc)	E^{2-red} (V vs. NHE)	EA (eV)	E_{EC} (eV)	E_{Opt}^a (eV)
3a	0.65	1.38	5.78	-2.42	-1.69	2.71	3.07	3.16
3c	0.67	1.40	5.80	-2.42	-1.69	2.71	3.09	3.18
3d	0.63	1.36	5.76	-2.46	-1.73	2.67	3.09	3.16
3g	0.60	1.33	5.73	-2.50	-1.77	2.63	3.10	3.17
3j	0.52	1.25	5.65	-2.47	-1.74	2.66	2.99	3.08
3m	0.68	1.41	5.81	-2.42	-1.69	2.71	3.10	3.20
5a	0.38	1.11	5.51	-2.89	-2.16	2.24	3.27	3.31

Calculations: IP = E^{1-ox} + 4.4 eV (HOMO) ; EA = E^{2-red} + 4.4 eV (LUMO);⁶⁰ E_{EC} = IP – EA (electrochemical band gap)⁶¹ aE_{Opt} estimated from the 0-0 transition from the intersection of the normalized absorption and emission spectra.⁶²

2.1.5. Density functional theory (DFT) calculations

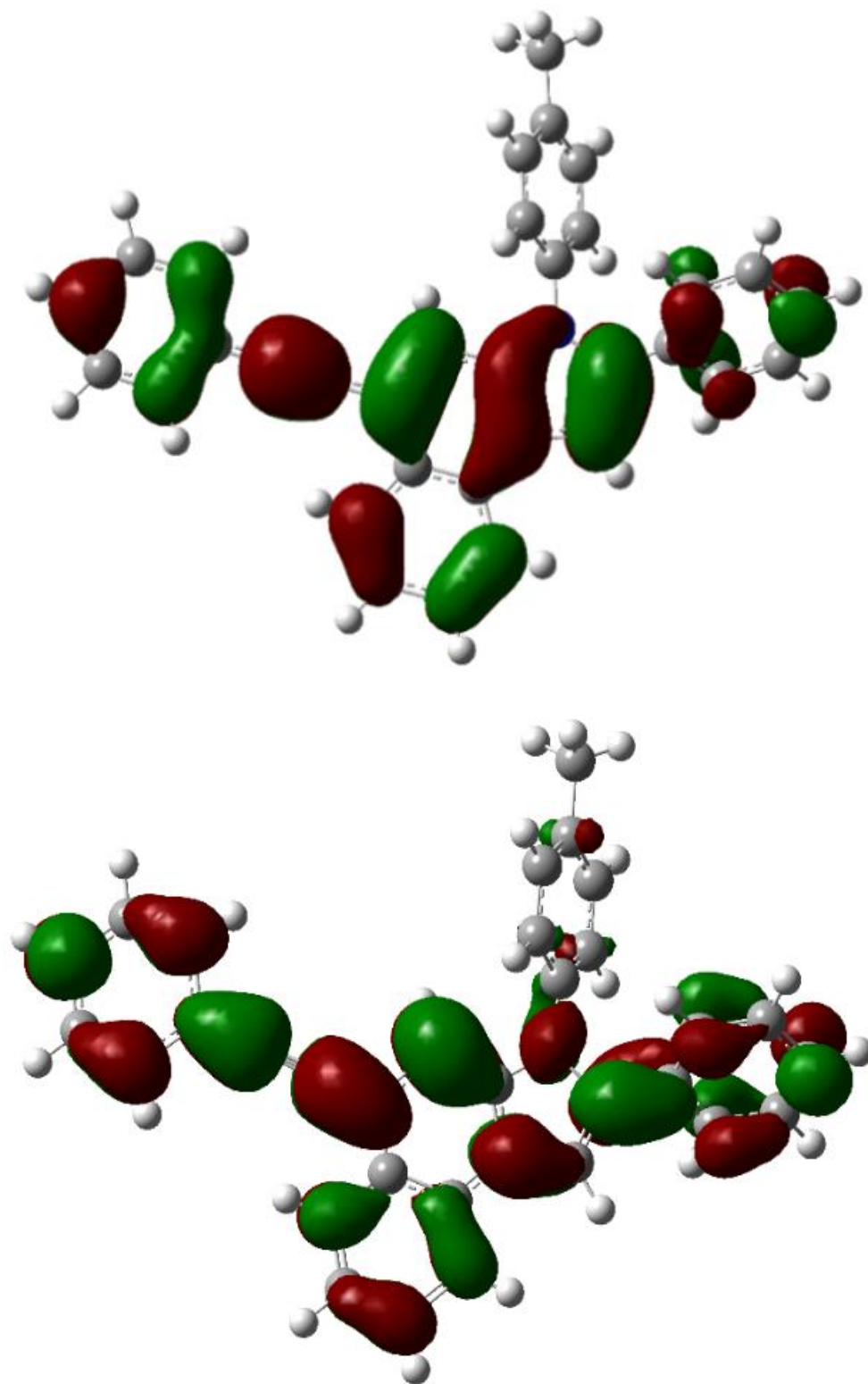


Figure 10. Frontier orbital for HOMO (top) and LUMO (bottom) of compound **3a**

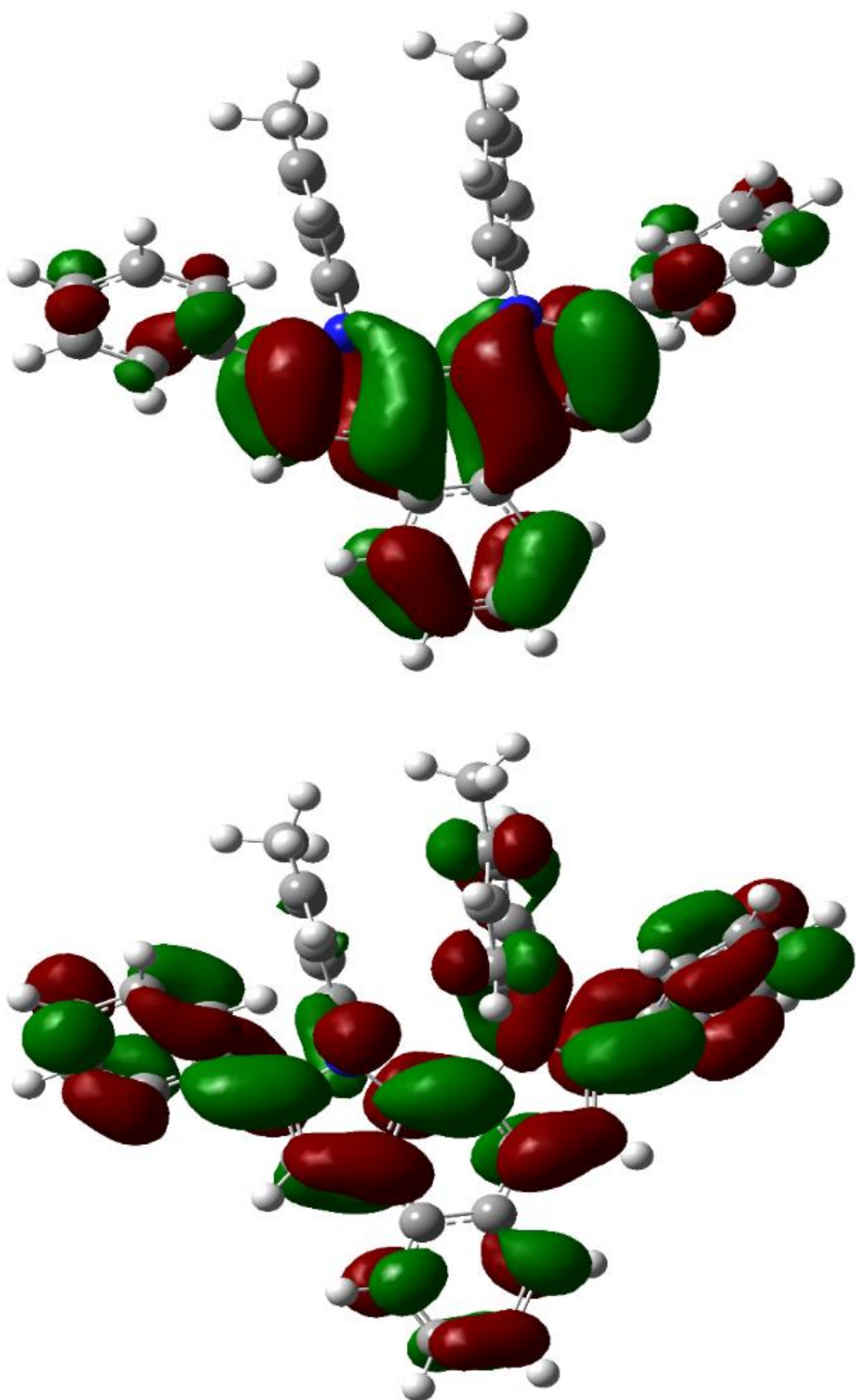


Figure 11. Frontier orbital for HOMO (top) and LUMO (bottom) of compound **5a**

For an improved understanding of the electronic structure of compounds **3a** and **5a**, DFT calculations with B3LYP/6-31G(d) basic set was used for HOMO and LUMO calculation and

the frontier orbital simulations. The experimental bandgaps and the theoretical bandgaps show a small difference of 3.16 eV vs. 3.47 eV for compound **3a** and 3.31 eV vs. 3.87 eV for compound **5a** (Table 7). The frontier orbitals for HOMO and LUMO of both compound **3a** and **5a** in Figure 10 and 11 demonstrates that the substituents at the nitrogen atoms give only very small contributions to the whole conjugated electronic system.

Table 7. Determined bandgaps of selected compounds **3** and **5a** in DMF.

cp	E_{EC} (eV)	E_{Opt}^a (eV)	E_{DFT}^b (eV)
3a	3.07	3.16	3.47
3c	3.09	3.18	3.48
3d	3.09	3.16	3.48
3g	3.10	3.17	3.51
3j	2.99	3.08	3.45
3m	3.10	3.20	3.49
5a	3.27	3.31	3.87

^a E_{Opt} estimated from the 0-0 transition from the intersection of the normalized absorption and emission spectrum.^{62b} Calculated at B3LYP/6-31G(d) level of theory.⁶³

2.2. Multiple Ethynylated Naphthalene

2.2.1. Introduction

Naphthalenes are well-known fluorophores and are frequently used as an interesting substructure of organic fluorescent materials.⁶⁴ Changes on the aromatic scaffold, such as multiple aryl- or ethynylene motifs have been the recent focus of new highly π conjugated compounds for fluorescence applications.⁶⁵ The planar conformation in the ground and excited states, make these derivatives potential candidates for application as nonlinear optical materials. Therefore alkynylated naphthalenes are an attractive target to improve the intramolecular electron transfer and stability for optical application of this class of compounds.⁶⁶

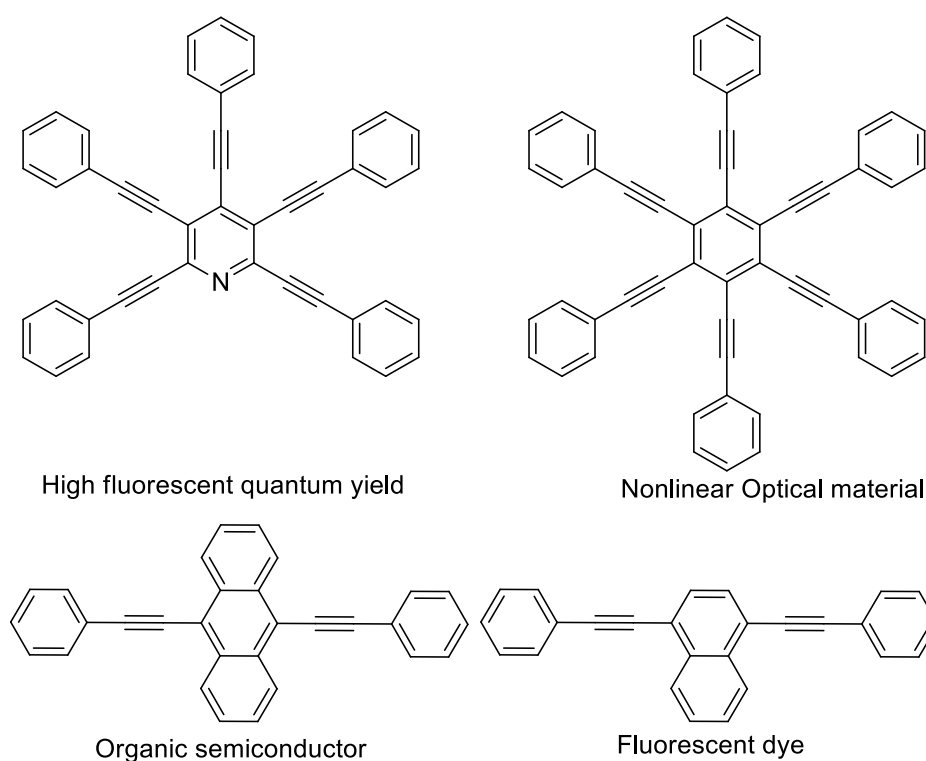


Figure 12. Examples of alkynylated compounds

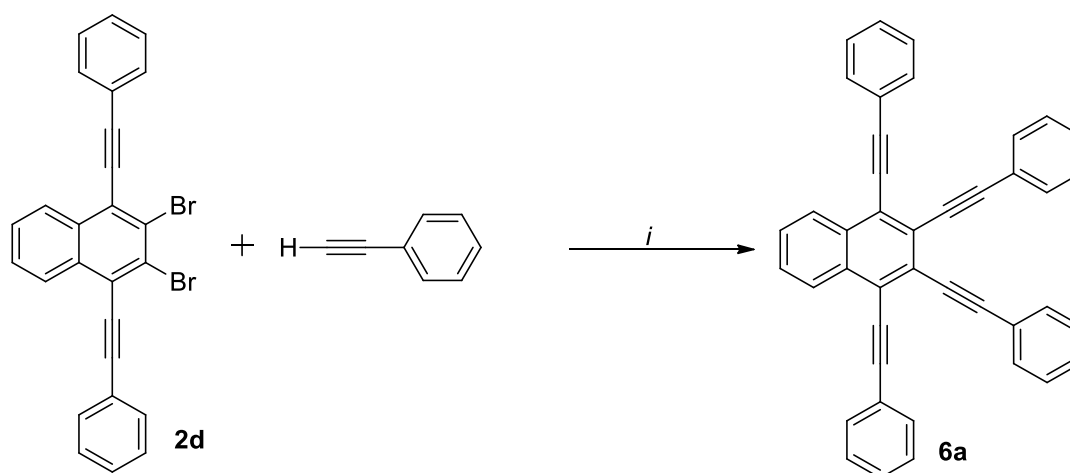
The synthesis of the prototypical 1,4-bis(phenylethynyl)naphthalene molecular frameworks and closely related materials featuring arylethynyl moieties are available via the Sonogashira cross-coupling of aryl halides with terminal alkynes in the presence of Palladium and a Copper co-catalyst.⁶⁷ Besides, the electrophilic carbonyl center in quinone, naphthoquinone, and anthraquinone reacting with alkynyllithium reagents are an alternative and useful methodology

for the preparation of simple diarylethynylene derivatives.⁶⁸ Y.Tobe *et al.* reported the synthesis of 1,2,3,4-tetrakis((isopropylsilyl)ethynyl) naphthalene.⁶⁹

The synthesis of polyalkynylated naphthalenes has not been extensively studied so far although increasing conjugation length has a strong influence on the molecular electronic system and causes red-shifted emission.⁶⁵ During my studies, I developed a new methodology for the synthesis of new tetra(arylethynyl)naphthalenes and 1,4-bis(arylethynyl)-2,3-bisarylnaphthalenes *via* Sonogashira cross-coupling and Suzuki–Miyaura cross-coupling of dibromodiethynylnaphthalenes **2d - f**. Furthermore, I investigated the photophysical properties of obtained compounds by steady-state absorption and emission measurements which had not been carried out for tetrakis(arylethynyl)naphthalenes before.

2.2.2. Results and Discussion

2.2.2.1. Synthesis of tetraarylethynylnaphthalenes **6a - l**



Scheme 15. Synthesis of tetraarylethynylnaphthalene **6a**.

Reaction condition, i, 2d (0.3 mmol), 2.0 equiv. phenylacetylene, PdCl₂(CH₃CN)₂ (5 mol%), ligand (10 mol%), CuI (5 mol%), base (1 ml), solvent (5 mL), 80 °C, 24 h.

Diethynyl derivatives **2d - f** in Scheme 7, section 2.1.2 were employed in the Sonogashira cross-coupling to synthesize tetraethynylnaphthalenes. To optimize the conditions, the reaction of the starting material **2d** and phenylacetylene were screened with a catalyst system consisting of PdCl₂(CH₃CN)₂ and a variety of phosphine ligands with CuI, solvent, base at different

temperatures (see Scheme 15 and Table 8). Up to 79% yield was achieved in the presence of the ligand XPhos, HN(*i*Pr)₂, dioxane at 80 °C. All applied bidentate phosphine ligands (BINAP, Xantphos, dppe, and dppf) were not employed successfully in this reaction due to the formation of an inseparable mixture of products.

Table 8. Optimization of the synthesis of **6a**.

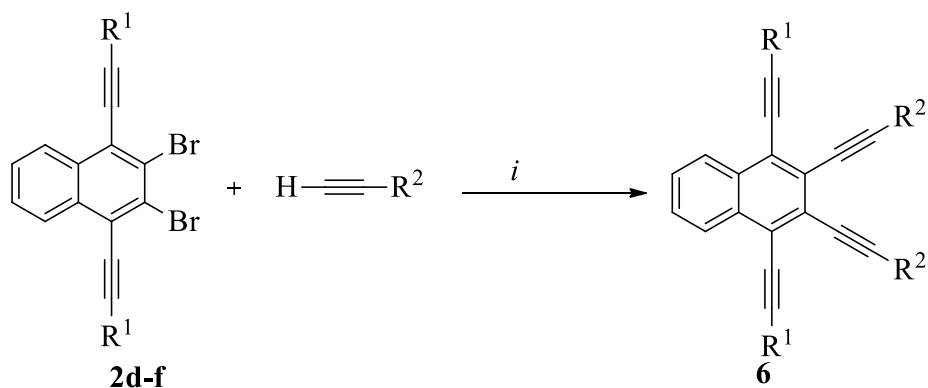
	Ligand	Base	Solvent	Temp (°C)	Yield (%)^a
1	XPhos	HN(<i>i</i> Pr) ₂	Dioxane	80	79
2	XPhos	HN(<i>i</i> Pr) ₂	Dioxane	100	55
3	XPhos	HN(<i>i</i> Pr) ₂	Dioxane	60	40
4	XPhos	HN(<i>i</i> Pr) ₂	THF	80	13
5	SPhos	HN(<i>i</i> Pr) ₂	Dioxane	80	54
6	XPhos	Cs ₂ CO ₃	Dioxane	80	22
7	SPhos	Cs ₂ CO ₃	Dioxane	80	-
8	P(<i>t</i> Bu) ₃ ·HBF ₄	HN(<i>i</i> Pr) ₂	Dioxane	80	34
9	Xantphos	HN(<i>i</i> Pr) ₂	Dioxane	80	38
10	RuPhos	HN(<i>i</i> Pr) ₂	Dioxane	80	42
11	Dppf	HN(<i>i</i> Pr) ₂	Dioxane	80	32
12	Dppe	HN(<i>i</i> Pr) ₂	Dioxane	80	12
13	DavePhos	HN(<i>i</i> Pr) ₂	Dioxane	80	17
14	BINAP	HN(<i>i</i> Pr) ₂	Dioxane	80	-

^a Yield of isolated products

The reaction of diethynylnaphthalenes **2d** - **f**, using optimized conditions with several acetylenes including those featuring electron-donating and electron-withdrawing substituents, afforded the desired products **6a** - **i** (Table 9) with good yield (42-79%). **2e** with tolyl group gave the products **6e** - **i** with lower yields (42-54%) when comparing to that of the products **6a** - **c** derived from **2d** (61-79%). Unfortunately, 1-hexyne was not successfully employed in

this reaction. Acetylenes with strong electron withdrawing groups like *p*-CN-C₆H₄ did not take part in this reaction.

Table 9. Synthesis of tetraalkynylnaphthalene **6a - l**.

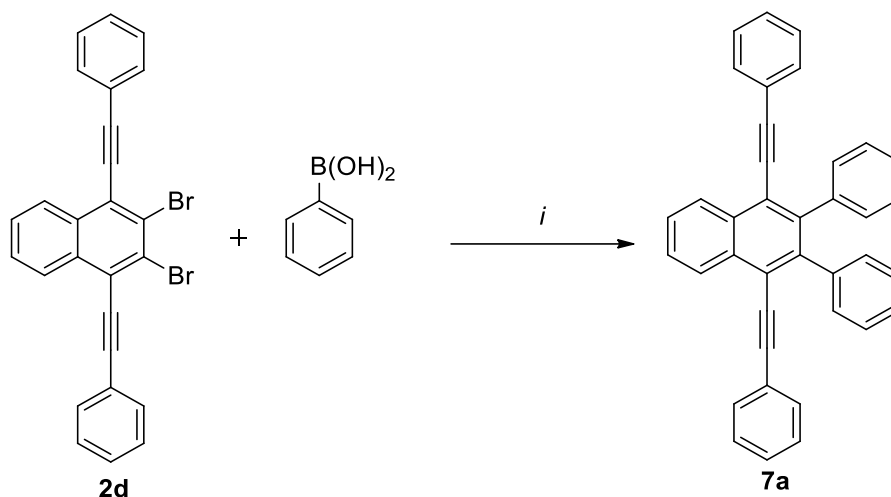


Compound	R ¹	R ²	Yield (%) ^a
6a	C ₆ H ₅	C ₆ H ₅	79
6b	C ₆ H ₅	<i>p</i> -FC ₆ H ₄	71
6c	C ₆ H ₅	<i>p</i> -MeOC ₆ H ₄	61
6d	1-Naphthyl	C ₆ H ₅	63
6e	<i>p</i> -MeC ₆ H ₄	C ₆ H ₅	54
6f	<i>p</i> -MeC ₆ H ₄	<i>p</i> -MeOC ₆ H ₄	52
6g	<i>p</i> -MeC ₆ H ₄	<i>p</i> -FC ₆ H ₄	52
6h	<i>p</i> -MeC ₆ H ₄	<i>p</i> - <i>t</i> BuC ₆ H ₄	54
6i	<i>p</i> -MeC ₆ H ₄	<i>p</i> -MeC ₆ H ₄	42
6k	<i>p</i> -MeC ₆ H ₄	C ₄ H ₉	-
6l	<i>p</i> -MeC ₆ H ₄	<i>p</i> -CNC ₆ H ₄	-

Reaction condition, *i*, **2d - f** (0.3 mmol), 2.0 equiv. alkyne, PdCl₂(CH₃CN)₂ (5 mol%), XPhos (10 mol%), CuI (5 mol%), diisopropylamine (1 ml) and dioxane (5 mL), 80 °C, 24 h. ^a Yield of isolated products

2.2.2.2. Synthesis of 2,3-diaryl-1,4-diethynynaphthalene **7a - k**.

After exploring the scope of the Sonogashira reaction, synthesizing various tetra-alkynyl derivatives of naphthalene, I turned the attention to the Suzuki-Miyaura cross-coupling reaction. The Suzuki-Miyaura reaction of **2d - f** with different arylboronic acids afforded 2,3-diaryl-1,4-diarylethynynaphthalenes **7a - k**. The reaction using Pd(PPh₃)₄ and sodium carbonate with the solvent system of 1,4-dioxane and water 5:1 gave **7a** with 88% yield. Further optimizations did not give better results (Table 10).



Scheme 16. Synthesis of 2,3-diaryl-1,4-diethynynaphthalene **7a**.

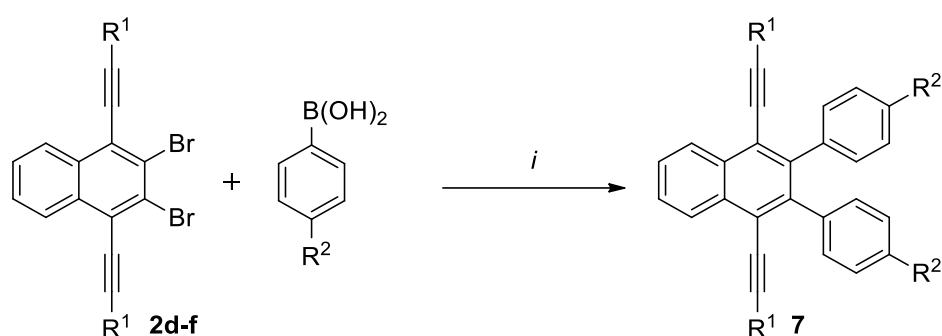
Reaction condition, i, 2d (0.3 mmol), 2.0 equiv. arylboronic acid, Palladium catalyst (5 mol%), 3.0 equiv. base, solvent (10 mL), H₂O (2 ml), 100 °C, 24 h.

Table 10. Optimization of the synthesis of **7a**.

	Catalyst	Base	Solvent	Temp (°C)	Yield (%)
1	Pd(PPh ₃) ₄	Na ₂ CO ₃	Dioxane/H ₂ O	100	88
2	Pd(PPh ₃) ₄	Na ₂ CO ₃	Dioxane/H ₂ O	80	51
3	Pd(PPh ₃) ₄	Na ₂ CO ₃	Dioxane/H ₂ O	60	-
4	Pd(PPh ₃) ₄	Na ₂ CO ₃	THF/H ₂ O	100	73
5	Pd(PPh ₃) ₄	NaOH	Dioxane/H ₂ O	100	46
6	Pd(OAc) ₂ + BINAP	Na ₂ CO ₃	Dioxane/H ₂ O	100	65
7	Pd(OAc) ₂ + RuPhos	Na ₂ CO ₃	Dioxane/H ₂ O	100	54

With optimized conditions in hand, I examined the scope of the reaction. The Suzuki-Miyaura reaction with various arylboronic acids afforded products **7a - l** in moderate to excellent yields (Table 11). The highest yield of 92% was obtained when employing [1,1'-biphenyl]-4-ylboronic acid. Naphthyl derivative **2f** gave product **7f** in 59% yield. Besides, starting material **2e** afforded products **7h - k** in generally lower yields (58-70%) compared to products **7b - e** derived from **2d** (77-92%).

Table 11. Synthesis of 2,3-diaryl-1,4-diarylethynynaphthalenes **7a - k**.



Compound	R ¹	R ²	Yield (%) ^a
7a	Ph	H	88
7b	Ph	Me	85
7c	Ph	CF ₃	82
7d	Ph	Ph	92
7e	Ph	MeO	77
7f	1-Naphthyl	H	59
7g	<i>p</i> -MeC ₆ H ₄	MeO	66
7h	<i>p</i> -MeC ₆ H ₄	<i>t</i> Bu	58
7i	<i>p</i> -MeC ₆ H ₄	CF ₃	67
7k	<i>p</i> -MeC ₆ H ₄	Ph	70

Reaction condition, *i*, **2d - f** (0.3 mmol), 2.0 equiv. arylboronic acid (0.6 mmol), Pd(PPh₃)₄ (5 mol%), 3.0 equiv. Na₂CO₃ (0.9 mmol), 1,4-dioxane (10 mL), H₂O (2 ml), 100 °C, 24 h. ^a Yield of isolated products

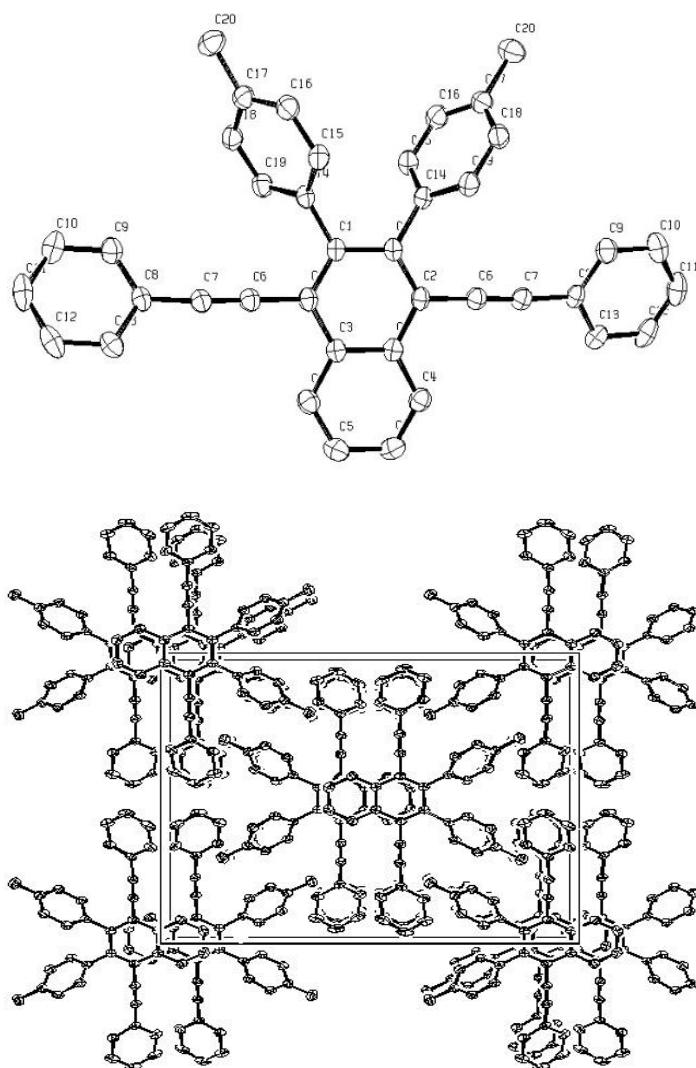


Figure 13. ORTEPs of compound **7b**. (The probability of ellipsoids: 45%)

The molecular structure of **7b** was independently confirmed by X-ray crystal structure analysis (Figure 13). In the solid state, the aryl rings at positions 2 and 3 of the naphthalene core are twisted by 60.5° while the arylolethynyl moieties are twisted only by 24.0° . Molecules of **7b** are ordered parallelly in the crystal lattice.

2.2.3. Absorption and fluorescence properties.

All compounds **6** and **7** emit strongly light in the violet region upon irradiation under UV light. UV-VIS absorption and fluorescence studies at the excitation wavelength of 360 nm of compounds **6** and **7** were carried out in acetonitrile at room temperature (Figure 14-15; Table 12). Compounds **6** and **7** possess a strong absorption band at 250-300 nm and broad bands with a certain fine structure in the range of 300-400 nm. The emission bands of the compounds

occupy bands around 397 – 470 nm with the presence of a shoulder in case of all compounds **6** and a clear second band in case of compounds **7**. There is no impact of the functional groups at the benzene rings on the absorption and emission bands of each series.

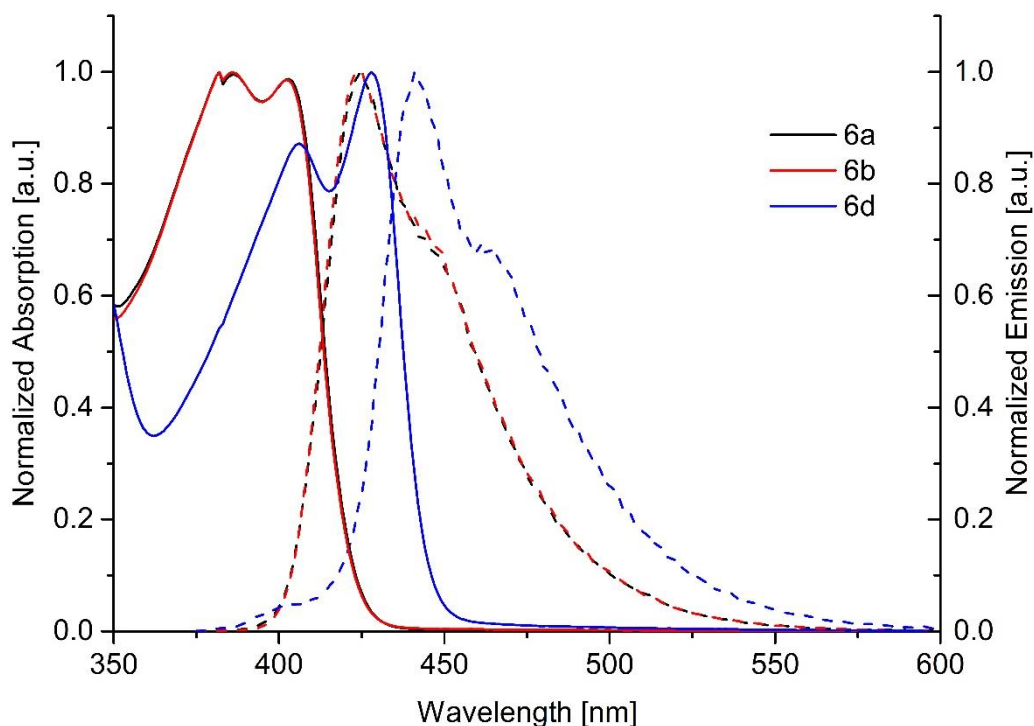


Figure 14. Absorption and corrected emission spectra of **6a**, **6b** and **6d**.

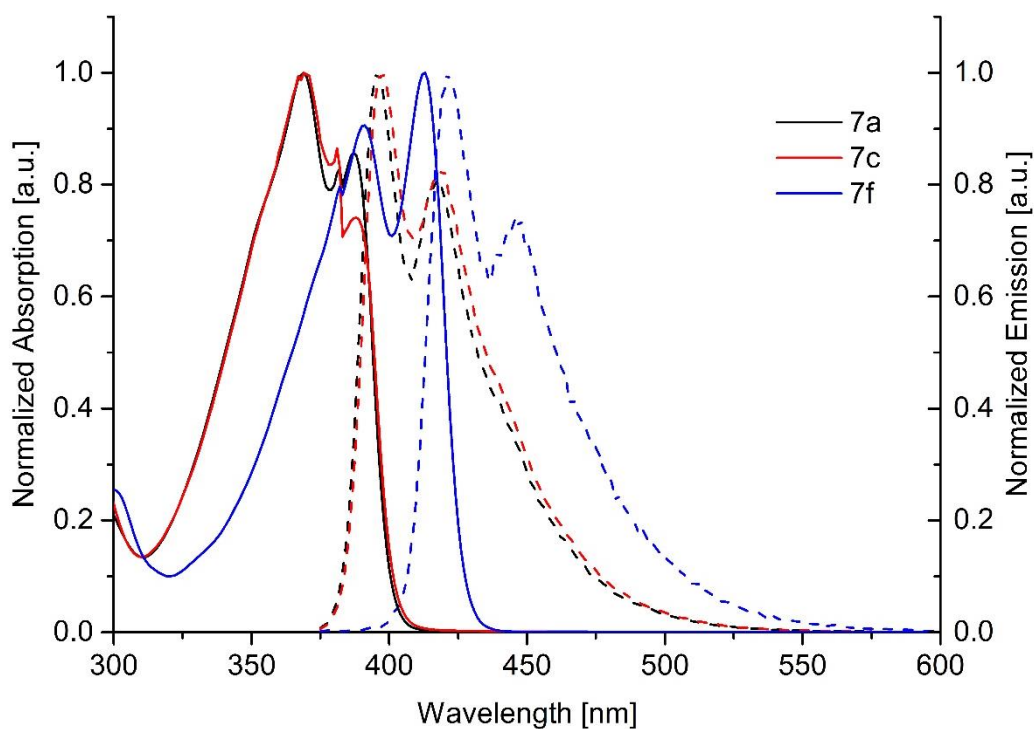


Figure 15. Absorption and corrected emission spectra of **7a**, **7c** and **7f**.

Table 12. Absorption and emission properties of **6** and **7**.

Cp	λ_{abs1} (nm)	$\text{Log } \epsilon(\lambda_{\text{abs1}})$ ($\text{l}\cdot\text{mol}^{-1}\cdot\text{cm}^{-1}$)	λ_{abs2} (nm)	$\text{Log } \epsilon(\lambda_{\text{abs2}})$ ($\text{l}\cdot\text{mol}^{-1}\cdot\text{cm}^{-1}$)	λ_{em1} (nm) (2 nd band)	Φ_{fluo} (%) ^a
6a	382	4.518	403	4.510	424 (448)	60
6b	382	4.386	402	4.379	423 (449)	78
6d	406	4.508	428	4.571	442 (470)	39
6e	326	4.581	408	4.615	426 (452)	59
6g	327	4.637	409	4.343	430 (456)	45
6h	332	5.881	409	5.519	429 (453)	56
6i	331	4.497	408	4.151	429 (456)	65
7a	369	3.713	387	4.647	401 (416)	76
7b	370	4.600	388	4.510	397 (420)	70
7c	369	5.096	387	5.060	397 (421)	78
7d	370	4.819	388	4.762	400 (424)	59
7e	371	4.754	389	4.605	405 (430)	52
7f	391	4.906	413	4.950	422 (448)	30
7g	373	4.685	392	4.623	406 (432)	28
7h	374	4.744	394	4.637	403 (427)	19
7i	374	4.933	393	4.845	402 (428)	68
7k	374	4.292	393	4.281	409 (435)	53

^a using quinine hemisulfate monohydrate in 0.05 M H₂SO₄, as standard for the determination of quantum yields ($\Phi = 51\%$)⁵⁹

Emission spectra of compounds **6d** and **7g** with an extended conjugated π -system show a red-shift by 22 nm in the emission spectrum comparing to their analog phenylderivatives **6a** and **7a**. Ethynyl moieties have a stronger influence on the emission spectra. The emission of compounds **6a** are more red shifted than compounds **7a** with the same substituents due to the different numbers of alkynyl moieties. This effect might be explained by the lower conjugated

system of compound **7a** compared to **6a**. The poor conjugation is ascribed from the worse orbital overlap of the more sterical phenyl rings to the naphthalene scaffold.

Compound **6a** and **7a**, which contain no substituent on the phenyl ring, possess very high quantum yields of 60% and 76%, respectively. Noteworthy, the quantum yields of compounds containing fluor or trifluoromethyl groups were observed to be even higher 78% (**6b**, **7c**), 68% (**7k**) while electron donating functional groups such as methoxy, methyl, *t*butyl groups possess lower quantum yields. Compounds with naphthyl or *t*butyl moieties have low quantum yields (39% (**6d**), 30% (**7g**), 19% (**7i**)).

2.3. Conclusion

Alkynylated benzoindoles **3** were prepared by a domino reaction consisting of a Buchwald-Hartwig amination and hydroamination. Tetraalkynylated naphthalenes **6** and diaryl-dialkynyl naphthalenes **7** were synthesized by the Sonogashira cross-coupling and Suzuki-Miyaura cross-coupling, respectively. The absorption and fluorescence properties of all products show promising photophysical properties, in particular, high quantum yields. Compounds **3a**, **5b**, **6a**, and **7a** possess different absorption and emission behaviors what might be explained by the charge transfer effect from the ethynyl and pyrrole moieties. The substituents on the amines have only a small effect on the absorption and fluorescence properties while incorporation of electron donating groups on the arylacetylenes leads to bathochromically shifted UV/Vis and fluorescence spectra. CV and DPV measurements of selected compounds **3** and **5** show a small impact of substituents on the electrochemical bandgaps of obtained compounds.

3. One-Pot Palladium-Catalyzed Synthesis of Benzo[*b*]carbazolediones

3.1. Introduction

Carbazolediones are one popular class of natural products with various excellent biological activities, for example, antitumor, antiprotozoal, and antibiotic properties.⁷⁰⁻⁷² Calothrixin shows significant cytotoxicity against human Hela cancer cells,⁷³ while Ellipticine quinone has antimalarial and cytotoxic properties (Figure 16).⁷⁴ Another example, murrayaquinone A which is extracted from the root bark of *Murrayaeuchrestifolia*, was demonstrated as an excellent inhibitor against tumor cell SK-MEL-5, Colo-20.⁷⁵ The carbazolequinone moiety has been reported to be a reversible fluorescent “on/off” molecule in a bio-sensor elements to determine energy transfer and local redox properties.⁷⁶

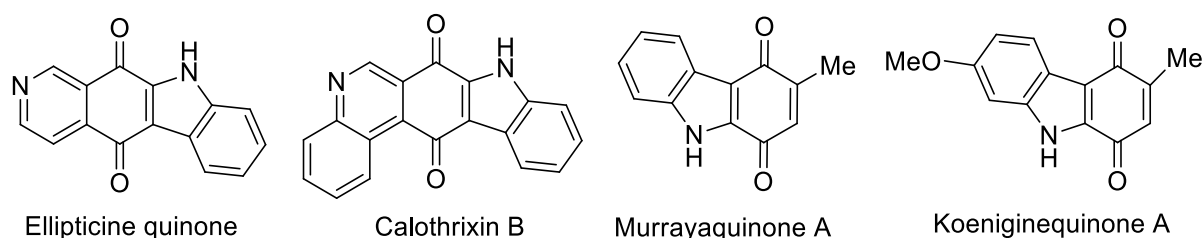
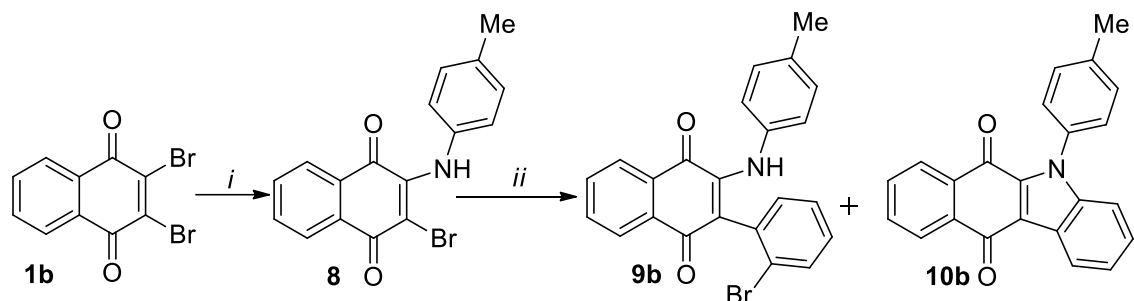


Figure 16. Naturally occurring carbazolequinone alkaloids

5*H*-Benzo[*b*]carbazoles have been previously approached by a Palladium(II) catalyzed oxidative biaryl coupling,^{77a-c} and two-fold Buchwald-Hartwig cross-coupling of 2-bromo-3-(2-bromophenyl)naphthalene-1,4-dione.^{77c} Besides, the methodologies based on Friedel-Crafts acylations,^{78a,b} organolithium coupling,^{78c} direct alkylations at a C-C double bond^{78d,e} are useful to synthesize benzocarbazolediones, too. However, the procedures are limited by the number of derivatives or are based on multiple step reactions which are time and cost consuming as well as waste producing. Therefore, I describe a new one-pot reaction for benzo[*b*]carbazolediones. The first step is a catalyst-free amination of 2,3-dibromonaphthoquinone in water. The second step is a domino reaction consisting of a Suzuki-Miyaura cross-coupling reaction and subsequent C–N cross-coupling reaction. Additionally, an alternative one-pot synthesis of benzo[*b*]carbazolediones is reported, which is based on Palladium-catalyzed domino reaction of 1,2-dibromobenzenes with secondary anilines.

3.3. Results and Discussion

3.3.1. One-pot synthesis of benzo[*b*]carbazolediones



Scheme 17. The three-step one-pot synthesis of **10b**.

Conditions, i, p-toluidine (0.3 mmol), H₂O (1 mL), 60 °C; *ii*, 1.1 equiv. 2-bromophenylboronic acid, catalyst (5 mol%), ligand (10 mol%), 3.0 equiv. K₃PO₄, dioxane (10 mL), 90 °C, 24 h.

The developed procedure is described in Scheme 17. The first step follows a previous report.⁷⁹ Michael addition of **1b** with *p*-toluidine gave 95% yield of intermediate **8** as a red solid. The reaction mixture was added 2-bromophenylboronic acid, the catalyst Pd(PPh₃)₄, K₃PO₄, water, and dioxane. After 24 h at 90 °C, the desired benzo[*b*]carbazoledione **10b** was obtained in 28% yield, while intermediate **9b** was formed with 47% yield.

Compound **9b** independently underwent intramolecular amination to form **10b** in 47% yield. The results proved that compound **9b** might be the intermediate of the domino reaction and the cyclization step from **9** to product **11** might be the limiting step in the domino process.

To optimize the intramolecular C-N cross-coupling, Pd₂(dba)₃ was added as a co-catalyst with several common ligands (see Table 13).⁸⁰ The system of Pd(PPh₃)₄ with Pd₂(dba)₃ and RuPhos (entry 5), improved the isolated yield of **10b** to 47% after 24h. However, the reaction, without Pd(PPh₃)₄ (entry 8) achieved only 17% yield. Bidentate phosphine ligands such as BINAP, Xantphos, dppe, or dppf were not employed successfully in this reaction. As a next step, the impact of temperature and solvents was investigated. The reaction temperature at 90 °C and 1,4-dioxane gave the best yield (entries 6-7, 9–11).

Table 13. Optimization of the one-pot synthesis of **11b**.

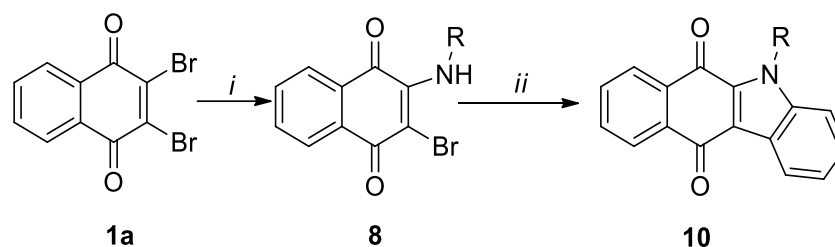
Entry	Catalyst	Co-catalyst/ligand	Yield (%) ^a	
			9b	10b
1	Pd(PPh ₃) ₄	-	47	28
2	Pd(PPh ₃) ₄	Pd ₂ (dba) ₃ + SPhos	36	35
3	Pd(PPh ₃) ₄	Pd ₂ (dba) ₃ + Dppe	28	37
4	Pd(PPh ₃) ₄	RuPhos	42	31
5	Pd(PPh ₃) ₄	Pd ₂ (dba) ₃ + RuPhos	17	47
6 ^b	Pd(PPh ₃) ₄	Pd ₂ (dba) ₃ + RuPhos	52	13
7 ^c	Pd(PPh ₃) ₄	Pd ₂ (dba) ₃ + RuPhos	24	26
8	-	Pd ₂ (dba) ₃ + RuPhos	31	17
9 ^d	Pd(PPh ₃) ₄	Pd ₂ (dba) ₃ + RuPhos	24	16
10 ^e	Pd(PPh ₃) ₄	Pd ₂ (dba) ₃ + RuPhos	33	39
11 ^f	Pd(PPh ₃) ₄	Pd ₂ (dba) ₃ + XPhos	27	22
12	Pd(PPh ₃) ₄	Pd ₂ (dba) ₃ + Xantphos	-	19
13	Pd(PPh ₃) ₄	Pd ₂ (dba) ₃ + dppf	19	14
14	Pd(PPh ₃) ₄	Pd ₂ (dba) ₃ + PtBu ₃ ·HBF ₄	42	29
15	Pd(PPh ₃) ₄	Pd ₂ (dba) ₃ + PCy ₃ ·HBF ₄	37	27
16	Pd(PPh ₃) ₄	Pd ₂ (dba) ₃ + BINAP	16	11

^a Yield of isolated products; ^b 60 °C in the second step; ^c 120 °C in the second step; ^d THF as solvent; ^e DMF as solvent; ^f toluene as solvent.

With optimized conditions, the desired benzo[*b*]carbazolediones **10a-g** were obtained in 42-70% yield using aromatic amines (Table 14). Electron donating groups like methyl, methoxy, gave moderate yields in the range of 48-49% (**10b**, **10e** and **10g**). Compound **10c** was isolated with improved 60% yield containing an electron withdrawing fluoro substituent. However **10d** with a nitro group in 4-position of aniline afforded only 42% yield. 4-aminophenol, *m*-(trifluoromethyl)aniline or *p*-cyanoaniline gave no desired products in the domino process.

Aliphatic and benzylic amines were employed successfully under optimized conditions (Table 14). 2-(3,4-dimethoxyphenyl)ethanamine gave product **10v** in the highest obtained yield (70%).

Table 14. One-pot synthesis of Benzo[*b*]carbazolediones **10a-v**.



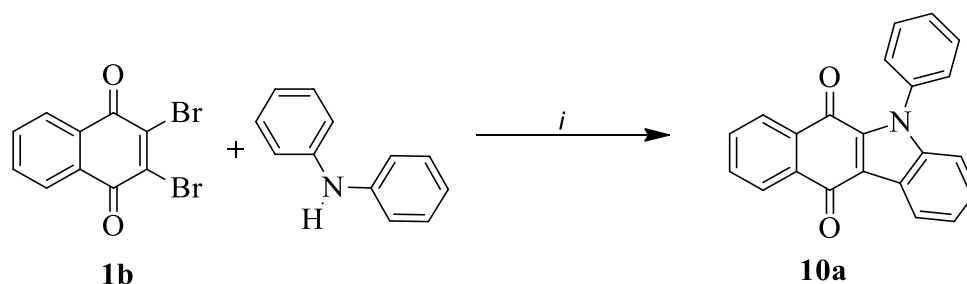
Compound	R	Yield ^a (%)
10a	C ₆ H ₅	61
10b	4-CH ₃ C ₆ H ₄	49
10c	4-FC ₆ H ₄	60
10d	4-(O ₂ N)C ₆ H ₄	42
10e	4-(MeO)C ₆ H ₄	49
10f	3,5-Me ₂ C ₆ H ₃	53
10g	4- <i>t</i> -BuC ₆ H ₄	48
10h	3-(F ₃ C)C ₆ H ₄	0
10i	4-(NC)C ₆ H ₄	0
10j	4-(HO)C ₆ H ₄	0
10k	<i>n</i> -C ₄ H ₉	42
10l	<i>n</i> -C ₅ H ₁₁	48
10m	<i>n</i> -C ₆ H ₁₃	57
10n	<i>n</i> -C ₇ H ₁₅	44
10o	<i>n</i> -C ₈ H ₁₇	46
10p	C ₆ H ₅ CH ₂	52
10q	C ₆ H ₅ (CH ₂) ₂	55

10r	C ₆ H ₅ (CH ₂) ₃	48
10s	4-FC ₆ H ₄ CH ₂	52
10t	4-(MeO)C ₆ H ₄ CH ₂	64
10u	4-(F ₃ C)C ₆ H ₄ CH ₂	59
10v	3,4-(MeO) ₂ C ₆ H ₃ (CH ₂) ₂	70

Conditions, i, amine (0.3 mmol), H₂O, 60 °C, 6 h; *ii*, 1.1 equiv. 2-bromophenylboronic acid, Pd(PPh₃)₄ (5 mol%), Pd₂(dba)₃ (5 mol%), RuPhos (10 mol%), 3.0 equiv. K₃PO₄, dioxane (10 mL), 90 °C, 24 h. ^a Yield of isolated products

3.3.2. Domino Synthesis of benzo[*b*]carbazolediones

Ackermann and coworkers developed a cyclization of 1,2-dibromobenzenes with secondary anilines, based on a domino C-N cross-coupling / CH activation reaction.⁸¹ Here, I report in the following the application of this methodology to the synthesis of benzo[*b*]carbazolediones.



Scheme 18. The two-step domino synthesis of **10a**.

Reaction conditions, i, 1.1 equiv. diphenylamine, Palladium catalyst (5 mol%), ligand (10 mol%), 4.0 equiv. base, toluene (10 mL), 90 °C, 24 h.

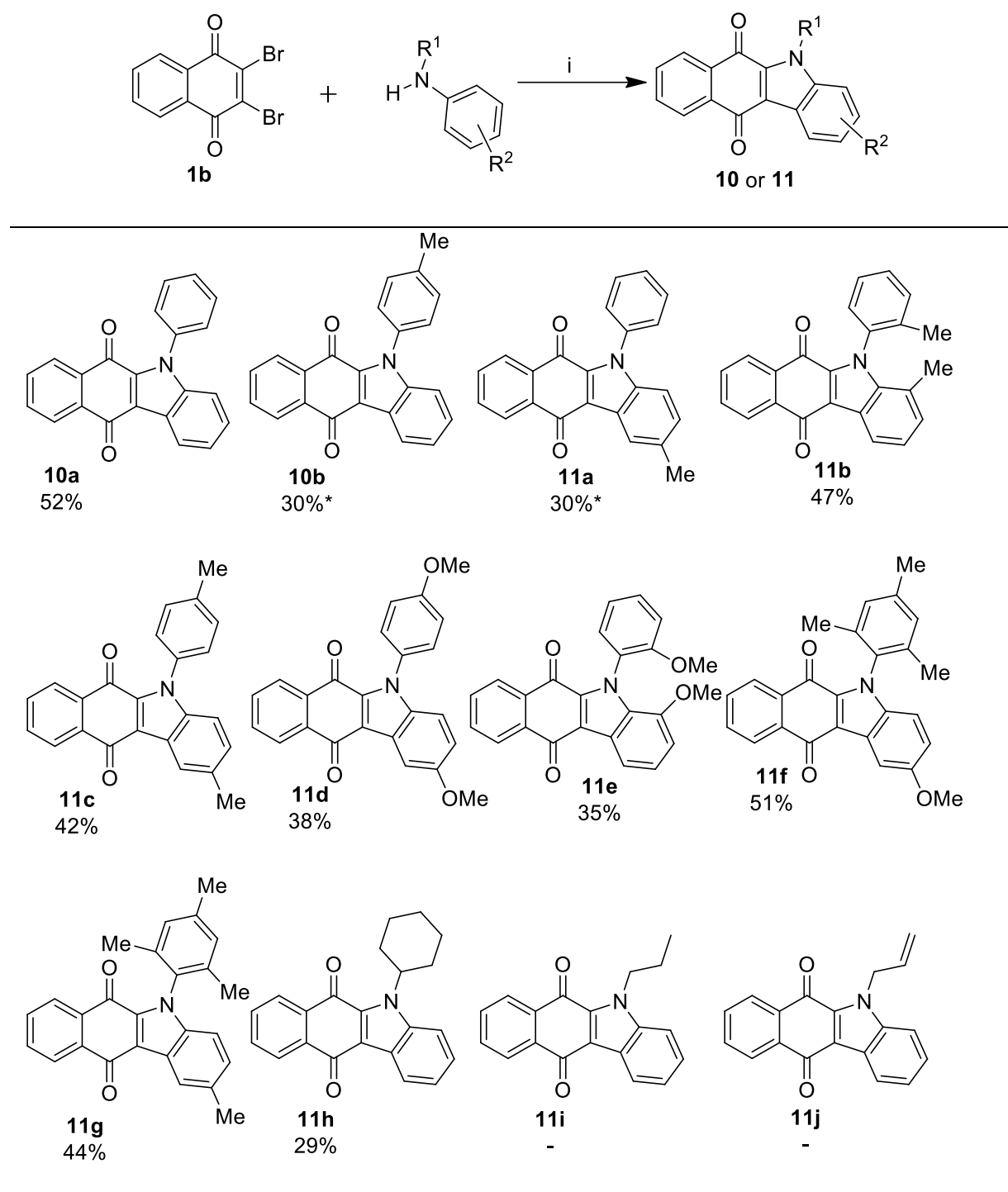
The reaction of **1b** with diphenylamine, using the ligand triphenylphosphine as reported by Ackermann,⁸¹ afforded benzo[*b*]carbazoledione **10a**, albeit, in only 38% yield (Scheme 18). For further optimization, PCy₃·HBF₄ was used in the reaction instead of triphenylphosphine, and the yield increased to 52%. Other ligands (RuPhos, BINAP, SPhos, Xphos, Xantphos, dppe, dppf) and Pd(PPh₃)₄ were not suitable for this reaction. Besides, a change of the solvent (DMF, dioxane, THF), base (NaOH, Na₂CO₃, Cs₂CO₃) did not result in an improvement of the yield (Table 15). Therefore, I continued to extend the scope with these conditions.

Table 15. Optimization of the two-step domino synthesis of **10a**.

entry	catalyst	ligand	Base	Solvent	Temp. °C	Yield ^a (%)
1	Pd(OAc) ₂	PPh ₃	<i>t</i> BuONa	Toluene	90	38
2	Pd(OAc) ₂	PCy ₃ ·HBF ₄	<i>t</i> BuONa	Toluene	90	52
3	Pd(PPh ₃) ₄	-	<i>t</i> BuONa	Toluene	90	33
4	Pd(OAc) ₂	RuPhos	<i>t</i> BuONa	Toluene	90	-
5	Pd(OAc) ₂	BINAP	<i>t</i> BuONa	Toluene	90	-
6	Pd(OAc) ₂	XPhos	<i>t</i> BuONa	Toluene	90	-
7	Pd(OAc) ₂	Xantphos	<i>t</i> BuONa	Toluene	90	-
8	Pd(OAc) ₂	Dppe	<i>t</i> BuONa	Toluene	90	-
9	Pd(OAc) ₂	Dppf	<i>t</i> BuONa	Toluene	90	-
10	Pd(OAc) ₂	SPhos	<i>t</i> BuONa	Toluene	90	-
11	Pd(OAc) ₂	SPhos	<i>t</i> BuONa	DMF	90	-
12	Pd(OAc) ₂	PCy ₃ ·HBF ₄	<i>t</i> BuONa	DMF	90	31
13	Pd(OAc) ₂	PCy ₃ ·HBF ₄	<i>t</i> BuONa	Dioxane	90	24
14	Pd(OAc) ₂	PCy ₃ ·HBF ₄	<i>t</i> BuONa	THF	90	12
15	Pd(OAc) ₂	PCy ₃ ·HBF ₄	NaOH	Toluene	90	35
16	Pd(OAc) ₂	PCy ₃ ·HBF ₄	Na ₂ CO ₃	Toluene	90	27
17	Pd(OAc) ₂	PCy ₃ ·HBF ₄	Cs ₂ CO ₃	Toluene	90	19
18	Pd(OAc) ₂	PCy ₃ ·HBF ₄	<i>t</i> BuONa	Toluene	130	42
19	Pd(OAc) ₂	PCy ₃ ·HBF ₄	<i>t</i> BuONa	Toluene	110	49
20	Pd(OAc) ₂	PCy ₃ ·HBF ₄	<i>t</i> BuONa	Toluene	70	-

Reaction conditions, 1.1 equiv. diphenylamine, Palladium catalyst (5 mol%), ligand (10 mol%), 4.0 equiv. base, toluene (10 mL), 90 °C, 24 h. ^a Yield of isolated products

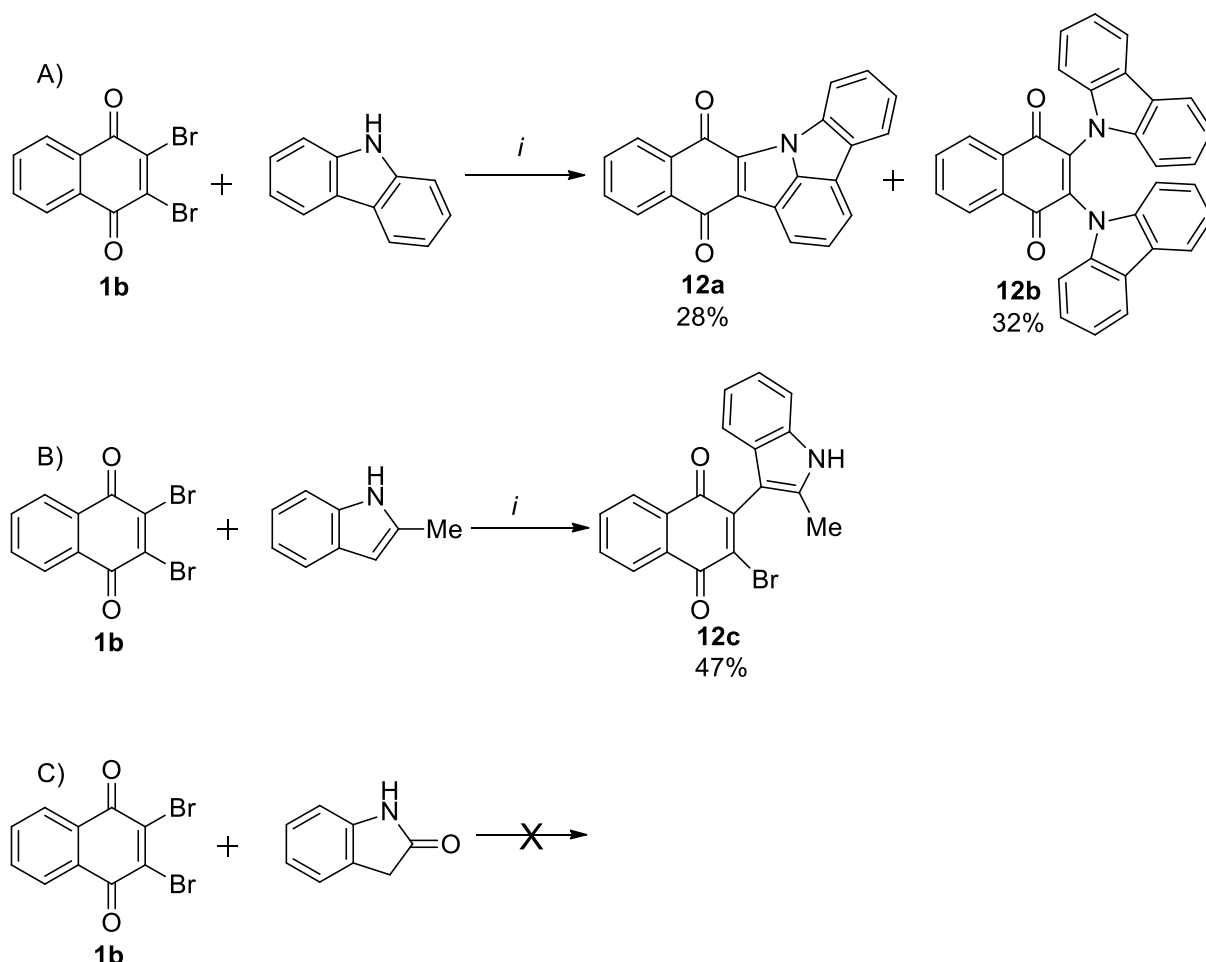
Table 16. Domino synthesis of benzo[*b*]carbazolediones (**10** and **11**).



Reaction condition *i*, 1.1 equiv. amine, Pd(OAc)₂ (5 mol%), PCy₃·HBF₄ (10 mol%), 4.0 equiv. *t*BuONa, toluene (10 mL), 90 °C, 24 h.

The reaction of **1b** with symmetrical diarylamines afforded benzo[*b*]carbazolediones **10a** and **11b-g** in 35-42% yield (Table 16). The employment of unsymmetrical phenyl-(*p*-tolyl)amine

gave an inseparable mixture of regioisomers **10b** and **11a**, due to the low regioselectivity of the C–H activation step. The asymmetrical products **11f** and **11g** were obtained with higher yields (51 and 41%). *N*-Cyclohexylaniline produces **11h** with a low yield of 29%. Other amines (**11i** - **j**) were not successfully employed in the reaction.



Scheme 19. Application of developed domino reaction with carbazole (A), methylindole (B), and indolinone (C).

Reaction conditions *i*, 1.2 equiv. *N*-heterocycle, Pd(OAc)₂ (5 mol%), PCy₃·HBF₄ (10 mol%), 4.0 equiv. *t*BuONa, toluene (10 mL), 90 °C, 24 h.

The reaction of **1b** with carbazole afforded the hexacyclic product **12a**, albeit, in only 28% isolated yield of the pure product, due to a competing second C–N cross-coupling reaction. The side-product **12b** was isolated in 32% yield (Scheme 19). 2-Methylindole does not react via CN cross-coupling reaction. However, compound **12c** was obtained, derived from CH-activation at position 3 of the indole. The reaction of **1b** with indolinone was also not successful and gave a

very complicated and inseparable reaction mixture what might be explained by the lower nucleophilicity of the amide.

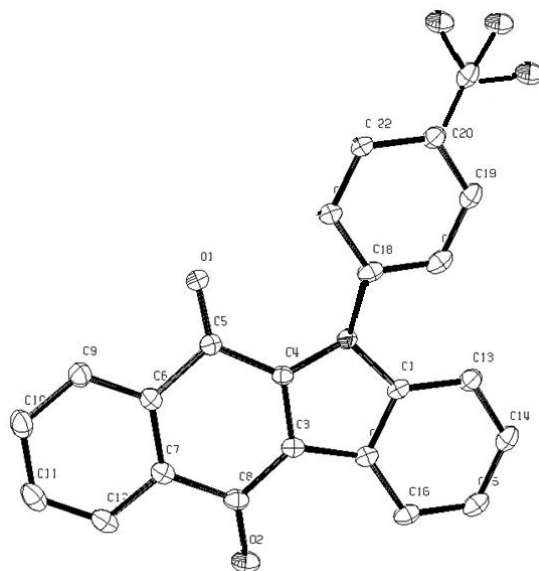


Figure 17. ORTEP of **10c** (The propability of ellipsoids: 45%)

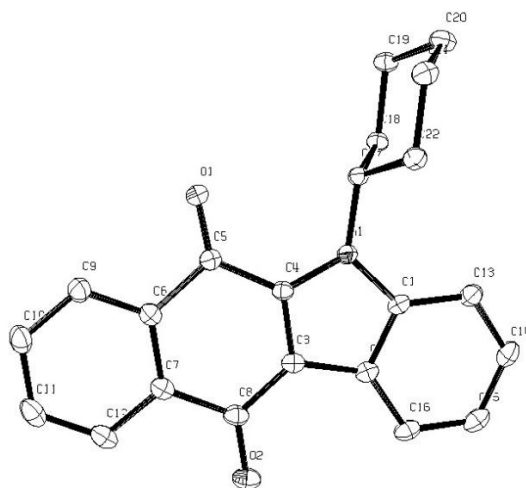


Figure 18. ORTEP of **11h** (The propability of ellipsoids: 45%)

The single crystal XRay diffraction measurement of product **10c** and **11h** was performed to independently confirm the corresponding structures.

3.4. Nucleotide Pyrophosphatase Activity

The enzyme nucleotide pyrophosphatases with seven members (NPP1-7) are attractive targets. Human nucleotide pyrophosphatases 1 (NPP-1) controls the bone mineralization. It also takes part in the insulin signaling process by controlling the tyrosine kinase activity. Human nucleotide pyrophosphatases 3 (NPP-3) is considered as a tumor marker and is associated with metastasis of cancer cells and carcinogenesis.⁸² Although studies of NPP structures and their behaviors in the human body were mentioned in the literature for a long time.⁸³ The inhibitors against two enzymes NPP-1 and NPP-3 have been limited by the number of them and their synthetic approaches. For instances, *N*⁶,*N*⁶-diethyl- β,γ -dibromomethylene-ATP (ARL67156), diadenosine 5',5''-boranopolyphosphonates, and adenosine 5'-(γ -thio)- α,β -methylene triphosphates⁸³ are some of a small number of NPP1 inhibitors. These inhibitors have limited applicability because of their weak metabolic stability. Oxadiazole, biscoumarine derivatives, quinazoline-4-piperidine-4-ethylsulfamide derivatives, imidazopyridine- and purine-substituted thioacetamide derivatives without nucleotides are found to be NPP1 inhibitors.⁸⁴

Different derivatives of compounds **10** and **11**, were tested for human recombinant NPP1 and NPP3. The bio-tests were performed in cooperation with the group of Professor Jamshed Iqbal in the Center for Advanced Drug Research, COMSATS Institute of Information Technology, Abbottabad, Pakistan. Synthesized compounds show significant inhibition of both enzymes when comparing with the previous inhibitors (Table 17).⁸⁴ The IC₅₀-value indicates how much of a drug is required to inhibit 50% of the enzyme activity. That value is considered as the major indicator to determine the selectivity and the inhibition of bio-active compounds.

Compound **10b** with a methyl group could be considered as the most potential inhibitor of NPP-1, which has the highest inhibitory value of IC₅₀ ± SEM = 0.57 ± 0.05 μ M. **10c**, **10t**, **10u** were more active against NPP-1 than NPP-3. The compound **10a** with the phenyl substituent is found to be the most active against NPP-3 with the inhibitory value of IC₅₀ ± SEM = 0.16 ± 0.06 μ M while **10a** is less active against NPP-1. The inhibitory value against NPP-1 is IC₅₀ ± SEM = 1.31 ± 0.08 μ M.

The compounds **10e** and **11d** substituted by a methoxy group are only active with NPP-3 IC₅₀ ± SEM = 0.28 ± 0.03 and 0.27 ± 0.02 μ M, respectively. Both of these compounds show no inhibition against NPP-1. The compounds **10d**, **10v**, **11b** represent also selective activity towards NPP-3 (IC₅₀ ± SEM = 0.30 ± 0.01 μ M, 3.72 ± 0.01 μ M, and 0.27 ± 0.02 μ M, respectively) in comparison to NPP-1 i.e, IC₅₀ ± SEM = 2.17 ± 0.09 μ M, 0.36 ± 0.06 μ M, and 2.39 ± 0.05 μ M, respectively.

The intermediate **9b** shows weak inhibition towards both nucleotide pyrophosphatases NPP-1 and NPP-3. The high inhibitory values of $IC_{50} \pm SEM = 1.74 \pm 0.04 \mu M$ for NPP-1 and $1.24 \pm 0.01 \mu M$ might be caused by the presence of the bromine atom. Hexacyclic compound **12a** displays no activity against both NPPs. **12a** has a highly conjugated and rigid structure what could be the reason of the low interaction of **12a** with studied NPP enzymes. In summary, the carbazolidione moiety may be the primary pharmacophore inhibiting against NPP enzymes. Methoxy functional groups may enhance the inhibition of these compounds.

Table 17. Inhibition activity of samples **9b**, **10**, **11**, **12a** against NPP-1 and NPP-3.*

Compound	NPP1	NPP3
	$IC_{50} (\mu M) \pm SEM$	$IC_{50} (\mu M) \pm SEM$
9b	1.74±0.04	1.24±0.01
10a	1.31±0.08	0.16±0.06
10b	0.57±0.05	1.01±0.08
10c	0.82±0.04	1.61±0.03
10d	2.17±0.09	0.30±0.01
10e	--	0.28±0.03
10m	2.84±0.07	2.43±0.01
10o	1.13±0.09	0.86±0.05
10t	0.59±0.01	1.16±0.04
10u	0.69±0.02	1.85±0.07
10v	3.72±0.06	0.36±0.01
11a	0.77±0.03	0.25±0.01
11b	2.39±0.05	0.38±0.03
11d	--	0.27±0.02
12a	--	--

Values \pm SEM are expressed deviation of three experiments (n = 3). The IC_{50} is the concentration, at which 50% of the enzyme activity is inhibited. *performed by Prof. Iqbal

3.5. Conclusion

Benzo[*b*]carbazolediones were synthesized successfully by a three-step domino reaction in moderate to good yields. In addition, the two-step domino reactions were performed with dibromonaphthoquinone and diarylamines to broaden the substrates scope. The yield of products from the first methodology are higher than those from the second. The second methodology, two-step domino reactions, resulted in the formation of regiosomers when asymmetrical diarylamines were used. Obtained benzo[*b*]carbazolediones show excellent inhibition against enzyme nucleotide pyrophosphatases NPP-1 and NPP-3 with high selectivity.

4. Palladium-Catalyzed Two-fold Buchwald-Hartwig Amination

4.1. Synthesis and Optical Properties of Indolo[2,3-*b*]quinoxalines and 5,7-dihydropyrido[3,2-*b*,5,6-*b'*]diindoles

4.1.1. Introduction

Highly π -conjugated heteroacenes are, nowadays, commercially used as possible, cheap and active elements in organic photovoltaic cells,^{85a} organic light-emitting diodes (OLEDs),^{85b} and especially in organic field-effect transistors (OFETs).^{85c} In particular, highly π -conjugated poly(hetero)aromatic structures are attractive because of their planar structure and the modifiability of their HOMO-LUMO level by substitutions.⁸⁶ These structures have usually strong inter- and intramolecular π - π interactions in the solid state.⁸⁷ Replacement of carbon atoms in π -systems with nitrogen heteroatoms has been considered as an effective strategy to modify the electronic structure and to change dipole moments.⁸⁸⁻⁸⁹

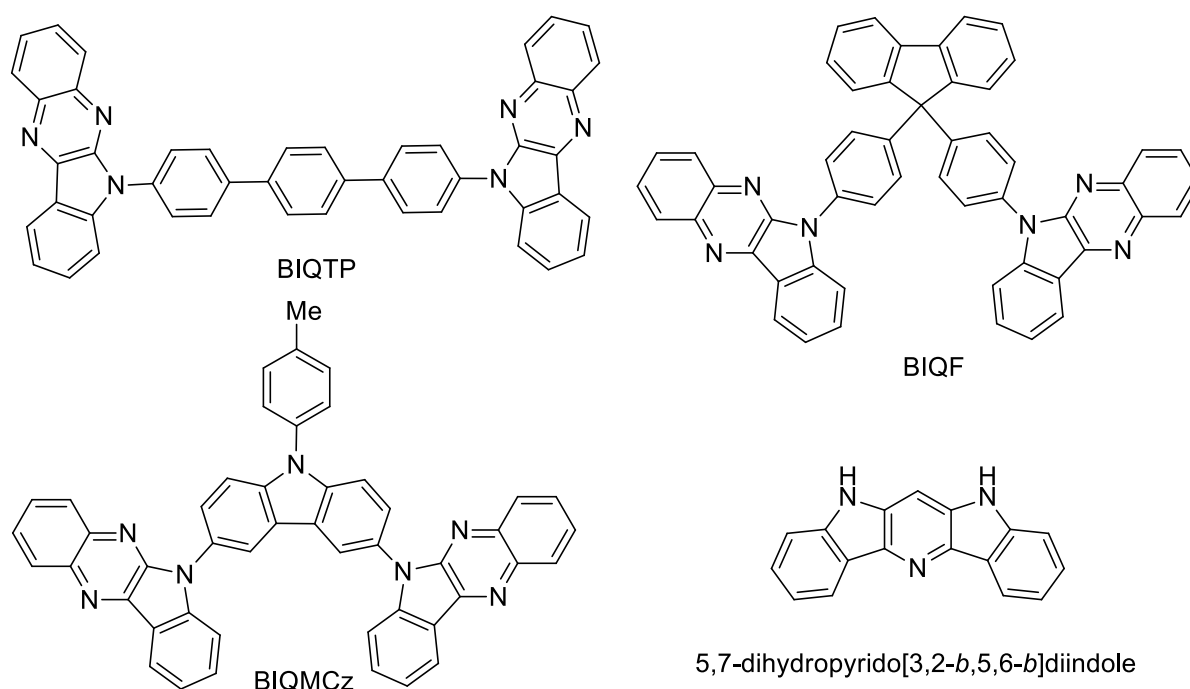


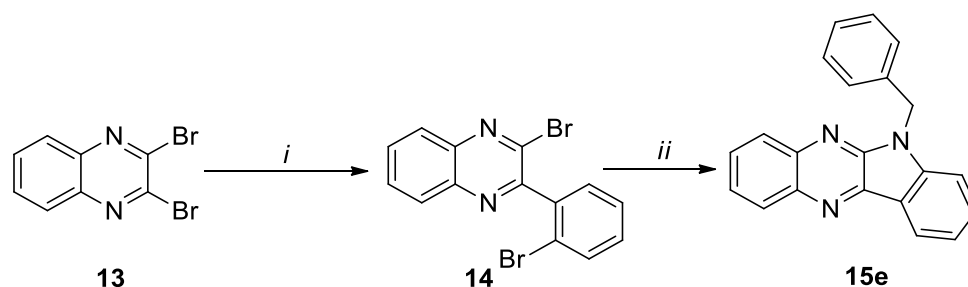
Figure 19. Selected examples of highly π -conjugated aza-carbazoles compounds

For example, BIQF, BIQTP, BIQMcz with two indoloquinoxaline moieties are known for their deep-red light emission (Figure 19).⁹⁰ Indolo[2,3-*b*]quinoxalines are, therefore, potential candidates for organic light-emitting diodes (OLEDs)⁹¹ and excitonic solar cells.⁹¹ The indolo[2,3-*b*]quinoxaline moieties are known to increase the thermal stability, and glass

transition temperature of these materials and are applied as electron transporting and emitting layers.⁹² Indolo[2,3-*b*]quinoxalines were firstly synthesized by Marchlewski via the cyclocondensation of isatin with *o*-phenylenediamine derivatives in the presence of AcOH as catalyst.^{93a} Indoloquinoxalines can be obtained via the cyclization of *o*-phenylenediamine with 1-acetyl-2-bromo-3-indolinone as well.^{93b}

Because of the importance of quinoxaline in the field of organic materials, I studied a practical and efficient two-step synthesis of indolo[2,3-*b*]quinoxalines. The procedure contains the first site-selective Suzuki-Miyaura reaction of 2,3-dibromoquinoxaline with 2-bromophenylboronic acid, followed by a two-fold Palladium-catalyzed C–N cross-coupling reaction with a primary amine. Additionally, I applied this strategy to 2,3,5,6-tetrabromopyridine for the synthesis of unknown pyridodiindoles. In literature, only 5,7-dihydropyrido[3,2-*b*,5,6-*b'*]diindole has been reported.⁹⁴

4.1.2. Synthesis of Indolo[2,3-*b*]quinoxalines



Scheme 20. Synthesis of indolo[2,3-*b*]quinoxalines **15e**.

Conditions, i, 1.2 equiv. 2-bromophenylboronic acid, Pd(PPh₃)₄ (5 mol%), 3.0 equiv. NaOH, THF, H₂O, 70 °C, 4 h. *ii*, 2.0 equiv. benzylamine, 3.0 equiv. base, Palladium catalyst (5 mol%), ligand (10 mol%), solvent, 100 °C, 6 h.

Indolo[2,3-*b*]quinoxalines were synthesized by a two-step synthesis. In the first step, the Suzuki-Miyaura reaction of **13** with 2-bromophenylboronic acid in the presence of Pd(PPh₃)₄ resulted in intermediate **14** in 84% isolated yield, followed by a two-fold C–N cross-coupling reaction (Scheme 20). The conditions of the amination of **14** with benzylamine were optimized afterwards (Table 18). Both, monodentate- and bidentate phosphine ligands were screened during the optimization. The results show that the bidentate ligand DPEPhos gave product **15e**

in up to 96% yield. Employing Pd(OAc)₂ gave lower yield of **15e**. Toluene was more appropriate than DMF under these conditions.

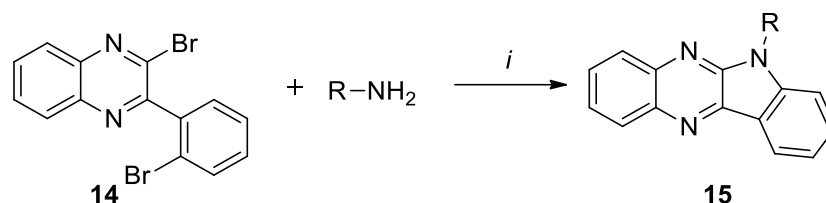
Table 18. Optimization for the Synthesis of **15e**.

Entry	Pd precursor	Ligand	Base	Solvent	Yield (%) ^a
1*	Pd ₂ (dba) ₃	BINAP	<i>t</i> BuONa	Toluene	51
2*	Pd(OAc) ₂	BINAP	<i>t</i> BuONa	Toluene	23
3*	Pd ₂ (dba) ₃	Xantphos	<i>t</i> BuONa	Toluene	63
4*	Pd ₂ (dba) ₃	DPEPhos	<i>t</i> BuONa	Toluene	96
5*	Pd ₂ (dba) ₃	Dppe	<i>t</i> BuONa	Toluene	14
6*	Pd ₂ (dba) ₃	Dppf	<i>t</i> BuONa	Toluene	73
7*	Pd ₂ (dba) ₃	PCy ₃ ·HBF ₄	<i>t</i> BuONa	Toluene	-
8*	Pd ₂ (dba) ₃	<i>Pt</i> Bu ₃ ·HBF ₄	<i>t</i> BuONa	Toluene	15
9	Pd ₂ (dba) ₃	XPhos	<i>t</i> BuONa	Toluene	61
10	Pd ₂ (dba) ₃	XPhos· <i>t</i> Bu ₂	<i>t</i> BuONa	Toluene	59
11	Pd ₂ (dba) ₃	SPhos	<i>t</i> BuONa	Toluene	25
12	Pd ₂ (dba) ₃	DavePhos	<i>t</i> BuONa	Toluene	34
13	Pd ₂ (dba) ₃	RuPhos	<i>t</i> BuONa	Toluene	39
14	Pd(OAc) ₂	DPEPhos	<i>t</i> BuONa	Toluene	12
15	Pd ₂ (dba) ₃	DPEPhos	Cs ₂ CO ₃	Toluene	32
16	Pd ₂ (dba) ₃	DPEPhos	<i>t</i> BuONa	DMF	56

* In the cooperation with Dr. Tran Quang Hung (50% of the optimisation reactions were obtained by myself).

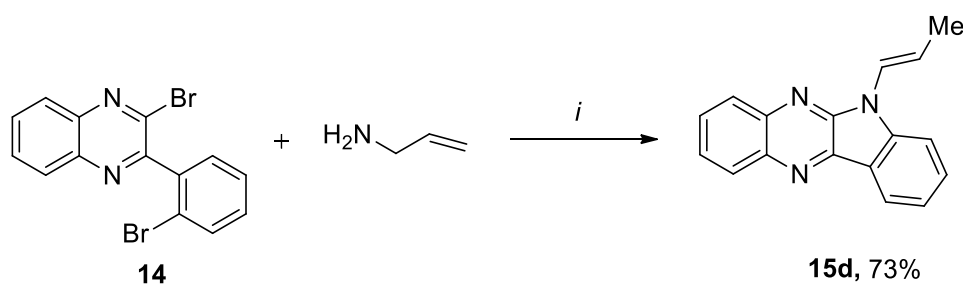
The application of these conditions allowed the synthesis of products **15a - f**, derived from aliphatic amines, allylamine, and benzylamines, with excellent yields (Table 19). The amination of allylamine underwent an isomerization of the double bond to form **15d** due to the presence of the strong base *t*BuONa (Scheme 21).

Table 19. Synthesis of **15a-f**.



Compound	R	Yield (%) ^a
15a	<i>n</i> -C ₃ H ₇	96
15b	<i>n</i> -C ₅ H ₁₁	93
15c	<i>n</i> -C ₇ H ₁₅	85
15d	Allyl	73 ^b
15e	Bn	94
15f	4-(MeO)C ₆ H ₄ CH ₂	92

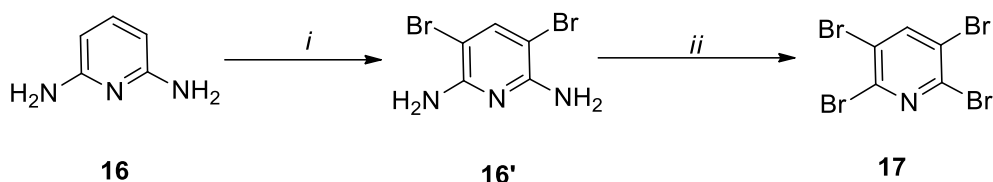
Conditions: *i*, 2.0 equiv. amine, 3.0 equiv. NaOtBu, Pd₂(dba)₃ (5 mol%), DPEPhos (10 mol%), toluene, 100 °C, 6 h. ^aYields of isolated products; ^bthe product 6-(prop-1-en-1-yl)-6*H*-indolo[2,3-*b*]quinoxaline **15d** was formed by isomerization of the allylic double bond (see Scheme 21).



Scheme 21. Synthesis of indolo[2,3-*b*]quinoxalines **15d**.

4.1.3. Synthesis of 5,7-dihydropyrido[3,2-*b*,5,6-*b'*]diindoles

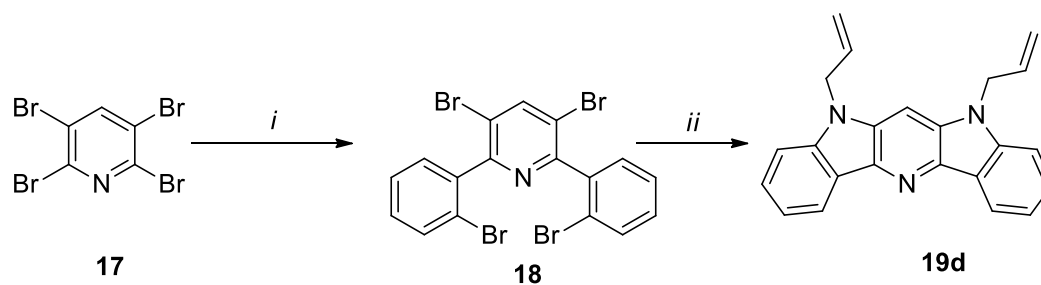
2,3,5,6-Tetrabromopyridine **16** was synthesized according to a literature procedure established by Flowers.⁹⁵



Scheme 22. Synthesis of 2,3,5,6-Tetrabromopyridine **17**

Condition, *i*, Br₂, AcOH, 0 °C. *ii*, HBr 48%, NaNO₂, H₂O, -3 °C → rt.

In the first step (Scheme 23), compound **18** was prepared by Suzuki–Miyaura reaction with 2-bromophenylboronic acid. The amination of **18** with allyl amine was optimized with various ligands, precatalysts and solvents at different reaction temperatures. The best yield of product **18d** (84%) was obtained when DPEPhos was used as the ligand in the presence of Pd₂(dba)₃ (i.e. see Table 20).



Scheme 23. Synthesis of 5,7-dihydropyrido[3,2-*b*,5,6-*b'*]diindoles **19d**.

Conditions, *i*, 2.2 equiv. 2-bromophenylboronic acid, Pd(PPh₃)₄ (5 mol%), 3.0 equiv. NaOH, THF, H₂O, 70 °C, 4 h. *ii*, 3.0 equiv. amine, 6.0 equiv. base, Pd₂(dba)₃ (5 mol%), ligand (10 mol%), solvent, 100 °C, 7 h.

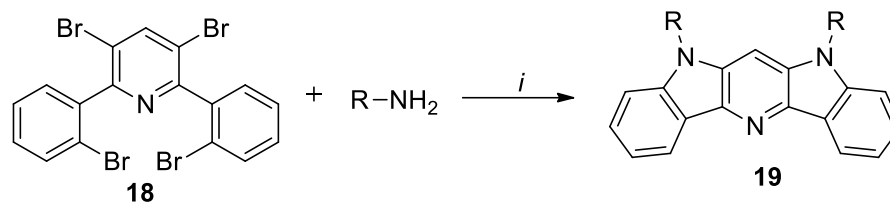
Table 20. Optimization for the Synthesis of **19d**.

Entry	Ligand	Solvent	Base	Temp. (°C)	Yield (%) ^a
1*	BINAP	Toluene	<i>t</i> BuONa	100	11
2*	Xantphos	Toluene	<i>t</i> BuONa	100	17
3*	DPEPhos	Toluene	<i>t</i> BuONa	100	74
4*	Dppe	Toluene	<i>t</i> BuONa	100	58
5*	Dppf	Toluene	<i>t</i> BuONa	100	41
6*	PCy ₃ ·HBF ₄	Toluene	<i>t</i> BuONa	100	-
7*	P <i>t</i> Bu ₃ ·HBF ₄	Toluene	<i>t</i> BuONa	100	6
8*	XPhos	Toluene	<i>t</i> BuONa	100	4
9	RuPhos	Toluene	<i>t</i> BuONa	100	7
10	SPhos	Toluene	<i>t</i> BuONa	100	8
11	DavePhos	Toluene	<i>t</i> BuONa	100	7
12	Dppe	Toluene	Cs ₂ CO ₃	100	37
13	Dppe	1,4-Dioxane	<i>t</i> BuONa	100	28
14	Dppe	THF	<i>t</i> BuONa	100	-
15	Dppe	Toluene	<i>t</i> BuONa	80	42
16	Dppe	Toluene	<i>t</i> BuONa	110	53

* In the co-operation with Dr. Tran Quang Hung (50% of the optimisation reactions was obtained by myself)

Under optimized conditions, the reaction of compounds **18** with aliphatic amines afforded desired 5,7-dihydropyrido[3,2-*b*,5,6-*b'*]diindoles **19a – c** in good to excellent yields (Table 21). Allyl substituted **19d** gave the highest yield (84%). Benzylamines and its derivatives gave good yields, too (products **19e** 60%, **19f** 70%).

Table 21. Synthesis of **19a - f**.



Compound	R	Yield (%) ^a
19a	<i>n</i> -C ₇ H ₁₅	80
19b	<i>n</i> -C ₃ H ₇	86
19c	<i>n</i> -C ₁₂ H ₂₅	71
19d	Allyl	84
19e	Bn	70
19f	4-(MeO)C ₆ H ₄ CH ₂	60

Conditions, *i*, 3.0 equiv. amine, 6.0 equiv. *t*BuONa, Pd₂(dba)₃ (5 mol%), DPEPhos (10 mol%), toluene, 100 °C, 7 h. ^a Yield of isolated products;

4.1.4. Absorption and Fluorescence Properties.

The fluorescence spectra were recorded at the excitation wavelength of 350 nm for compounds **15** and 360 nm for compounds **19** (Figure 20, 21). Absorption maxima and fluorescent data are listed in Table 22. The UV/VIS spectra of selected compounds **19** show strong absorption bands in a range of 290-310 nm and weak absorption bands at about 380 nm. Compounds **15a**, **15c** and **15e** have two strong absorption bands around 270 and 350 nm and a very weak band between 350-400 nm. In each series, there are small differences in the shape and the position of maxima in the absorption- and emission bands due to different substituents. The emission spectra of **19** display a narrow emission band with 3 maxima around 383, 393 and 403 nm. While compounds **15** possess a broad emission band with a band at about 480 nm. The Stokes shifts of compounds **19** are about 1700 cm⁻¹ while ones of compounds **15** are larger, in the range of 7600 cm⁻¹. All measured compounds of **19** give similar quantum yields of about 33%. Derivatives **19** show very low quantum yields (~5%).

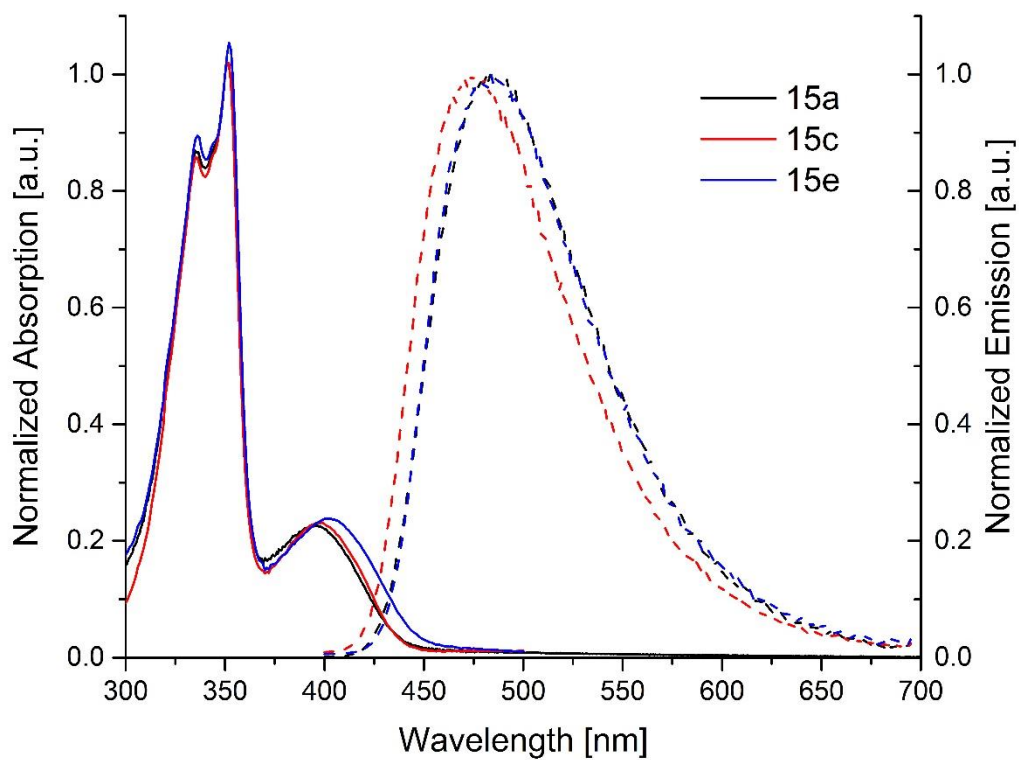


Figure 20. Absorption and emission spectra of selected compounds **15**.

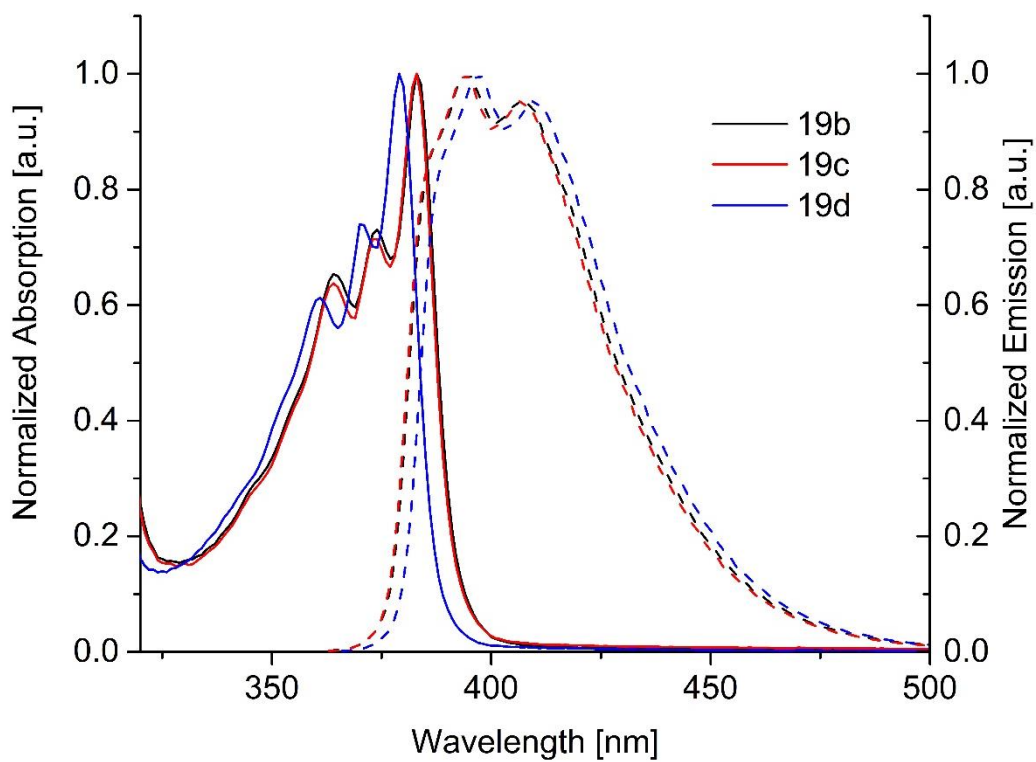


Figure 21. Absorption and emission spectra of selected compounds **19**.

Table 22. Absorption and emission spectroscopic data of **15** and **19**.

Cp	λ_{abs1} (nm)	Log $\epsilon(\lambda_{\text{abs1}})^{\text{a}}$	λ_{abs2} (nm)	Log $\epsilon(\lambda_{\text{abs2}})^{\text{a}}$	λ_{abs3} (nm)	Log $\epsilon(\lambda_{\text{abs3}})^{\text{a}}$	λ_{em} (nm) (shoulders)	$E_{\text{opt}}^{\text{b}}$ (eV)	$\Phi_{\text{fluo}}^{\text{c}}$
15a	336	3.626	352	3.728	394	3.043	475	3.25	5
15c	336	4.834	352	4.939	394	4.240	483	3.28	6
15e	334	4.822	351	4.934	395	4.238	477	3.22	5
19b	364	4.274	375	4.348	382	4.471	406 (392, 381)	3.44	33
19c	364	4.249	375	4.329	382	4.413	406 (392, 382)	3.48	31
19d	362	4.149	371	4.233	380	4.488	404 (393, 380)	3.36	35
19f	360	4.090	370	4.135	381	4.184	404 (392, 381)	3.34	34

^a($\text{l}\cdot\text{mol}^{-1}\cdot\text{cm}^{-1}$); ^b E_{opt} estimated from the absorption edge wavelength⁶²; ^cusing quinine hemisulfate monohydrate in 0.05 M H_2SO_4 ($\Phi = 51\%$)⁵⁹

4.1.5. Electrochemical properties

The corresponding redox peaks in cyclic voltammograms for selected compounds of **15** and **19** were overlapped by the background current and the signal from the solvent. Therefore, the DPV method was employed using DMF as solvent at room temperature and under argon atmosphere for electrochemical investigations. In voltammograms (Figure 23, 24), the oxidation and the reduction processes of compounds **15** and **19** show clear and symmetrical redox peaks. These symmetrical peaks could suggest that the oxidation and the reduction processes are reversible. The reduction and oxidation of compounds **19** occurred at considerably lower potential than that of compounds **15**.

The values for the electronic properties IP (HOMO) and EA (LUMO) of selected compounds **15** and **19** are shown in Table 23. Band gaps E_{EC} of compounds **19** are larger than that of compounds **15**. Comparing HOMO and LUMO values among compounds **19**, substrates **19e** with a benzyl group had the highest HOMO level and the lowest LUMO level resulting in the smallest band gap (3.47 eV). The same trend was observed for **15e** containing a benzyl substituent when comparing among compounds **15**.

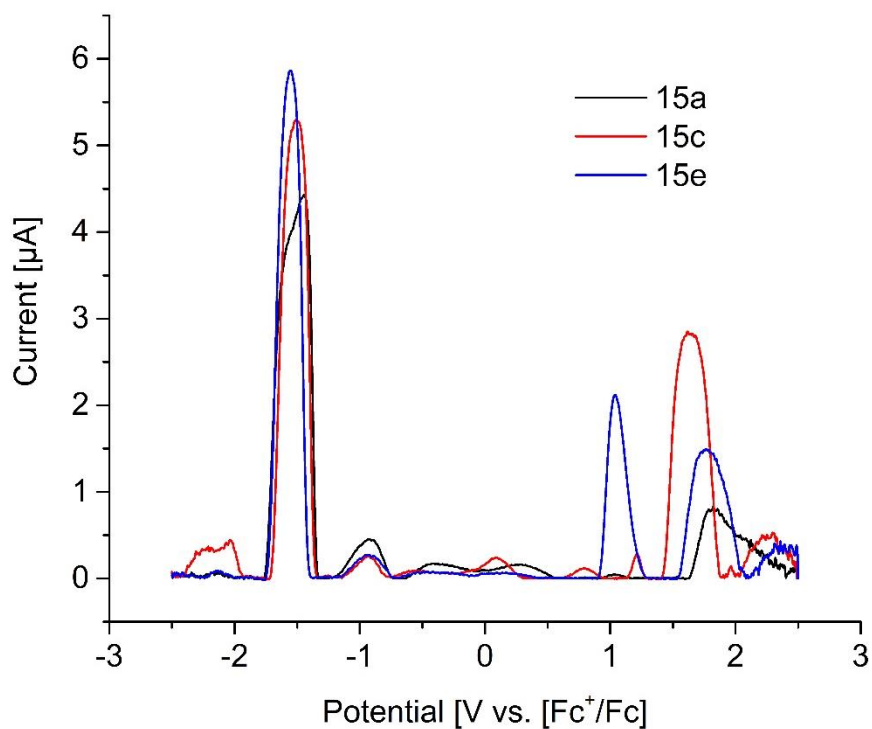


Figure 22. Differential Pulse Voltammetry Plot of **15**.

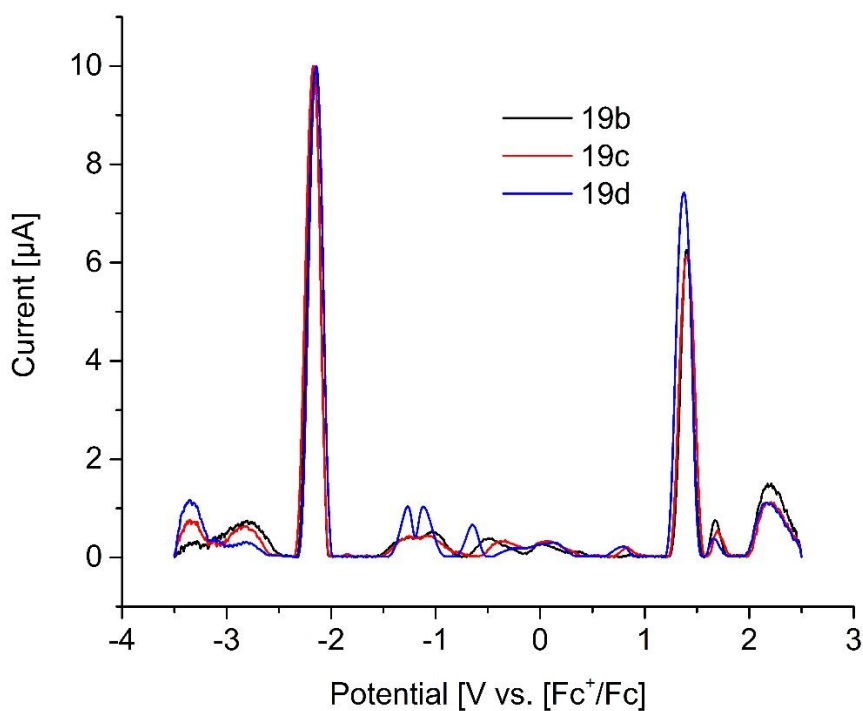


Figure 23. Differential Pulse Voltammetry Plot of **19**.

The optical band gaps are lower than the electrochemical band gaps. The optical bandgap is determined by the excitation of electron from HOMO to LUMO. Meanwhile, the

electrochemical bandgap is determined by the reduction potential and oxidation potential of the substances on the electrode surface in a solvent. Therefore, the effect of solvation and the limitation of the interface between the substances and electrodes can attribute to the redox behaviors.

Table 23. Electrochemical properties of selected compounds of **15** and **18**.

Cp	E^{1-ox} (V vs Fc/Fc ⁺)	E^{2-red} (V vs Fc/Fc ⁺)	IP (eV) ^a	EA (eV) ^a	E_{EC} (eV) ^a
15a	1.819	-1.496	6.22	2.90	3.32
15c	1.813	-1.508	6.21	2.89	3.32
15d	1.787	-1.545	6.19	2.86	3.33
15e	1.874	-1.512	6.27	2.89	3.38
19a	1.263	-2.268	5.64	2.13	3.51
19c	1.265	-2.35	5.67	2.05	3.62
19d	1.312	-2.197	5.71	2.20	3.52
19e	1.457	-2.003	5.87	2.40	3.47
19f	1.312	-2.256	5.71	2.14	3.57

^aCalculations: IP = E^{1-ox} + 4.4 eV (HOMO) ; EA = E^{2-red} + 4.4 eV (LUMO); E_{EC} = IP – EA (electrochemical band gap)^{60,61}

4.1.6. Conclusion

The 2-step procedure: Suzuki-Miyaura cross-coupling reactions, followed by Pd-catalyzed double amination is a useful strategy to synthesize indolo[2,3-*b*]quinoxalines **15** and 5,7-dihydropyrido[3,2-*b*,5,6-*b'*]diindoles **19** in excellent yields. Selected compounds **15** and **19** show fluorescence properties with low quantum yields (about 5% for compounds **15** and about 30% for compound **19**). The substituents have a small effect on the electrochemical and fluorescence properties. Compounds **19** possess larger bandgaps than compounds **15**.

4.2. Palladium-Catalyzed Synthesis and Nucleotide Pyrophosphatase Activity of Benzo[4,5]-furo[3,2-*b*]indoles and Furo[3,2-*b*,4,5-*b'*]diindoles

4.2.1. Introduction

The poly(hetero)aromatic compounds consisting of thiophenes and pyrroles have been well-known motifs for light-emitting applications due to their advancements for conducting properties and stability.⁹⁶ Recently, organic semiconductors containing furan moieties instead of thiophenes became attractive due to their isoelectronic properties.⁹⁷ With the presence of the furan and pyrrole moieties, benzofuroindoles have been mentioned as highly efficient light-emitting components in optical devices⁹⁸ Moreover, 10*H*-benzo[4,5]-furo[3,2-*b*]indole, was reported with remarkable activity in the treatment of sexual steroid hormone receptor mediated diseases.^{99a} 10*H*-benzo[4,5]-furo[3,2-*b*]indole-1-carboxylic acid can control the potassium channel in the human body for the treatment of smooth muscle dysfunctional contraction.^{99b}

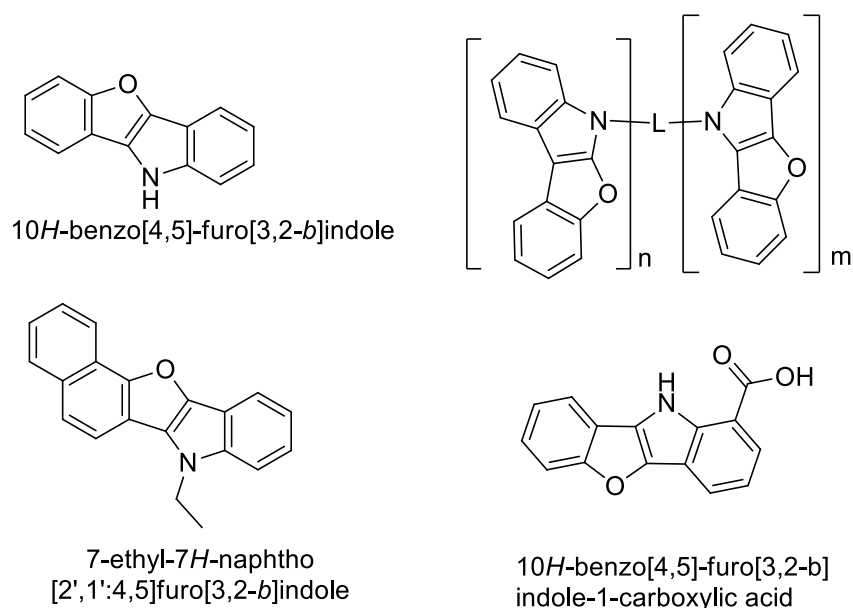


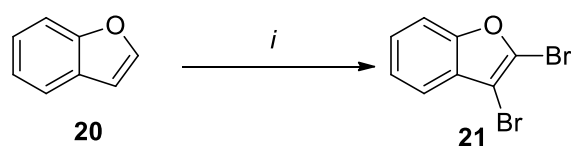
Figure 24. Selected examples of furoindole derivatives

Benzofuro[2,3-*b*]indoles can be prepared via classic Fischer-indole cyclization¹⁰⁰ with phenylhydrazine under acidic conditions. Besides, the Palladium catalyzed cross-coupling with indole derivatives is a noticeable strategy to obtain these compounds.¹⁰¹ Based on previous work related to Pd-catalyzed Suzuki-Miyaura reactions of 2-bromophenylboronic acid with 2,3,5,6-tetrabromopyridine, 2,3-dibromoquinoxaline, tetrabromothiophene,^{80a} and 2,3-dibromo-1-methyl-1*H*-indole in my research group,^{80b} I studied the synthesis of various

benzofuro[2,3-*b*]indolo derivatives by this approach. At the same time, Truong *et al.* have, mentioned the double Buchwald-Hartwig amination resulting the same products *via* iodine-mediated electrophilic cyclization for the starting material synthesis.^{101c} In comparison, I propose a convenient two-step procedure: regioselective Suzuki-Miyaura reaction of 2,3-dibromobenzofuran and subsequent cyclization by double Buchwald-Hartwig reaction. In addition, I applied this strategy, for the first time, to tetrabromofuran as starting material. This interesting and highly symmetrical substrate has only been scarcely used so far in Palladium catalyzed reactions. These reactions lead to furodiindoles – a highly symmetrical heterocyclic core structure which has, to the best of my knowledge, not been reported so far.

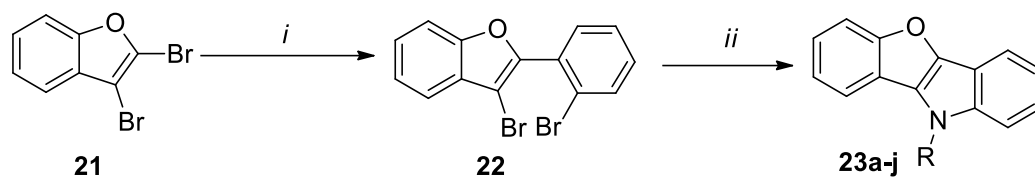
4.2.2. Synthesis of benzo[4,5]-furo[3,2-*b*]indoles

2,3,-dibromobenzofuran (**21**) was synthesized according to a literature procedure.¹⁰² Intermediate **22** (84% yield) was prepared by a Suzuki-Miyaura cross-coupling of **21** and 2-bromophenylboronic acid using Pd(PPh₃)₄ as catalyst.



Scheme 24. Synthesis of 2,3-Dibromobenzofuran **21**

Condition, *i*, Br₂, AcOK, CH₂Cl₂, 4 h, reflux.

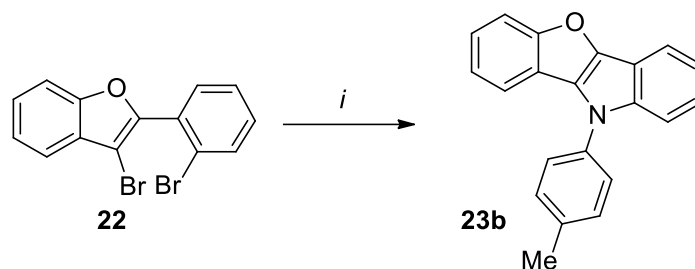


Scheme 25. Synthesis of benzo[4,5]-furo[3,2-*b*]indoles **23a-j**.

Conditions, *i*, 1.1 equiv. 2-bromophenylboronic acid, Pd(PPh₃)₄ (2.5 mol%), 3.0 equiv. K₃PO₄, 1,4-dioxane, H₂O, 100 °C, 8 h.⁸⁰ *ii*, 1.1 equiv. amine, 3.0 equiv. *t*BuONa, Palladium catalyst (5 mol%), ligand, solvent (10 mol%), 110 °C, 12 h.

To develop a more efficient procedure for the synthesis of benzo[4,5]-furo[3,2-*b*]indoles **23**, the conditions of the double CN cross-coupling of **22** were optimized using *p*-toluidine (Scheme 25, Table 24).

Table 24. Optimization for the synthesis of **21b**.



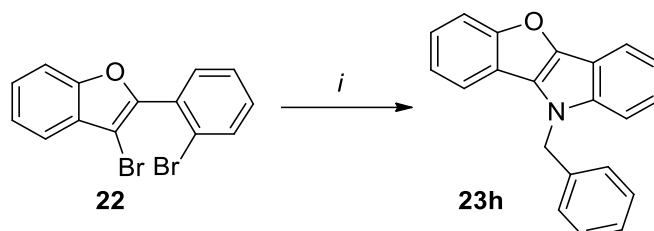
Entry	Pd precursor	Ligand	Solvent	Yield (%) ^a
1	Pd ₂ (dba) ₃	Dppf	Toluene	57
2	Pd ₂ (dba) ₃	Xantphos	Toluene	44
3	Pd ₂ (dba) ₃	Dppe	Toluene	62
4	Pd ₂ (dba) ₃	BINAP	Toluene	75
5	Pd ₂ (dba) ₃	<i>t</i> Bu ₃ ·HBF ₄	Toluene	41
6	Pd ₂ (dba) ₃	XPhos	Toluene	36
7	Pd ₂ (dba) ₃	SPhos	Toluene	54
8	Pd ₂ (dba) ₃	DavePhos	Toluene	35
9	Pd ₂ (dba) ₃	RuPhos	Toluene	45
10	Pd(OAc) ₂	BINAP	Toluene	52
11	Pd ₂ (dba) ₃	BINAP	Dioxane	61
12	Pd ₂ (dba) ₃	BINAP	DMF	14

Condition, *i*, 1.1 equiv. amine, 3.0 equiv. *t*BuONa, Pd₂(dba)₃ (5 mol%), ligand (10 mol%), toluene, 110 °C, 12 h. ^aYield calculated by ¹H-NMR of the crude product using 1,4-dioxane as an internal standard.

According to my observation, monodentate phosphine ligands were not suitable for this reaction while bidentate phosphine ligands gave compound **23b** in better yields. Compound **23b** was

obtained with the highest yield (75%) when BINAP, Pd₂(dba)₃ as the catalyst system in toluene was used for this reaction. The reaction afforded 52% yield with Pd(OAc)₂ as the catalyst precursor.

Table 25. Optimization for the synthesis of **23h**.



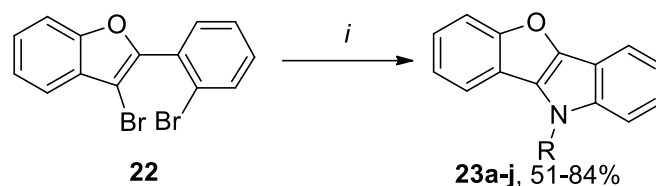
Entry	Ligand	Yield (%) ^a
1	Dppf	23
2	Xantphos	47
3	Dppe	34
4	BINAP	57
5	PtBu ₃ ·HBF ₄	43
6	XPhos	32
7	SPhos	44
8	DavePhos	67
9	RuPhos	52

Condition, *i*, 1.1 equiv. amine, 3.0 equiv. *t*BuONa, Pd₂(dba)₃ (5 mol%), ligand (10 mol%), toluene, 110 °C, 12 h. ^aYield calculated by ¹H-NMR of the crude product using 1,4-dioxane as an internal standard

Using optimized conditions, different anilines were used for the double amination to afford products **23a - g** with good to excellent yields. The substituents of aniline derivatives have no effect on the yield. However, the conditions were not suitable for the double amination using alkyl- or benzyl amines. Therefore, an additional screening of ligands was performed for the reaction with benzylamine (Table 25). The best yield of the product **23h** was 67% in the

presence of Pd₂(dba)₃ and DavePhos. Aliphatic amines like *n*-heptyl and cyclohexylamine gave the final products **23i** - **j** with moderate yields (53 and 57%, respectively) (Table 26).

Table 26. Synthesis of **23a-j**.

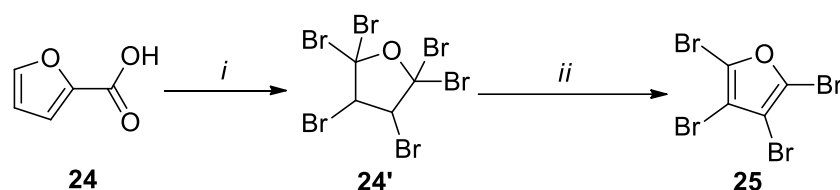


Compound	R	Yield (%) ^a
23a	Ph	63 ^b
23b	4-MeC ₆ H ₄	75 ^b
23c	4-FC ₆ H ₄	79 ^b
23d	3-(CF ₃)C ₆ H ₄	81 ^b
23e	4-(MeO)C ₆ H ₄	65 ^b
23f	3,4-(MeO) ₂ C ₆ H ₃	51 ^b
23g	4- <i>t</i> BuC ₆ H ₄	84 ^b
23h	Bn	67 ^c
23i	<i>n</i> -C ₇ H ₁₅	53 ^c
23j	Cyclohexyl	57 ^c

Condition, i, 1.1 equiv. amine, 3.0 equiv. *t*BuONa, Pd₂(dba)₃ (5 mol%), ligand (10 mol%), toluene, 110 °C, 12 h. ^aYield calculated by ¹H-NMR of the crude product using 1,4-dioxane as an internal standard. ^aIsolated yields; ligand,^bBINAP;^cDavePhos

4.2.3. Synthesis of furo[3,2-*b*,4,5-*b'*]diindole

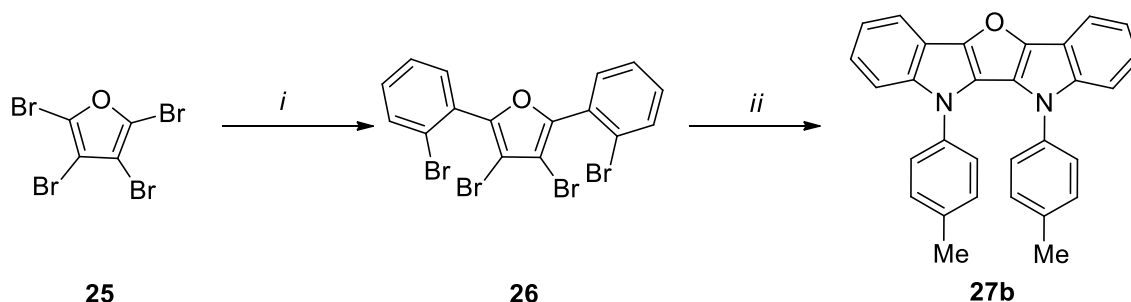
2,3,4,5-Tetrabromofuran **25** was prepared following a literature procedure (Scheme 26).¹⁰³



Scheme 26. Synthesis of 2,3,4,5-Tetrabromofuran **25**.

Condition, *i*, Br₂, KOH, H₂O; *ii*, KOH, MeOH, reflux.

The precursor 3,4-dibromo-2,5-bis(2-bromophenyl)furan **26** (78% isolated yield) was obtained via the Suzuki-Miyaura reaction of tetrabromofuran **25** with 2-bromophenylboronic acid. Various amines were employed to afford the desired furo[3,2-*b*,4,5-*b'*]diindoles **27** by twofold double Buchwald-Hartwig amination (Scheme 27).



Scheme 27. Synthesis of furo[3,2-*b*,4,5-*b'*]diindole **27b**.

Conditions, *i*, 2.2 equiv. 2-bromophenylboronic acid, Pd(PPh₃)₄ (2.5 mol%), 5.0 equiv. K₃PO₄, dioxane (10 ml), H₂O, 90 °C, 8 h. *ii*, 3.0 equiv. amine, 5.0 equiv. *t*BuONa, Palladium catalyst (5 mol%), ligand (10 mol%), solvent, 110 °C, 6 h.

However, previously optimized conditions for compound **23** could not be applied to synthesize compounds **27** due to the occurrence of an inseparable mixture of products. The ligands, Palladium precursor, reaction temperature and solvents were screened in an additional optimization for compound **27b** (Scheme 27, Table 27). The reaction with Pd₂(dba)₃ and dppf gave compound **27b** in the best yield (65%).

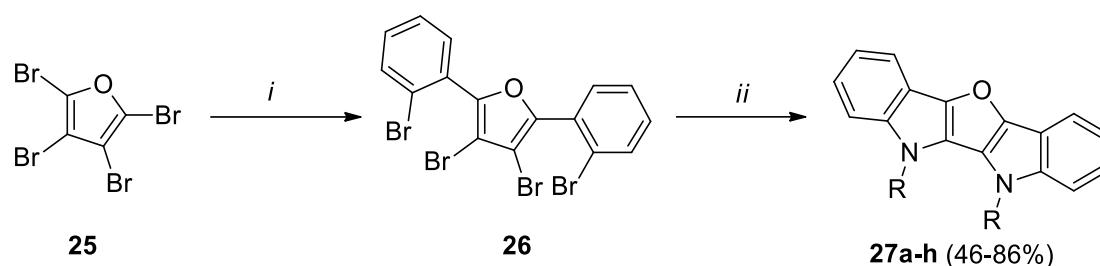
Table 27. Optimization for the synthesis of **27b**.

Entry	Pd precursor	Ligand	Solvent	Yield (%) ^a
1	Pd ₂ (dba) ₃	Dppf	Toluene	65
2	Pd ₂ (dba) ₃	Xantphos	Toluene	44
3	Pd ₂ (dba) ₃	Dppe	Toluene	48
4	Pd ₂ (dba) ₃	BINAP	Toluene	55
5	Pd ₂ (dba) ₃	P <i>t</i> Bu ₃ ·HBF ₄	Toluene	41
6	Pd ₂ (dba) ₃	XPhos	Toluene	29
7	Pd ₂ (dba) ₃	SPhos	Toluene	33
8	Pd ₂ (dba) ₃	DavePhos	Toluene	22
9	Pd ₂ (dba) ₃	RuPhos	Toluene	25
10	Pd(OAc) ₂	Dppf	Toluene	52
11	Pd ₂ (dba) ₃	Dppf	Dioxane	61
12	Pd ₂ (dba) ₃	PCy ₃ ·HBF ₄	DMF	22
13	Pd ₂ (dba) ₃	DPEPhos	DMF	23
14	Pd ₂ (dba) ₃	Dppf	THF	8
15	Pd(OAc) ₂	Dppf	THF	18
16	Pd(OAc) ₂	BINAP	Toluene	38
17	Pd ₂ (dba) ₃	Dppf	DMF	14

^aYield calculated by ¹H-NMR using 1,4-dioxane as an internal standard

The newly developed conditions allowed to extend the scope of reaction with various anilines and aliphatic amines. The products **27** were obtained in moderate to good yields. The product **27f** substituted with 4-*t*BuC₆H₄ was synthesized with the best yield (86%). The amination with benzylamine and *n*-heptylamine gave the product **27h** and **27g** in the yield of 37% and 22%, respectively. Using dppe instead of dppf gave the products **27h** and **27g** in improved yields (53% and 46%). There is no relation between the electron donor or acceptor ability of substituents and the yields of reaction products.

Table 28. Synthesis of **27a-h**.



Compound	R	Yield (%) ^a
27a	Ph	51
27b	4-MeC ₆ H ₄	65
27c	4-FC ₆ H ₄	59
27d	3-(CF ₃)C ₆ H ₄	66
27e	4-(MeO)C ₆ H ₄	53
27f	4- <i>t</i> BuC ₆ H ₄	86
27g	Bn	37 (53) ^b
27h	<i>n</i> -C ₇ H ₁₅	22 (46) ^b

Conditions, *i*, 2.2 equiv. 2-bromophenylboronic acid, Pd(PPh₃)₄ (2.5 mol%), 5 equiv. K₃PO₄, dioxane, H₂O, 90 °C, 8 h. *ii*, 3.0 equiv. amine, 5 equiv. NaOtBu, Pd₂(dba)₃ (5 mol%), dppf (10 mol%), toluene, 110 °C, 6 h. ^a Isolated yields; ^b dppe was used as ligand

X-ray crystal structure analysis was performed to independently prove the structures of **23c** and **27d** (Figures 25, 26). The compound **23c** was crystallized in the monoclinic form in which the molecules are packed into layers. The 4-fluorophenyl substituent is twisted by 49.4° compared to the planar furoindole core structure. The molecules of **27d** are ordered into layers to form monoclinic system (needles form). The two substituents at the Nitrogen atom are not parallel and twisted by 43.6° and 51.0° compared to the planar furodiindole scaffold.

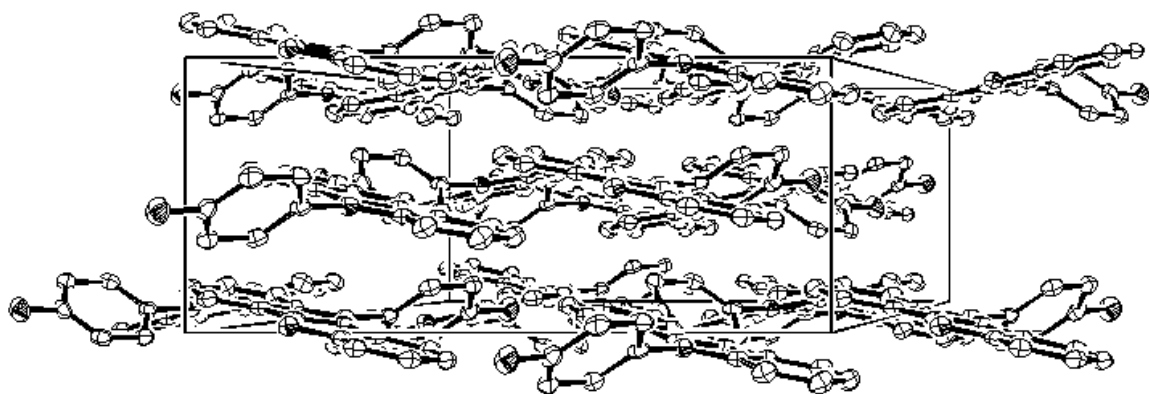
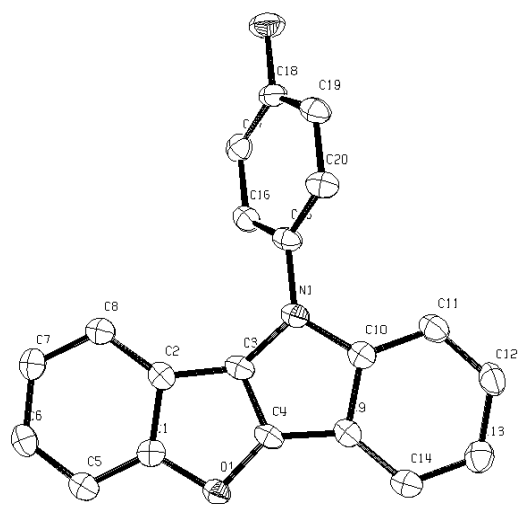


Figure 25. ORTEPs of **23c** (The probability of ellipsoids: 45%).

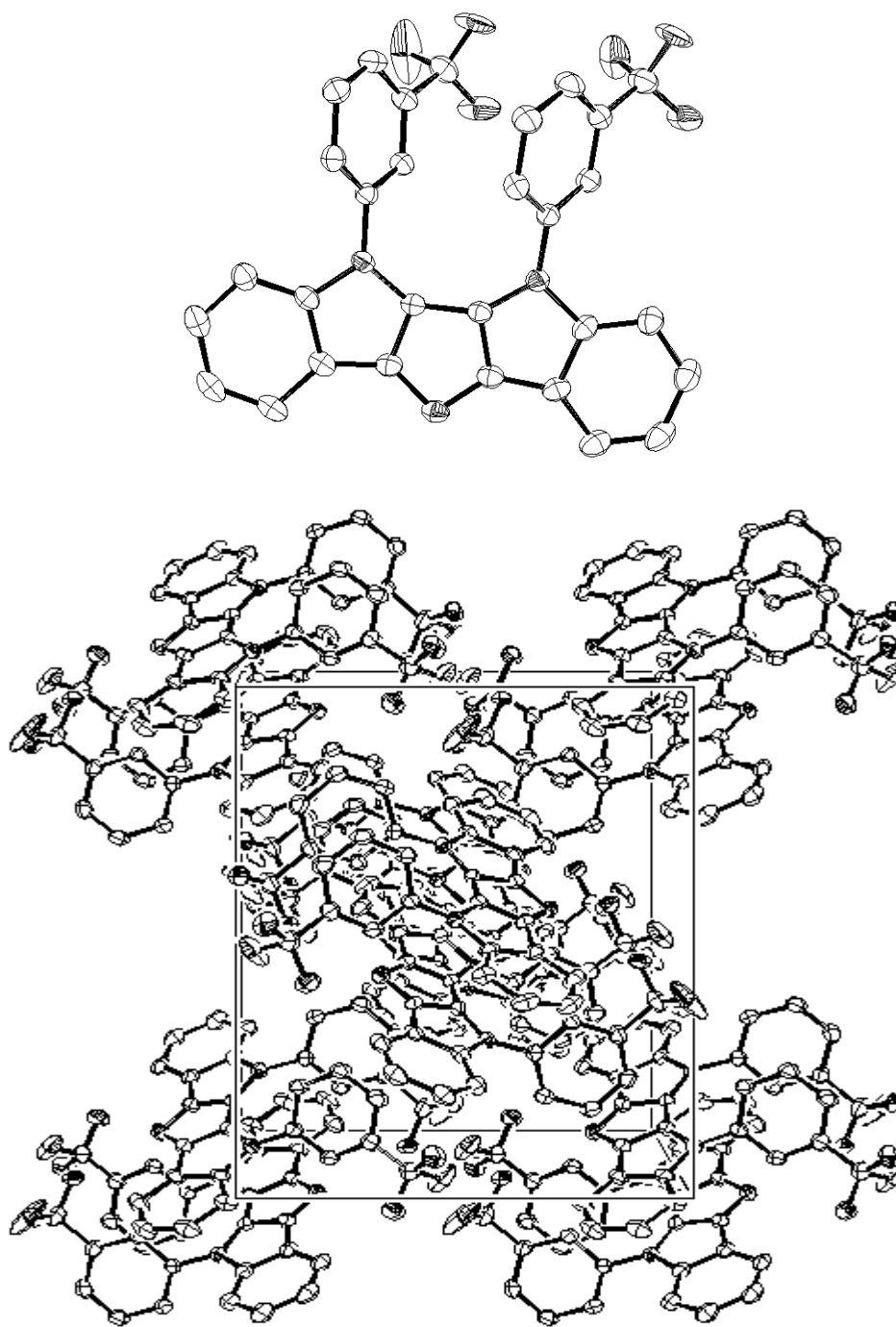


Figure 26. ORTEPs of **27d** (The propability of ellipsoids: 45%).

4.2.4. Absorption and fluorescence properties.

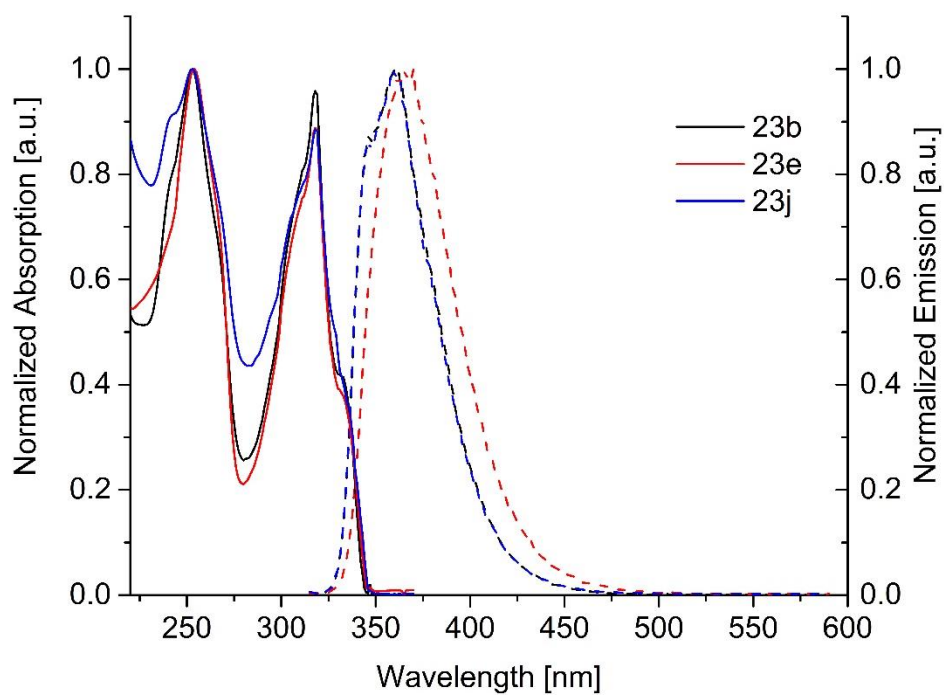


Figure 27. Absorption and emission spectra of selected compounds **23**.

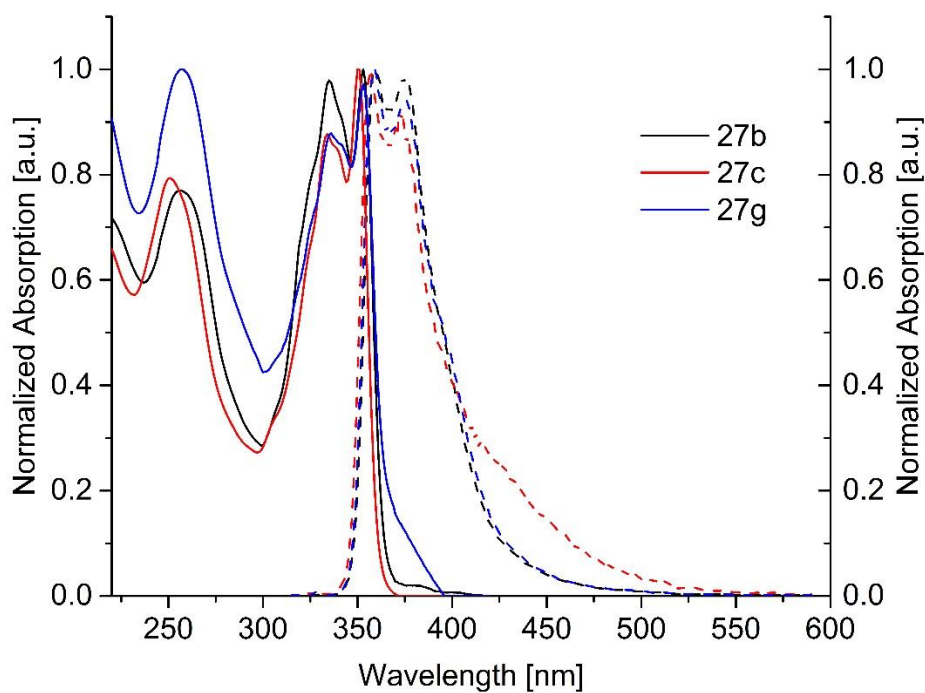


Figure 28. Absorption and emission spectra of selected compounds **27**.

Steady-state UV-VIS absorption and emission spectra of selected compounds **23** and **27** were measured in acetonitrile at 25 °C and are displayed in Figure 27 and 28. The determined absorption-, emission maxima and quantum yields are listed in Table 29.

Table 29. Absorption and emission properties of **23** and **27**.

Cp	λ_{abs1} [nm]	Log $\epsilon(\lambda_{\text{abs1}})^{\text{a}}$	λ_{abs2} [nm]	Log $\epsilon(\lambda_{\text{abs2}})^{\text{a}}$	λ_{abs3} [nm]	Log $\epsilon(\lambda_{\text{abs3}})^{\text{a}}$	λ_{em1} [nm]	λ_{em2} [nm]	$E_{\text{opt}}^{\text{b}}$ [eV]	$\Phi_{\text{fluo}}^{\text{c}}$
23b	253	5,169	318	5,137	-	-	366		3.70	72
23c	253	5,072	318	5,048	-	-	365		3.70	48
23e	254	4,468	318	4,395	-	-	369		3.72	59
23h	252	4,615	318	4,581	-	-	370		3.73	64
23j	252	4,387	318	4,369	-	-	363		3.75	82
27b	256	4,514	335	4,542	353	4,582	359	378	3.41	87
27c	252	4,319	334	4,321	349	4,405	357	377	3.44	57
27e	257	4,551	336	4,572	353	4,602	358	375	3.38	69
27g	256	4,415	338	4,429	355	4,489	361	379	3.39	52

^a($\text{l}\cdot\text{mol}^{-1}\cdot\text{cm}^{-1}$), ^b E_{opt} estimated from the absorption edge wavelength.⁶² ^cusing quinine hemisulfate monohydrate in 0.05 M H_2SO_4 , ($\Phi = 51\%$)⁵⁹

The strong absorption bands at about 250 nm and around 300-370 nm were recorded for all compounds **23** and **27**. For each kind of compounds **23** and compounds **27**, the spectra possess the same shape with small differences in intensity and the position of the absorption maxima. Such small differences indicate that substituents at the Nitrogen atoms have only small impact on the optical properties and the furoindol scaffold is the main chromophore. Compounds **27** gave a moderate red-shift about 20 nm when comparing with compounds **23** due to the extension of the π -system by the second pyrrole ring in compounds **27**. Based on the absorption maxima, the measurements of fluorescence spectra were performed with an excitation wavelength of 300 nm. The emission maxima of compounds **23** were in a range from 363 to 370 nm, while compounds **27** emit at 360 nm with no real difference in shape and position of

the emission maxima (Table 29). The emission spectra of **23** show a single asymmetrical band while these of **27** consist of two emission bands. The Stokes shift values of compounds **23** and **27** were about 3000 cm^{-1} and 500 cm^{-1} , respectively. All measured compounds **23** and **27**, possess remarkably high quantum yields (48-87%). Compound **27b** gave the highest quantum yield (87%). Substituents had a weak effect on the absorption behaviors, but a strong effect on the emission quantum yields is observed. The substances with methyl groups (compounds **23b**, **27b**; quantum yield: 72% and 87%) possess higher quantum yields than these with electron withdrawing fluoro groups (compounds **23c**, **17c**; with quantum yields: 48% and 57%). The presence of oxygen in compounds **23e** and **27e** accompanies with a decrease of the quantum yields to 59 % and 69% compared to compounds **23b**, **27b**, respectively.

4.2.5. Electrochemical studies

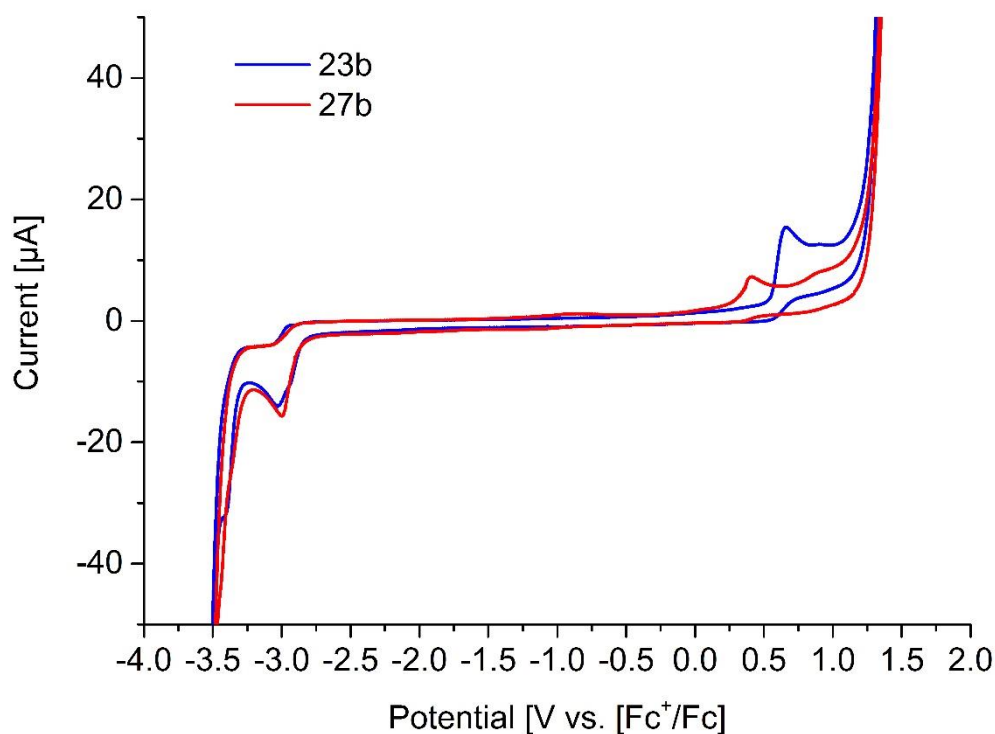


Figure 29. Cyclic Voltammetry plot of **23b** and **27b** in DMF.

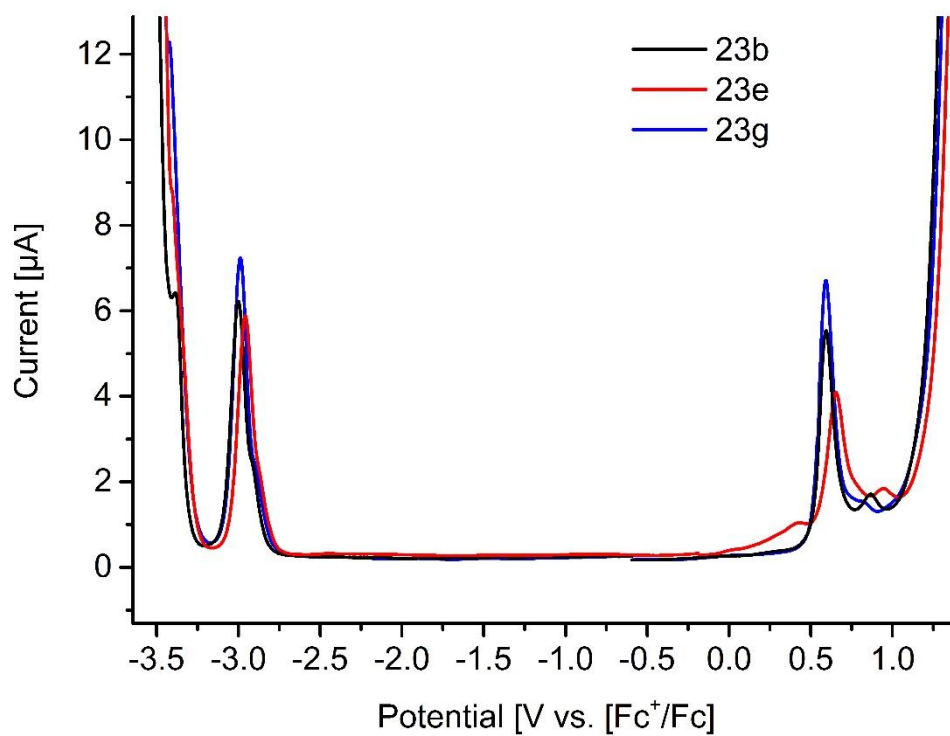


Figure 30. Differential Pulse Voltammetry plot of selected compounds **23**.

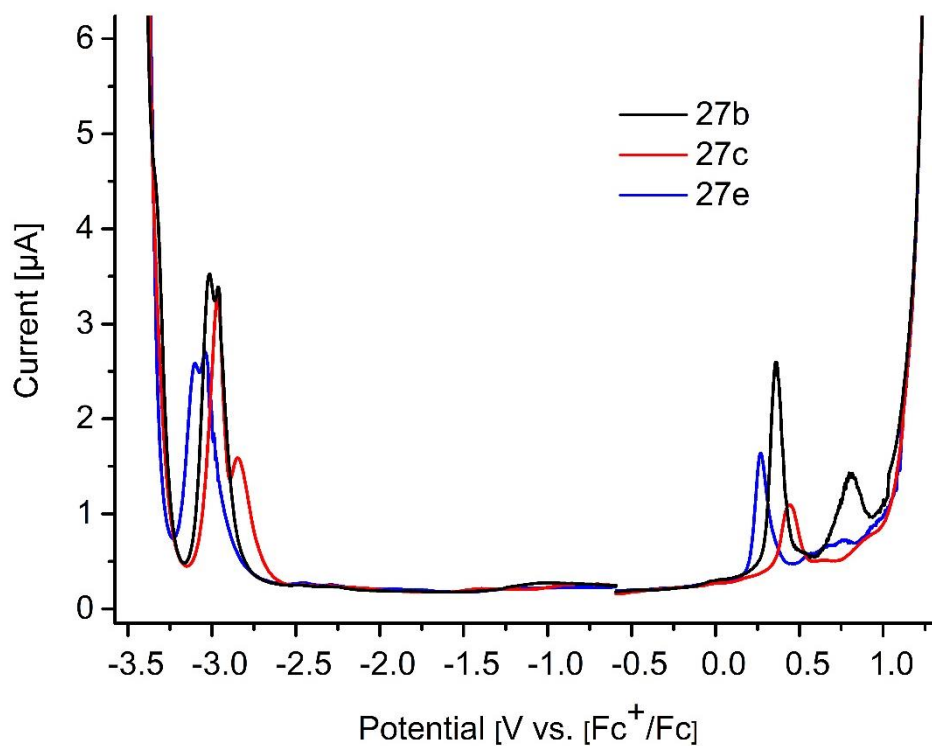


Figure 31. Differential Pulse Voltammetry plot of selected compounds **27**.

23b and **27b** possess non-reversible oxidation and reduction events, shown in the cyclic voltammograms (Figure 29). There is no difference of the reduction events of compounds **23b** and **27d** which is ascribed for the furan moiety. The oxidation event of compound **27b** is by 0.236 V earlier than that of compound **23b** due to the electron donating input of the second indole moiety in compound **27b**. Furthermore, Differential Pulse Voltammetry (DPV) was performed to evaluate the HOMO and LUMO energies, described in Figure 30, 31 and Table 30.

Table 30. Redox data of **23** and **27** in DMF.

Cp	E ^{1-ox} (V vs Fc/Fc ⁺)	E ^{2-red} (V vs Fc/Fc ⁺)	IP (eV) ^a	EA (eV) ^a	E _{EC} (eV) ^a
23b	-2.270	1.327	-5.727	-2.130	3.597
23c	-2.225	1.388	-5.788	-2.175	3.613
23e	-2.255	1.327	-5.727	-2.145	3.582
23h	-2.300	1.282	-5.682	-2.100	3.582
23j	-2.235	1.362	-5.762	-2.165	3.597
27b	-2.230	1.091	-5.491	-2.170	3.321
27c	-2.114	1.176	-5.576	-2.286	3.290
27e	-2.305	1.005	-5.405	-2.095	3.310
27g	-2.270	1.101	-5.501	-2.130	3.371

^aCalculations: IP = E^{1-ox} + 4.4 eV (HOMO) ; EA = E^{2-red} + 4.4 eV (LUMO); E_{EC} = IP – EA (electrochemical band gap)^{60, 61}

An influence of substituents cannot be recognized for compounds **23**. All derivatives possess similar electronic behaviors despite various substituents. Only a small difference can be detected for the oxidation peaks. Therefore, they possess very similar LUMO and HOMO energy levels. The redox events of compounds **27** are more complicated with high dependency on the substituents. However, their electrochemical band gaps are not much different with the

value of 3.6 eV for compounds **23b**, **23c**, **23e**, **23h** and **23j** and 3.3 eV for compounds **27b**, **27c**, **27e** and **27g**. The electrochemical band gaps are slightly lower than the optical band gaps.

4.2.6. Nucleotide Pyrophosphatase Activity.

Derivatives of compounds **23** and **27** were tested for human recombinant NPPs, i.e. NPP1-3. These compounds show significant inhibition of both enzymes of NPP-1 and NPP-3 (Table 31).

Table 31. Biological activity of **23** and **27**.

Compound	NPP-1	NPP-3
	IC ₅₀ (μM)±SEM	IC ₅₀ (μM)±SEM
23a	--	1.38±0.03
23b	2.84±0.06	0.59±0.02
23c	1.29±0.07	3.14±0.09
23d	3.57±0.03	0.49±0.04
23e	--	0.26±0.01
23h	2.62±0.03	0.27±0.06
23i	3.27±0.08	2.55±0.07
23j	6.14±0.09	2.39±0.05
27b	0.11±0.06	0.61±0.09
27c	--	0.13±0.06
27d	--	0.28±0.04
27e	1.38±0.09	0.18±0.01
27g	0.53±0.09	0.21±0.04
27h	--	0.24±0.02

Values ± SEM are expressed as deviation of three experiments (n = 3). The IC₅₀ is the concentration, at which 50% of the enzyme activity is inhibited. *performed by Prof. Iqbal

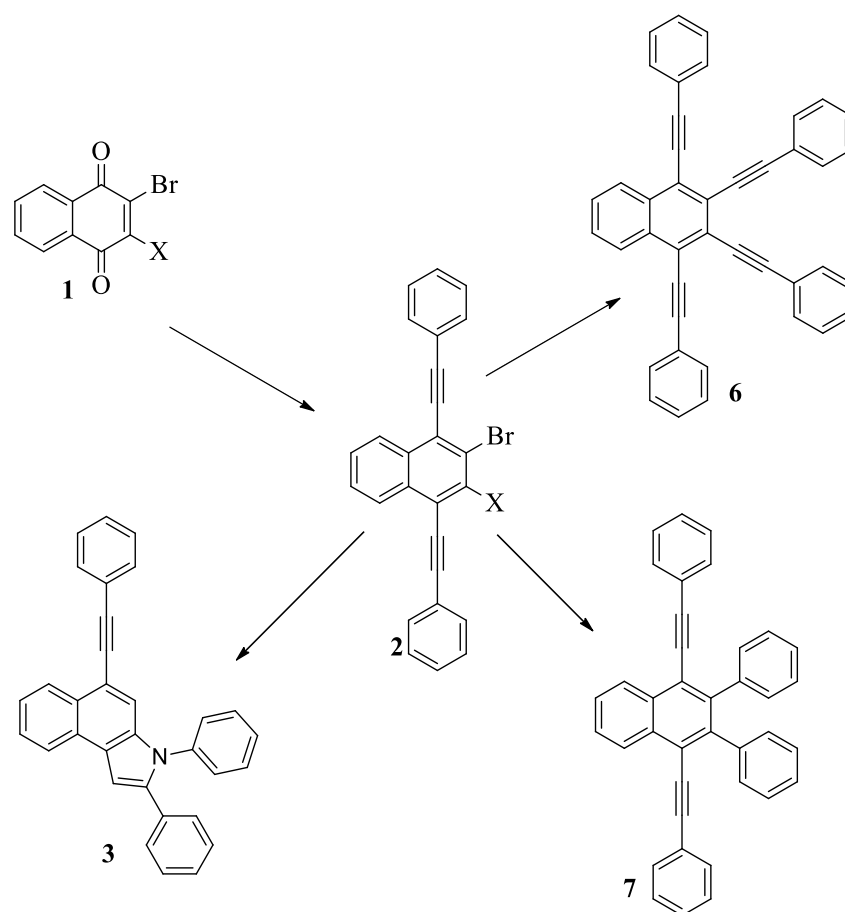
Compound **23a** with phenyl group and **23e** with 4-MeOC₆H₄ group, respectively, show high selectivity against the nucleotide pyrophosphatase enzyme NPP-3. Compound **23c** is more sensitive against NPP1 than NPP3 with an inhibitory value of NPP-1, $IC_{50} \pm SEM = 1.29 \pm 0.07 \mu M$, while compounds **23b**, **23d**, **23h** were more sensitive against NPP3 than NPP1. Aliphatic substituted compounds **23j**, **23i** show no selectivity against both enzymes. Interestingly, compounds **27** could be potential inhibitors against nucleotide pyrophosphatases NPP-3. Compound **27b** is highly active against both NPP-3 and NPP-1 ($IC_{50} \pm SEM = 0.11 \pm 0.06 \mu M$). In contrast, compounds **27e** and **27g** are more active against NPP-3 than NPP-1. Compounds **27c**, **27d** and **27h** are only selective to NPP-3 ($IC_{50} \pm SEM = 0.13 \pm 0.06$, 0.28 ± 0.04 and $0.24 \pm 0.02 \mu M$, respectively). With high inhibitory value of $IC_{50} \pm SEM = 0.13 \pm 0.06 \mu M$, compound **27c** may be considered as the most potential candidate applied for the inhibition of NPP-3. Furo[3,2-*b*,4,5-*b'*]diindoles **27** exhibit an even stronger activity to both enzymes than indole derivatives **23**.

4.2.7. Conclusion.

Benzo[4,5]-furo[3,2-*b*]indoles **23** and furo[3,2-*b*:4,5-*b'*]diindoles **27** were successfully prepared *via* a 2-step procedure using a Suzuki-Miyaura cross-coupling reaction in the first step, followed by Pd-catalyzed double N-arylation. The electrochemical and fluorescence studies demonstrated that both compounds **23** and **27** are promising candidates for optical application with high quantum yields. Compound **27** with two indole moieties have a smaller bandgap (3.3 eV for the electrochemical bandgap and 3.4 eV for the optical bandgap) comparing with compound **23** with one indole moiety (3.6 eV for the electrochemical bandgap and 3.7 eV for the optical bandgap). Effects on the optical and electrochemical properties of obtained compounds induced by the N-substituents are very small but allow to verify the electron affinity and the ionization potential. In addition, compounds **23** and **27** show high inhibition against nucleotide pyrophosphatase NPP-1 and NPP-3. The biological activities of these compounds are dependent on the substituents on the Nitrogen atom.

5. Summary

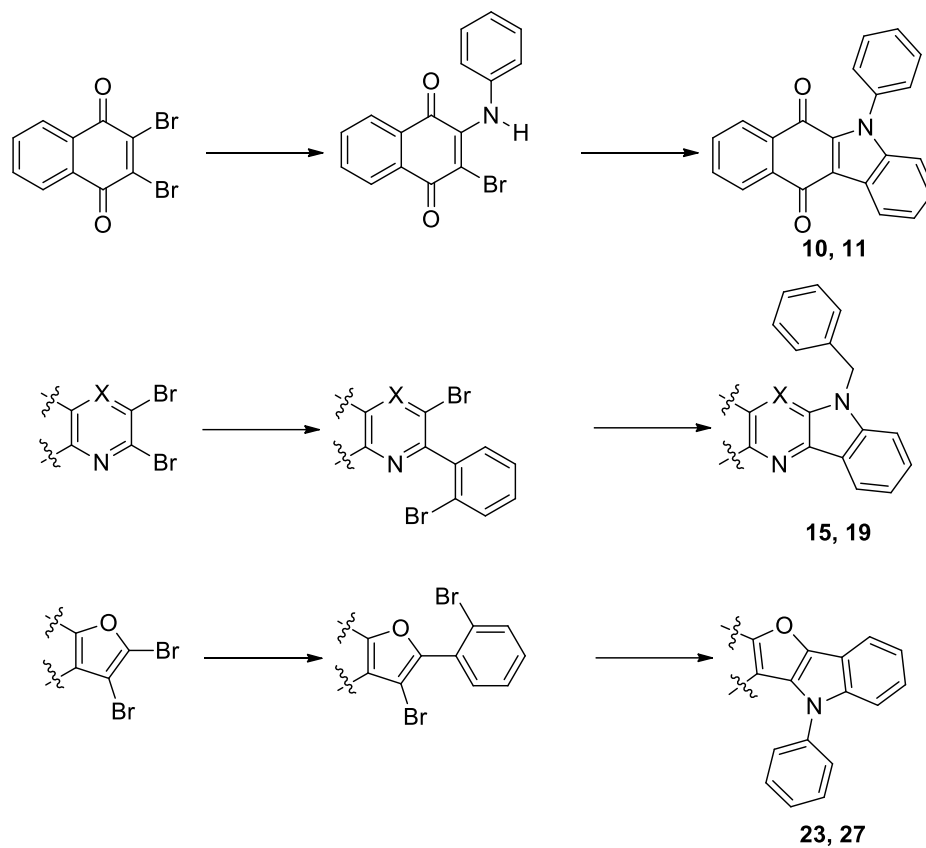
I have prepared highly-conjugated systems from cheap and commercial available precursors. In detail, introducing one or two bromine atoms into positions 2 and 3, corresponding brominated naphthoquinones are attractive building blocks for further structural modification. Thus in this thesis I have shown that various, highly functionalized naphthalene- and quinone derivatives are easily accessible from these simple starting materials by application of Palladium catalyzed cross-coupling reactions.



Scheme 28. The modification of naphthoquinone structure

Moreover, polyhalogenated quinoxalines, furans and pyridines have been used as easily available starting materials for the synthesis of heterocyclic ladder-type tetracene and pentacene analogs, using a two-step procedure consisting of a Suzuki-Miyaura reaction of the halogenated heterocycle with 2-bromophenylboronic acid followed by a double Buchwald-Hartwig reaction. Preliminary optical and electrochemical studies of selected compounds have been

undertaken to get first insights into the structure-property relationship of newly synthesized compounds.



Scheme 29. The combination of Suzuki-Miyaura and Buchwald-Hartwig cross-coupling reactions.

An additional selected compounds, namely benzocarbazolediones and furoindoles have been studied regarding their inhibition activity related to human nucleotide pyrophosphatase and show to some extent high activity and selectivity to these enzymes

6. References

1. a) Fleming, A.; *Br. J. Exp. Pathol.* **1929**, *10*, 226–236; b) Roncali, J.; *Chem. Rev.* **1997**, *97*, 173–205.
2. a) Atanasov, A. G.; Waltenberger, B.; Pferschy-Wenzig, E. M.; Linder, T.; Wawrosch, C.; Uhrin, P.; Temml, V.; Wang, L.; Schwaiger, S.; Heiss, E. H.; Rollinger, J. M.; Schuster, D.; Breuss, J. M.; Bochkov, V.; Mihovilovic, M. D.; Kopp, B.; Bauer, R.; Dirsch, V. M.; Stuppner, H. *Biotechnol Adv.* **2015**, *33*, 1582–614; b) Sneader, W. “*Drug Discovery, A History*” **2005**, John Wiley & Sons; c) Paul, S. M.; Mytelka, D. S.; Dunwiddie, C. T.; Persinger, C. C.; Munos, B. H.; Lindborg, S. R.; Schacht, A. L. *Nat. Rev. Drug Discov.* **2010**, *9*, 203–214.
3. a) Stefano, G. B.; Ptáček, R.; Kuželová, H.; Kream, R. M.; *Folia Biol. (Praha)*. **2012**, *58*, 49–56; b) Jonsson, T.; Christensen, C. B.; Jordening, H.; Frølund, C. *Pharmacol. Toxicol.* **1988**, *62*, 203–205
4. a) Rook, E. J.; van-Ree, J. M.; van-den-Brink, W.; Hillebrand, M. J.; Huitema, A. D.; Hendriks, V. M.; Beijnen, J. H. *Basic Clin. Pharmacol. Toxicol.* **2006**, *98*, 86–96; b) Prommer, E. *J. Opioid Manag.* **2011**, *7*, 401–406.
5. Bentley, K. W.; Hardy, D. G. *J. Am. Chem. Soc.* **1967**, *89*, 3281–3292.
6. a) Jordan, R. H.; Dodabalapur, A.; Strukelj, M.; Miller, T.M. *Appl. Phys. Lett.* **1996**, *68*, 1192–1194; b) Facchetti, A.; *Chem. Mater.* **2010**, *23*, 733–758; c) Yang, J.; Nguyen, T.-Q. *Org. Electron.* **2007**, *8*, 566–574.
7. a) Dimitrakopoulos, C. D.; Malenfant, P. R. L. *Adv. Mater.* **2002**, *14*, 99–118. b) Chen, K.-Y.; Hsieh, H. H.; Wu, C. C.; Hwang, J. J.; Chow, T. J. *Chem. Commun.* **2007**, 1065–1067.
8. a) Chenguang, W.; Zuolun, Z.; Yue, W. *J. Mater. Chem. C.* **2016**, *4*, 9918–9936; b) Kwon, J.-H.; Kang, I. M.; Bae, J. H. *Eur. Phys. J. Appl. Phys.* **2014**, *65*, 30202–30208; c) Salzmann, I.; Duhm, S.; Heimel, G.; Rabe, J. P.; Koch, N.; Oehzelt, M.; Sakamoto, Y.; Suzuki, T. *Langmuir.* **2008**, *24*: 7294–7298.
9. a) Kalman, B.; Clarke, N.; Johansson, L. B. A. *J. Phys. Chem.* **1989**, *93*, 4608–4615; b) Hasegawa, T.; Takeya, J. *Sci. Technol. Adv. Mater.* **2009**, *10*, 024314–024330, c) Yang, C.-H.; Tai, C.-C.; Sun, I-W. *J. Mater. Chem.* **2004**, *14* , 947–950.
10. Seechurn, C. C. C. J.; Kitching, M. O.; Colacot, T. J.; Snieckus, V. *Angew. Chem. Int. Ed.* **2012**, *51*, 5062–5085.
11. Adams, C. *Top. Catal.* **2009**, *52*, 924–934.

12. Martin, T.; Moody, C. J. *J. Chem. Soc. Perkin Trans.* **1988**, *1*, 241-246.
13. Knoelker, H.-J.; Reddy, K. R. *Heterocycles*, **2003**, *60*, 1049-1052.
14. Maruyama, K.; Katagiri, T. *J. Phys. Org. Chem.* **1989**, *2*, 205-213.
15. a) Normant, J. F. *Synthesis*. **1972**, 63-80; b) Wu, G.; Huang, M. *Chem. Rev.* **2006**, *106*, 2596-2616.; c) Alt, H. G.; Koppl, A. *Chem. Rev.* **2000**, *100*, 1205-1222; d) Hsieh, J.-C.; Cheng, C.-H. *Chem. Comm.* **2005**, 2459-2461.
16. a) Zhang, L.; Sun, J.; Kozmin, S. A. *Adv. Synth. Catal.* **2006**, *348*, 2271-2296; b) Ito, Y.; Sawamura, M.; Hayashi, T. *J. Am. Chem. Soc.* **1986**, *108*, 6405-6406; c) Samojłowicz, C.; Bieniek, M.; Grela, K. *Chem. Rev.* **2009**, *109*, 3708-3742. d) Fürstner, A.; Leitner, A.; Méndez, M.; Krause, H. *J. Am. Chem. Soc.* **2002**, *124*, 13856-13863.
17. Negishi, E.-I. „*Handbook of Organopalladium Chemistry for Organic Synthesis*“ **2002**, John Wiley
18. a) Hussain, M.; Khera, R. A.; Nguyen, T. H.; Langer, P. *Org. Biomol. Chem.* **2011**, *9*, 370-373; b) Reimann, S.; Ehlers, P.; Ohlendorf, L.; Langer, P. *Org. Biomol. Chem.* **2017**, *15*, 1510 - 1520; c) Tran, Q. H.; Dang, T. T.; Villinger, A.; Tran, V. S.; Langer, P. *Org. Biomol. Chem.* **2012**, *10*, 9041 - 9044.
19. Fortman, G. C.; Nolan, S. T. *Chem. Soc. Rev.* **2011**, *40*, 5151-5169.
20. a) Dehli, J. R.; Legros, J.; Bolm, C. *Chem. Commun.* **2005**, 973-986; b) Frlan, R.; Kikelj, D. *Synthesis* **2006**, 2271-2285; c) Schlummer, B.; Scholz, U. *Adv. Synth. Catal.* **2004**, *346*, 1599-1626; d) Fernandez-Rodriguez, M. A.; Shen, Q.; Hartwig, J. F.; *J. Chem. Soc.* **2006**, *128*, 2180-2181;
21. a) Negishi, E.-i. *J. Organomet. Chem.* **2002**, *653*, 34-40; b) Nicolaou, K. C.; Bulger, P. G.; Sarlah, D. *Angew. Chem. Int. Ed.* **2005**, *44*, 4442-4489; c) Stanforth, S. P. *Tetrahedron* **1998**, *54*, 263-303.
22. a) Wu, X.-F.; Neumann, H.; Beller, M. *Chem. Rev.* **2013**, *113*, 1-35. b) Knowles, J. P.; Whiting, A. *Org. Biomol. Chem.* **2007**, *5*, 31- 44.
23. Carey, F. A.; Sundberg, R. J. “*Advanced Organic Chemistry*” **2007**, Springer.
24. a) San, F.-S. *Chem. Soc. Rev.* **2013**, *42*, 5270-5298; b) Miyaura, N.; Yamada, K.; Suzuki, A. *Tetrahedron Lett.* **1979**, *20*, 3437-3440.
25. (a) Noel, T.; Buchwald, S. L. *Chem. Soc. Rev.* **2011**, *40*, 5010-5029; (b) Batail, N.; Genelot, M.; Dufaud, V.; Joucla, L.; Djakovitch, L. *Catal. Today* **2011**, *173*, 2-14; (c) Magano, J.; Dunetz, J. R. *Chem. Rev.* **2011**, *111*, 2177-2250.

26. a) De Koning, P. D.; McAndrew, D.; Moore, R.; Moses, I. B.; Boyles, D. C.; Kissick, K.; Stanchina, C. L.; Cuthbertson, T.; Kamatani, A.; Rahman, L.; Rodriguez, R.; Urbina, A.; Sandoval, A.; Rose, P. R. *Org. Process Res. Dev.* **2011**, *15*, 1018-1026; b) Ishikura, M.; Imaizumi, K.; Katagiri, N. *Heterocycles* **2000**, *53*, 553-556; c) Xu, G.; Fu, W.; Liu, G.; Senanayake, C. H.; Tang, W. *J. Am. Chem. Soc.* **2014**, *136*, 570-573; d) Lan, P.; Banwell, M. G.; Ward, J. S.; Willis, A. C. *Org. Lett.* **2014**, *16*, 228-231; e) Nicolaou, K. C.; Bheema Rao, P.; Hao, J.; Reddy, M. V.; Rassias, G.; Huang, X.; Chen, D. Y.; Snyder, S. A. *Angew. Chem. Int. Ed.* **2003**, *42*, 1753-1758; f) Torrado, A.; Iglesias, B.; López, S.; de Lera, A. R. *Tetrahedron* **1995**, *51*, 2435-2454; g) Dalby, A.; Mo, X.; Stoa, R.; Wroblewski, N.; Zhang, Z.; Hagen, T. J. *Tetrahedron Lett.* **2003**, *54*, 2737-2739.
27. Rouhi, A. M. *Chem. Eng. News*, **2004**, *82*, 49-58.
28. a) Suzuki, A. *J. Org. Chem.* **1999**, *576*, 147-168; b) Matos, K.; Soderquist, J. A.; *J. Org. Chem.* **1998**, *63*, 461-470; c) Lennox, A. J. J.; Lloyd-Jones, G. C. *Chem. Soc. Rev.* **2014**, *43*, 412-443.
29. Lima, C. F. R. A. C.; Rodrigues, A. S. M. C.; Silva, V. L. M.; Silva, A. M. S.; Santos, L. M. N. B. F. *Chem. Cat. Chem.* **2014**, *6*, 1291-1302.
30. Röhlich, C.; Wirth, A. S.; Köhler, K. *Chem. Eur. J.* **2012**, *18*, 15485-15494,
31. a) Sonogashira, K. *J. Organomet. Chem.* **2002**, *653*, 46-49; b) Sonogashira, K.; Tohda, Y.; Hagihara, N. *Tetrahedron Lett.* **1975**, *16*, 4467-4470.
32. a) Mujahidin, D.; Doye, S. *Eur. J. Org. Chem.* **2005**, 2689-2693; b) Bleicher, L.S.; Cosford, N.D.P.; Herbaut, A.; McCallum, J. S.; McDonald, I. A. *J. Org. Chem.* **1998**, *63*, 1109-1118.
33. Hong, B.-C.; Nimje, R. Y. *Curr. Org. Chem.* **2006**, *10*, 2191-2225.
34. a) Chinchilla, R.; Nájera, C. *Chem. Soc. Rev.* **2011**, *40*, 5084-5121; b) King, A. O.; Yasuda, N. *Top. Organomet. Chem.* **2005**, *9*, 646-650;
35. Yang, L.; Zhao, L.; Li, C.-J. *Chem. Commun.* **2010**, *46*, 4184-4186.
36. a) Driver, M.S.; Hartwig, J. F. *J. Am. Chem. Soc.* **1995**, *117*, 4708-4709; b) Widenhoefer, R. A.; Buchwald, S. L. *Organometallics* **1996**, *15*, 2755-2763.
37. a) Allen, C. F. H.; McKee, G. H. W. *Org. Synth. Coll.* **1943**, *2*, 15-18; b) Mannich, C.; Krösche, W. *Arch. Pharm. (Weinheim)* **1912**, *250*, 647-667. c) Sato, S.; Sakamoto, T.; Miyazawa, E.; Kikugawa, Y. *Tetrahedron.* **2004**, *60*, 7899-906.

38. a) Wolfe, J. P.; Wagaw, S.; Marcoux, J.-F.; Buchwald, S. L. *Acc. Chem. Res.* **1998**, *31*, 805–818; b) Surry, A. S.; Buchwald, S. L. *Chem. Sci.* **2011**, *2*, 27-50.
39. Hartwig, J.F. *Pure Appl. Chem*, **1999**, *71*, 1416–1423.
40. a) Deadman, B. J.; Hopkin, M. D.; Baxendale, L. R.; Ley, S. V. *Org. Biomol. Chem.* **2013**, *11*, 1766-1800; b) Mari, M.; Bartoccini, F.; Piersanti, G. *J. Org. Chem.* **2013**, *78*, 7727-7734.
41. a) Murahashi, S. *J. Am. Chem. Soc.* **1955**, *77*, 6403–6404; b) Fujawara, Y.; Moritani, I.; Danno, S. Asano, R.; Teranishi, S. *J. Am. Chem. Soc.* **1969**, *91*, 7166-7169
42. a) Rossi, R.; Bellina, F.; Lessi, M.; Manzini, C. *Adv. Synth. Catal.* **2014**, *356*, 17- 117; b) Mei, T. S.; Kou, L.; Ma, S.; Engle, K. M.; Yu, J. Q. *Synthesis* **2012**, *44*, 1778-1791.
43. a) Chen, X.; Engle, K. M.; Wang, D.-H.; Yu, J.-Q. *Angew. Chem. int. Ed.* **2009**, *48*, 5094-5115; b) Ackermann, L. *Chem. Rev.* **2011**, *111*, 1315-1345; c) Kuhl, N.; Hopkinson, M. N.; Wencel-Delord, J.; Glorius, F. *Angew. Chem. Int. Ed.* **2012**, *51*, 10236–10254; d) Neufeldt, S. R.; Sanford, M. S. *Acc. Chem. Res.* **2012**, *45*, 936– 946.
44. a) Schmidt, A. W.; Reddy, K. R.; Knolker, H. J. *Chem. Rev.* **2012**, *112*, 3193-3328; b) O'Malley, S. J.; Tan, K. L.; Watzke, A.; Bergman, R. G.; Ellman, J. A. *J. Am. Chem. Soc.* **2005**, *127*, 13496–13497; c) Butler, J. R.; Wang, C.; Bian, J.; Ready, J. M. *J. Am. Chem. Soc.* **2011**, *133*, 9956- 9959; d) Gutekunst, W. R.; Baran, P. S. *J. Am. Chem. Soc.* **2011**, *133*, 19076-19079.
45. a) Gong, M.-S.; Lee, H.-S.; Jeon, Y.-M. *J. Mater. Chem.* **2010**, *20*, 10735; b) Liu, D.; Du, M.; Chen, D.; Ye, K.; Zhang, Z.; Liu, Y.; Wang, Y. *J. Mater. Chem. C*, **2015**, *3*, 4394-4401; c) Jiang, W.; Li, Y.; Wang, Z. *Chem. Soc. Rev.* **2013**, *42*, 6113-6127.
46. Bridges, J. W.; Williams, R. T. *Biochem. J.* **1968**, *107*, 225-237.
47. Chen, Y.; Zhu, Y.; Yang, D.; Luo, Q.; Yang, L.; Huang, Y.; Zhao, S.; Lu, Z.; *Chem. Commun.* **2015**, *51*, 6133-6136.
48. a) Dalton, L. R.; Sullivan, P. A.; Bale, D. H. *Chem. Rev.* **2010**, *110*, 25-55; b) Xiao, J.; Duong, H. M.; Liu, Y.; Shi, W.; Ji, L.; Li, G.; Li, S.; Liu, X.-W.; Ma, J.; Wudl, F.; Zhang, Q.; *Angew. Chem. Int. Ed.* **2012**, *51*, 6094-6098; c) Chen, Y.; Zhu, Y.; Yang, D.; Luo, Q.; Yang, L.; Huang, Y.; Zhao, S.; Lu, Z.; *Chem. Commun.* **2015**, *51*, 6133.
49. a) Jia, G.; Lown, W. J. *Bioorg. Med. Chem.* **2000**, *8*, 1607-1617; b) Yang, S.; Denny, W. A. *J. Org. Chem.* **2002**, *67*, 8958-8961; c) Ham, Y.-W.; Boger, D. L. *J. Am. Chem. Soc.* **2004**, *126*, 9194-9195.
50. Jones, G. B.; Mathews, J. E. *Tetrahedron* **1997**, *53*, 14599-14614.
51. Sjögren, M.; Johnson, A.-L.; Hedner, E.; Dahlstöm, M.; Göransson, U.; Shirani, H.; Bergman, J.; Jonsson, P. R.; Bohlin, L. *Peptides* **2006**, *27*, 2058-2064.

52. a) Gassman, P. G.; Schenk, W. N. *J. Org. Chem.* **1977**, *42*, 3240-3243; b) Pennington, F. C.; Jellinex, M.; Thurn, R. D. *J. Org. Chem.* **1958**, *24*, 565; c) Bartoli, G.; Bosco, G. P. M.; Dalpozzo, R. *Tetrahedron Lett.* **1989**, *30*, 2129-2132; d) Im, G.-Y. J.; Bronner, S. M.; Goetz, A. E.; Paton, R. S.; Cheong, P. H.-Y.; Houk, K. N.; Garg, N. K. *J. Am. Chem. Soc.* **2010**, *132*, 17933-17944; e) Hulcoop, D. G.; Lautens, M. *Org. Lett.* **2007**, *9*, 1761-1764; f) Rawal, V. H.; Jones, R. J.; Cava, M. P. *Tetrahedron Lett.* **1985**, *26*, 2423-2426; g) Sakamoto, T.; Kondo, Y.; Yamanaka, H.; *Heterocycles* **1986**, *24*, 1845;-1847 h) Ferretti, F.; El-Atawy, M. A.; Muto, S.; Hagar, M.; Gallo, E.; Ragaini, F. *Eur. J. Org. Chem.* **2015**, 5712-5715.
53. Meng, Q.; Gao, J.; Li, R.; Jiang, L.; Wang, C.; Zhao, H.; Liu, C.; Li, H.; Hu, W. *J. Mater. Chem.* **2009**, *19*, 1477-1482.
54. Anthony, J. E. *Chem. Rev.* **2006**, *106*, 5028-5048.
55. a) Zhao, N.; Xuan, S.; Fronczek, F. R.; Smith, K. M.; Vicente, M. G. H. *J. Org. Chem.* **2015**, *80*, 8377-8383; b) Guan, M.; Chen, C.; Zhang, J.; Zeng, R.; Zhao, Y. *Chem. Commun.* **2015**, *51*, 12103-12106; c) Danilkina, N. A.; Kulyashova, A. E.; Khlebnikov, A. F.; Brase, S.; Balova, I. A.; *J. Org. Chem.* **2014**, *79*, 9018-9045.
56. Brachet, E.; Belmont, P.; *J. Org. Chem.* **2015**, *80*, 7519-7529.
57. Ehlers, P.; Neubauer, A.; Lochbrunner, S.; Villinger, A.; Langer, P. *Org. Lett.* **2011**, *12*, 1618-1621.
58. Lehnerr, D.; McDonald, R.; Tykwinski, R. R. *Org. Lett.*, **2008**, *10*, 4163-4166.
59. Brouwe, M. A. *Pure Appl. Chem.* **2011**, *83*, 2213-2228.
60. Zhu, Y.; Champion, R. D.; Jenekhe, S. A. *Macromolecules*, **2006**, *39*, 8712-8719.
61. Trasatti, S. *Pure Appl. Chem.* **1986**, *58*, 955-966.
62. Köhler, A.; Bässler, H. *"Electronic Processes in Organic Semiconductors: An Introduction"*, **2015**, Wiley-VCH, 129-131
63. a) Wang, T.; Hoyer, T. R. *J. Am. Chem. Soc.* **2016**, *138*, 13870-13873; b) Shimizu, S.; Murayama, A.; Haruyama, T.; Iino, T.; Mori, S.; Furuta, H.; Kobayashi, N. *Chem. Eur. J.* **2015**, *21*, 12996-13003; c) Kapur, A.; Kumar, K.; Singh, L.; Singh, P.; Elango, M.; Subramanian, V.; Gupta, V.; Kanwal, P.; Ishar, M. P. S. *Tetrahedron* **2009**, *65*, 4593-4603.
64. a) Lee, H. W.; Kim, H. J.; Kim, Y. S.; Kim, J.; Lee, S. E.; Lee, H. W.; Kim, Y. K.; *J. Lumin.* **2015**, *165*, 99-104; b) Yoon, J.-A.; Kim, Y.-H.; Kim, N. H.; Lee, S. Y.; Zhu, F. R.; Kim, W. Y. *Nanoscale Res. Lett.* **2014**, *9*, 191-198; c) Wang, C.; Dong, H.; Hu, W.; Liu, Y.; Zhu, D. *Chem. Rev.* **2012**, *112*, 2208-2267.
65. a) Zhang, J.; Smith, Z. C.; Thomas III, S. W. *J. Org. Chem.* **2014**, *79*, 10081-10093; b) Narita, T.; Takase, M.; Nishinaga, T.; Iyoda, M.; Kamada, K.; Ohta, K. *Chem. Eur. J.* **2010**, *16*,

12108-12113; c) Kivala, M.; Stanoeva, T.; Michinobu, T.; Frank, B.; Gescheidt, G.; Diederich, F. *Chem. Eur. J.* **2008**, *14*, 7638-7647; d) Piao, M. J.; Chajara, K.; Yoon, S. J.; Kim, H. M.; Jeon, S.-J.; Kim, T.-H.; Song, K.; Asselberghs, I.; Persoons, A.; Clays, K.; Cho, B. R. *J. Mater. Chem.* **2006**, *16*, 2273-2281.

66. a) Rodríguez, J. G.; Tejedor, J. L. *J. Org. Chem.* **2002**, *67*, 7631-7640; b) Morozov, O. S.; Asachenko, A. F.; Antonov, D. V.; Kochurov, V. S.; Paraschuk, D. Y.; Nechaev, M. S. *Adv. Synth. Catal.* **2014**, *356*, 2671-2678; c) Shinohara, K.; Nishida, T.; Wada, R.; Peng, L.; Minoda, Y.; Orita, A.; Otera, J. *Tetrahedron* **2016**, *72*, 4427-4434.

67. a) Khan, M. S.; Al-Mandhary, M. R. A.; Al-Suti, M. K.; Al-Battashi, F. R.; Al-Saadi, S.; Ahrens, B.; Bjernemose, J. K.; Mahon, M. F.; Raithby, P. R. Younus, M.; Chawdhury, N.; Köhler, A.; Marseglia, E. A.; Tedesco, E.; Feeder, N.; Teat, S. J. *Dalton Trans.* **2004**, 2377-2385; b) Alvey, P. M.; Ono, R. J.; Bielawski, C. W.; Iverson, B. L. *Macromolecules*, **2013**, *46*, 718-726; c) Z. Zhao, Z.; Yu, S.; Xu, L.; Wang, H.; Lu, P.; *Tetrahedron*, **2007**, *63*, 7809-7815; d) Gole, B.; Shanmugaraju, S.; Kumar, A.; Partha, B.; Mukherjee, S. *Chem. Commun.* **2011**, *47*, 10046-10048; e) Lamm, J.-H.; Glatthor, J.; Weddeling, J.-H.; Mix, A.; Chmiel, J.; Neumann, B.; Stammeler, H.-G.; Mitzel, N. W. *Org. Biomol. Chem.* **2014**, *12*, 7355-7364.

68. a) Bholá, R.; Bally, T.; Valente, A.; Cyranski, M. K.; Dobrzycki, L.; Spain, St. M.; Rempala, P.; Chin, Matthew R.; King, Benjamin T. *Angew. Chem. Int. Ed.* **2010**, *49*, 399-402; b) Park, Y. S.; Dibble, David J.; Kim, Juhwan; Lopez, Robert C.; Vargas, E.; Gorodetsky, A. A. *Angew. Chem. Int. Ed.* **2016**, *55*, 3352-3355; c) Lehnerr, D.; McDonald, R.; Tykwinski, R. R. *Org. Lett.*, **2008**, *10*, 4163-4166.

69. Tobe, Y.; Kubota, K.; Naemura, K.; *J. Org. Chem.* **1997**, *62*, 3430-3431

70. (a) Shaaban, S.; Negm, A.; Ashmawy, A. M.; Ahmed, D. M.; Wessjohann, L. A. *Eur. J. Med. Chem.* **2016**, *122*, 55-71; (b) Boncel, S.; Herman, A. P.; Budniok, S.; Jędrysiak, R. G. Jakóbiak-Kolon, A.; Skepper, J. N.; Müller, K. H. *ACS Biomater. Sci. Eng.* **2016**, *2*, 1273-1285; c) Bass, P. D.; Gubler, D. A.; Judd, T. C.; Williams, R. M. *Chem. Rev.* **2013**, *113*, 6816-6863.

71. a) Hata, T.; Sano, Y.; Sugawara, R.; Matsumae, A.; Kanamori, K.; Shima, T.; Hoshi, T.; *J. Antibiot.* **1956**, *9*, 141-146. (b) Cone, M.C.; Melville, C.R.; Gore, M.P.; Gould, S.J. *J. Antibiot.* **1989**, *42*, 179-188;

72. a) Inman, M.; Carvalho, C.; Lewis, W.; Moody, J. C. *J. Org. Chem.* **2016**, *81*, 7924-7930; b) Asche, C.; Frank, W.; Albertb, A.; Kucklaenderc, U. *Bioorg. Med. Chem.* **2005**, *13*, 819-837.

73. Rickards, R. W.; Rothschild, J. M.; Willis, A. C.; De Chazal, N. M.; Kirk, J.; Kirk, K.; Saliba, K. J.; Smith, G. D.; *Tetrahedron* **1999**, *55*, 13513-13520.
74. Bernardo, P. H.; Chai, C. L. L.; Heath, G. A.; Mahon, P. J.; Smith, G. D.; Waring, P.; Wilkes, B. A. *J. Med. Chem.* **2004**, *47*, 4958-4963.
75. Itoigawa, M.; Kashiwada, Y.; Ito, C.; Furukawa, H.; Tachibana, Y.; Bastow, K. F.; Lee, K.-H. *J. Nat. Prod.* **2000**, *63*, 893-897.
76. a) Illos, R. A.; Shamir, D.; Shimon, L. J. W.; Zilbermann I.; Bittnera, S. *Tetrahedron Lett.* **2006**, *47*, 5543-5546; b) Macías-Ruvalcaba, N.; Cuevas, G.; González, I.; Aguilar-Martínez, M. *J. Org. Chem.* **2002**, *67*, 3673-3681;
77. a) Yogo, M.; Ito, C.; Furukawa, H. *Chem. Pharm. Bull.* **1991**, *39*, 328-334; b) Sridharan, V.; Martín, M. A.; Menéndez, J. C. *Eur. J. Org. Chem.* **2009**, 4614-4621; c) Tu, S.; Ding, C.; Hu, W.; Li, F.; Yao, Q.; Zhang, A. *Molec. Divers.* **2011**, *15*, 91-99; d) Echavarren, A. M.; Tamayo, N.; Paredes, M. C. *Tetrahedron Lett.* **1993**, *34*, 4713-4716; e) Bolibrukh, K.; Khoumer, Polovkovich, S.; Noviko, V.; Terme, T.; Vanelle, P. *Synlett.* **2014**, *25*, 2765-2768.
78. a) Tseng, C. M.; Wu, Y. L.; Chuang, C.-P. *Tetrahedron* **2004**, *60*, 12249-12264; b) Patil, P.; Nimonkar, A.; Akamanchi, K. G.; *J. Org. Chem.* **2014**, *79*, 2331-2336; c) Liu, Y.; Gribbl, G. W. *Tetrahedron Lett.* **2001**, *42*, 2949-2951; d) Ketcha, D. M.; Gribble, G. W. *J. Org. Chem.* **1985**, *50*, 5451-5457; e) Corral, J. M. M. D.; Castro, M. A.; Gordaliza, M.; Martín, M. L.; Gamito, A. M.; Cuevasb, C.; Felicianoa, A. S. *Bioorg. Med. Chem.* **2006**, *14*, 2816-2827; f) Hu, H. Y.; Liu, Y.; Ye, M.; Xu, J. H. *Synlett.* **2006**, *12*, 1913-1917; f) Miki, Y.; Tsuzaki, Y.; Matsukida, H. *Heterocycles* **2002**, *57*, 1645-1651; g) Guo, J.; Kiran, I. N. C.; Reddy, R. S.; Gao, J.; Tang, M.; Lui, Y.; He, Y. *Org. Lett.* **2016**, *18*, 2499-2502.
79. a) Tandon, V. K.; Maurya, H. K.; Mishra, N. N.; Shukl, P. K.; *Euro. J. Med. Chem.* **2009**, *44*, 3130-3134; b) Tandon, V. K.; Maury, H. K.; *Tetrahedron Lett.* **2009**, *50*, 5896-5902.
80. a) Hung, T. Q.; Dang, T. T.; Villinger, A.; Sung, T. V.; Langer, P. *Org. Biomol. Chem.* **2012**, *10*, 9041 – 9044; b) Hung, T. Q.; Do, H. H.; Ngo, N. T.; Dang, T. T.; Ayub, K.; Villinger, A.; Lochbrunner, S.; Flechsig, G.-U.; Langer, P. *Org. Biomol. Chem.* **2014**, *12*, 6151–6166.
81. a) Ackermann, L.; Althammer, A. *Angew. Chem. Int. Ed.* **2007**, *46*, 1627-1629; b) Ackermann, L.; Althammer, A.; Mayer, P. *Synthesis*, **2009**, *20*, 3493-3503.
82. a) Terkeltaub, R.; *Purinergic Signal.* **2006**, *2*, 371–377; b) Goding, J. W.; Grobber, B.; Slegers, H.; *Biochim. Biophys. Acta*, **2003**, *1638*, 1–19; c) Dong, H.; Maddux, B. A.; Altomonte, J.; Meseck, M.; Accili, D.; Terkeltaub, R.; Johnson, K.; Youngren, J. F.; Goldfine, I. D.; *Diabetes.* **2005**, *54*, 367–372; d) Zalatan, J. G.; Fenn, T. D.; Brunger, A. T.; Herschlag, D. *Biochem.* **2006**, *45*, 9788–803.

83. a) Shayhidin E. E.; Forcellini E.; Boulanger M. C.; Mahmut A.; Dautrey S.; Barbeau X.; Lagüe P.; Sévigny J.; Paquin J. F.; Mathieu P.; *Br. J. Pharmacol.* **2015**, *172*, 4189-99; b) Joseph, S. M.; Pifer, M. A.; Przybylski, R. J.; Dubyak, G. R. *Br. J. Pharmacol.* **2004**, *142*, 1002–1014; c) Eliahu, S.; Lecka, J.; Reiser, G.; Haas, M.; Bigonnesse, F.; Lévesque, S. A.; Pelletier, J.; Sévigny, J.; Fischer, B. *J. Med. Chem.* **2010**, *53*, 8485–8497; d) Nadel, Y.; Gilad, Y.; Förster, D.; Reiser, G.; Kenigsberg, S.; Camden, J.; Weisman, G. A.; Senderowitz, H.; Lecka, J.; Ben-David, G.; Simhaev, L.; Eliahu, S.; Oscar J.; Fischer, B.; Senderowitz, H.; Sévigny, J. *J. Med. Chem.* **2014**, *57*, 4677–4691.
84. a) Patel S. D.; Habeski W. M.; Cheng A. C.; de la Cruz E.; Loh C.; Kablaoui N. M. *Bioorg. Med. Chem. Lett.* **2009**, *19*, 3339-3343; b) Khan, K. M., Fatima, N.; Rasheed, M.; Jalil S.; Ambreen, N.; Perveen, S.; Choudhary, M. I. *Bioorg. Med. Chem.* **2009**, *17*, 7816-7822; c) Choudhary M. I.; Fatima N.; Khan K. M.; Jalil S.; Iqbal S.; Atta-Ur-Rahman. *Bioorg. Med. Chem.* **2006**, *14*, 8066-8075; d) Chang, L.; Lee, S.-Y.; Leonczak, P.; Rozenski, J.; Jonghe, S. D.; Hanck, T.; Müller, C. E.; Herdewijn, P. *J. Med. Chem.* **2014**, *57*, 10080–10100.
85. a) Katz, H. E. *J. Mater. Chem.* **1997**, *7*, 369-376; b) Tang, W. C.; Slyke, S. A. V. *Appl. Phys. Lett.* **1987**, *51*, 913-915; c) Yu, G.; Wang, J.; McElvain, J.; Heeger, A. J. *Adv. Mater.* **1998**, *17*, 1431-1434.
86. Xiao, J.; Duong, H. M.; Liu, Y.; Shi, W.; Ji, L.; Li, G.; Li, S.; Liu, X.-W.; Ma, J.; Wudl, F.; Zhang, Q.; *Angew. Chem. Int. Ed.* **2012**, *51*, 6094-6098.
87. Tyagi, P.; Venkateswararao, A.; Thomas, K. R. J.; *J. Org. Chem.* **2011**, *76*, 4571–4581.
88. a) Kim, S. J.; Kim, Y. J.; Son, Y. H.; Hur, A.; Um, H. A.; Shin, J.; Lee, T. W.; Cho, M. J.; Kim, J. K., Joo, S.; Yang, J. H.; Chae, G. S.; Choi, K.; Kwon, J. H.; Choi, D. H.; *Chem. Commun.* **2013**, *49*, 6788–6790; b) Im, Y.; Lee, J. Y.; *Chem. Commun.* **2013**, *49*, 5948–5950.
89. a) Son, Y. H.; Kim, Y. J.; Park, M. J.; Oh, H.-Y.; Park, J. S.; Yang, J. H.; Suh, M. C.; Kwon, J. H.; *J. Mater. Chem. C* **2013**, *1*, 5008–5014; b) Lee, C. W.; Im, Y.; Seo, J. A.; Lee, J. Y.; *Chem. Commun.* **2013**, *49*, 9860–9862; c) Lee, C. W., Im, Y., Seo, J.-A.; Lee, J. Y.; *Org. Electron.* **2013**, *14*, 2687–2691; d) Jiang, W.; Tang, J.; Yang, W.; Ban, X.; Huang, B.; Dai, Y.; Sun, Y.; Duan, L.; Qiao, J.; Wang, L.; Qiu, Y.; *Tetrahedron* **2012**, *68*, 5800–5805.
90. Su, T.-H.; Fan, C.-H.; Ou-Yang, Y.-H.; Hsu, L.-C.; Cheng, C.-H.; *J. Mater. Chem. C* **2013**, *1*, 5084–5092.
91. Fan, C.-H.; Sun, P.; Su, T.-H.; Cheng, C.-H. *Adv. Mater.* **2011**, *23*, 2981–2985.
92. Thomas, K. R. J.; Tyagi, P.; *J. Org. Chem.* **2010**, *75*, 8100–8011.
93. a) Schunck, E.; Marchlewski, L. *Ber. Dtsch. Chem. Ges.* **1895**, *28*, 2525-2531; b) Wentrup, V. C.; Thetaz, C.; Tagliaferri, E.; Lindner, H. J.; Kitschke, B.; Winter, H.-W. *Angew. Chem.*

- 1980**, 4, 556–557; c) Pratima, N. A.; Alphonse, F.-A.; Routier, S.; Coudert, G.; Mérour, J.-Y. *Heterocycles* **2001**, 55, 925–940
94. Kim, T. H.; Kim, S. M.; Beak, Y. M.; Kim, H. M.; Park, H. C.; Shin, J. Y.; *PCT Int. Patent Appl.* WO 2013133575 A2013133571 2020130912, **2013**.
95. Chen, T. K.; Flowers, W. T. *J. Chem. Soc., Chem. Commun.* **1980**, 1139-1140.
96. a) Takimiya, K.; Shinamura, S.; Osaka, I.; Miyazaki, E. *Adv. Mater.* **2011**, 23, 4347-4370; b) Cinar, M. E.; Ozturk, T. *Chem. Rev.* **2015**, 115, 3036-3140; c) Li, Y. N.; Wu, Y. L.; Gardner, S.; Ong, B. S. *Adv. Mater.* **2005**, 17, 849–853; d) Wu, Y. L.; Li, Y. N.; Gardner, S.; Ong, B. S. *J. Am. Chem. Soc.* **2005**, 127, 614–618; e) Simokaitiene, J.; Stanislovaityte, E.; Grazulevicius, J. V.; Jankauskas, V.; Gu, R.; Dehaen, W.; Hung, Y.-C.; Hsu, C.-P. *J. Org. Chem.* **2012**, 77, 4924–4931.
97. a) Gidron, Ori; Bendikov, M. *Angew. Chem. Int. Ed.* **2014**, 53, 2546-2555; b) Jin, X.-H.; Sheberla, D.; Shimon, L. J. W.; Bendikov, M. *J. Am. Chem. Soc.* **2014**, 136, 2592-2601; c) Gidron, O.; Diskin-Posner, Y.; Bendikov, M. *J. Am. Chem. Soc.* **2010**, 132, 2149-2150.
98. a) Sawada, Y.; Hotta, M.; Matsumoto, *Pat.* WO 2012050003 A1, **2012**; b) Nagaoka, M.; Kase, K.; Naito, K.; Otsuka, K.; Kusano, S.; *PCT Int. Appl.* WO 2015125679 A1, **2015**; c) Sakamoto, N.; Miyata, Y.; *U.S. Pat. Appl. Publ.* US 20150171338 A1, **2015**.
99. a) Sui, Z.; Zhangand, X.; Li, X. *Pat.* 2006047017 A1, **2006**; b) Butera, J. A.; Antane, S. A.; Hirth, B.; Lennox, J. R.; Sheldon, J. H.; Norto, N.W.; Warga, D.; Argentieri, T. M. *Bioorg. Med. Chem. Lett.* **2001**, 11, 2093–2097.
100. a) Gormemis, A. E.; Ha, T. S.; Im, I.; Jung, K.-Y.; Lee, J. Y.; Park, C.-S.; Kim, Y.-C.; *Chem. Bio. Chem.* **2005**, 6, 1745–1748; b) Schroeder, D. C.; Corcoran, P. O.; Holden, C. A.; Mulligan, M. C.; *J. Org. Chem.* **1962**, 27, 586–591.
101. a) Srour, H.; Doan, T.-H.; Silva, E. D.; Whitby, R. J.; Witulski, B. *J. Mater. Chem. C*, **2016**, 4, 6270-6279; b) Takamatsu, K.; Hirano K.; Satoh, T.; Miura, M. *Org. Lett.* **2014**, 16, 2892–2895; c) Saito, K.; Chikkade, P. K.; Kanai, M.; Kuninobu, Y. *Chem. Eur. J.* **2015**, 21, 8365-8368; d) Truong, M. A.; Nakano, K.; *J. Org. Chem.* 2015, 80, 11566–11572.
102. Vollmayer, P.; Clair, T.; Goding, J. W.; Sano, K.; Servos, J.; Zimmermann, H.; *Eur. J. Biochem.* **2003**, 270, 2971–2978.
103. Shopee, C. W.; *J. Chem. Soc., Perkin Trans.* **1985**, 1, 45-52.

7. Appendix

7.1 General information

All used chemicals, if not otherwise stated, are commercially available and used without further purification. All reactions were carried out in dried glass pressure tubes under an argon atmosphere. Analytical TLC on Merck silica gel 60 F254 plates was visualized by fluorescence quenching. Column chromatography was performed on Merck *Geduran Si 60 (0.063-0.200 mm)*. ¹H NMR and ¹³C NMR spectra were carried out on a Bruker Advance DRX-500 MHz, 300 MHz or 250 MHz. Chemical shifts in ppm were corrected by residual solvent. Multiplicities: s = singlet, d = doublet, dd = doublet of doublets, t = triplet, td = triplet of doublets, tt = triplet of triplets, m = multiplet, q = quartet. Nicolet 550 FT – IR spectrometer was used with ATR sampling technique for solids and liquids. Signal characterization: w = weak, m = medium, s = strong. Gas chromatography - mass analysis was performed on an Agilent HP-5890 instrument with an Agilent HP-5973 Mass Selective Detector (EI) and HP-5 capillary column using helium carrier gas. Agilent 1969A TOF mass spectrometer was used for ESI HR-MS measurements. High Resolution MS (HRMS) was performed on a Finnigan MAT 95 XP. Single crystal X-Ray structure determination was carried out on a Bruker X8Apex diffractometer with CCD camera (Mo K α radiation and graphite monochromator, $a = 0.071073$ Å). Melting points were determined on a Micro-Hot-Stage GalenTM III Cambridge Instruments. The melting points are not corrected.

Electrochemical protocols

All electrochemical studies were performed with an Autolab (PGSTAT 302N, Metrohm) at 22 °C in dried dimethylformamide under an Argon atmosphere. 0.1 M tetrabutylammonium hexafluorophosphate (Fluka) was used as conducting support. The working electrode was a glassy carbon disk electrode ($d = 2$ mm), a Pt-electrode as the counter electrode, an Ag/AgCl/LiCl sat. in EtOH-system as the reference electrode (all electrodes: Metrohm) and the ferrocenium/ferrocene as internal reference system (potential of Fc⁺/Fc: 0.51 V [vs. Ag/AgCl/LiCl sat. in EtOH]). The CV scans were repeated three times at a scan rate of 40 mV·s⁻¹. The DPV measurements in oxidative and anodic directions were performed with a step potential of 5 mV, modulation amplitude of 0.025 V, modulation time of 0.05 s and an interval time of 0.5 s

Biological protocols

Cell Transfection with Human NPPs. COS-7 cells were transfected with plasmids expressing human NPPs ((NPP-1)¹ or (NPP-3)²) in 10-cm plates, by using Lipofectamine. The confluent cells were incubated for 5 hr at 37 °C in DMEM/F-12 in the absence of fetal bovine serum and with 6 µg of plasmid DNA and 24 µL of Lipofectamine reagent. Subsequently, the same volume of DMEM/F-12 containing 20% FBS was added to stop the transfection and cells were harvested 48–72 h later.

Preparation of membrane fractions. The transfected cells were washed three times with Tris–saline buffer at 4 °C and then the cells were collected by scraping in the harvesting buffer (95 mM NaCl, 0.1 mM PMSF, and 45 mM Tris buffer, pH 7.5). Afterwards, the cells were washed twice by centrifugation at 300×g for 5 min at 4 °C.³ These cells were resuspended in the harvesting buffer containing 10 µg/mL aprotinin and then sonicated. Cellular and nuclear debris were discarded by 10 min centrifugation (300×g at 4 °C). Glycerol (final concentration of 7.5%) was added to the resulting supernatant and all the samples were kept at -80 °C until used. Bradford microplate assay⁴ was used for the estimation of protein concentration. Bovine serum albumin was used as a reference standard.

Protocol of Nucleotide pyrophosphatase (NPP-1 & NPP-3) activity. The conditions for the assay were optimized with slight modifications in previously used spectrophotometric method.⁵ The reaction was carried out in the assay buffer which contained 5 mM MgCl₂, 0.1 mM ZnCl₂, 25% glycerol and 50 mM tris-hydrochloride (pH: 9.5). Initial screening was performed at a concentration of 0.1 mM of the tested compounds. The total volume of 100 µL contained 70 µL of the assay buffer, 10 µL of tested compound (0.1 mM with final DMSO 1% (v/v)) and 10 µL of NPP-1 (27 ng of protein from COS cell lysate in assay buffer) or 10 µL of h-NPP-3 (25 ng of protein from COS cell lysate in assay buffer). The mixture was pre-incubated for 10 minutes at 37 °C and absorbance was measured at 405 nm as pre-read using microplate reader (BioTek FLx800, Instruments, Inc. USA). The reaction was then initiated by the addition of 10 µL of p-Nph-5-TMP substrate at a final concentration of 0.5 mM and the reaction mixture was incubated for 30 more min at 37 °C. The change in the absorbance was measured as after-read. The activity of each compound was compared with the reaction in absence of tested compounds/inhibitors. The compounds which exhibited over 50% inhibition of either the NPP-

1 activity or NPP-3 activity were further evaluated for determination of IC_{50} values. For this purpose their dose response curves were obtained by assaying each inhibitor concentration against both NPPs using the above mentioned reaction conditions. All experiments were repeated three times in triplicate. The IC_{50} values, determined by the non-linear curve fitting program PRISM 5.0 (GraphPad, San Diego, California, USA).

7.2. Supplement for optical spectra of compounds 3, 6, 7

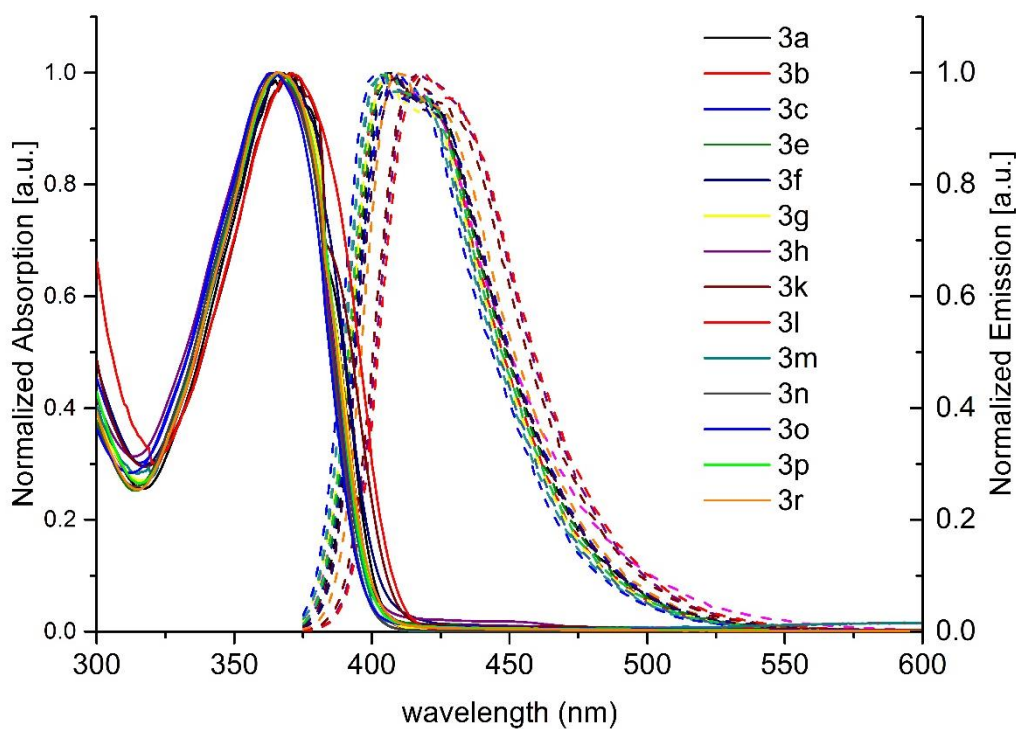


Figure S1. Absorption and corrected emission spectra of **3**

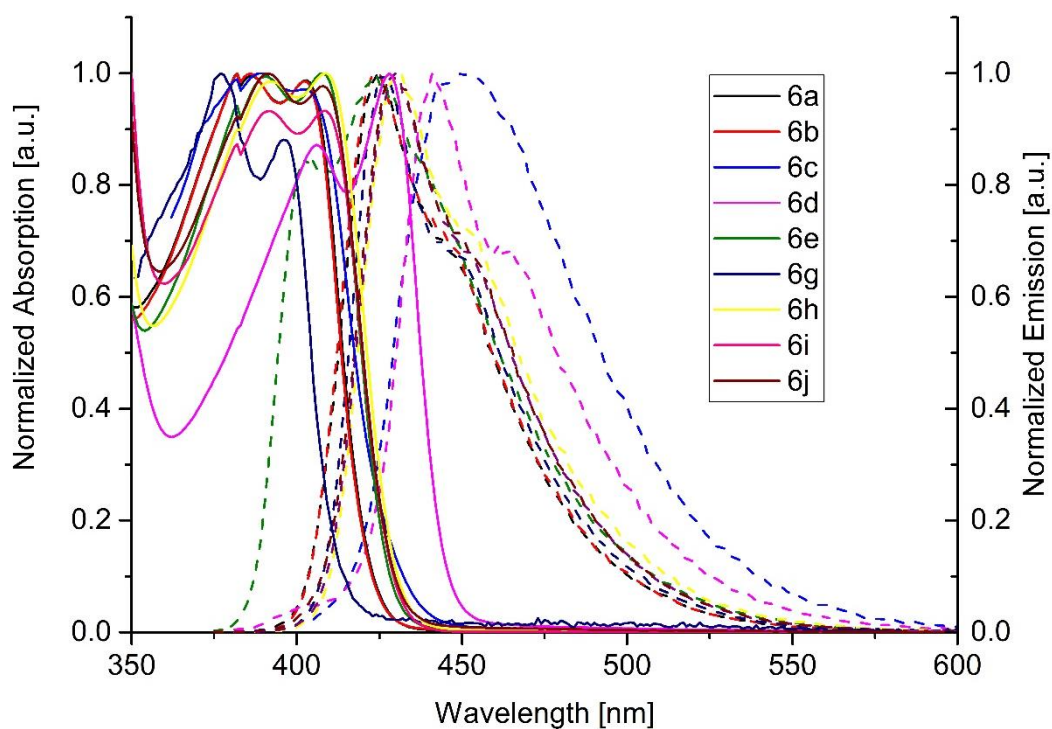


Figure S2. Absorption and fluorescence spectra of compounds **6**.

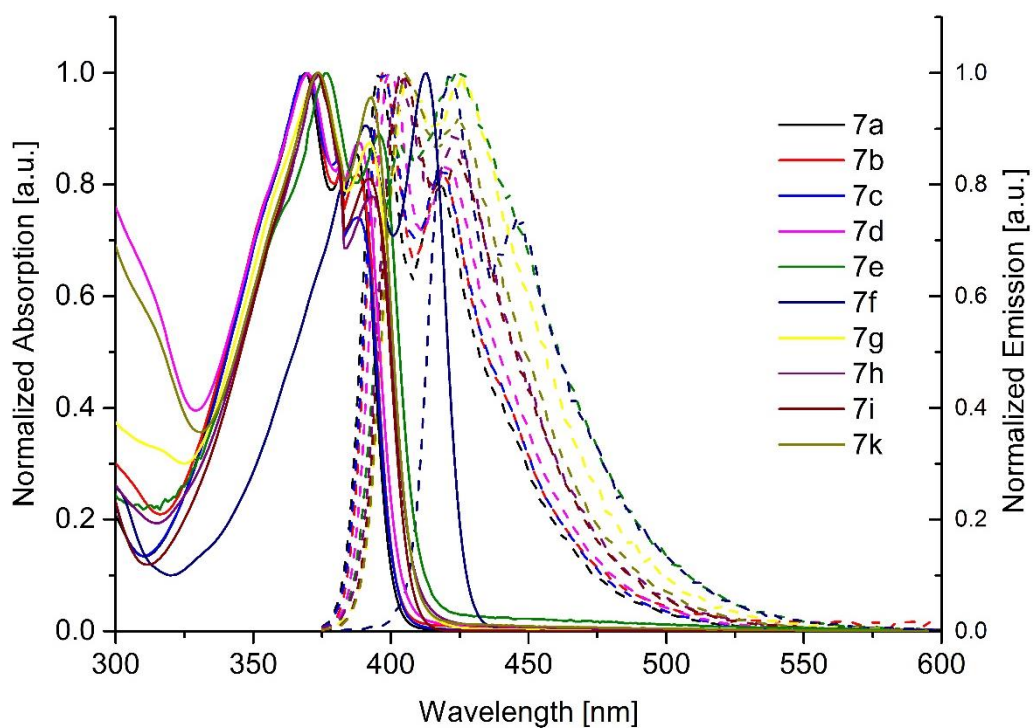
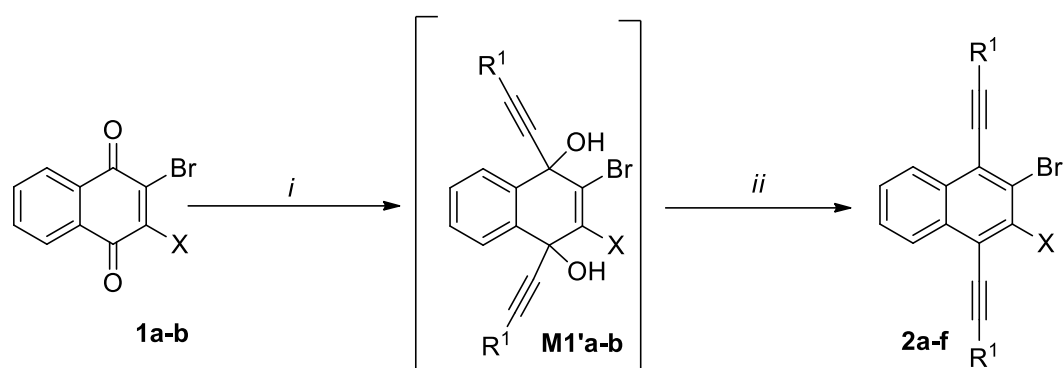


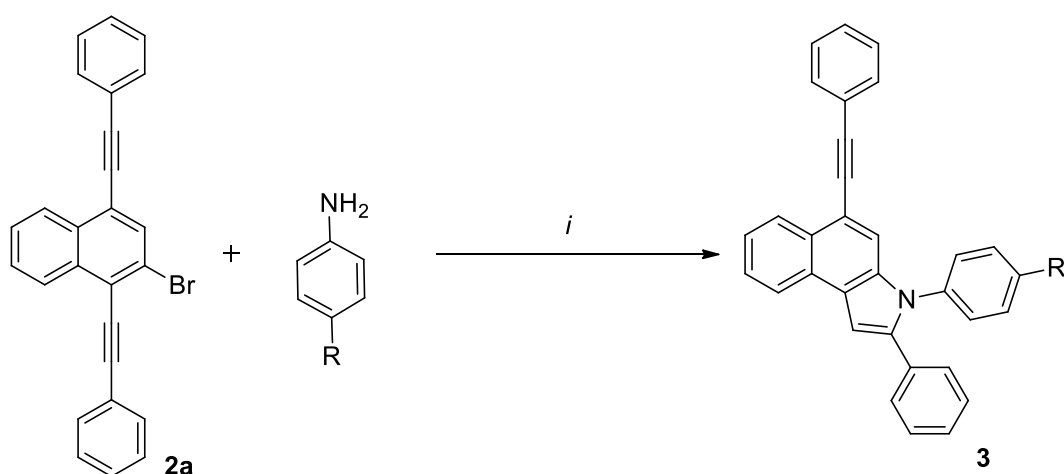
Figure S3. Absorption and fluorescence spectra of compounds **7**.

6.3. Supplement for Chapter 2



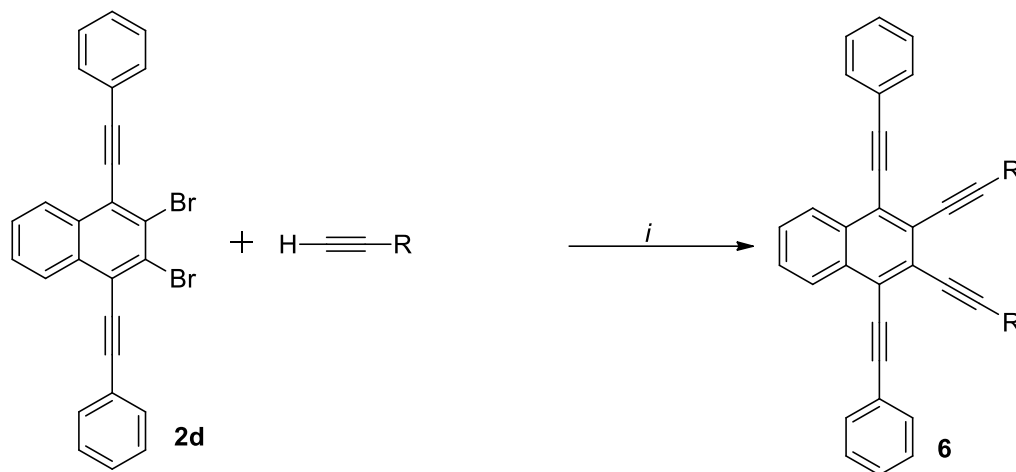
Scheme S1. Synthesis of diarylethynynaphthalenes **2a-f**.

Procedure for the starting compounds 2: The solution of 1,4-naphthoquinones in THF was dropped into the mixture of *n*-Buli and arylacetylenes. The reaction was stirred for 10 minutes at room temperature, then, was heated to 60 °C for 30 minutes. After cooling down, a saturated solution of ammonium chloride was added. The mixture was extracted with ethyl acetate, dried for the next step. The obtained brown solid was dissolved in MeCN (20 ml) and water (1 ml), then SnCl₂ was added. The reaction was refluxed for 6h. After cooling down to room temperature, the mixture was diluted with water and extracted with ethyl acetate. The combined organic layers were dried over sodium sulfate and concentrated under vacuum. The crude material was purified by flash column chromatography (silica gel, heptane/ethylacetate).



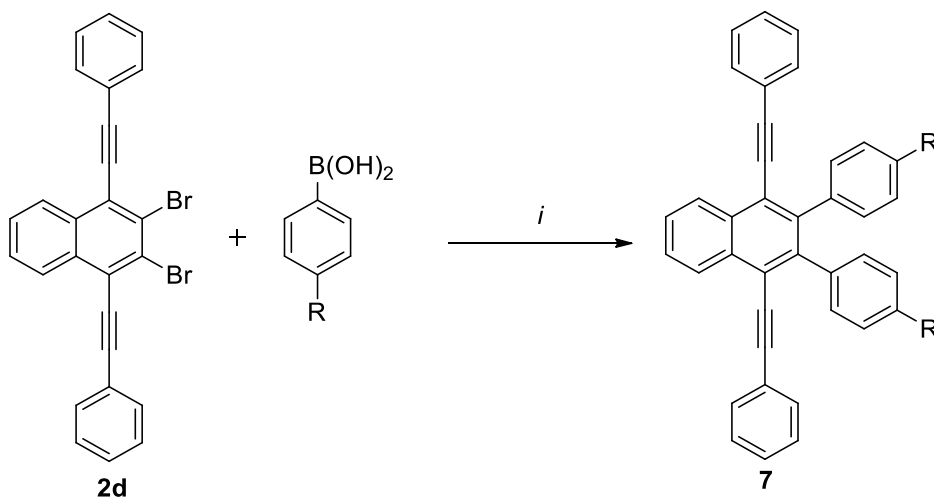
Scheme S2. Synthesis of ethynylbenzoindole **3**.

Procedure for ethynylbenzoindole 3 (amination), An argon purged pressure tube was charged with brominated 1,4-diethynyl-naphthalene(0.3 mmol) and the amine (0.3 mmol), Pd(OAc)₂ (5 mol%), SPhos (10 mol%), base (0.9 mmol) and DMF (10 mL). The reaction was set up at 90 °C for 48 h. Afterwards the mixture was allowed to reach room temperature, was diluted with water and extracted with ethyl acetate. The combined organic layers were dried over sodium sulfate and concentrated under vacuum. The crude material was purified by flash column chromatography (silica gel, heptane/ethylacetate).



Scheme S3. Synthesis of tetraarylethynyl-naphthalene **6**.

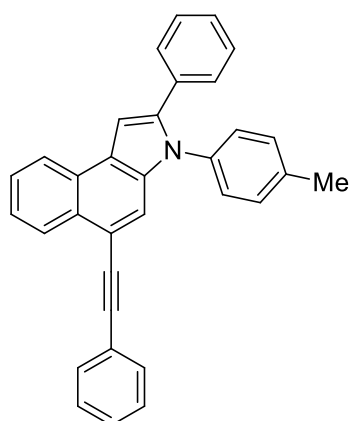
Procedure for tetraarylethynyl-naphthalene 6a (Sonogashira reaction), An argon purged pressure tube was charged with 2,3-dibromo-1,4-diethynyl-naphthalene **1** (0.3 mmol) and PdCl₂(CH₃CN)₂ (5 mol%), SPhos (or XPhos) (10 mol%), CuI (5 mol%), diisopropylamine (1 ml) and dioxane (5 mL), then the arylacetylene (0.3 mmol) was added. The reaction was set up at 80 °C for 24 h. Afterwards the mixture was allowed to reach room temperature, was diluted with water and extracted with ethyl acetate. The combined organic layers were dried over sodium sulfate and concentrated under vacuum. The crude material was purified by flash column chromatography (silica gel, heptane/ethylacetate).



Scheme S4. Synthesis of 2,3-diaryl-1,4-diethynynaphthalene **7**.

Procedure for 2,3-diaryl-1,4-diethynynaphthalene **7 (Suzuki-Miyaura reaction)**, An argon purged pressure tube was charged with 2,3-dibromo-1,4-diethynynaphthalene (0.3 mmol) and arylboronic acid (0.3 mmol), Pd(PPh₃)₄ (5 mol%), Na₂CO₃ (0.9 mmol) and dioxane (10 mL). The reaction was set up at 100 °C for 24 h. Afterwards the mixture was allowed to reach room temperature, was diluted with water and extracted with ethyl acetate. The combined organic layers were dried over sodium sulfate and concentrated under vacuum. The crude material was purified by flash column chromatography (silica gel, heptane/ethylacetate).

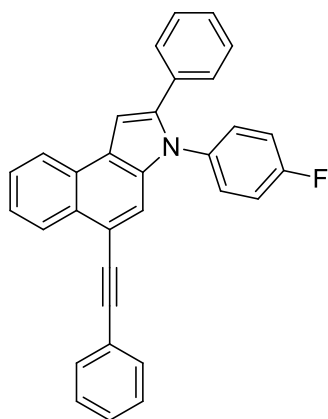
2-Phenyl-5-(phenylethynyl)-3-(*p*-tolyl)-3*H*-benzo[e]indole (3a**)**



Following the general procedure, **3a** was obtained as a yellow solid (96 mg, 74 %), mp = 166 – 168 °C. ¹H NMR (250 MHz, CDCl₃) δ 8.55 (dd, ³J = 8.1 Hz, ⁴J = 0.9 Hz, 1H, CH_{Ar}), 8.38 – 8.31 (m, 1H, CH_{Ar}), 7.71 (s, 1H, CH_{Ar}), 7.68 – 7.62 (m, 3H, CH_{Ar}), 7.60 – 7.55 (m, 1H, CH_{Ar}), 7.44 – 7.19 (m, 13H, CH_{Ar}), 2.45 (s, 3H, CH₃). ¹³C NMR (63 MHz, CDCl₃) δ 140.7, 137.9, 135.5, 135.0, 132.5 (C_{Ar}), 131.6, 130.3 (2CH_{Ar}), 129.6 (C_{Ar}), 129.0, 128.5, 128.4 (2CH_{Ar}), 128.1 (CH_{Ar}), 128.0 (2CH_{Ar}), 127.8 (C_{Ar}), 127.4, 127.1, 126.5, 124.6 (CH_{Ar}), 124.4, 124.0 (C_{Ar}), 123.5, 117.0 (CH_{Ar}), 115.2 (C_{Ar}), 103.0 (CH_{Ar}), 93.2, 89.3 (C≡C), 21.4 (CH₃). IR (ATR, cm⁻¹), $\tilde{\nu}$ = 1585 (m), 1475 (s), 1363 (s), 1282 (m), 1257 (m), 1228 (m), 750 (s), 705 (m), 692 (s), 684 (s), 665 (s), 657 (s), 646 (s). MS (EI,

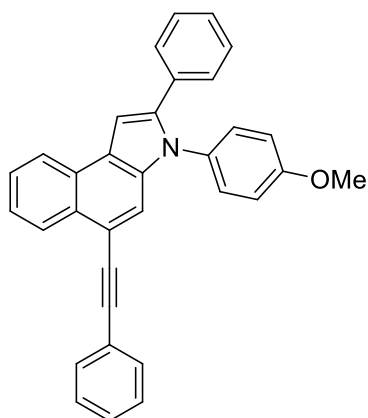
70 eV), m/z (%) = 435 (6), 434 (33), 433 (M^+ , 100), 417 (4), 340 (3), 315 (6), 208 (6), 77 (5). HRMS (EI), calcd for $C_{33}H_{23}N$ ($[M]^+$), 433.18250, found, 435.18283.

3-(4-Fluorophenyl)-2-phenyl-5-(phenylethynyl)-3H-benzo[e]indole (3b)



Following the general procedure, **3b** was obtained as a yellow solid (64 %), mp = 208 – 209 °C. 1H NMR (300 MHz, $CDCl_3$) δ 8.53 – 8.46 (m, 1H, CH_{Ar}), 8.32 – 8.26 (m, 1H, CH_{Ar}), 7.66 – 7.48 (m, 5H, CH_{Ar}), 7.39 – 7.22 (m, 11H, CH_{Ar}), 7.19 – 7.07 (m, 2H, CH_{Ar}). ^{19}F NMR (282 MHz, $CDCl_3$) δ -113.20. ^{13}C NMR (75 MHz, $CDCl_3$) δ 161.8 (d, $^1J = 248.3$ Hz, CF), 140.6, 134.8 (C_{Ar}), 134.0 (d, $^4J = 3.2$ Hz, C_{Ar}), 132.0 (C_{Ar}), 131.5 (2 CH_{Ar}), 129.9 (d, $^3J = 8.6$ Hz, 2 CH_{Ar}), 129.5 (C_{Ar}), 128.9 (2 CH_{Ar}), 128.4 (4 CH_{Ar}), 128.1 (CH_{Ar}), 127.6 (C_{Ar}), 127.5, 127.0, 126.5, 124.6 (CH_{Ar}), 124.3, 123.7 (C_{Ar}), 123.3 (CH_{Ar}), 116.5 (d, $^2J = 22.9$ Hz, 2 CH_{Ar}), 116.4 (CH_{Ar}), 115.4 (C_{Ar}), 103.2 (CH_{Ar}), 93.2, 88.9 ($C\equiv C$). IR (ATR, cm^{-1}), $\tilde{\nu} = 3070$ (w), 1598 (m), 1508 (s), 1477.28 (s), 1390 (m), 1220 (s), 1068 (m), 1029 (m), 1014 (m), 948 (m), 862 (m), 840 (s). MS (EI, 70 eV), m/z (%) = 438 (31), 437 (M^+ , 100), 413 (1), 333 (6), 313 (7), 219 (19), 218 (25), 179 (12). HR-MS (EI), Calcd for $C_{32}H_{20}FN$ (M^+) = 437.15743, found 437.15706.

3-(4-Methoxyphenyl)-2-phenyl-5-(phenylethynyl)-3H-benzo[e]indole (3c)

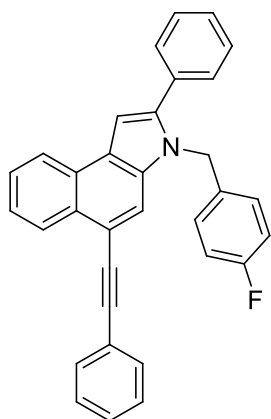


Following the general procedure C, **3c** was obtained as a yellow solid (80 %), mp = 201 – 202 °C. 1H NMR (250 MHz, $CDCl_3$) δ 8.58 – 8.51 (m, 1H, CH_{Ar}), 8.38 – 8.30 (m, 1H, CH_{Ar}), 7.68 – 7.57 (m, 5H, 5 CH_{Ar}), 7.43 – 7.27 (m, 10H, CH_{Ar}), 7.24 (s, 1H, CH_{Ar}), 7.04 – 6.97 (m, 2H, CH_{Ar}), 3.88 (s, 3H, OCH_3). ^{13}C NMR (63 MHz, $CDCl_3$) δ 159.1, 140.8, 135.25, 132.4 (C_{Ar}), 131.6 (2 CH_{Ar}), 130.9, 129.6 (C_{Ar}), 129.4, 129.0, 128.5, 128.4 (2 CH_{Ar}), 128.1 (CH_{Ar}), 127.8 (C_{Ar}), 127.5, 127.1, 126.5, 124.6 (CH_{Ar}), 124.3, 123.9 (C_{Ar}), 123.5, 117.0 (CH_{Ar}), 115.1 (C_{Ar}), 114.8 (2 CH_{Ar}), 102.7 (CH_{Ar}), 93.2, 89.2 ($C\equiv C$), 55.7 (OCH_3). IR (ATR, cm^{-1}), $\tilde{\nu} = 3099$ (w), 3056 (w), 3029 (w), 3002 (w), 2956 (w), 2919 (w), 2848 (w), 2200 (w), 1724 (w), 1596 (w), 1587 (m), 1510 (s), 1492 (m), 1475 (m), 1465 (m), 1454 (m). MS (EI, 70 eV), m/z (%) = 452 (30), 451 (84), 450 (71), 449

(M⁺, 100), 362 (12), 184 (4), 155 (6), 91 (4), 44 (14). HR-MS (EI), Calcd for C₃₃H₂₃NO₂ (M⁺), 449.17741, found 449.17690.

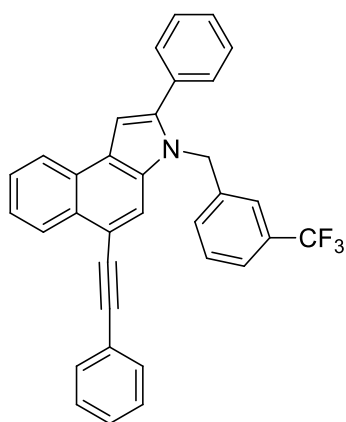
3-(4-Fluorobenzyl)-2-phenyl-5-(phenylethynyl)-3H-benzo[e]indole (3d)

Following the general procedure C, **3d** was obtained as a yellow solid (52 %), mp = 171 – 173 °C



¹H NMR (300 MHz, CDCl₃) δ 8.65 – 8.60 (m, 1H, CH_{Ar}), 8.40 – 8.35 (m, 1H, CH_{Ar}), 7.79 – 7.63 (m, 5H, CH_{Ar}), 7.55 – 7.40 (m, 8H, CH_{Ar}), 7.26 (s, 1H, CH_{Ar}), 7.11 – 6.93 (m, 4H, CH_{Ar}), 5.50 (s, 2H, CH₂). ¹⁹F NMR (282 MHz, CDCl₃) δ - 115.0. ¹³C NMR (75 MHz, CDCl₃) δ 162.1 (d, ¹J = 245.8 Hz, CF), 141.5 (C_{Ar}), 133.6 (d, ⁴J = 3.2 Hz, C_{Ar}), 133.5, 132.3 (C_{Ar}), 131.6 (2CH_{Ar}), 129.3 (C_{Ar}), 129.2, 128.7, 128.5 (2CH_{Ar}), 128.2 (d, ³J = 9.3 Hz, 2CH_{Ar}), 127.8 (C_{Ar}), 127.5, 127.4, 127.1, 126.5 (CH_{Ar}), 124.6 (C_{Ar}), 124.5 (CH_{Ar}), 123.8 (C_{Ar}), 123.3 (CH_{Ar}), 116.1 (d, ²J = 23.1 Hz, 2CH_{Ar}), 115.7 (CH_{Ar}), 115.0 (C_{Ar}), 102.4 (CH_{Ar}), 93.2, 89.1 (C≡C), 47.2 (CH₂). IR (ATR, cm⁻¹), $\tilde{\nu}$ = 3049 (w), 3029 (w), 2993 (w), 2906 (w), 2858 (w), 2200 (w), 1602 (m), 1585 (m), 1567 (w), 1519 (w), 1508 (s), 1492 (m), 1477 (s), 1459 (m), 1438 (m), 1417 (w). MS (EI, 70 eV), m/z (%) = 453.18 (7), 452 (25), 451 (M⁺, 84), 342 (100), 313 (7), 265 (4), 237 (3), 109 (5). HR-MS (EI), Calcd for C₃₃H₂₂NF (M⁺), 451.17308 found 451.17264.

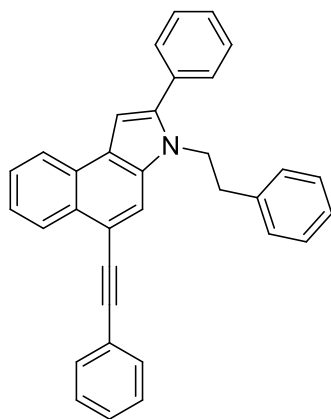
2-Phenyl-5-(phenylethynyl)-3-(3-(trifluoromethyl)benzyl)-3H-benzo[e]indole (3e)



Following the general procedure C, **3e** was obtained as a yellow solid (47 %), mp = 179 – 180 °C. ¹H NMR (250 MHz, CDCl₃) δ 8.62 - 8.49 (m, 1H), 8.38 – 8.26 (m, 1H, CH_{Ar}), 7.71 – 7.28 (m, 16H, CH_{Ar}), 7.22 (s, 1H, CH_{Ar}), 7.09 (d, ³J = 7.8 Hz, 1H, CH_{Ar}), 5.54 (s, 2H, CH₂). ¹⁹F NMR (235 MHz, CDCl₃) δ -62.64. ¹³C NMR (63 MHz, CDCl₃) δ 141.4, 139.0, 133.4, 132.2 (C_{Ar}), 131.5 (2CH_{Ar}), 131.2 (q, ²J = 33.0 Hz, CCF₃), 129.6 (CH_{Ar}), 129.3 (C_{Ar}), 129.1 (3CH_{Ar}), 128.8, 128.4 (2CH_{Ar}), 128.4, 128.1 (CH_{Ar}), 127.8 (C_{Ar}), 127.0, 126.5 (CH_{Ar}), 124.6 (C_{Ar}), 124.5 (CH_{Ar}), 124.4 (q, ³J = 3.8 Hz, CH_{Ar}), 123.8 (q, ¹J = 272.7 Hz, CF₃), 123.6 (C_{Ar}), 123.3 (CH_{Ar}), 122.8 (q, ³J = 3.8 Hz, CH), 115.9 (CH_{Ar}),

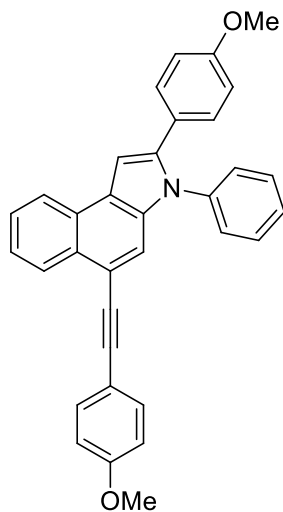
115.2 (C_{Ar}), 102.6 (CH_{Ar}), 93.2, 88.9 (C≡C), 47.4 (CH₂). IR (ATR, cm⁻¹), $\tilde{\nu}$ = 3052 (w), 2919 (w), 2198 (w), 1614 (w), 1598 (w), 1585 (m), 1567 (w), 1537 (w), 1519 (w), 1490 (m). MS (EI, 70 eV), m/z (%) = 503 (22), 502 (73), 501 (M⁺, 100), 424 (6), 342 (94), 315 (15), 265 (5). 178 (3), 109 (1). HR-MS (EI), Calcd for C₃₄H₂₂NF₃ (M⁺), 501.16989, found 501.16999.

3-Phenethyl-2-phenyl-5-(phenylethynyl)-3H-benzo[e]indole (3f)



Following the general procedure C, **3f** was obtained as a yellow solid (19 %), mp = 154 – 155 °C. ¹H NMR (250 MHz, CDCl₃) δ 8.63 – 8.50 (m, 1H, CH_{Ar}), 8.35 – 8.21 (m, 1H, CH_{Ar}), 7.91 (s, 1H, CH_{Ar}), 7.76 – 7.67 (m, 2H, CH_{Ar}), 7.66 – 7.51 (m, 2H, CH_{Ar}), 7.48 – 7.33 (m, 8H, CH_{Ar}), 7.19 (dd, ³J = 6.6 Hz, ⁴J = 3.7 Hz, 3H, CH_{Ar}), 7.04 (s, 1H, CH_{Ar}), 6.97 – 6.85 (m, 2H, CH_{Ar}), 4.67 – 4.37 (m, 2H, CH₂), 3.20 – 2.91 (m, 2H, CH₂). ¹³C NMR (63 MHz, CDCl₃) δ 141.4, 138.0, 132.9, 132.8 (C_{Ar}), 131.7, 131.7 (CH_{Ar}), 129.6 (2CH_{Ph}), 129.2 (C_{Ar}), 128.8, 128.7, 128.6, 128.6, 128.2 (2CH_{Ph}), 128.0 (C_{Ar}), 127.1, 126.8, 126.4 (CH_{Ar}), 124.6 (C_{Ar}), 124.4 (CH_{Ar}), 124.0 (C_{Ar}), 123.4, 116.3 (CH_{Ar}), 114.6 (C_{Ar}), 102.2 (CH_{Ar}), 93.1, 89.4 (C≡C), 45.9, 37.0 (CH₂). IR (ATR, cm⁻¹), $\tilde{\nu}$ = 3027 (w), 2850 (w), 1585 (m), 1452 (m), 1357 (s), 1230 (m), 1178 (m), 1072 (m), 981 (m), 968 (m), 946 (m), 842 (m). MS (EI, 70 eV), m/z (%) = 448 (44), 447 (100), 358 (9), 357 (33), 356 (99), 355 (20), 354 (21). HR-MS (EI), Calcd for C₃₄H₂₅N (M⁺), 447.19815, found 447.19765.

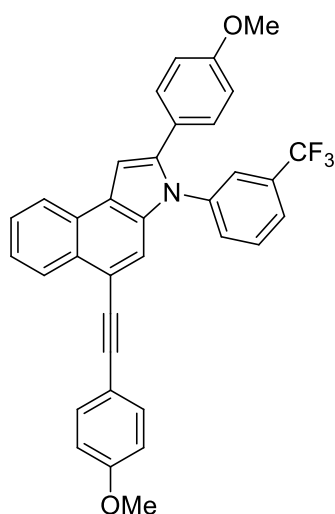
2-(4-Methoxyphenyl)-5-((4-methoxyphenyl)ethynyl)-3-phenyl-3H-benzo[e]indole (3g)



Following the general procedure C, **3g** was obtained as a yellow solid (42 %), mp = 185 – 186 °C. ¹H NMR (250 MHz, CDCl₃) δ 8.66 – 8.49 (m, 1H, CH_{Ar}), 8.37 – 8.32 (m, 1H, CH_{Ar}), 7.74 – 7.23 (m, 13H, CH_{Ar}), 6.98 – 6.79 (m, 4H, CH_{Ar}), 3.86 (s, 3H, OCH₃), 3.82 (s, 3H, OCH₃). ¹³C NMR (63 MHz, CDCl₃) δ 159.5, 159.0, 140.3, 138.1, 134.5 (C_{Ar}), 132.9, 130.1 (2 CH_{Ar}), 129.0 (C_{Ar}), 129.5, 128.3 (2 CH_{Ar}), 127.7 (CH_{Ar}), 127.6 (C_{Ar}), 127.0, 126.2 (CH_{Ar}), 124.8 (C_{Ar}), 124.3 (CH_{Ar}), 124.2 (C_{Ar}), 123.3, 116.4 (CH_{Ar}), 116.0, 115.1 (C_{Ar}), 114.0, 113.8 (2CH_{Ar}), 102.2 (CH_{Ar}), 92.9, 87.7 (C≡C), 55.3, 55.2 (OCH₃). IR (ATR, cm⁻¹), $\tilde{\nu}$ = 3047 (w), 2921 (w), 2850 (w), 1737 (w), 1731 (w),

1614 (w), 1596 (m), 1562 (w), 1529 (w), 1506 (s), 1498 (s), 1484 (s), 1456 (m), 1446 (m), 1430 (w), 1411 (w). MS (EI, 70 eV), m/z (%) = 481 (19), 480 (56), 479 (M^+ , 100), 464 (43), 392 (11), 240 (12), 218 (8), 196 (12), 130 (1). HR-MS (EI), Calcd for $C_{34}H_{25}NO_2$ (M^+), 479.18798, found 479.18701.

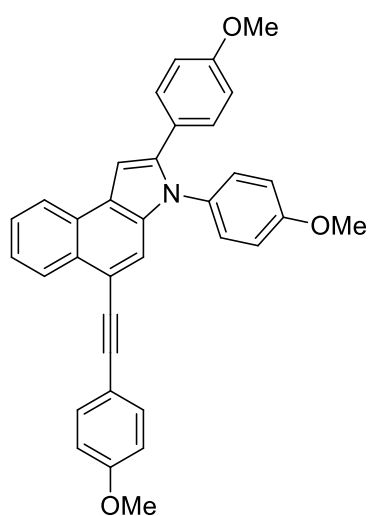
2-(4-methoxyphenyl)-5-((4-methoxyphenyl)ethynyl)-3-(3-(trifluoromethyl)phenyl)-3H-benzo[e]indole (3h)



Following the general procedure C, **3h** was obtained as a yellow solid (75 %), mp = 216 – 2178 °C. 1H NMR (250 MHz, $CDCl_3$) δ 8.59 – 8.49 (m, 1H, CH_{Ar}), 8.35 – 8.25 (m, 1H, CH_{Ar}), 7.72 – 7.43 (m, 9H, CH_{Ar}), 7.28 – 7.12 (m, 3H, CH_{Ar}), 6.92 – 6.77 (m, 4H, CH_{Ar}), 3.82 (s, 3H, OCH_3), 3.77 (s, 3H, OCH_3). ^{19}F NMR (235 MHz, $CDCl_3$) δ -62.55. ^{13}C NMR (63 MHz, $CDCl_3$) δ 159.6, 159.2, 140.3, 138.8, 134.3 (C_{Ar}), 133.0 (2 CH_{Ar}), 132.0 (q, $^2J = 33.0$ Hz, CCF_3), 131.6 (CH_{Ar}), 130.2 (2 CH_{Ar}), 130.1 (CH_{Ar}), 129.6, 127.6 (C_{Ar}), 127.1, 126.5 (CH_{Ar}), 125.1 (q, $^3J = 3.7$ Hz, CH_{Ar}), 124.6 (CH_{Ar}), 124.5 (C_{Ar}), 124.4 (q, $^3J = 3.8$ Hz, CH_{Ar}), 124.2 (C_{Ar}), 123.5 (q, $^1J = 275.36$ Hz, CF_3), 123.4 (CH_{Ar}), 115.8, 115.8 (C_{Ar}), 115.6 (CH_{Ar}), 114.1, 114.0 (2 CH_{Ar}), 103.0 (CH_{Ar}), 93.4, 87.5 ($C\equiv C$), 55.3, 55.2 (OCH_3). IR (ATR, cm^{-1}), $\tilde{\nu}$ = 3070 (w), 3037 (w), 2996 (w), 2952 (w), 2935 (w), 2908 (w), 2836 (w), 1604 (m), 1583 (m), 1565 (m), 1510 (s), 1486 (s), 1457 (s), 1438 (s), 1415 (w). MS (EI, 70 eV), m/z (%) = 549 (10), 548 (18), 547 (M^+ , 50), 532 (14), 499 (18), 497 (100), 483 (10), 482 (28). HRMS (ESI-TOF), Calcd for $C_{35}H_{24}F_3NO_2$ (M^+), 547.17587, found 547.17591.

2,3-Bis(4-methoxyphenyl)-5-((4-methoxyphenyl)ethynyl)-3H-benzo[e]indole (3i)

Following the general procedure C, **3i** was obtained as a yellow solid (65 %),

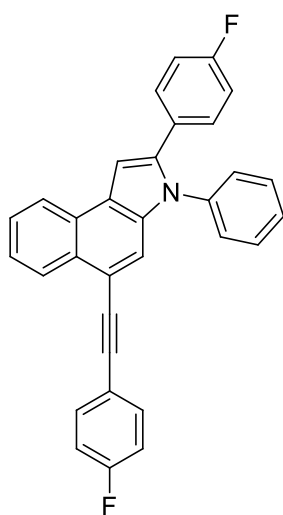


mp = 222 – 223 °C. ^1H NMR (300 MHz, CDCl_3) δ 8.43 (dd, $^3J = 8.1$ Hz, $^4J = 0.8$ Hz, 1H, CH_{Ar}), 8.22 (dd, $^3J = 8.0$ Hz, $^4J = 0.8$ Hz, 1H, CH_{Ar}), 7.57 – 7.40 (m, 5H, CH_{Ar}), 7.22 – 7.10 (m, 5H, CH_{Ar}), 6.91 – 6.69 (m, 6H, CH_{Ar}), 3.77 (s, 3H, OCH_3), 3.74 (s, 3H, OCH_3), 3.69 (s, 3H, OCH_3). ^{13}C NMR (75 MHz, CDCl_3) δ 159.6 (C_{Ar}), 159.1 (2C_{Ar}), 140.6, 135.0 (C_{Ar}), 133.0 (2CH_{Ar}), 131.0 (C_{Ar}), 130.2 (2CH_{Ar}), 129.6 (C_{Ar}), 129.5 (2CH_{Ar}), 127.7 (C_{Ar}), 127.2 (CH_{Ar}), 126.3 (C_{Ar}), 125.0 (CH_{Ar}), 124.4 (C_{Ar}), 124.1, 123.4, 116.6 (CH_{Ar}), 116.1, 115.1 (C_{Ar}), 114.8, 114.2, 113.9 (2CH_{Ar}), 101.9 (CH_{Ar}), 93.0, 87.9 ($\text{C}\equiv\text{C}$), 55.6, 55.4, 55.3

(OCH_3). IR (ATR, cm^{-1}), $\tilde{\nu} = 3000$ (w), 2954 (m), 2923 (s), 2852 (m), 2202 (w), 1724 (m), 1650 (w), 1600 (m), 1567 (m), 1556 (m), 1508 (s), 1456 (s), 1438 (m). MS (EI, 70 eV), m/z (%) = 511 (14), 510 (34), 509 (M^+ , 100), 494 (25), 479 (5), 255 (7), 189 (9), 44 (4), HR-MS (EI), Calcd for $\text{C}_{35}\text{H}_{27}\text{NO}_3$ (M^+), 509.19855, found 509.19782.

2-(4-Fluorophenyl)-5-((4-fluorophenyl)ethynyl)-3-phenyl-3H-benz[e]indole (3j)

Following the general procedure C, **3j** was obtained as a yellow solid (74 %), mp = 236 – 238 °C.

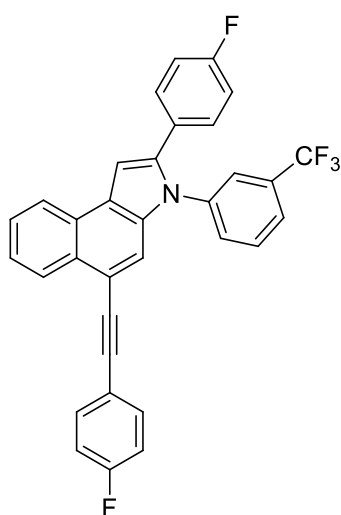


^1H NMR (300 MHz, CDCl_3) δ 8.49 (dd, $^3J = 8.2$ Hz, $^4J = 0.8$ Hz, 1H, CH_{Ar}), 8.35 – 8.29 (m, 1H, CH_{Ar}), 7.70 – 7.43 (m, 8H, CH_{Ar}), 7.35 – 7.27 (m, 5H, CH_{Ar}), 7.12 – 6.93 (m, 4H, CH_{Ar}). ^{19}F NMR (235 MHz, CDCl_3) δ -111.27, -114.06. ^{13}C NMR (63 MHz, CDCl_3) δ 163.4 (d, $^1J = 249.2$ Hz, CF), 161.4 (d, $^1J = 247.6$ Hz, CF), 139.7, 137.9, 134.8 (C_{Ar}), 133.5 (d, $^3J = 8.3$ Hz, 2CH_{Ar}), 130.7 (d, $^3J = 8.1$ Hz, 2CH_{Ar}), 129.7 (2CH_{Ar}), 129.6 (C_{Ar}), 128.5 (d, $^4J = 3.4$ Hz, C_{Ar}), 128.3 (2CH_{Ar}), 128.1 (CH_{Ar}), 127.8 (C_{Ar}), 127.1, 126.6, 124.7 (CH_{Ar}), 124.5 (C_{Ar}), 123.5 (CH_{Ar}), 120.0 (d, $^4J = 3.5$ Hz, C_{Ar}), 116.8 (CH_{Ar}), 115.8 (d, $^2J = 21.2$ Hz, 2CH_{Ar}), 115.5 (d, $^2J = 22.8$ Hz, 2CH_{Ar}), 115.3 (C_{Ar}),

103.1 (CH_{Ar}), 92.2, 88.8 ($\text{C}\equiv\text{C}$). IR (ATR, cm^{-1}), $\tilde{\nu} = 3050$ (w), 2921 (w), 2852 (w), 1596 (m), 1562 (w), 1529 (w), 1506 (s), 1498 (s), 1484 (s), 1456 (m), 1446 (m), 1430 (m). MS (EI, 70 eV),

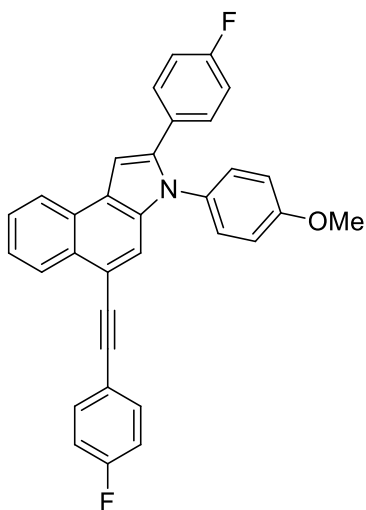
m/z (%) = 456 (43), 455 (M^+ , 100), 407 (2), 281 (10), 217 (35), 166 (11), 73 (8), 44 (3). HRMS (ESI-TOF), calcd for $C_{32}H_{19}NF_2$ ($[M+H]^+$), 456.15583, found, 456.15445.

2-(4-Fluorophenyl)-5-((4-fluorophenyl)ethynyl)-3-(4-(trifluoromethyl)phenyl)-3H-benzo[e]indole (3k)



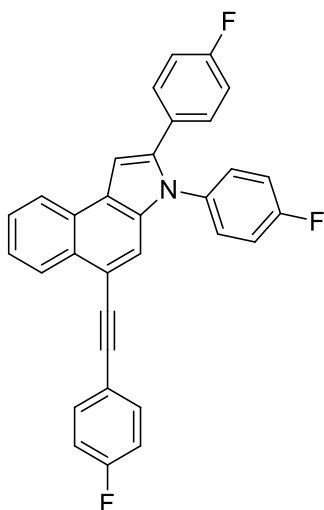
Following the general procedure C, **3k** was obtained as a yellow solid (45 %), mp = 243 – 244 °C. 1H NMR (300 MHz, DMSO) δ 8.50 (d, $^3J = 7.5$ Hz, 1H, CH_{Ar}), 8.46 (d, $^3J = 7.6$ Hz, 1H, CH_{Ar}), 7.92 – 7.61 (m, 10H, CH_{Ar}), 7.41 – 7.19 (m, 6H, CH_{Ar}). ^{19}F NMR (235 MHz, DMSO) δ -61.42, -111.04, -113.72. ^{13}C NMR (63 MHz, DMSO) δ 162.1 (d, $^1J = 247.8$ Hz, CF), 161.9 (d, $^1J = 246.5$ Hz, CF), 139.9, 138.2, 134.3 (C_{Ar}), 133.5 (d, $^3J = 8.5$ Hz, $2CH_{Ar}$), 132.2, 132.2 (CH_{Ar}), 131.8 (q, $^2J = 34.2$ Hz, CCF_3), 131.0 (CH_{Ar}), 130.9 (d, $^3J = 8.3$ Hz, $2CH_{Ar}$), 129.0 (C_{Ar}), 128.0 (d, $^4J = 3.3$ Hz, C_{Ar}), 127.4 (C_{Ar}), 126.5 (d, $^2J = 24.0$ Hz, $2CH_{Ar}$), 125.0 (q, $^3J = 3.7$ Hz, CH_{Ar}), 124.9 (q, $^3J = 3.9$ Hz, CH_{Ar}), 124.4 (C_{Ar}), 123.6 (CH_{Ar}), 119.3 (d, $^4J = 3.4$ Hz, C_{Ar}), 119.0 (q, $^1J = 276.4$ Hz, CF_3), 115.9 (CH_{Ar}), 115.8 (d, $^2J = 22.5$ Hz, $2CH_{Ar}$), 115.4, 115.1 (CH_{Ar}), 114.7 (C_{Ar}), 104.0 (CH_{Ar}), 92.3, 88.4 ($C\equiv C$). IR (ATR, cm^{-1}), $\tilde{\nu} = 3070$ (w), 2921 (w), 2852 (w), 2202 (w), 1612 (w), 1598 (m), 1583 (w), 1562 (w), 1506 (s), 1484 (s), 1459 (m), 1440 (m). MS (EI, 70 eV) = m/z (%) = 525 (9), 524 (53), 523 (M^+ , 100), 453 (2), 377(2), 262 (7), 227 (2), 144 (1). HR-MS (EI), Calcd for $C_{33}H_{18}NF_5$ (M^+), 523.13539, found 523.13481.

2-(4-Fluorophenyl)-5-((4-fluorophenyl)ethynyl)-3-(4-methoxyphenyl)-3H-benzo[e]indole (3l)



Following the general procedure C, **3l** was obtained as a yellow solid (66 %), mp = 197 – 198 °C. ^1H NMR (250 MHz, CDCl_3) δ 8.50 (dd, $^3J = 8.1$ Hz, $^4J = 1.0$ Hz, 1H, CH_{Ar}), 8.35 – 8.29 (m, 1H, CH_{Ar}), 7.72 – 7.51 (m, 5H, CH_{Ar}), 7.34 – 7.20 (m, 5H, CH_{Ar}), 7.14 – 6.91 (m, 6H, CH_{Ar}), 3.88 (s, 3H, OCH_3). ^{19}F NMR (235 MHz, CDCl_3) δ -111.33, -114.19. ^{13}C NMR (63 MHz, CDCl_3) δ 162.5 (d, $^1J = 249.2$ Hz, CF), 162.3 (d, $^1J = 247.8$ Hz, CF), 159.3, 139.8, 135.1 (C_{Ar}), 133.5 (d, $^3J = 8.3$ Hz, 2CH_{Ar}), 130.6 (d, $^3J = 8.0$ Hz, 2CH_{Ar}), 130.6, 129.5 (C_{Ar}), 129.4 (2CH_{Ar}), 128.6 (d, $^4J = 3.4$ Hz, C_{Ar}), 127.8 (C_{Ar}), 127.1, 126.6, 124.6 (CH_{Ar}), 124.3 (C_{Ar}), 123.5 (CH_{Ar}), 120.0 (d, $^4J = 3.5$ Hz, C_{Ar}), 116.9 (CH_{Ar}), 115.8 (d, $^2J = 22.1$ Hz, 2CH_{Ar}), 115.5 (d, $^2J = 21.6$ Hz, 2CH_{Ar}), 115.1 (C_{Ar}), 114.9 (2CH_{Ar}), 102.6 (CH_{Ar}), 92.1, 88.8 ($\text{C}\equiv\text{C}$), 55.7 (OCH_3). IR (ATR, cm^{-1}), $\tilde{\nu} = 3049$ (w), 2956 (w), 2923 (w), 2850 (w), 1612 (w), 1600 (w), 1583 (w), 1506 (s), 1483 (s), 1452 (m), 1440 (m). MS (EI, 70 eV), m/z (%) = 487 (13), 486 (40), 485 (M^+ , 100), 470 (7), 440 (10), 346 (6), 320 (6), 210 (9), 173 (4), 110 (6), 71 (4), 44 (36). HR-MS (EI), Calcd for $\text{C}_{33}\text{H}_{21}\text{NOF}_2$ (M^+), 485.15857, found 485.15792.

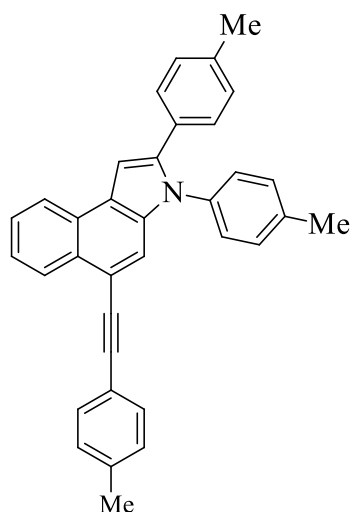
2,3-Bis(4-fluorophenyl)-5-((4-fluorophenyl)ethynyl)-3H-benzo[e]indole (3m)



Following the general procedure C, **3m** was obtained as a yellow solid (65 %), mp = 234 – 235 °C. ^1H NMR (250 MHz, DMSO) δ 8.09 – 7.98 (m, 2H, CH_{Ar}), 7.33 – 7.16 (m, 4H, CH_{Ar}), 7.12 (d, $^3J = 3.4$ Hz, 2H, CH_{Ar}), 7.07 – 6.89 (m, 6H, CH_{Ar}), 6.83 – 6.67 (m, 4H, CH_{Ar}). ^{19}F NMR (235 MHz, DMSO) δ -111.09, -113.11, -113.93. ^{13}C NMR (63 MHz, DMSO) δ 161.5 (d, $^1J = 247.83$ Hz, CF), 161.3 (d, $^1J = 247.26$ Hz, CF), 161.0 (d, $^1J = 247.07$ Hz, CF), 139.4, 134.1 (C_{Ar}), 133.1 (d, $^4J = 3.1$ Hz, C_{Ar}), 132.9 (d, $^3J = 8.5$ Hz, 2CH_{Ar}), 130.2 (d, $^3J = 8.3$ Hz, 2CH_{Ar}), 129.8 (d, $^3J = 8.9$ Hz, 2CH_{Ar}), 128.3 (C_{Ar}), 127.6 (d, $^4J = 3.4$ Hz, C_{Ar}), 126.9 (C_{Ar}), 126.0, 125.7 (CH_{Ar}), 124.2 (C_{Ar}), 123.6 (C_{Ar}), 123.0 (CH_{Ar}), 118.8 (d, $^4J = 3.5$ Hz, C_{Ar}), 115.9 (d, $^2J = 23.0$ Hz, 2CH_{Ar}), 115.6 (CH_{Ar}), 115.2 (d, $^2J = 22.2$ Hz, 2CH_{Ar}), 114.6 (d, $^2J = 21.8$ Hz, 2CH_{Ar}), 113.9, 102.7 (CH_{Ar}), 91.6, 87.9 ($\text{C}\equiv\text{C}$). IR (ATR, cm^{-1}), $\tilde{\nu} = 3064$ (m), 2921 (m), 2850 (m), 1598 (m), 1506 (s), 1486 (s), 1432 (m), 1417 (m). MS (EI, 70 eV), m/z (%) = 475 (9), 474 (35), 473 (M^+ , 100), 429 (8),

351 (14), 281 (9), 221 (10), 147 (8), 73 (14), 44 (12). HR-MS (EI), Calcd for C₃₂H₁₈NF₃ (M⁺), 473.13859, found 473.13801.

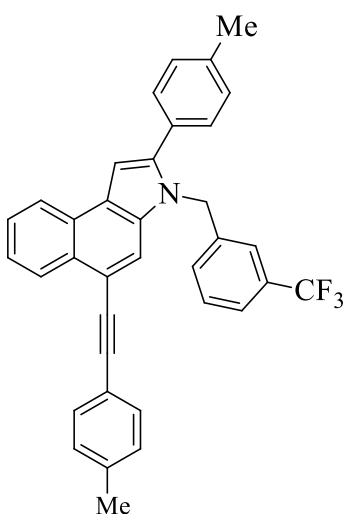
2,3-Di-*p*-tolyl-5-(*p*-tolylethynyl)-3*H*-benzo[*e*]indole (3n)



Following the general procedure C, **3n** was obtained as a yellow solid (57 %), mp = 182 – 183 °C. ¹H NMR (250 MHz, CDCl₃) δ 8.56 – 8.49 (m, 1H, CH_{Ar}), 8.36 – 8.28 (m, 1H, CH_{Ar}), 7.69 – 7.49 (m, 5H, CH_{Ar}), 7.33 – 7.26 (m, 3H, CH_{Ar}), 7.25 – 7.16 (m, 6H, CH_{Ar}), 7.09 (d, ³J = 8.0 Hz, 2H, CH_{Ar}), 2.45 (s, 3H, CH₃), 2.39 (s, 3H, CH₃), 2.34 (s, 3H, CH₃). ¹³C NMR (63 MHz, CDCl₃) δ 140.8, 138.2, 137.8, 137.3, 135.6, 135.0 (C_{Ar}), 131.5, 130.2 (2CH_{Ar}), 129.6 (2C_{Ar}), 129.3, 129.2, 128.8, 128.1 (2CH_{Ar}), 127.8 (C_{Ar}), 127.2, 126.4, 124.5 (CH_{Ar}), 124.3 (C_{Ar}), 123.4 (CH_{Ar}), 120.9 (C_{Ar}), 116.8 (CH_{Ar}), 115.2 (C_{Ar}), 102.6 (CH_{Ar}), 93.3, 88.6 (C≡C), 21.7 (CH₃), 21.4 (2CH₃). IR (ATR, cm⁻¹), $\tilde{\nu}$ = 3029 (w), 2919 (w), 2850 (w), 1704 (w), 1699 (w), 1693 (w), 1683 (w), 1673 (w), 1668 (w), 1658 (w), 1650 (w), 1608 (w), 1587 (w), 1558 (w), 1510 (s). MS (EI, 70 eV), m/z (%) = 464 (14), 464 (48), 462 (44), 461 (M⁺, 100), 445 (4), 360 (8), 329 (12). HR-MS (EI), Calcd for C₃₅H₂₇N (M⁺), 461.21380, found 461.21295.

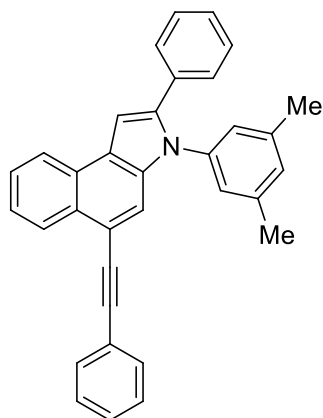
2-(*p*-Tolyl)-5-(*p*-tolylethynyl)-3-(3-(trifluoromethyl)benzyl)-3*H*-benzo[*e*]indole (3o)

Following the general procedure C, **3o** was obtained as a yellow solid (60 %), mp = 1181 – 182 °C. ¹H NMR (250 MHz, CDCl₃) δ 8.53 (dd, ³J = 8.1 Hz, ⁴J = 1.0 Hz, 1H, CH_{Ar}), 8.30 (dd, ³J = 7.9 Hz, ⁴J = 1.0 Hz, 1H, CH_{Ar}), 7.69 – 7.45 (m, 6H, CH_{Ar}), 7.43 – 7.28 (m, 4H, CH_{Ar}), 7.20 (m, 5H, CH_{Ar}), 7.08 (d, ³J = 7.8 Hz, 1H, CH_{Ar}), 5.53 (s, 2H, CH₂), 2.41 (s, 3H, CH₃), 2.39 (s, 3H, CH₃). ¹⁹F NMR (235 MHz, CDCl₃) δ -62.65. ¹³C NMR (63 MHz, CDCl₃) δ 141.4, 139.1, 138.3, 138.2, 133.3 (C_{Ar}), 131.8 (q, ²J = 32.6 Hz, CCF₃), 131.4 (2CH_{Ar}), 129.5 (CH_{Ar}), 129.5 (2CH_{Ar}), 129.3, 129.6 (C_{Ar}), 129.2 (CH_{Ar}), 129.2, 129.1 (2CH_{Ar}), 127.8 (C_{Ar}), 127.1, 126.4 (CH_{Ar}), 124.5 (C_{Ar}), 124.4 (CH_{Ar}), 124.3 (q, ³J = 3.8 Hz, CH_{Ar}), 124.1 (q, ¹J = 276.0 Hz, CF₃), 123.2 (CH_{Ar}), 122.8 (q, ³J = 3.8 Hz, CH_{Ar}), 120.6 (C_{Ar}), 115.8 (CH_{Ar}), 115.2 (C_{Ar}), 102.3 (CH_{Ar}), 93.3, 88.3 (C≡C), 47.3 (CH₂), 21.5, 21.2



(CH₃).IR (ATR, cm⁻¹), $\tilde{\nu}$ = 3060 (w), 3027 (w), 2995 (w), 2956 (w), 2921 (w), 2863 (w), 1616 (w), 1589 (w), 1564 (w), 1510 (m), 1488 (m), 1444 (m), 1430 (w). MS (EI, 70 eV), m/z (%) = 531 (8), 530 (41), 529 (M⁺, 100), 370 (48), 159 (10). HR-MS (ESI-TOF/MS), Calcd for C₃₆H₂₆NF₃ (M+H)⁺, 530.20901, found 530.20797.

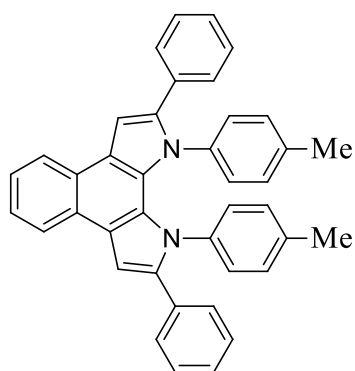
3-(3,5-Dimethylphenyl)-2-phenyl-5-(phenylethynyl)-3H-benzo[e]indole (3p)



Following the general procedure, **3b** was obtained as a yellow solid (96 mg, 74 %), mp = 176 – 178 °C. ¹H NMR (250 MHz, CDCl₃) δ 8.55 – 8.43 (m, 1H, CH_{Ar}), 8.29 – 8.21 (m, 1H, CH_{Ar}), 7.65 – 7.61 (m, 1H, CH_{Ar}), 7.59 – 7.44 (m, 4H, CH_{Ar}), 7.35 – 7.10 (m, 9H, CH_{Ar}), 6.97 (s, 1H, CH_{Ar}), 6.86 (s, 2H, CH_{Ar}), 2.25 (s, 6H, 2CH₃). ¹³C NMR (63 MHz, CDCl₃) δ 140.6 (C_{Ar}), 139.3 (2C_{Ar}), 138.0, 135.1, 132.5(C_{Ar}), 131.6 (2CH_{Ar}), 129.8 (CH_{Ar}), 129.6 (C_{Ar}), 128.8, 128.5, 128.3 (2CH_{Ar}), 128.1 (CH_{Ar}), 127.8 (C_{Ar}), 127.4, 127.1, 126.4 (CH_{Ar}), 126.0 (2CH_{Ar}), 124.5 (CH_{Ar}), 124.4, 123.9 (C_{Ar}), 123.5, 117.1 (CH_{Ar}), 115.0 (C_{Ar}), 102.9 (CH_{Ar}), 93.2, 89.4 (C≡C), 21.4 (2CH₃). IR (ATR, cm⁻¹), $\tilde{\nu}$ = 3060 (w), 2918 (w), 1644 (m), 1589 (s), 1505 (s), 1218 (s), 1155 (m), 1090 (m). MS (EI, 70 eV), m/z (%) = 449 (17), 448 (60), 447 (M⁺, 100), 431 (4), 315 (6), 324 (5). HR-MS (EI), Calcd for C₃₄H₂₅N (M⁺), 447.19815, found 447.19765.

2,9-Diphenyl-1,10-di-*p*-tolyl-1,10-dihydrobenzo[e]pyrrolo[3,2-*g*]indole (5a)

Following the general procedure C, **5a** was obtained as a yellow solid (35 %), mp = 166 – 168 °C.

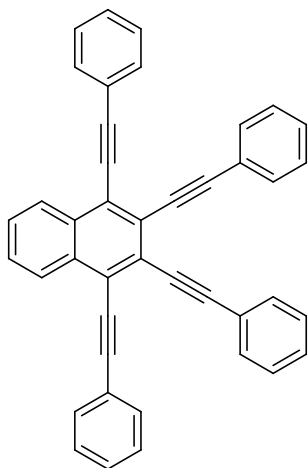


¹H NMR (300 MHz, CDCl₃) δ 8.36 – 8.26 (m, 2H, CH_{Ar}), 7.56 – 7.50 (m, 2H, CH_{Ar}), 7.24 (s, 2H, CH_{Ar}), 7.20 – 7.08 (m, 6H, CH_{Ar}), 7.07 – 6.94 (m, 4H, CH_{Ar}), 6.65 (d, ³J = 8.0 Hz, 4H, CH_{Ar}), 6.41 (m, 4H, CH_{Ar}), 2.23 (s, 6H, 2CH₃). ¹³C NMR (75 MHz, CDCl₃) δ 140.8, 138.2, 136.5, 134.0 (2C_{Ar}), 130.6, 129.2, 128.1, 128.1 (4CH_{Ar}), 127.5 (2CH_{Ar}), 125.9, 125.8 (2C_{Ar}), 124.5, 123.7 (2CH_{Ar}), 123.7 (2C_{Ar}), 105.8 (2CH_{Ar}), 21.7 (2CH₃).

IR (ATR, cm^{-1}), $\tilde{\nu} = 2915$ (w), 2850 (w), 2740 (w), 1899 (w), 1666 (w), 1656 (w), 1596 (m), 1585 (m), 1573 (w), 1548 (w), 1510 (s), 1479 (m), 1444 (m). HR-MS (ESI-TOF/MS), Calcd for $\text{C}_{40}\text{H}_{30}\text{N}_2$ (M^+), 538.24021, found 538.24021.

1,2,3,4-tetrakis(phenylethynyl)naphthalene (6a)

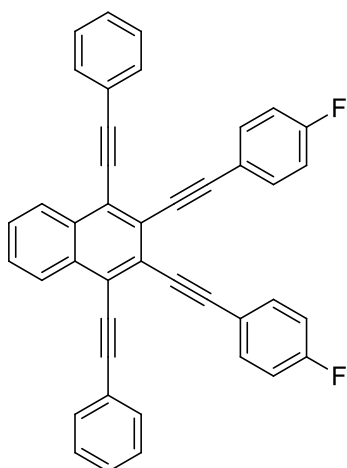
Following the general procedure, **6a** was obtained as a yellow solid (79 %), mp = 166 – 168 °C.



^1H NMR (300 MHz, CDCl_3) δ 8.49 - 8.41 (m, 2H, CH_{Ar}), 7.77 – 7.60 (m, 10H, CH_{Ar}), 7.47 – 7.31 (m, 12H, CH_{Ar}). ^{13}C NMR (75 MHz, CDCl_3) δ 132.1 (2C_{Ar}), 131.8, 131.8 (4CH_{Ph}), 128.8, 128.7 (2CH_{Ar}), 128.5, 128.5 (4CH_{Ph}), 128.2, 126.9 (2CH_{Ar}), 125.7, 124.1, 123.5, 123.2 (2C_{Ar}), 100.6, 98.1, 88.1, 86.7 ($2\text{C}\equiv\text{C}$). IR (ATR, cm^{-1}), $\tilde{\nu} = 2206$ (m), 1943 (w), 1899 (w), 1886 (w), 1828 (w), 1801 (w), 1754 (w), 1673 (w), 1594 (m), 1569 (m), 1533 (m), 1513 (w), 1488 (s), 1454 (m), 1440 (m). MS (EI, 70 eV), m/z (%) = 530 (20), 529 (43), 528 ($[\text{M}]^+$, 100), 527 (10), 524 (12), 450 (16), 224 (10), 155

(7). HR-MS (EI), Calcd for $\text{C}_{42}\text{H}_{24}$ (M^+), 528.18725, found 528.18713.

2,3-bis((4-fluorophenyl)ethynyl)-1,4-bis(phenylethynyl)naphthalene (6b)

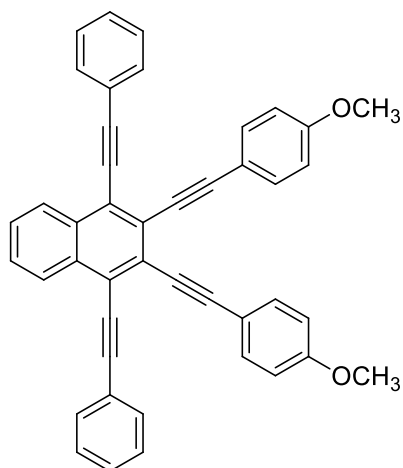


Following the general procedure, **6b** was obtained as a white solid (71 %), mp = 208 – 209 °C.¹ ^1H NMR (300 MHz, CDCl_3) δ 8.38 – 8.28 (m, 2H, CH_{Ar}), 7.65 – 7.47 (m, 10H, CH_{Ar}), 7.37 – 7.29 (m, 6H, CH_{Ar}), 7.02 – 6.93 (m, 4H, CH_{Ar}). ^{19}F NMR (282 MHz, CDCl_3) δ 110.10 ^{13}C NMR (75 MHz, CDCl_3) δ 162.9 (d, $^1J = 250.4$ Hz, 2CF), 133.8 (d, $^3J = 8.4$ Hz, 4CH_{Ar}), 132.2 (2C_{Ar}), 131.9 (4CH_{Ar}), 129.1 (2CH_{Ar}), 128.7 (4CH_{Ar}), 128.3, 127.0 (2CH_{Ar}), 125.5, 124.3, 123.3 (2C_{Ar}), 119.7 (d, $^4J = 3.5$ Hz, 2C_{Ar}), 116.0 (d, $^2J = 22.1$ Hz, 4CH_{Ar}), 100.8, 97.0, 88.0, 86.8

($2\text{C}\equiv\text{C}$). IR (ATR, cm^{-1}), $\tilde{\nu} = 3058$ (m), 3022 (w), 2962 (w), 1596 (m), 1538 (w), 1510 (s), 1490 (s). MS (EI, 70 eV), m/z (%) = 466 (14), 565 (41), 564 ($[\text{M}]^+$, 100), 486 (11), 66 (18), 44 (22).

HR-MS (EI), Calcd for $\text{C}_{42}\text{H}_{22}\text{F}_2$ (M^+), 564.16841, found 564.16689.

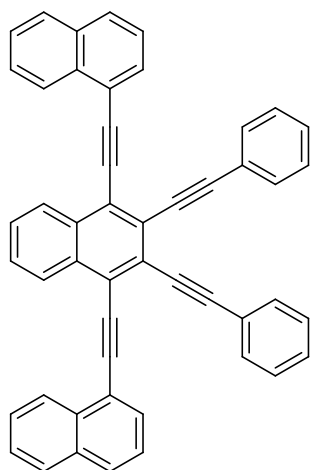
2,3-bis((4-methoxyphenyl)ethynyl)-1,4-bis(phenylethynyl)naphthalene (6c)



Following the general procedure, **6c** was obtained as a yellow solid (61 %), mp = 198 – 200 °C. ¹H NMR (250 MHz, CDCl₃) δ 8.48 – 8.37 (m, 2H, CH_{Ar}), 7.71 (m, 4H, CH_{Ar}), 7.65 – 7.56 (m, 6H, CH_{Ar}), 7.47 – 7.36 (m, 6H, CH_{Ar}), 6.96 – 6.85 (m, 4H, CH_{Ar}), 3.85 (s, 6H, 2OCH₃). ¹³C NMR (63 MHz, CDCl₃) δ 160.1 (2C_{Ar}), 133.5 (4CH_{Ar}), 132.1 (2C_{Ar}), 131.9 (4CH_{Ar}), 128.9 (2CH_{Ar}), 128.6 (4CH_{Ar}), 128.0, 127.0 (2CH_{Ar}), 126.1, 123.8, 123.5, 115.8 (2C_{Ar}), 114.3 (4CH_{Ar}), 100.5, 98.4, 87.3, 87.0 (2C≡C), 55.5 (2OCH₃). IR (ATR, cm⁻¹), $\tilde{\nu}$ = 3074 (w), 3058 (w), 2991. (w), 2958 (w), 2933 (w), 2910 (w), 2833 (w), 2194 (m), 1604 (m), 1569 (w), 1533 (m). MS (EI, 70 eV), m/z (%) = 590 (10), 589 (26), 588 ([M]⁺, 59), 545 (4), 424 (4), 249 (10), 97 (4), 66 (17), 44 (100). HR-MS (EI), Calcd for C₄₄H₂₈O₂ (M⁺), 588.20838, found 588.20702.

1,1'-((2,3-bis(phenylethynyl)naphthalene-1,4-diyl)bis(ethyne-2,1-diyl))dinaphthalene (6d)

(6d)

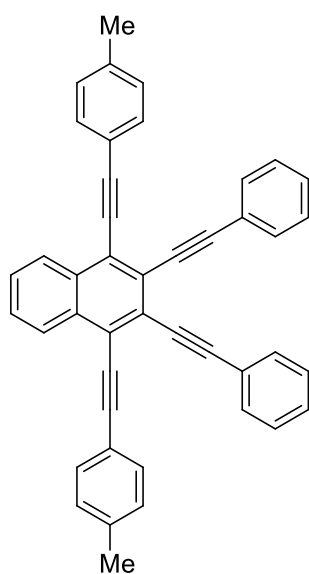


Following the general procedure, **6d** was obtained as a yellow solid (63 %), mp = 266 – 268 °C. ¹H NMR (300 MHz, CDCl₃) δ 8.73 (d, ³J = 8.2 Hz, 2H, 2CH_{Ar}), 8.67 – 8.60 (m, 2H, CH_{Ar}), 8.01 (dd, ³J = 7.2 Hz, ³J = 1.1 Hz, 2H, CH_{Ar}), 7.91 (t, ³J = 8.2 Hz, 4H, CH_{Ar}), 7.77 – 7.71 (m, 2H, CH_{Ar}), 7.68 – 7.64 (m, 4H, CH_{Ar}), 7.57 – 7.47 (m, 4H, CH_{Ar}), 7.39 – 7.27 (m, 8H, CH_{Ar}). ¹³C NMR (75 MHz, CDCl₃) δ 133.4 (4C_{Ar}), 133.4 (2C_{Ar}), 132.4 (4CH_{Ar}), 131.2, 129.6, 128.8 (2CH_{Ar}), 128.5 (6CH_{Ar}), 128.4, 127.4, 127.2, 126.8, 126.7 (2CH_{Ar}), 125.9 (2C_{Ar}), 125.5 (2CH_{Ar}), 124.3, 123.4, 121.0 (2C_{Ar}), 99.2, 98.5, 91.6, 88.6 (2C≡C).

IR (ATR, cm⁻¹), $\tilde{\nu}$ = 2956 (m), 2923 (m), 2210 (m), 2198 (m), 1934 (m), 1918 (w), 1822 (w), 1803 (m), 1702 (w), 1598 (m), 1585 (m), 1575 (m), 1538 (m), 1504 (m), 1488 (m). MS (EI, 70 eV), m/z (%) = 628 ([M]⁺, 5), 429 (2), 281 (6), 267 (4), 207 (13), 57 (29), 44 (100). HR-MS (EI), Calcd for C₅₀H₂₈ (M⁺), 628.21855, found 628.21810.

2,3-bis(phenylethynyl)-1,4-bis(*p*-tolylethynyl)naphthalene (6e)

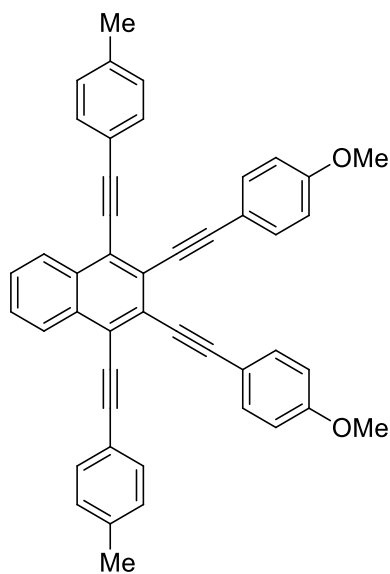
Following the general procedure, **6e** was obtained as a yellow solid (54 %), mp = 196 – 197 °C.



$^1\text{H NMR}$ (300 MHz, CDCl_3) δ 8.50 – 8.37 (m, 2H, CH_{Ar}), 7.77 – 7.52 (m, 10H, CH_{Ar}), 7.44 – 7.34 (m, 6H, CH_{Ar}), 7.22 (d, $^3J = 7.9$ Hz, 4H, CH_{Ar}), 2.42 (s, 6H, 2 CH_3). $^{13}\text{C NMR}$ (75 MHz, CDCl_3) δ 139.2, 132.2 (2 C_{Ar}), 132.0, 131.8, 129.4 (4 CH_{Ar}), 128.7 (2 CH_{Ar}), 128.6 (4 CH_{Ar}), 128.2, 127.1 (2 CH_{Ar}), 125.6, 124.3, 123.7, 120.3 (2 C_{Ar}), 101.0, 98.0, 88.4, 86.3 (2 $\text{C}\equiv\text{C}$), 21.8 (2 CH_3). IR (ATR, cm^{-1}), $\tilde{\nu} = 3056$ (w), 3041 (w), 3029 (w), 2917 (w), 2852 (w), 2200 (w), 1731 (w), 1724 (w), 1594 (w), 1569 (w), 1533 (w), 1508 (m), 1488 (m), 1463 (w), 1440 (m), 1405 (w). MS (EI, 70 eV), m/z (%) = 557 (6), 556 ($[\text{M}]^+$, 12), 57 (7). 464 (1), 262 (1), 169 (1), 154 (2), 104 (1) 43 (100), . HR-MS (EI), Calcd for $\text{C}_{44}\text{H}_{28}$ (M^+), 556.21855, found

556.21681.

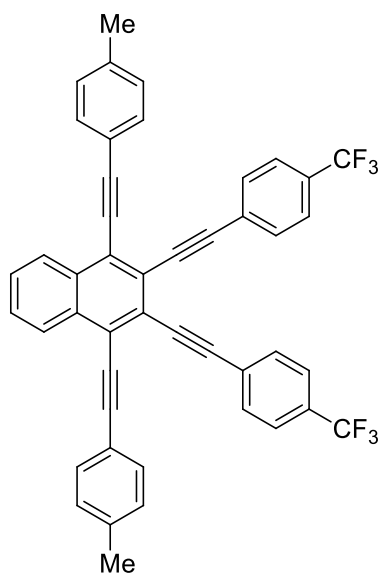
2,3-bis((4-methoxyphenyl)ethynyl)-1,4-bis(*p*-tolylethynyl)naphthalene (6f)



Following the general procedure, **6f** was obtained as a yellow solid (51 %), mp = 224 – 225 °C. $^1\text{H NMR}$ (300 MHz, CDCl_3) δ 8.53 – 8.34 (m, 2H, CH_{Ar}), 7.68 – 7.55 (m, 10H, CH_{Ar}), 7.33 – 7.16 (m, 4H, CH_{Ar}), 6.98 – 6.80 (m, 4H, CH_{Ar}), 3.86 (s, 6H, 2 OCH_3), 2.42 (s, 6H, 2 CH_3). $^{13}\text{C NMR}$ (63 MHz, CDCl_3) δ 159.9, 139.0 (2 C_{Ar}), 133.3 (4 CH_{Ar}), 132.0 (2 C_{Ar}), 131.7, 129.3 (4 CH_{Ar}), 127.8, 126.8 (2 CH_{Ar}), 125.8, 123.7, 120.3, 115.8 (2 C_{Ar}), 114.1 (4 CH_{Ar}), 100.6, 98.0, 87.2, 86.3 (2 $\text{C}\equiv\text{C}$), 55.3 (2 OCH_3), 21.6 (2 CH_3). IR (ATR, cm^{-1}), $\tilde{\nu} = 3056$ (w), 3031 (w), 2989 (w), 2915 (w), 2208 (w), 1606 (w), 1573 (w), 1564 (w), 1513 (m), 1481 (m), 1461 (w), 1450 (m), 1434 (s).

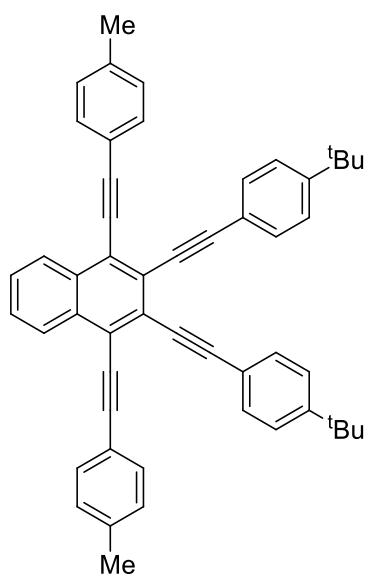
MS (EI, 70 eV), m/z (%) = 617 (14), 616 ($[\text{M}]^+$, 30), 57 (5), 43 (100), 42 (39), 41 (61). HR-MS (EI), Calcd for $\text{C}_{46}\text{H}_{32}\text{O}_2$ (M^+), 616.23968, found 616.23954.

1,4-bis(*p*-tolylethynyl)-2,3-bis((4-(trifluoromethyl)phenyl)ethynyl)naphthalene (6g)



Following the general procedure, **6g** was obtained as a yellow solid (52 %), mp = 242 – 243 °C. $^1\text{H NMR}$ (300 MHz, CDCl_3) δ 8.43 – 8.33 (m, 2H, CH_{Ar}), 7.72 – 7.49 (m, 14H, CH_{Ar}), 7.21 (d, $^3J = 7.9$ Hz, 4H, CH_{Ar}), 2.43 (s, 6H, 2 CH_3). $^{19}\text{F NMR}$ (282 MHz, CDCl_3) δ -62.8. $^{13}\text{C NMR}$ (63 MHz, CDCl_3) δ 139.6, 132.3 (2 C_{Ar}), 132.0, 131.8 (4 CH_{Ar}), 130.4 (q, $^2J = 33.7$ Hz, 2 CCF_3), 129.5 (4 CH_{Ar}), 128.6 (2 CH_{Ar}), 127.4 (2 C_{Ar}), 127.2 (2 CH_{Ar}), 125.6 (q, $^3J = 3.8$ Hz, 4 CH_{Ar}), 125.0, 124.6 (2 C_{Ar}), 123.3 (q, $^1J = 243.8$ Hz, 2 CF_3), 120.1 (2 C_{Ar}), 101.5, 96.2, 90.5, 86.0 (2 $\text{C}\equiv\text{C}$), 21.8 (2 CH_3). IR (ATR, cm^{-1}), $\tilde{\nu} = 2919$ (w), 2861 (w), 2200 (w), 1610 (m), 1537 (w), 1510 (m), 1488 (m), 1463 (w), 1440 (m), 1405 (w). MS (EI, 70 eV), m/z (%) = 693 (17), 692 ($[\text{M}]^+$, 38), 673 (1), 532 (1), 461 (1), 57 (7), 43 (100). HR-MS (EI), Calcd for $\text{C}_{46}\text{H}_{26}\text{F}_6$ (M^+), 692.68906, found 692.68742.

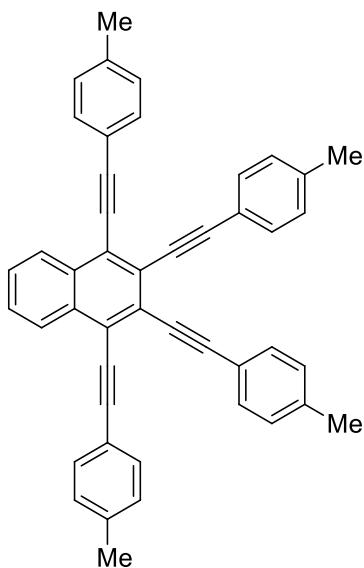
2,3-bis((4-(tert-butyl)phenyl)ethynyl)-1,4-bis(p-tolylethynyl)naphthalene (6h)



Following the general procedure, **6h** was obtained as a yellow solid (54 %), mp = 230 – 231 °C. $^1\text{H NMR}$ (300 MHz, CDCl_3) δ 8.47 – 8.41 (m, 2H, CH_{Ar}), 7.66 – 7.58 (m, 10H, CH_{Ar}), 7.40 (d, $^3J = 8.4$ Hz, 4H, CH_{Ar}), 7.23 (d, $^3J = 7.9$ Hz, 4H, CH_{Ar}), 2.42 (s, 6H, 2 CH_3), 1.37 (s, 18H, 6 CH_3). $^{13}\text{C NMR}$ (63 MHz, CDCl_3) δ 152.0, 139.1, 132.2 (2 C_{Ar}), 131.8, 131.7, 129.4 (4 CH_{Ar}), 128.0, 127.0 (2 CH_{Ar}), 125.8 (2 C_{Ar}), 125.5 (4 CH_{Ar}), 124.1, 120.8, 120.5 (2 C_{Ar}), 100.8, 98.3, 87.9, 86.5 (2 $\text{C}\equiv\text{C}$), 35.0 (2 $\text{C}(\text{CH}_3)_3$), 31.4 (6 CH_3), 21.8. (2 CH_3). IR (ATR, cm^{-1}), $\tilde{\nu} = 3076$ (w), 3058 (w), 3029 (w), 2960 (m), 2902 (m), 2863 (m), 2204 (w), 1658 (w), 1650 (w), 1606 (w), 1537 (m), 1508 (m). MS (EI, 70 eV), m/z (%) = 669 (7), 668 ($[\text{M}]^+$, 13), 44 (17), 43 (100), 42 (40), 41 (67). HR-MS (EI), Calcd for $\text{C}_{52}\text{H}_{44}$ (M^+), 668.34375, found 668.34478.

1,2,3,4-tetrakis(p-tolylethynyl)naphthalene (6i)

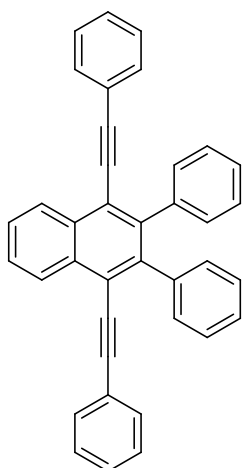
Following the general procedure, **6i** was obtained as a yellow solid (42 %), mp = 226 – 227 °C.



$^1\text{H NMR}$ (300 MHz, CDCl_3) δ 8.48 – 8.39 (m, 2H, CH_{Ar}), 7.69 – 7.52 (m, 10H, CH_{Ar}), 7.25 – 7.10 (m, 8H, CH_{Ar}), 2.41 (s, 12H, 4 CH_3). $^{13}\text{C NMR}$ (63 MHz, CDCl_3) δ 139.0, 138.8, 132.0 (2 C_{Ar}), 131.7, 131.7, 129.3, 129.2 (4 CH_{Ar}), 127.9, 126.9 (2 CH_{Ar}), 125.7, 123.9, 120.5, 120.3 (2 C_{Ar}), 100.7, 98.2, 87.7, 86.3 (2 $\text{C}\equiv\text{C}$), 21.6, 21.6 (2 CH_3). IR (ATR, cm^{-1}), $\tilde{\nu}$ = 3079 (w), 3060 (w), 3031 (w), 2935 (w), 2915 (w), 2198 (w), 2171 (w), 1901 (w), 1789 (w), 1778 (w), 1693 (w), 1681 (w), 1673 (w), 1666 (w), 1633 (w), 1604 (w), 1581 (w), 1564 (w). MS (EI, 70 eV), m/z (%) = 586 (8), 585 (28), 584 ($[\text{M}]^+$, 67), 44 (15), 43 (100), 42 (38), 41 (60). HR-MS (EI), Calcd for $\text{C}_{46}\text{H}_{32}$

(M^+), 584.24985, found 584.25013.

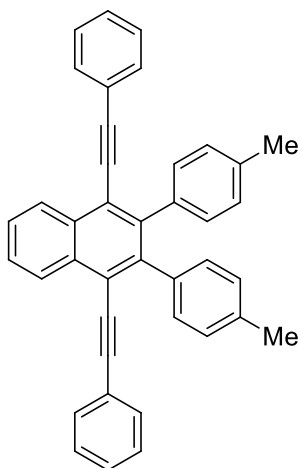
2,3-diphenyl-1,4-bis(phenylethynyl)naphthalene (7a)



Following the general procedure, **7a** was obtained as a yellow solid (88 %), mp = 212 – 213 °C. $^1\text{H NMR}$ (250 MHz, CDCl_3) δ 8.65 – 8.54 (m, 2H, CH_{Ar}), 7.76 – 7.63 (m, 2H, CH_{Ar}), 7.34 – 7.17 (m, 20H, CH_{Ar}). $^{13}\text{C NMR}$ (63 MHz, CDCl_3) δ 143.1, 140.0, 132.3 (2 C_{Ar}), 131.4, 130.9 (4 CH_{Ar}), 128.3 (2 CH_{Ar}), 128.2 (4 CH_{Ar}), 127.4 (2 CH_{Ar}), 127.2 (4 CH_{Ar}), 127.0, 126.7 (2 CH_{Ar}), 123.4, 120.9 (2 C_{Ar}), 99.6, 87.8. (2 $\text{C}\equiv\text{C}$). IR (ATR, cm^{-1}), $\tilde{\nu}$ = 3054 (m), 3022 (m), 1942 (w), 1874 (w), 1818 (w), 1799 (w), 1754 (w), 1594 (m), 1579 (w), 1569 (m), 1544 (w). MS (EI, 70 eV), m/z (%) = 482 (8), 481 (38), 480 ($[\text{M}]^+$, 100), 478 (9), 400 (28), 326 (5), 281 (7), 230 (10), 201 (7), 73 (10). HR-MS (EI), Calcd for $\text{C}_{38}\text{H}_{24}$ (M^+), 480.18725, found

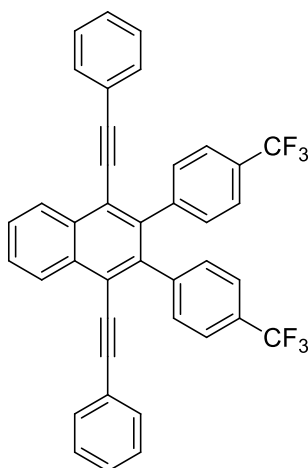
480.18687.

1,4-bis(phenylethynyl)-2,3-di-*p*-tolynaphthalene (7b)



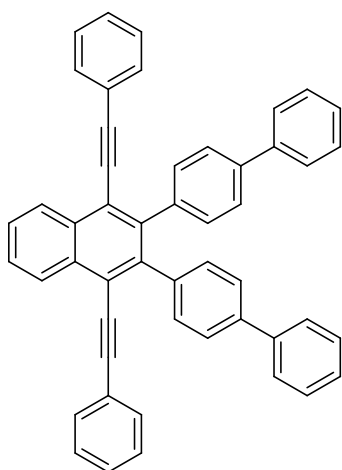
Following the general procedure, **7b** was obtained as a yellow solid (85 %), mp = 180 – 181 °C. ¹H NMR (300 MHz, CDCl₃) δ 8.65 – 8.52 (m, 2H, CH_{Ar}), 7.76 – 7.64 (m, 2H, CH_{Ar}), 7.45 – 7.27 (m, 10H, CH_{Ar}), 7.18 – 7.6 (m, 8H, CH_{Ar}), 2.35 (s, 6H, 2CH₃). ¹³C NMR (75 MHz, CDCl₃) δ 143.3, 137.1, 136.1, 132.3 (2C_{Ar}), 131.4, 130.8, 128.2 (4CH_{Ar}), 128.2 (2CH_{Ar}), 127.9 (4CH_{Ar}), 127.3, 126.9 (2CH_{Ar}), 123.5, 120.9 (2C_{Ar}), 99.4, 88.0 (2C≡C), 21.3 (2CH₃). IR (ATR, cm⁻¹), $\tilde{\nu}$ = 3077 (w), 2968 (w), 2923 (w), 2867 (w), 1901 (w), 1797 (w), 1596 (w), 1569 (w), 1544 (w), 1515 (w), 1510 (w). MS (EI, 70 eV), m/z (%) = 510 (31), 509 (55), 508 ([M]⁺, 100), 507 (11), 493 (20), 419 (19), 326 (3), 237 (12), 200 (17), 57 (11), 43 (23). HR-MS (EI), Calcd for C₄₀H₂₈ (M⁺), 508.21855, found 508.21834.

1,4-bis(phenylethynyl)-2,3-bis(4-(trifluoromethyl)phenyl)naphthalene (7c)



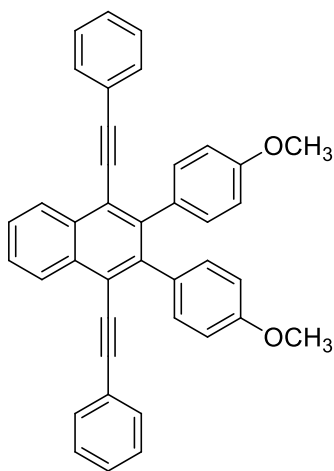
Following the general procedure, **7c** was obtained as a yellow solid (82 %), mp = 255 – 256 °C. ¹H NMR (300 MHz, CDCl₃) δ 8.60 (dd, ³J = 6.3 Hz, ⁴J = 3.3 Hz, 2H, CH_{Ar}), 7.75 (dd, ³J = 6.3 Hz, ⁴J = 3.3 Hz, 2H, CH_{Ar}), 7.55 (d, ³J = 8.1 Hz, 4H, CH_{Ar}), 7.38 (d, ³J = 8.2 Hz, 6H, CH_{Ar}), 7.30 (dd, ³J = 6.7 Hz, ⁴J = 3.7 Hz, 4H, CH_{Ar}), 7.23 – 7.14 (m, 4H, CH_{Ar}). ¹⁹F NMR (282 MHz, CDCl₃) δ -62.55. ¹³C NMR (63 MHz, CDCl₃) δ 143.6, 141.1 (2C_{Ar}), 134.4 (q, ²J = 33.2 Hz, 2CCF₃), 132.5 (2C_{Ar}), 131.5, 131.4 (4CH_{Ar}), 128.9 (2CH_{Ar}), 128.5 (4CH_{Ar}), 128.2, 127.2 (2CH_{Ar}), 124.6 (q, ³J = 3.5 Hz, 4CH_{Ar}), 124.3 (q, ¹J = 275.8 Hz, 2CF₃), 122.9, 121.4 (2C_{Ar}), 100.8, 87.1 (2C≡C). IR (ATR, cm⁻¹), $\tilde{\nu}$ = 3077 (w), 3049 (w), 3031 (w), 3022 (w), 2935 (w), 2208 (w), 1920 (w), 1616 (m), 1596 (w), 1571 (w), 1540 (w). MS (EI, 70 eV), m/z (%) = 618 (8), 617 (42), 616 ([M]⁺, 100), 545 (5), 468 (10), 400 (8), 237 (6), 77 (9). HR-MS (EI), Calcd for C₄₀H₂₂F₆ (M⁺), 616.16202, found 616.16186.

2,3-di([1,1'-biphenyl]-4-yl)-1,4-bis(phenylethynyl)naphthalene (7d)



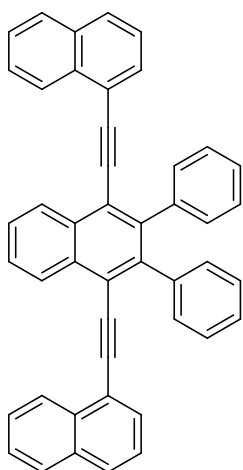
Following the general procedure, **7d** was obtained as a white solid (92 %), mp = 229 – 230 °C. ¹H NMR (300 MHz, CDCl₃) δ 8.63 (dd, ³J = 6.4 Hz, ⁴J = 3.3 Hz, 2H, CH_{Ar}), 7.76 – 7.69 (m, 4H, CH_{Ar}), 7.68 – 7.59 (m, 5H, CH_{Ar}), 7.52 (d, ³J = 8.3 Hz, 5H, CH_{Ar}), 7.48 – 7.29 (m, 16H, CH_{Ar}). ¹³C NMR (63 MHz, CDCl₃) δ 142.7, 140.9, 139.3, 139.1, 132.3 (2C_{Ar}), 131.4, 131.4, 128.7 (4CH_{Ar}), 128.3 (4CH_{Ar}), 127.5, 127.2 (2CH_{Ar}), 127.0 (4CH_{Ar}), 125.9 (2CH_{Ar}), 125.9 (4CH_{Ar}), 123.3, 121.1 (2C_{Ar}), 99.8, 87.9 (2C≡C) (1 signal of CH_{Ar} was overlapped). IR (ATR, cm⁻¹), $\tilde{\nu}$ = 3056.77 (m), 3029 (m), 2196 (w), 1594 (m), 1581 (w), 1571 (w), 1538 (w), 1519 (w). MS (EI, 70 eV), m/z (%) = 635 (16), 634 (52), 633 (87), 632 ([M]⁺, 100), 631 (21), 555 (25), 478 (18), 400 (7), 277 (10), 238 (15), 125 (4), 43 (10). HR-MS (EI), Calcd for C₅₀H₃₂ (M⁺), 632.24985, found 632.24807.

2,3-bis(4-methoxyphenyl)-1,4-bis(phenylethynyl)naphthalene (7e)



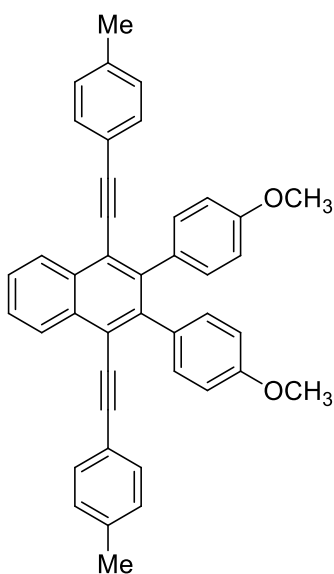
Following the general procedure, **7e** was obtained as a yellow solid (77 %), mp = 235 – 236 °C. ¹H NMR (300 MHz, CDCl₃) δ 8.61 – 8.55 (m, 2H, 2CH_{Ar}), 7.72 – 7.65 (m, 2H, CH_{Ar}), 7.36 – 7.27 (m, 10H, CH_{Ar}), 7.23 – 7.14 (m, 4H, CH_{Ar}), 6.84 – 6.74 (m, 4H, CH_{Ar}), 3.81 (s, 6H, 2OCH₃). ¹³C NMR (75 MHz, CDCl₃) δ 158.3, 142.9, 132.5, 132.3 (2C_{Ar}), 132.1, 131.5, 128.3 (4CH_{Ar}), 128.2, 127.3, 126.9 (2CH_{Ar}), 123.5, 121.0 (2C_{Ar}), 112.7 (4CH_{Ar}), 99.3, 88.0 (C≡C), 55.2 (2OCH₃). IR (ATR, cm⁻¹), $\tilde{\nu}$ = 3076 (w), 3018 (w), 2993 (w), 2956 (w), 2931 (w), 2906 (w), 2848 (w), 1889 (w), 1731 (w), 1606 (m), 1594 (m), 1579 (w), 1569 (w), 1508 (s). MS (EI, 70 eV), m/z (%) = 543 (9), 542 (29), 541 (43), 540 ([M]⁺, 100), 509 (13), 451 (15), 389 (7), 224 (170), 187 (8), 97 (10), 43 (24). HR-MS (EI), Calcd for C₄₀H₂₈O₂ (M⁺), 540.20838, found 540.20769.

1,1'-((2,3-diphenylnaphthalene-1,4-diyl)bis(ethyne-2,1-diyl))dinaphthalene (7f)



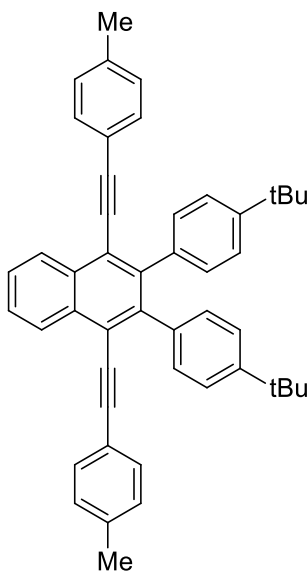
Following the general procedure, **7f** was obtained as a yellow solid (59 %), mp = 233 – 234 °C. ¹H NMR (300 MHz, CDCl₃) δ 8.82 – 8.76 (m, 2H, CH_{Ar}), 7.86 – 7.75 (m, 6H, CH_{Ar}), 7.68 (dd, ³J = 7.1 Hz, ⁴J = 1.1 Hz, 2H, CH_{Ar}), 7.51 – 7.38 (m, 6H, CH_{Ar}), 7.37 – 7.27 (m, 12H, CH_{Ar}). ¹³C NMR (75 MHz, CDCl₃) δ 143.3, 140.4 (2C_{Ar}), 133.1 (4C_{Ar}), 132.5 (2C_{Ar}), 130.6 (4CH_{Ar}), 130.5, 128.7, 128.0 (2CH_{Ar}), 127.7 (4CH_{Ar}), 127.6, 127.1, 126.8, 126.7, 126.4, 126.3, 125.2 (2CH_{Ar}), 121.1, 121.0 (2C_{Ar}), 98.2, 92.4 (2C≡C). IR (ATR, cm⁻¹), $\tilde{\nu}$ = 3056 (w), 3047 (w), 1600 (w), 1583 (w), 1575 (w), 1558 (w), 1542 (w), 1504 (w), 1486 (m). MS (EI, 70 eV), m/z (%) = 583 (8), 582 (22), 581 (41), 580 ([M]⁺, 100), 501 (5), 441 (11), 376 (3), 326 (2), 281 (9), 207 (7), 165 (7), 128 (5), 44 (20). HR-MS (EI), Calcd for C₄₆H₂₈ (M⁺), 580.21855, found 580.21733.

2,3-bis(4-methoxyphenyl)-1,4-bis(p-tolylethynyl)naphthalene (7g)



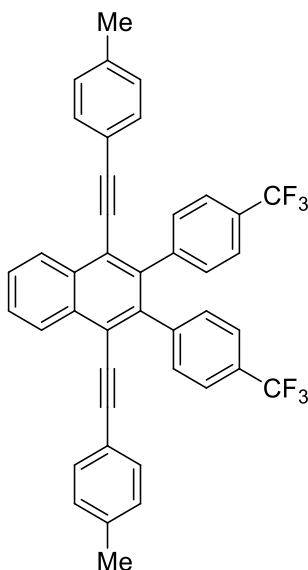
Following the general procedure, **7g** was obtained as a yellow solid (66 %), mp = 230 – 231 °C. ¹H NMR (300 MHz, CDCl₃) δ 8.63 – 8.52 (m, 2H, CH_{Ar}), 7.72 – 7.62 (m, 2H, CH_{Ar}), 7.24 – 7.08 (m, 12H, CH_{Ar}), 6.85 – 6.73 (m, 4H, CH_{Ar}), 3.80 (s, 6H, 2OCH₃), 2.35 (s, 6H, 2CH₃). ¹³C NMR (63 MHz, CDCl₃) δ 158.2, 142.7, 138.4, 132.6, 132.3 (2C_{Ar}), 132.1, 131.3, 129.0 (4CH_{Ar}), 127.7, 126.9 (2CH_{Ar}), 121.0, 120.5 (2C_{Ar}), 112.7 (4CH_{Ar}), 99.5, 87.5 (2C≡C), 55.2 (2OCH₃), 21.5 (2CH₃). IR (ATR, cm⁻¹), $\tilde{\nu}$ = 3076 (w), 3029 (w), 2996 (w), 2954 (w), 2929 (w), 2908 (w), 2833 (w), 2204 (w), 1905 (w), 1893 (w), 1606 (m), 1575 (w), 1564 (w), 1544 (w), 1510 (s). MS (EI, 70 eV), m/z (%) = 569 (8), 568 ([M]⁺, 20), 69 (11), 44 (22), 43 (100), 42 (26), 41 (40). HR-MS (EI), Calcd for C₄₂H₃₂O₂ (M⁺), 568.23968, found 568.23805.

2,3-bis(4-tert-butylphenyl)-1,4-bis(p-tolylethynyl)naphthalene (7h)



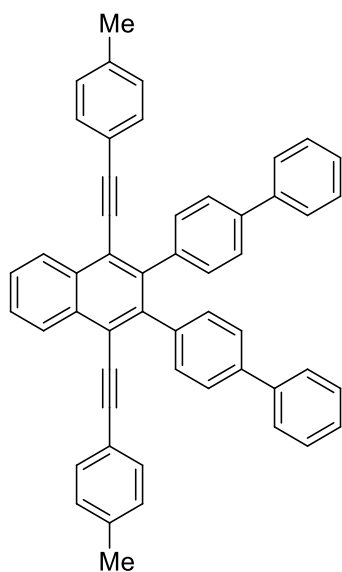
Following the general procedure, **7h** was obtained as a yellow solid (58 %), mp = 204 – 205 °C. ^1H NMR (250 MHz, CDCl_3) δ 8.58 (dd, $^3J = 6.4$ Hz, $^4J = 3.3$ Hz, 2H, CH_{Ar}), 7.67 (dd, $^3J = 6.4$ Hz, $^4J = 3.3$ Hz, 2H, CH_{Ar}), 7.23 – 7.14 (m, 8H, CH_{Ar}), 7.10 – 7.05 (m, 8H, CH_{Ar}), 2.33 (s, 6H, 2 CH_3), 1.32 (s, 18H, 6 CH_3). ^{13}C NMR (63 MHz, CDCl_3) δ 149.2, 143.4, 138.3, 137.2, 132.1, (2 C_{Ar}), 131.5, 130.7, 129.0 (4 CH_{Ar}), 127.3, 127.0 (2 CH_{Ar}), 124.0 (4 CH_{Ar}), 120.9, 120.7 (2 C_{Ar}), 99.7, 87.8 (2 $\text{C}\equiv\text{C}$), 34.5 (2C), 31.5 (6 CH_3), 21.6 (2 CH_3). IR (ATR, cm^{-1}), $\tilde{\nu}$ = 2956 (m), 2923 (m), 2902 (w), 2861 (w), 2202 (w), 1903 (w), 1722 (w), 1714 (w), 1681 (w), 1673 (w), 1592 (w), 1573 (w), 1564 (w), 1485(m), 1471 (m). MS (EI, 70 eV), m/z (%) = 622 (13), 621 (38), 620 ($[\text{M}]^+$, 82), 563 (43), 507 (18), 430 (62), 262 (27), 183 (22), 108 (10), 57 (21), 43 (100). HR-MS (EI), Calcd for $\text{C}_{48}\text{H}_{44}$ (M^+), 620.34375, found 620.34350.

1,4-bis(*p*-tolylethynyl)-2,3-bis(4-(trifluoromethyl)phenyl)naphthalene (7i)



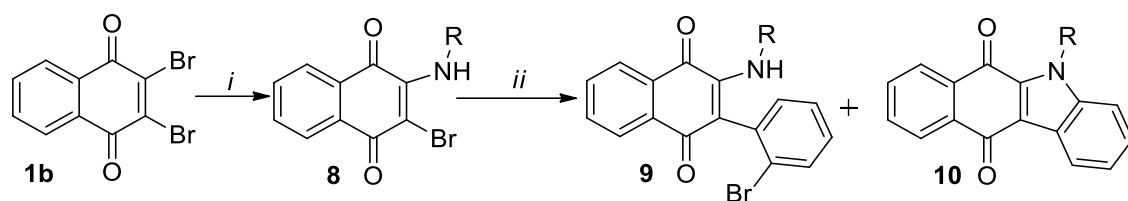
Following the general procedure, **7i** was obtained as a yellow solid (67 %), mp = 238 – 239 °C. ^1H NMR (300 MHz, CDCl_3) δ 8.62 – 8.54 (m, 2H, 2 CH_{Ar}), 7.78 – 7.72 (m, 2H, CH_{Ar}), 7.59 – 7.46 (m, 4H, CH_{Ar}), 7.35 (d, $^3J = 8.0$ Hz, 4H, CH_{Ar}), 7.12 – 7.03 (m, 8H, CH_{Ar}), 2.35 (s, 6H, 2 CH_3). ^{19}F NMR (282 MHz, CDCl_3) δ -62.50. ^{13}C NMR (63 MHz, CDCl_3) δ 143.7, 140.8, 139.1, 132.4 (2 C_{Ar}), 131.4 (8 CH_{Ar}), 129.3 (4 CH_{Ar}), 129.3 (q, $^2J = 32.5$ Hz, 2 CCF_3), 128.1, 127.2 (2 CH_{Ar}), 124.5 (q, $^3J = 3.7$ Hz, 4 CH_{Ar}), 124.3 (q, $^1J = 272.0$ Hz, 2 CF_3), 121.4, 119.9 (2 C_{Ar}), 101.0, 86.6 (2 $\text{C}\equiv\text{C}$), 21.7 (2 CH_3). IR (ATR, cm^{-1}), $\tilde{\nu}$ = 3060 (w), 3029 (w), 2993 (w), 2925 (w), 2204 (w), 1920 (w), 1616 (w), 1575 (w), 1542 (w), 1510 (m), 1488 (w), 1454 (w), 1438 (w). MS (EI, 70 eV), m/z (%) = 647 (5), 645 (40), 644 ($[\text{M}]^+$, 100), 69 (9), 43 (81), 42 (23), 41 (32). HR-MS (EI), Calcd for $\text{C}_{42}\text{H}_{26}\text{F}_6$ (M^+), 644.19332, found 644.19143.

2,3-di([1,1'-biphenyl]-4-yl)-1,4-bis(*p*-tolylethynyl)naphthalene (7k)



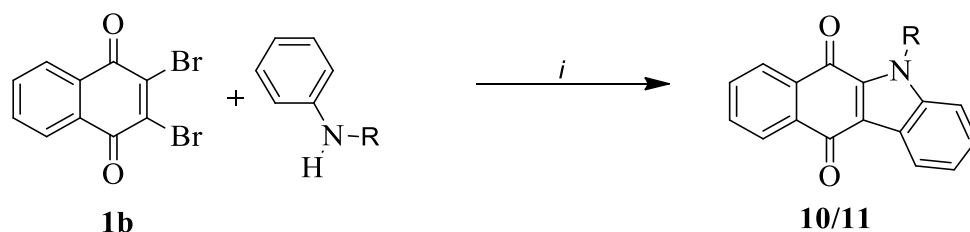
Following the general procedure, **7k** was obtained as a yellow solid (74 %), mp = 260 – 261 °C. ^1H NMR (300 MHz, CDCl_3) δ 8.69 – 8.57 (m, 2H, CH_{Ar}), 7.78 – 7.68 (m, 2H, CH_{Ar}), 7.64 – 7.58 (m, 4H, CH_{Ar}), 7.54 – 7.32 (m, 14H, CH_{Ar}), 7.17 (d, $^3J = 8.1$ Hz, 4H, CH_{Ar}), 7.07 (d, $^3J = 8.0$ Hz, 4H, CH_{Ar}), 2.33 (s, 4H, 2 CH_3). ^{13}C NMR (63 MHz, CDCl_3) δ 142.5, 141.0 (2 C_{Ar}), 139.2 (4 C_{Ar}), 138.5, 132.3 (2 C_{Ar}), 131.5, 131.3, 129.1, 128.7 (4 CH_{Ar}), 127.4, 127.1, 1270.0 (2 CH_{Ar}), 127.0 (4 CH_{Ar}), 125.9 (4 CH_{Ar}), 121.1, 120.3 (2 C_{Ar}), 100.0, 87.3 (2 $\text{C}\equiv\text{C}$), 21.5 (2 CH_3) (one signal of CH was overlapped). IR (ATR, cm^{-1}), $\tilde{\nu} = 1911$ (w), 1799 (w), 1673 (w), 1658 (w), 1650 (w), 1598 (w), 1579 (w), 1558 (w), 1538 (w), 1510 (m), 1484 (m), 1446 (m). MS (EI, 70 eV), m/z (%) = 662 (18), 661 (59), 660 ($[\text{M}]^+$, 100), 645 (13), 476 (4), 284 (4). HR-MS (EI), Calcd for $\text{C}_{52}\text{H}_{36}$ (M^+), 660.28115, found 660.28042.

7.4. Supplement for Chapter 3



Scheme S5. The three-step one-pot synthesis of **10**.

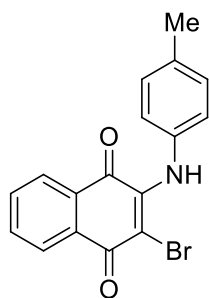
Procedure A (one-pot synthesis), 2,3-dibromo-1,4-naphthoquinone **1** (0.3 mmol), the appropriate amine (0.3 mmol) and H₂O (1 mL) were poured into a pressure tube. The reaction was set up at 60 °C for 6 h, then, 2-bromophenylboronic acid (0.33 mmol), Pd(PPh₃)₄ (5 mol%), Pd₂(dba)₃ (5 mol%), RuPhos (10 mol%), K₃PO₄ (0.9 mmol) and 1,4-dioxane (10 mL) were added under argon. The tube was sealed with a Teflon valve and stirred at 90 °C. After 24 h, the mixture was allowed to reach room temperature, diluted with water and extracted with dichloromethane. The combined organic layers were dried over sodium sulfate and concentrated under vacuum. The crude material was purified by flash column chromatography (silica gel, heptane/ethylacetate).



Scheme S6. The two-step domino synthesis of **10a**.

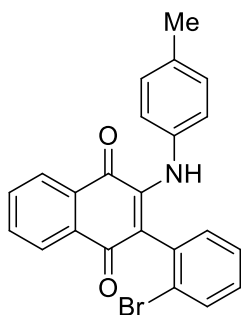
Procedure B (domino synthesis), An argon purged pressure tube was charged with 2,3-dibromo-1,4-naphthoquinone **1** (0.3 mmol) and the secondary amine (0.36 mmol), Pd(OAc)₂ (5 mol%), PPh₃ (10 mol%), *t*BuONa (1.2 mmol) and toluene (10 mL). The reaction was set up at 90 °C for 24 h. Afterwards the mixture was allowed to reach room temperature, was diluted with water and extracted with ethyl acetate. The combined organic layers were dried over sodium sulfate and concentrated under vacuum. The crude material was purified by flash column chromatography (silica gel, heptane/ethylacetate).

2-bromo-3-(*p*-tolylamino)naphthalene-1,4-dione (8)



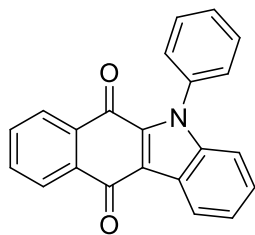
Starting from *p*-toluidine with 2,3-dibromonaphthalene-1,4-dione in water at 60 °C for 12 h, **8** was obtained as a dark red solid, mp = 157 - 158 °C. ¹H NMR (300 MHz, CDCl₃) δ = 8.19 (dd, ³J = 7.6 Hz, ⁴J = 1.3 Hz, 1H, CH_{Ar}), 8.14 – 8.05 (m, 1H, CH_{Ar}), 7.81 – 7.60 (m, 3H, CH_{Ar}), 7.15 (d, ³J = 8.2 Hz, 2H, CH_{Ar}), 7.00 (d, ³J = 8.3 Hz, 2H, CH_{Ar}), 2.36 (s, 3H, CH₃). ¹³C NMR (75 MHz, CDCl₃) δ = 180.26, 177.44 (C=O), 144.43, 135.98 (C_{Ar}), 135.08 (CH_{Ar}), 135.01 (C_{Ar}), 132.96 (CH_{Ar}), 132.62, 130.01 (C_{Ar}), 129.24 (2CH_{Ar}), 127.54, 127.18 (CH_{Ar}), 124.98 (2CH_{Ar}), 107.00 (C_{Ar}), 21.21 (CH₃). IR (ATR, cm⁻¹), $\tilde{\nu}$ = 3302 (m), 3223 (w), 3095 (w), 3024 (w), 2916 (w), 1672 (s), 1645 (m), 1630 (m), 1591 (m), 1581 (m), 1566 (m), 1547 (s). MS (EI, 70 eV), m/z (%) = 341 (M⁺, 73), 326 (4), 262 (100), 247 (12), 219 (9), 178 (10), 105 (13), 91 (29). HRMS (EI), calcd C₁₇H₁₂BrNO₂ (M⁺) 341.00459, found 341.00382;

2-(2-bromophenyl)-3-(*p*-tolylamino)naphthalene-1,4-dione (9b)



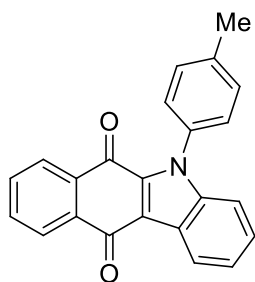
Following the general procedure, **9b** was obtained as a red solid (17 %), mp = 175 – 176 °C. ¹H NMR (250 MHz, CDCl₃) δ = 8.23 – 8.11 (m, 2H, CH_{Ar}), 7.82 – 7.66 (m, 3H, CH_{Ar}), 7.27 – 7.20 (m, 1H, CH_{Ar}), 7.04 – 6.81 (m, 3H, CH_{Ar}), 6.78 – 6.62 (m, 4H, CH_{Ar}), 2.14 (s, 3H, CH₃). ¹³C NMR (63 MHz, CDCl₃) δ 182.9, 181.5 (C=O), 142.2, 135.2 (C_{Ar}), 135.1 (CH_{Ar}), 134.6, 134.3, 133.6 (C_{Ar}), 132.9, 132.4, 132.2 (CH_{Ar}), 130.4 (C_{Ar}), 128.7 (CH_{Ar}), 128.47 (2CH_{Ar}), 127.0, 126.5, 126.5 (CH_{Ar}), 125.3 (C_{Ar}), 124.6 (2CH_{Ar}), 115.9 (C_{Ar}), 20.9 (CH₃). IR (ATR, cm⁻¹), $\tilde{\nu}$ = 3331 (w), 3298 (s), 3064 (w), 3045 (w), 3010 (w), 2920 (w), 1674 (s), 1633 (m), 1612 (w), 1595 (m), 1569 (s), 1516 (s), 1505 (s). MS (EI, 70 eV), m/z (%) = 419 (4), 417 (M⁺, 5), 339 (27), 338 (100), 324 (7), 323 (26), 295 (3), 294 (5), 190 (6), 176 (7), 165 (6), 161 (9). HRMS (EI), calcd for C₂₃H₁₆BrNO₂ (M⁺) 417.03589, found 417.03524; calcd for C₂₃H₁₆⁸¹BrNO₂ (M⁺) 419.03385, found 419.03478.

5-phenyl-5*H*-benzo[*b*]carbazole-6,11-dione (10a)



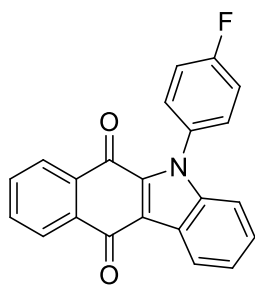
Following the general procedure, **10a** was obtained as a light red solid (51 %), and starting from diphenylamine, following the general procedure the same compound was isolated in 38 % yield, mp = 253 – 255 °C. ¹H NMR (250 MHz, CDCl₃) δ = 8.58 – 8.48 (m, 1H, CH_{Ar}), 8.25 (dd, ³J = 7.6 Hz, ⁴J = 1.3 Hz, 1H, CH_{Ar}), 8.05 (dd, ³J = 7.5 Hz, ⁴J = 1.4 Hz, 1H, CH_{Ar}), 7.78 – 7.57 (m, 5H, CH_{Ar}), 7.49 - 7.37 (m, 4H, CH_{Ar}), 7.21 – 7.14 (m, 1H, CH_{Ar}). ¹³C NMR (63 MHz, CDCl₃) δ = 181.8, 177.7 (C=O), 141.2, 136.9, 135.7, 134.2 (C_{Ar}), 133.9 (CH_{Ar}), 133.7 (C_{Ar}), 133.1 (CH_{Ar}), 129.7 (2CH_{Ar}), 129.3, 127.8 (CH_{Ar}), 127.8 (2CH_{Ar}), 126.6, 126.5, 124.9 (CH_{Ar}), 124.0 (C_{Ar}), 123.7 (CH_{Ar}), 120.0 (C_{Ar}), 112.3 (CH_{Ar}). IR (ATR, cm⁻¹), $\tilde{\nu}$ = 3070 (m), 3047 (w), 2924 (w), 1649 (s), 1612 (m), 15894 (s), 1570 (m), 1516 (s), 1499 (m). MS (EI, 70 eV), m/z (%) = 323 (M⁺, 100), 294 (11), 265 (14), 190 (6), 161 (7), 132 (9), 1. HR-MS (EI), Calcd for C₂₂H₁₃O₂N (M⁺), 323.09406; found 323.09334.

5-(*p*-tolyl)-5H-benzo[*b*]carbazole-6,11-dione (10b)



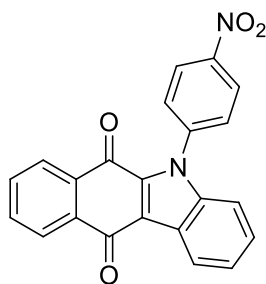
Following the general procedure, **10b** was obtained as an orange solid (49 %), mp = 266 – 268 °C. ¹H NMR (250 MHz, CDCl₃) δ = 8.56 – 8.46 (m, 1H, CH_{Ar}), 8.30 – 8.19 (m, 1H, CH_{Ar}), 8.10 – 7.96 (m, 1H, CH_{Ar}), 7.79 – 7.58 (m, 2H, CH_{Ar}), 7.46 – 7.29 (m, 6H, CH_{Ar}), 7.21 – 7.09 (m, 1H, CH_{Ar}), 2.52 (s, 3H, CH₃). ¹³C NMR (63 MHz, CDCl₃) δ = 181.7, 177.7 (C=O), 141.3, 139.3, 135.7, 134.3, 134.2 (C_{Ar}), 133.8 (CH_{Ar}), 133.7 (C_{Ar}), 133.1 (CH_{Ar}), 130.3 (2CH_{Ar}), 127.7 (CH_{Ar}), 127.4 (2CH_{Ar}), 126.6, 126.4, 124.9 (CH_{Ar}), 124.0 (C_{Ar}), 123.8 (CH_{Ar}), 119.9 (C_{Ar}), 112.3 (CH_{Ar}), 21.5 (CH₃). IR (ATR, cm⁻¹), $\tilde{\nu}$ = 3062 (w), 3050 (w), 2956 (w), 2921 (m), 2851 (m), 1732 (w), 1660 (m), 1641 (m), 1612 (w), 1588 (m), 1516 (s). MS (EI, 70 eV), m/z (%) = 337 (M⁺, 100), 322 (38), 308 (9), 278 (12), 168 (11), 163 (5), 139 (4), 132 (7), 2). HR-MS (EI), Calcd for C₂₃H₁₅NO₂ (M⁺), 337.10973, found 337.10925.

5-(4-fluorophenyl)-5H-benzo[*b*]carbazole-6,11-dione (10c)



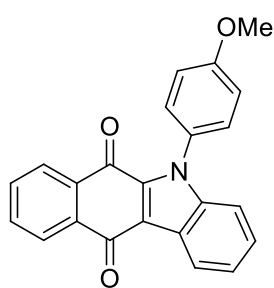
Following the general procedure, **10c** was obtained as an orange solid (60 %), mp = 275 - 277 °C. ^1H NMR (300 MHz, CDCl_3) δ = 8.56 – 8.48 (m, 1H, CH_{Ar}), 8.24 (dd, 3J = 7.6 Hz, 4J = 1.2 Hz, 1H, CH_{Ar}), 8.04 (dd, 3J = 7.5 Hz, 4J = 1.2 Hz, 1H, CH_{Ar}), 7.77 – 7.63 (m, 2H, CH_{Ar}), 7.47 – 7.40 (m, 4H, CH_{Ar}), 7.34 - 7.27 (m, 2H, CH_{Ar}), 7.18 – 7.11 (m, 1H, CH_{Ar}). ^{19}F NMR (282 MHz, CDCl_3) δ = -111.41; ^{13}C NMR (126 MHz, CDCl_3) δ = 181.7, 177.8 (C=O), 162.9 (d, 1J = 249.7 Hz, CF), 141.2, 135.7, 134.1, 134.0 (C_{Ar}), 133.6 (CH_{Ar}), 133.2 (CH_{Ar}), 132.9 (d, 4J = 3.5 Hz, C_{Ar}), 129.6 (d, 3J = 9.0 Hz, 2 CH_{Ar}), 128.0, 126.6, 126.6, 125.0, 124.0, 124.0 (CH_{Ar}), 120.2 (C_{Ar}), 116.7 (d, 2J = 23.1 Hz, 2 CH_{Ar}), 112.0 (C_{Ar}), IR (ATR, cm^{-1}), $\tilde{\nu}$ = 3062 (w), 3047 (w), 3009 (w), 2959 (w), 2921 (m), 2850 (m), 1658 (s), 1650 (s), 1613 (m), 1590 (m), 1552 (w), 1512 (s). MS (EI, 70 eV), m/z (%) = 341 (M^+ , 100), 312 (16), 296 (7), 283 (15), 257 (4), 170 (9), 141 (6). HR-MS (EI), Calcd for $\text{C}_{22}\text{H}_{12}\text{NO}_2\text{F}$ (M^+), 341.08466, found, 341.08426.

5-(4-nitrophenyl)-5H-benzo[b]carbazole-6,11-dione (10d)



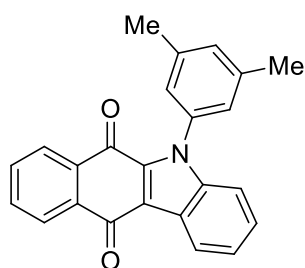
Starting from 4-Nitroaniline, following the general procedure, **10d** was obtained as an orange solid (37 %), mp = 286 - 288 °C. ^1H NMR (300 MHz, DMSO) δ = 8.52 – 8.45 (m, 2H, CH_{Ar}), 8.40 – 8.34 (m, 1H, CH_{Ar}), 8.13 (dd, 3J = 7.4 Hz, 4J = 1.3 Hz, 1H, CH_{Ar}), 8.00 – 7.92 (m, 3H, CH_{Ar}), 7.90 – 7.78 (m, 2H, CH_{Ar}), 7.55 – 7.45 (m, 2H, CH_{Ar}), 7.32 – 7.24 (m, 1H, CH_{Ar}). ^{13}C NMR (63 MHz, DMSO) δ = 180.9, 176.7 (C=O), 147.4, 142.1, 139.8, 135.8 (C_{Ar}), 134.2, 133.6 (CH_{Ar}), 133.2, 133.0 (C_{Ar}), 129.3 (2 CH_{Ar}), 128.1, 126.2, 125.9, 125.1 (CH_{Ar}), 124.7 (2 CH_{Ar}), 123.4 (C_{Ar}), 122.8 (CH_{Ar}), 119.3 (C_{Ar}), 112.0 (CH_{Ar}). IR (ATR, cm^{-1}), $\tilde{\nu}$ = 3116 (w), 3077 (w), 2922 (w), 2851 (w), 1662 (m), 1646 (m), 1607 (w), 1590 (m), 1556 (w), 1518 (m). MS (EI, 70 eV), m/z (%) = 368 (M^+ , 100), 339 (4), 322 (16), 293 (9), 265 (23), 190 (5), 161 (4), 133 (7). HR-MS (EI), calcd for $\text{C}_{22}\text{H}_{12}\text{N}_2\text{O}_4$ (M^+), 368.07916, found 368.07895.

5-(4-methoxyphenyl)-5H-benzo[b]carbazole-6,11-dione (10e)



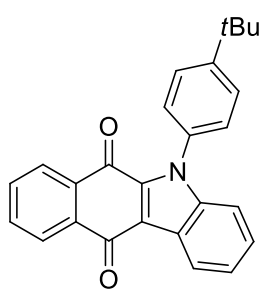
Following the general procedure, **10e** was obtained as a light orange solid (47 %), mp = 237 - 239 °C. ¹H NMR (300 MHz, CDCl₃) δ = 8.56 – 8.47 (m, 1H, CH_{Ar}), 8.25 (dd, ³J = 7.6 Hz, ⁴J = 1.2 Hz, 1H, CH_{Ar}), 8.11 – 8.01 (m, 1H, CH_{Ar}), 7.77 – 7.61 (m, 2H, CH_{Ar}), 7.45 – 7.33 (m, 4H, CH_{Ar}), 7.21 – 7.15 (m, 1H, CH_{Ar}), 7.13 – 7.07 (m, 2H, CH_{Ar}), 3.93 (s, 3H, OCH₃). ¹³C NMR (126 MHz, CDCl₃) δ = 181.6, 177.7 (C=O), 156.0, 141.4, 135.6, 134.1 (CH_{Ar}), 133.7 (C_{Ar}), 133.6 (CH_{Ar}), 133.0 (C_{Ar}), 129.4 (CH_{Ar}), 128.7 (2CH_{Ar}), 127.6, 126.5, 126.3, 124.8 (C_{Ar}), 123.8 (CH_{Ar}), 123.7 (C_{Ar}), 119.7 (CH_{Ar}), 114.7 (2CH_{Ar}), 112.2 (C_{Ar}), 55.6 (OCH₃). IR (ATR, cm⁻¹), $\tilde{\nu}$ = 3296 (m), 3228 (w), 3091 (m), 3072 (m), 3006 (m), 2957 (m), 2923 (m), 2849 (m), 2835 (m), 1651 (s), 1610 (m), 1593 (s), 1514 (s), 1486 (s), 1471 (m), 1456 (s), 1441 (s). MS (EI, 70 eV), m/z (%) = 353 (M⁺, 100), 338 (9), 322 (11), 310 (8), 265 (6), 254 (9), 176 (8), 163 (4), 126 (6). HR-MS (EI), calcd for C₂₃H₁₅NO₃ (M⁺), 353.10464, found 353.10441.

5-(3,5-dimethylphenyl)-5H-benzo[b]carbazole-6,11-dione (10f)



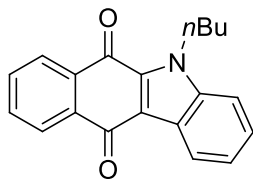
Following the general procedure, **10f** was obtained as a yellow solid (47 %), mp = 248 - 250 °C. ¹H NMR (300 MHz, CDCl₃) δ = 8.57 – 8.47 (m, 1H, CH_{Ar}), 8.25 (dd, ³J = 7.6 Hz, ⁴J = 1.2 Hz, 1H, CH_{Ar}), 8.06 (dd, ³J = 7.6 Hz, ⁴J = 1.3 Hz, 1H, CH_{Ar}), 7.77 – 7.61 (m, 2H, CH_{Ar}), 7.47 – 7.35 (m, 2H, CH_{Ar}), 7.22 – 7.14 (m, 2H, CH_{Ar}), 7.04 (s, 2H, CH_{Ar}), 2.43 (s, 6H, 2CH₃). ¹³C NMR (75 MHz, CDCl₃) δ = 181.8, 177.6 (C=O), 141.3 (C_{Ar}), 139.4 (2C_{Ar}), 136.7, 135.7, 134.2 (C_{Ar}), 133.8 (CH_{Ar}), 133.7 (C_{Ar}), 133.1, 131.1, 127.6, 126.6, 126.4 (CH_{Ar}), 125.3 (2CH_{Ar}), 124.8 (CH_{Ar}), 124.0 (C_{Ar}), 123.7 (CH_{Ar}), 119.8 (C_{Ar}), 112.5 (CH_{Ar}), 21.5 (2CH₃). IR (ATR, cm⁻¹), $\tilde{\nu}$ = 3055 (w), 3010 (w), 2918 (w), 2861 (w), 1660 (s), 1650 (s), 1614 (m), 1594 (m), 1586 (m), 1571 (w), 1518 (s), 1491 (m), 1473 (m). MS (EI, 70 eV), m/z (%) = 351 (M⁺, 100), 336 (88), 322 (6), 306 (4), 291 (7), 278 (11), 190 (4), 176 (8), 168 (8), 163 (5), 154 (4), 139 (8). HR-MS (EI), calcd for C₂₄H₁₇NO₂ (M⁺), 351.12538, found 351.12488.

5-(4-(tert-butyl)phenyl)-5H-benzo[b]carbazole-6,11-dione (10g)



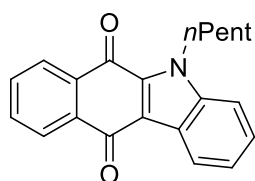
Following the general procedure, **10g** was obtained as a yellow solid (48 %), mp = 294 - 296 °C. ¹H NMR (300 MHz, CDCl₃) δ = 8.56 – 8.48 (m, 1H, CH_{Ar}), 8.25 (dd, ³J = 7.6 Hz, ⁴J = 1.3 Hz, 1H, CH_{Ar}), 8.07 (dd, ³J = 7.6, ⁴J = 1.2 Hz, 1H, CH_{Ar}), 7.79 – 7.57 (m, 4H, CH_{Ar}), 7.49 – 7.32 (m, 4H, CH_{Ar}), 7.24 – 7.13 (m, 1H, CH_{Ar}), 1.44 (s, 9H, 3CH₃). ¹³C NMR (75 MHz, CDCl₃) δ = 181.8, 177.8 (C=O), 152.3, 141.4, 135.7, 134.2, 134.2 (C_{Ar}), 133.9 (CH_{Ar}), 133.7 (C_{Ar}), 133.1, 127.7 (CH_{Ar}), 127.1 (2CH_{Ar}), 126.6 (CH_{Ar}), 126.5 (2CH_{Ar}), 126.5, 124.9 (CH_{Ar}), 124.0 (C_{Ar}), 123.8 (CH_{Ar}), 120.0 (C_{Ar}), 112.5 (CH_{Ar}), 35.1 (C-(CH₃)₃), 31.6 (3CH₃). IR (ATR, cm⁻¹), $\tilde{\nu}$ = 3309 (w), 3292 (w), 3069 (w), 3041 (w), 2965 (m), 2868 (m), 1663 (s), 1650 (s), 1613 (m), 1591 (m), 1584 (m), 1556 (m), 1519 (s), 1488 (s). MS (EI, 70 eV), m/z (%) = 379 (M⁺, 60), 364 (100), 336 (5), 322 (10), 265 (4), 168 (9), 154 (2), 139 (3). HR-MS (EI), Calcd for C₂₆H₂₁NO₂ (M⁺) 379.15668, found 379.15654.

5-butyl-5H-benzo[b]carbazole-6,11-dione (10k)



Following the general procedure, **10k** was obtained as a yellow solid (42 %), mp = 109 – 111 °C. ¹H NMR (300 MHz, CDCl₃) δ = 8.50 – 8.46 (m, 1H, CH_{Ar}), 8.25 – 8.11 (m, 2H, CH_{Ar}), 7.78 – 7.63 (m, 2H, CH_{Ar}), 7.52 – 7.35 (m, 3H, CH_{Ar}), 4.78 – 4.67 (m, 2H, CH₂), 1.96 – 1.79 (m, 2H, CH₂), 1.54 – 1.41 (m, 2H, CH₂), 0.99 (t, ³J = 7.3 Hz, 3H, CH₃). ¹³C NMR (63 MHz, CDCl₃) δ = 181.4, 179.1 (C=O), 139.6, 135.0, 134.3 (C_{Ar}), 133.9 (CH_{Ar}), 133.8 (C_{Ar}), 132.9, 127.3, 126.6, 126.4, 124.6 (CH_{Ar}), 124.22 (C_{Ar}), 124.1 (CH_{Ar}), 119.2 (C_{Ar}), 111.2 (CH_{Ar}), 45.3 (CH₂), 32.5 (CH₂), 20.3 (CH₂), 14.0 (CH₃). IR (ATR, cm⁻¹), $\tilde{\nu}$ = 3063 (w), 3010 (w), 2997 (w), 2960 (m), 2916 (m), 2862 (m), 2848 (m), 1657 (s), 1643 (s), 1614 (m), 1593 (s), 1576 (m), 1516 (s). MS (EI, 70 eV), m/z (%) = 303 (M⁺, 80), 274 (17), 260 (100), 247 (31), 232 (7), 219 (9), 203 (8), 190 (17), 176 (10). HR-MS (EI), Calcd for C₂₀H₁₇NO₂ (M⁺), 303.12538, found, 303.12599

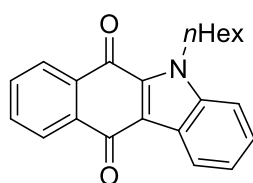
5-pentyl-5H-benzo[b]carbazole-6,11-dione (10l)



Following the general procedure, **10l** was obtained as a yellow solid (48 %), mp = 102 - 104 °C. ¹H NMR (300 MHz, CDCl₃) δ = 8.46 (d, ³J = 7.9 Hz, 1H, CH_{Ar}), 8.26 – 8.09 (m, 2H, CH_{Ar}), 7.78 – 7.60 (m, 2H, CH_{Ar}), 7.49 – 7.32 (m, 3H, CH_{Ar}), 4.79 – 4.59 (m, 2H, CH_{Ar}), 1.99 – 1.79 (m, 2H, CH₂), 1.46 – 1.34 (m, 4H, 2CH₂), 0.91 (t, ³J = 6.9 Hz, 3H, CH₃). ¹³C NMR (75 MHz,

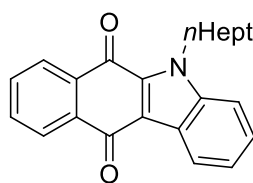
CDCl₃) δ = 181.3, 179.0 (C=O), 139.5, 134.9, 134.3 (C_{Ar}), 133.8 (CH_{Ar}), 133.8 (C_{Ar}), 132.9, 127.3, 126.6, 126.4, 124.5 (CH_{Ar}), 124.2 (C_{Ar}), 124.1 (CH_{Ar}), 119.1 (C_{Ar}), 111.2 (CH_{Ar}), 45.5 (CH₂), 30.1 (CH₂), 29.1 (CH₂), 22.6 (CH₂), 14.1 (CH₃) IR (ATR, cm⁻¹), $\tilde{\nu}$ = 3061 (w), 3030 (w), 3012 (w), 2957 (m), 2947 (m), 2926 (m), 2866 (m), 2727 (w), 1660 (s), 1643 (s), 1614 (m), 1591 (s), 1518 (s), 1495 (m), 1475 (s), 1456 (m). MS (EI, 70 eV), m/z (%) = 317 (M⁺, 86), 288 (11), 274 (16), 260 (100), 247 (32), 219 (11), 204 (10), 190 (20), 176 (12), 163 (7), HRMS (ESI-TOF), calcd for C₂₁H₁₉NO₂ ([M+H]⁺), 318.14886, found, 318.14889

5-hexyl-5H-benzo[b]carbazole-6,11-dione (10m)



Following general procedur, **10m** was obtained as a yellow solid (57 %), mp = 115 - 117 °C. ¹H NMR (250 MHz, CDCl₃) δ = 8.46 (d, ³J = 7.8 Hz, 1H, CH_{Ar}), 8.26 – 8.09 (m, 2H, CH_{Ar}), 7.77 – 7.60 (m, 2H, CH_{Ar}), 7.51 – 7.33 (m, 3H, CH_{Ar}), 4.74 – 4.63 (m, 2H, CH₂), 1.95 – 1.78 (m, 2H, CH₂), 1.53 – 1.28 (m, 6H, 3CH₂), 0.88 (t, ³J = 6.7 Hz, 3H, CH₃). ¹³C NMR (63 MHz, CDCl₃) δ = 181.3, 179.0 (C=O), 139.5, 134.9, 134.3, 133.8 (C_{Ar}), 133.8, 132.9, 127.3, 126.6, 126.4, 124.6 (CH_{Ar}), 124.2 (C_{Ar}), 124.1 (CH_{Ar}), 119.1 (C_{Ar}), 111.2 (CH_{Ar}), 45.5 (CH₂), 31.6 (CH₂), 30.3 (CH₂), 26.7 (CH₂), 22.7 (CH₂), 14.1 (CH₃). IR (ATR, cm⁻¹), $\tilde{\nu}$ = 2968 (w), 2953 (m), 2922 (m), 2870 (w), 2854 (m), 1657 (s), 1643 (s), 1612 (m), 1591 (s), 1516 (s). MS (EI, 70 eV), m/z (%) = 331 (M⁺, 96), 302 (8), 260 (100), 247 (30), 232 (11), 190 (18), 176 (13). HR-MS (EI), calcd for C₂₂H₂₁NO₂ (M⁺), 331.15668, found, 331.15677.

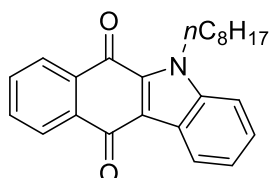
5-heptyl-5H-benzo[b]carbazole-6,11-dione (10n)



Following the general procedure, **10n** was obtained as a yellow solid (44 %), mp = 106 - 108 °C. ¹H NMR (300 MHz, CDCl₃) δ = 8.05 – 8.43 (m, 1H, CH_{Ar}), 8.26 – 8.12 (m, 2H, CH_{Ar}), 7.78 – 7.62 (m, 2H, CH_{Ar}), 7.51 – 7.34 (m, 3H, CH_{Ar}), 4.70 (m, 2H, CH₂), 1.98 – 1.77 (m, 2H, CH₂), 1.47 – 1.26 (m, 8H, 4CH₂), 0.87 (t, ³J = 6.8 Hz, 3H, CH₃). ¹³C NMR (63 MHz, CDCl₃) δ = 181.3, 179.0 (C=O), 139.5, 134.9, 134.3 (C_{Ar}), 133.8 (CH_{Ar}), 133.8 (C_{Ar}), 132.9, 127.3, 126.6, 126.4, 124.6 (CH_{Ar}), 124.2 (C_{Ar}), 124.1 (CH_{Ar}), 119.1 (C_{Ar}), 111.2 (CH_{Ar}), 45.5 (CH₂), 31.8 (CH₂), 30.4 (CH₂), 29.1 (CH₂), 27.0 (CH₂), 22.7 (CH₂), 14.2 (CH₃). IR (ATR, cm⁻¹), $\tilde{\nu}$ = 2953 (m), 2918 (s), 2870 (m), 2854 (m), 1657 (vs), 1640 (s), 1614 (m), 1593 (s), 1514 (s), 1495 (s), 1475 (s). MS (EI, 70 eV), m/z (%) = 345 (M⁺, 100), 302 (6), 260 (83), 247 (28),

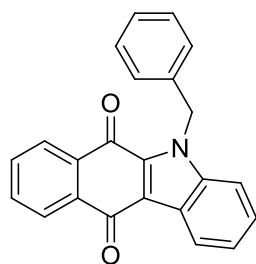
232 (13), 190 (14), 105 (5), 88 (1), 77 (4), 55 (2), 41 (10). HRMS (ESI-TOF), calcd for $C_{23}H_{23}NO_2$ ($[M+H]^+$), $m/z=346.18016$, found 346.18013; calcd for $C_{23}H_{23}NaNO_2$ ($[M+Na]^+$), 368.1621, found 368.16218.

5-octyl-5H-benzo[b]carbazole-6,11-dione (10o)



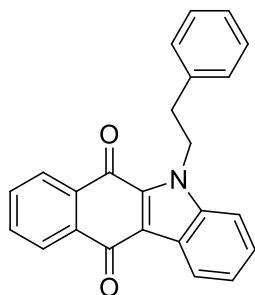
Following the general procedure, **10o** was obtained as a yellow solid (33 %), mp = 77 - 78 °C. 1H NMR (250 MHz, $CDCl_3$) δ = 8.52 – 8.39 (m, 1H, CH_{Ar}), 8.26 – 8.08 (m, 2H, CH_{Ar}), 7.79 – 7.61 (m, 2H, CH_{Ar}), 7.50 – 7.31 (m, 3H, CH_{Ar}), 4.81 – 4.60 (m, 2H, CH_2), 1.96 – 1.77 (m, 2H, CH_2), 1.47 – 1.24 (m, 10H, 5 CH_2), 0.93 – 0.81 (m, 3H, CH_3). ^{13}C NMR (63 MHz, $CDCl_3$) δ = 181.3, 179.0 (C=O), 139.5, 134.9, 134.3 (C_{Ar}), 133.8 (CH_{Ar}), 133.8 (C_{Ar}), 132.9, 127.3, 126.6, 126.4, 124.6 (CH_{Ar}), 124.2 (C_{Ar}), 124.1 (CH_{Ar}), 119.1 (C_{Ar}), 111.2 (CH_{Ar}), 45.5 (CH_2), 31.9 (CH_2), 30.4 (CH_2), 29.4 (CH_2), 29.3 (CH_2), 27.1 (CH_2), 22.7 (CH_2), 14.2 (CH_3). IR (ATR, cm^{-1}), $\tilde{\nu}$ = 2955 (w), 2920 (m), 2854 (m), 1657 (s), 1641 (s), 1612 (w), 1595 (s), 1512 (s), 1493 (m), 1477 (s), 1454 (m), 1433 (w), 1421 (m). MS (EI, 70 eV), m/z (%) = 359 (M^+ , 100), 330 (3), 274 (13), 260 (80), 247 (21), 232 (8), 190 (12), 77 (2), 41 (9). HR-MS (EI), calcd for $C_{24}H_{25}NO_2$ (M^+), 359.18798, found, 359.18793.

5-benzyl-5H-benzo[b]carbazole-6,11-dione (10p)



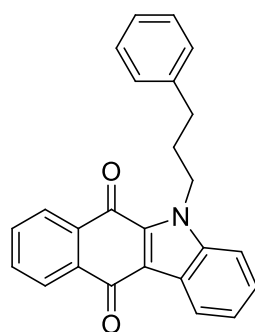
Following the general procedure, **10p** was obtained as a yellow solid (52 %), mp = 175 – 177 °C. 1H NMR (300 MHz, $CDCl_3$) δ = 8.55 – 8.46 (m, 1H, CH_{Ar}), 8.28 – 8.19 (m, 1H, CH_{Ar}), 8.17 – 8.12 (m, 1H, CH_{Ar}), 7.78 – 7.62 (m, 2H, CH_{Ar}), 7.49 – 7.38 (m, 3H, CH_{Ar}), 7.32 – 7.26 (m, 2H, CH_{Ar}), 7.25 – 7.17 (m, 3H, CH_{Ar}), 6.01 (s, 2H, CH_2); ^{13}C NMR (63 MHz, $CDCl_3$) δ = 181.5, 179.2 (C=O), 140.0, 136.7, 135.0, 134.3 (C_{Ar}), 134.0 (CH_{Ar}), 133.8 (C_{Ar}), 133.1 (CH_{Ar}), 129.1 (2 CH_{Ar}), 128.0, 127.8 (CH_{Ar}), 126.9 (2 CH_{Ar}), 126.8, 126.5, 124.9 (CH_{Ar}), 124.4 (C_{Ar}), 124.2 (CH_{Ar}), 119.7 (C_{Ar}), 111.7 (CH_{Ar}), 48.6 (CH_2). IR (ATR, cm^{-1}), $\tilde{\nu}$ = 3305 (w), 3282 (w), 3086 (w), 3056 (w), 3029 (m), 3007 (w), 2922 (w), 2850 (w), 1658 (s), 1645 (vs), 1594 (m), 1585 (s), 1520 (s), 1493 (s), 1466 (s). MS (EI, 70 eV), m/z (%) = 337 (M^+ , 100), 320 (5), 292 (3), 278 (3), 260 (6), 231 (3), 204 (3), 190 (6), 163 (4), 139 (3), 114 (2), 91 (98). HR-MS (EI), calcd for $C_{23}H_{15}NO_2$ (M^+) 337.10973, found 337.10948.

5-phenethyl-5H-benzo[b]carbazole-6,11-dione (10q)



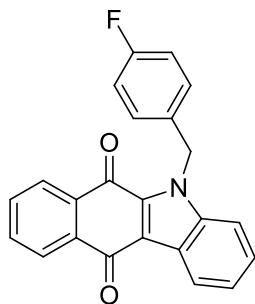
Following the general procedure, **10q** was obtained as a yellow solid (55 %), mp = 171 – 172 °C. ¹H NMR (250 MHz, CDCl₃) δ = 8.52 – 8.41 (m, 1H, CH_{Ar}), 8.26 – 8.12 (m, 2H, CH_{Ar}), 7.80 – 7.59 (m, 2H, CH_{Ar}), 7.48 – 7.32 (m, 3H, CH_{Ar}), 7.29 – 7.16 (m, 5H, CH_{Ar}), 4.97 – 4.84 (m, 2H, CH₂), 3.23 – 3.11 (m, 2H, CH₂). ¹³C NMR (63 MHz, CDCl₃) δ = 181.4, 179.0 (C=O), 139.4, 137.9, 134.8, 134.3 (C_{Ar}), 133.9 (CH_{Ar}), 133.7 (C_{Ar}), 133.0 (CH_{Ar}), 129.1, 128.8 (2CH_{Ar}), 127.4, 127.0, 126.6, 126.4, 124.6 (CH_{Ar}), 124.1 (C_{Ar}), 124.1 (CH_{Ar}), 119.3 (C_{Ar}), 111.0 (CH_{Ar}), 47.0 (CH₂), 36.7 (CH₂). IR (ATR, cm⁻¹), $\tilde{\nu}$ = 3074 (m), 3055 (m), 3022 (m), 2958 (m), 2920 (m), 1655 (s), 1643 (s), 1587 (s), 1514 (s), 1491 (s), 1468 (s), 1450 (s), 1419 (s), 1398 (s), 1369 (m). MS (EI, 70 eV), m/z (%) = 351 (M⁺, 33), 260 (100), 247 (14), 232 (4), 203 (6), 176 (9), 151 (3), 128 (2). HR-MS (EI), calcd for C₂₄H₁₇NO₂ (M⁺), 351.12538, found 351.12567

5-(3-phenylpropyl)-5H-benzo[b]carbazole-6,11-dione (10r)



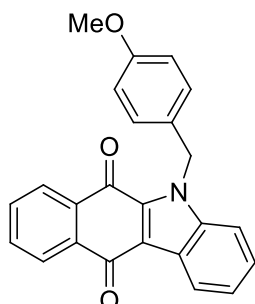
Following the general procedure, **10r** was obtained as a yellow solid (48 %), mp = 155 – 156 °C. ¹H NMR (250 MHz, CDCl₃) δ = 8.49 – 8.42 (m, 1H, CH_{Ar}), 8.25 – 8.13 (m, 2H, CH_{Ar}), 7.77 – 7.64 (m, 2H, CH_{Ar}), 7.41 – 7.27 (m, 5H, CH_{Ar}), 7.24 – 7.16 (m, 3H, CH_{Ar}), 4.91 – 4.59 (m, 2H, CH₂), 2.92 – 2.64 (m, 2H, CH₂), 2.35 – 2.06 (m, 2H, CH₂). ¹³C NMR (63 MHz, CDCl₃) δ = 181.3, 179.1 (C=O), 140.9, 139.4, 134.9, 134.3 (C_{Ar}), 133.9 (CH_{Ar}), 133.7 (C_{Ar}), 132.9 (CH_{Ar}), 128.6, 128.4 (2CH_{Ar}), 127.4, 126.6, 126.4, 126.3, 124.6 (CH_{Ar}), 124.2 (C_{Ar}), 124.1 (CH_{Ar}), 119.2 (C_{Ar}), 111.1 (CH_{Ar}), 45.0, 33.2, 31.5 (CH₂). IR (ATR, cm⁻¹), $\tilde{\nu}$ = 3024 (w), 2960 (w), 2947 (w), 2931 (w), 2914 (w), 1576 (w), 1516 (s), 1421 (m), 1398 (m), 1356 (m), 1344 (m), 1275 (w), 1242 (s), 1221 (m), 1207 (s), 1167 (m). MS (EI, 70 eV), m/z (%) = 365 (M⁺, 72), 336 (2), 274 (23), 261 (100), 247 (6), 232 (9), 204 (10), 190 (9), 176 (8), 91 (12). HR-MS (EI), calcd for C₂₅H₁₉O₂N (M⁺) 365.14103, found 365.14055.

5-(4-fluorobenzyl)-5H-benzo[b]carbazole-6,11-dione (10s)



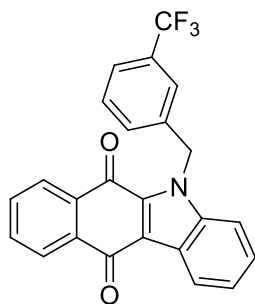
Starting from (4-fluorophenyl)methanamine, following the general procedure, **10s** was obtained as a yellow solid (52 %), mp = 200 – 201 °C. ^1H NMR (250 MHz, CDCl_3) δ = 8.53 – 8.44 (m, 1H, CH_{Ar}), 8.25 – 8.18 (m, 1H, CH_{Ar}), 8.16 – 8.09 (m, 1H, CH_{Ar}), 7.78 – 7.62 (m, 2H, CH_{Ar}), 7.48 – 7.35 (m, 3H, CH_{Ar}), 7.23 – 7.14 (m, 2H, CH_{Ar}), 7.03 – 6.90 (m, 2H, CH_{Ar}), 5.94 (s, 2H, CH_2). ^{19}F NMR (235 MHz, CDCl_3) δ = -114.39. ^{13}C NMR (63 MHz, CDCl_3) δ = 181.4, 179.1 (C=O), 162.4 (d, 1J = 246.5 Hz, CF), 139.7, 134.7, 134.2 (C_{Ar}), 134.0 (CH_{Ar}), 133.6 (C_{Ar}), 133.0 (CH_{Ar}), 132.4 (d, 4J = 3.2 Hz, C_{Ar}), 128.7 (d, 3J = 8.2 Hz, 2CH_{Ar}), 127.8, 126.7, 126.8, 124.8 (CH_{Ar}), 124.2 (C_{Ar}), 124.2 (CH_{Ar}), 119.6 (C_{Ar}), 115.9 (d, 2J = 21.7 Hz, 2CH_{Ar}), 111.4 (CH_{Ar}), 47.7 (CH_2). IR (ATR, cm^{-1}), $\tilde{\nu}$ = 3284 (w), 3066 (w), 3055 (w), 3003 (w), 1645 (s), 1595 (s), 1508 (s), 1464 (s), 1194 (s), 1165 (s), 1155 (m), 1146 (m), 1126 (m), 1099 (m). MS (EI, 70 eV), m/z (%) = 355 (M^+ , 73), 296 (1), 296 (1), 260 (2), 222 (3), 190 (6), 130 (2), 109 (100), 83 (10). HRMS (ESI-TOF), calcd for $\text{C}_{23}\text{H}_{14}\text{NFO}_2$ ($[\text{M}+\text{H}]^+$), 356.10813.

5-(4-methoxybenzyl)-5H-benzo[b]carbazole-6,11-dione (10t)



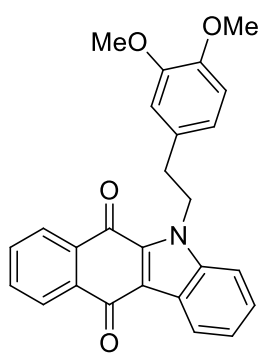
Following the general procedure, **10t** was obtained as a yellow solid (58 %), mp = 182 – 183 °C. ^1H NMR (300 MHz, CDCl_3) δ = 8.50 – 8.44 (m, 1H, CH_{Ar}), 8.20 (dd, 3J = 7.5 Hz, 4J = 1.3 Hz, 1H, CH_{Ar}), 8.14 (dd, 3J = 7.4 Hz, 4J = 1.4 Hz, 1H, CH_{Ar}), 7.61 – 7.75 (m, 2H, CH_{Ar}), 7.51 – 7.34 (m, 3H, CH_{Ar}), 7.10 (d, 3J = 5.8 Hz, 2H, CH_{Ar}), 6.84 – 6.77 (m, 2H, CH_{Ar}), 5.90 (s, 2H, CH_2), 3.73 (s, 3H, OCH_3). ^{13}C NMR (75 MHz, CDCl_3) δ = 181.4, 179.0 (C=O), 159.3, 139.8, 134.8, 134.2 (C_{Ar}), 133.9 (CH_{Ar}), 133.7 (C_{Ar}), 132.9 (CH_{Ar}), 128.8 (C_{Ar}), 128.3 (2CH_{Ar}), 127.6, 126.7, 126.4, 124.7 (CH_{Ar}), 124.3 (C_{Ar}), 124.1 (CH_{Ar}), 119.5 (C_{Ar}), 114.3 (2CH_{Ar}), 111.6 (CH_{Ar}), 55.4 (OCH_3), 48.0 (CH_2). IR (ATR, cm^{-1}), $\tilde{\nu}$ = 3289 (w), 3052 (m), 2933 (m), 1612 (m), 1591 (s), 1584 (s), 1515 (vs), 1493 (s), 1466 (s), 1439 (s), 1420 (m), 1396 (s), 1316 (m), 1252 (s), 1239 (vs), 1189 (s), 1166 (s). MS (EI, 70 eV), m/z (%) = 367 (M^+ , 37), 203 (2), 190 (7), 139 (2), 121 (100), 91 (6), 78 (8), 77 (9). HR-MS (EI), calcd for $\text{C}_{24}\text{H}_{17}\text{O}_3\text{N}$ ($[\text{M}+\text{H}]^+$) 368.12812, found 368.12771.

5-(3-(trifluoromethyl)benzyl)-5H-benzo[b]carbazole-6,11-dione (10u)



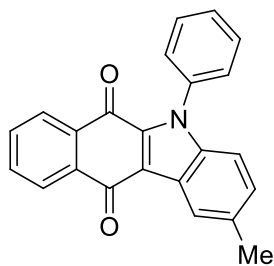
Following the general procedure, **10u** was obtained as a yellow solid (59 %), mp = 198 – 199 °C. ^1H NMR (300 MHz, CDCl_3) δ = 8.56 – 8.47 (m, 1H, CH_{Ar}), 8.28 – 8.19 (m, 1H, CH_{Ar}), 8.18 – 8.10 (m, 1H, CH_{Ar}), 7.80 – 7.64 (m, 2H, CH_{Ar}), 7.60 – 7.34 (m, 6H, CH_{Ar}), 7.30 – 7.27 (m, 1H, CH_{Ar} overlap with solvent signal), 6.04 (s, 2H, CH_2). ^{19}F NMR (282 MHz, CDCl_3) δ = -62.62. ^{13}C NMR (75 MHz, CDCl_3) δ = 181.4, 179.1 (C=O), 139.7, 137.7, 134.76, 134.2 (C_{Ar}), 134.1 (CH_{Ar}), 133.6 (C_{Ar}), 133.1 (CH_{Ar}), 131.4 (q, 2J = 32.5 Hz, C- CF_3), 130.01 (q, 4J = 1.1 Hz, CH_{Ar}), 129.6, 128.0, 126.7, 126.5, 125.0 (CH_{Ar}), 124.9 (q, 3J = 3.7 Hz, CH_{Ar}), 124.3 (q, 1J = 273 Hz, CF_3), 124.3 (CH_{Ar}), 124.3 (C_{Ar}), 123.8 (q, 3J = 3.9 Hz, CH_{Ar}), 119.8 (C_{Ar}), 111.2 (CH_{Ar}), 48.2 (CH_2). IR (ATR, cm^{-1}), $\tilde{\nu}$ = 3290 (w), 3078 (w), 2989 (w), 1612 (w), 1597 (m), 1585 (m), 1419 (m), 1396 (m), 1362 (w), 1352 (w), 1329 (s), 1282 (m), 1219 (m), 1198 (s). MS (EI, 70 eV), m/z (%) = 405 (M^+ , 100), 376 (6), 260 (16), 190 (7), 159 (49), 139 (4), 109 (12). HRMS (ESI-TOF), calcd for $\text{C}_{24}\text{H}_{14}\text{NF}_3\text{O}_2$ ($[\text{M}+\text{H}]^+$), 406.10494, found 406.10512; calcd for $\text{C}_{24}\text{H}_{14}\text{NaNF}_3\text{O}_2$ ($[\text{M}+\text{Na}]^+$), 428.08688, found 428.08715.

5-(3,4-dimethoxyphenylethyl)-5H-benzo[b]carbazole-6,11-dione (10v)



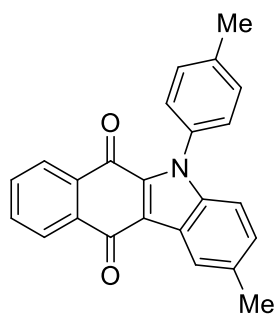
Starting from 2-(3,4-dimethoxyphenyl)ethanamine, following the general procedure, **10v** was obtained as a yellow solid (66 %), mp = 153 – 154 °C. ^1H NMR (250 MHz, CDCl_3) δ = 8.51 – 8.24 (m, 1H, CH_{Ar}), 8.20 – 7.86 (m, 2H, CH_{Ar}), 7.73 – 7.45 (m, 2H, CH_{Ar}), 7.41 – 7.06 (m, 3H, CH_{Ar}), 6.74 – 6.43 (m, 3H, CH_{Ar}), 5.05 – 4.48 (m, 2H, CH_2), 3.69 (s, 3H, CH_3), 3.67 (s, 3H, CH_3), 3.09 – 2.85 (m, 2H, CH_2). ^{13}C NMR (63 MHz, CDCl_3) δ = 181.20, 178.81 (C=O), 149.1, 148.0, 139.4, 134.8, 134.1 (C_{Ar}), 133.8 (CH_{Ar}), 133.6 (C_{Ar}), 132.9 (CH_{Ar}), 130.4 (C_{Ar}), 127.3, 126.5, 126.3, 124.5 (CH_{Ar}), 124.0 (C_{Ar}), 123.9, 121.1 (CH_{Ar}), 119.1 (C_{Ar}), 112.3, 111.4, 111.0 (CH_{Ar}), 56.0, 55.9 (OCH_3), 46.9 (CH_2), 36.2 (CH_2). IR (ATR, cm^{-1}), $\tilde{\nu}$ = 3063 (w), 2997 (w), 2918 (m), 2848 (m), 1655 (s), 1643 (m), 1616 (w), 1605 (w), 1539 (w), 1512 (s), 1437 (m), 1375 (m), 1281 (m), 1257 (s). MS (EI, 70 eV), m/z (%) = 411 (M^+ , 54), 260 (49), 247 (13), 203 (8), 176 (11), 164 (29), 151 (100), 107 (10). HR-MS (EI), calcd for $\text{C}_{26}\text{H}_{21}\text{O}_4\text{N}$ (M^+) 411.14651, found 411.14639.

2-methyl-5-phenyl-5H-benzo[b]carbazole-6,11-dione (11a)



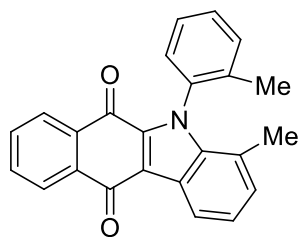
Starting from 4-methyl-*N*-phenylaniline, following the general procedure, the mixture **11a** and **10b** was obtained as a yellow solid (41.7 mg, 41 %). The pure of **11a** was isolated by recrystallizing from heptane and ethyl acetate (5:1), and washing the precipitate with cold ethyl acetate, (25 %) mp = 301 - 302 °C. ¹H NMR (300 MHz, CDCl₃) δ = 8.34 – 8.22 (m, 2H, CH_{Ar}), 8.07 – 8.01 (m, 1H, CH_{Ar}), 7.77 – 7.56 (m, 5H, CH_{Ar}), 7.47 – 7.41 (m, 2H, CH_{Ar}), 7.25 – 7.18 (m, 1H, CH_{Ar}), 7.06 (d, ³*J* = 8.6 Hz, 1H, CH_{Ar}), 2.53 (s, 3H, CH₃). ¹³C NMR (75 MHz, CDCl₃) δ = 181.8, 177.7 (C=O), 139.8, 137.1, 135.0, 134.3 (C_{Ar}), 133.8 (CH_{Ar}), 133.8 (C_{Ar}), 133.1, 129.8 (CH_{Ar}), 129.6 (2CH_{Ar}), 129.3 (CH_{Ar}), 127.7 (2CH_{Ar}), 126.6 (CH_{Ar}), 126.5, 124.9 (C_{Ar}), 124.3 (CH_{Ar}), 123.1 (CH_{Ar}), 119.6 (C_{Ar}), 111.9 (CH_{Ar}), 21.7 (CH₃). IR (ATR, cm⁻¹), $\tilde{\nu}$ = 3061 (w), 2910 (w), 1651 (s), 1590 (m), 1518 (s), 1219 (s), 1176 (m), 1157 (m), 1093 (m), 1047 (m), 1030 (m). MS (EI, 70 eV), *m/z* (%) = 337 (M⁺, 100), 308 (7), 278 (9), 233 (1), 203 (3), 168 (12), 153 (3), 139 (4), 77 (4). HR-MS (EI), calcd for C₂₃H₁₅NO₂ (M⁺) 337.10973, found 337.10948.

2-methyl-5-(*p*-tolyl)-5H-benzo[b]carbazole-6,11-dione (11b)



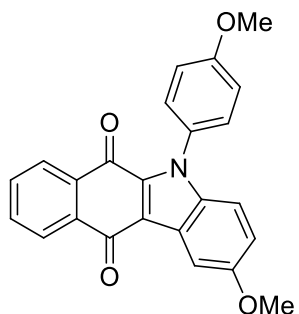
Starting from di-*p*-tolylamine, following the general procedure, **11b** was obtained as a yellow solid (42 %), mp = 301 – 302 °C. ¹H NMR (300 MHz, CDCl₃) δ = 8.33 – 8.28 (m, 1H, CH_{Ar}), 8.26 - 8.21 (m, 1H, CH_{Ar}), 8.09 – 8.02 (m, 1H, CH_{Ar}), 7.68 (m, 2H, CH_{Ar}), 7.40 (d, ³*J* = 8.1 Hz, 2H, CH_{Ar}), 7.34 – 7.29 (m, 2H, CH_{Ar}), 7.21 (dd, ³*J* = 8.6 Hz, ⁴*J* = 1.4 Hz, 1H, CH_{Ar}), 7.06 (d, ³*J* = 8.6 Hz, 1H, CH_{Ar}), 2.52, 2.51 (CH₃). ¹³C NMR (63 MHz, CDCl₃) δ = 181.9, 177.8 (C=O), 139.9, 139.4, 135.7, 135.0, 134.5, 134.4 (C_{Ar}), 133.9, 133.1 (CH_{Ar}), 130.4 (2CH_{Ar}), 130.0 (CH_{Ar}), 129.8 (C_{Ar}), 127.5 (2CH_{Ar}), 126.7, 126.5 (CH_{Ar}), 124.4 (C_{Ar}), 123.2 (CH_{Ar}), 119.6 (C_{Ar}), 112.1 (CH_{Ar}), 21.8, 21.6 (CH₃). IR (ATR, cm⁻¹), $\tilde{\nu}$ = 3063 (w), 2997 (w), 2933 (w), 2922 (m), 1643 (s), 1591 (s), 1512 (s), 1462 (s), 1452 (s), 1419 (s), 1398 (s), 1257 (s), 1234 (s), 1182 (s), 1088 (m), 1063 (s), 1047 (m). MS (EI, 70 eV), *m/z* (%) = 351 (M⁺, 100), 336 (29), 322 (6), 294 (6), 278 (6), 168 (9), 151 (3), 132 (4). HRMS (ESI-TOF), calcd for C₂₄H₁₇NO₂ ([M+H]⁺), *m/z* = 352.13321, found 352.13327; calcd for C₂₄H₁₇NaNO₂ ([M+Na]⁺), *m/z* = 374.11515, found 374.11509.

4-methyl-5-(*o*-tolyl)-5*H*-benzo[*b*]carbazole-6,11-dione (11c)



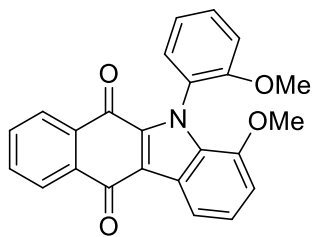
Following the general procedure, **11c** was obtained as an orange solid (47 %), mp = 189 – 190 °C. ¹H NMR (300 MHz, CDCl₃) δ = 8.46 (d, ³J = 8.1 Hz, 1H, CH_{Ar}), 8.25 (dd, ³J = 7.6 Hz, ⁴J = 1.4 Hz, 1H, CH_{Ar}), 8.01 (dd, ³J = 7.6 Hz, ⁴J = 1.3 Hz, 1H, CH_{Ar}), 7.71 – 7.66 (m, 2H, CH_{Ar}), 7.55 – 7.28 (m, 4H, CH_{Ar}), 7.14 (d, ³J = 7.1 Hz, 2H, CH_{Ar}), 2.02 (s, 3H, CH₃), 1.85 (s, 3H, CH₃). ¹³C NMR (63 MHz, CDCl₃) δ = 181.8, 177.7 (C=O), 138.5, 138.5, 136.9, 135.6, 134.3, 133.8 (C_{Ar}), 133.6, 133.0, 130.7, 130.4, 129.8, 128.7 (CH_{Ar}), 126.7 (C_{Ar}), 126.6, 126.4, 126.3, 124.9 (CH_{Ar}), 123.8 (C_{Ar}), 121.9 (CH_{Ar}), 119.7 (C_{Ar}), 18.3, 17.5 (CH₃). IR (ATR, cm⁻¹), $\tilde{\nu}$ = 3054 (w), 2917 (m), 1646 (s), 1515 (s), 1471 (m), 1454 (s), 1394 (s), 1290 (s), 1214 (s), 1176 (m), 1147 (s), 1106 (m). MS (EI, 70 eV), m/z (%) = 353 (3), 352 (26), 351 (100), 350 (18), 337 (14), 336 (48), 334 (24), 322 (17), 278 (11), 218 (15), 176 (7), 139 (6). HRMS (EI), calcd for C₂₄H₁₇NO₂ (M⁺), m/z = 351.12538, found 351.12555.

2-methoxy-5-(4-methoxyphenyl)-5*H*-benzo[*b*]carbazole-6,11-dione (11d)



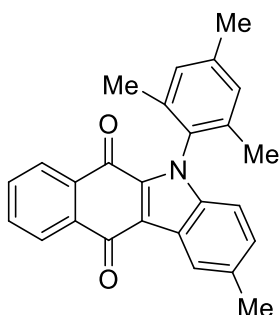
Following the general procedure, **11d** was obtained as an orange solid (38 %), mp = 239 – 240 °C. ¹H NMR (300 MHz, CDCl₃) δ 8.19 (dd, ³J = 7.5 Hz, ⁴J = 1.2 Hz, 1H, CH_{Ar}), 8.02 (dd, ³J = 7.5 Hz, ⁴J = 1.2 Hz, 1H, CH_{Ar}), 7.85 (d, ⁴J = 1.9 Hz, 1H, CH_{Ar}), 7.69 – 7.58 (m, 2H, CH_{Ar}), 7.40 – 7.31 (m, 2H, CH_{Ar}), 7.15 – 6.95 (m, 4H, CH_{Ar}), 3.93 (s, 3H, OCH₃), 3.92 (s, 3H, OCH₃). ¹³C NMR (75 MHz, CDCl₃) δ 181.7, 177.4 (C=O), 160.0, 158.1, 136.7, 135.4, 134.2, 133.8 (C_{Ar}), 133.7, 133.0 (CH_{Ar}), 129.5 (C_{Ar}), 128.7 (2CH_{Ar}), 126.6, 126.3 (CH_{Ar}), 124.7 (C_{Ar}), 119.7 (CH_{Ar}), 119.2 (C_{Ar}), 114.7 (2CH_{Ar}), 113.4, 102.8 (CH_{Ar}), 55.9, 55.7 (OCH₃). IR (ATR, cm⁻¹), $\tilde{\nu}$ = 1648 (s), 1612 (m), 1587 (m), 1513 (s), 1490 (s), 1475 (s), 1463 (s), 1438 (m), 1423 (m). MS (EI, 70 eV), m/z (%) = 385 (4), 384 (25), 383 (100), 368 (19), 340 (3), 297 (3), 277 (2). HRMS (EI), calcd for C₂₄H₁₇NO₄ (M⁺), m/z = 383.11576, found 383.39608

1-methoxy-5-(2-methoxyphenyl)-5*H*-benzo[*b*]carbazole-6,11-dione (11e)



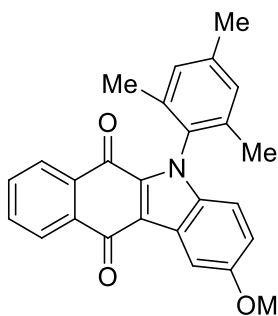
Following the general procedure, **11e** was obtained as an orange solid (35 %), mp = 239 – 240 °C. ¹H NMR (300 MHz, CDCl₃) δ = 8.22 (d, ³J = 7.5 Hz, 1H, CH_{Ar}), 8.04 (dd, ³J = 7.5 Hz, ⁴J = 1.2 Hz, 1H, CH_{Ar}), 7.88 (d, ³J = 1.8 Hz, 1H, CH_{Ar}), 7.75 – 7.59 (m, 2H, CH_{Ar}), 7.39 – 7.32 (m, 2H, CH_{Ar}), 7.15 – 6.99 (m, 4H, CH_{Ar}), 3.95 (s, 3H, OCH₃), 3.93 (s, 3H, OCH₃). ¹³C NMR (75 MHz, CDCl₃) δ = 181.8, 177.5 (C=O), 160.1, 158.1, 136.8, 135.5, 134.3, 133.9 (C_{Ar}), 133.7, 133.0 (CH_{Ar}), 129.5 (C_{Ar}), 128.7 (2CH_{Ar}), 126.6, 126.3 (CH_{Ar}), 124.8 (C_{Ar}), 119.7 (CH_{Ar}), 119.3 (C_{Ar}), 114.8 (2CH_{Ar}), 113.4, 102.9 (CH_{Ar}), 56.0, 55.7 (OCH₃). IR (ATR, cm⁻¹), $\tilde{\nu}$ = 3061 (w), 2997 (w), 2550 (w), 2355 (w), 1649 (s), 1612 (m), 1514 (s), 1491 (s), 1439 (m), 1423 (m), 1398 (m), 1344 (m), 1317 (m), 1286 (m), 1128 (m), 1109 (m), 1092 (m). MS (EI, 70 eV), m/z (%) = 383 (M⁺, 100), 368 (30), 340 (7), 297 (6), 269 (3), 240 (5), 192 (5). HRMS (EI), calcd for C₂₄H₁₇NO₄ (M⁺), m/z = 383.11521, found 383.11509.

5-mesityl-2-methyl-5H-benzo[b]carbazole-6,11-dione (11f)



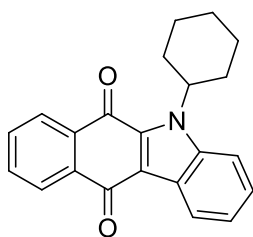
Following the general procedure, **11f** was obtained as an orange solid (44 %), mp = 239 – 240 °C. ¹H NMR (250 MHz, CDCl₃) δ 8.38 - 8.29 (m, 1H, CH_{Ar}), 8.27 (dd, ³J = 7.6 Hz, ³J = 1.4 Hz, 1H, CH_{Ar}), 8.04 (dd, ³J = 7.6 Hz, ⁴J = 1.3 Hz, 1H, CH_{Ar}), 7.77 – 7.60 (m, 2H, CH_{Ar}), 7.23 (dd, ³J = 8.6 Hz, ⁴J = 1.6 Hz, 1H, CH_{Ar}), 7.08 (s, 2H, CH_{Ar}), 6.86 (d, ³J = 8.6 Hz, 1H, CH_{Ar}), 2.54 (s, 3H, CH₃), 2.42 (s, 3H, CH₃), 1.86 (s, 6H, 2CH₃). ¹³C NMR (63 MHz, CDCl₃) δ 181.6, 177.6 (C=O), 138.9, 138.1 (C_{Ar}), 135.5 (2C_{Ar}), 135.3, 134.8, 134.3 (C_{Ar}), 133.6 (CH_{Ar}), 133.4 (C_{Ar}), 132.8 (CH_{Ar}), 132.6 (C_{Ar}), 129.7 (C_{Ar}), 129.3 (2CH_{Ar}), 126.4 (CH_{Ar}), 126.4 (CH_{Ar}), 124.2 (C_{Ar}), 123.0 (CH_{Ar}), 119.0 (C_{Ar}), 111.4 (CH_{Ar}), 21.6 (CH₃), 21.2 (CH₃), 17.3 (2CH₃). IR (ATR, cm⁻¹), $\tilde{\nu}$ = 2946 (w), 1654 (s), 1619 (m), 1592 (s), 1521 (s), 1483 (s), 1461 (s), 1442 (m), 1415 (s), 1380 (s), 1373 (m), 1330 (m), 1047 (s). MS (EI, 70 eV), m/z (%) = 381 (4), 380 (28), 379 (100), 378 (15), 364 (28), 362 (12), 351 (11), 350 (22), 246 (25), 182 (7), 146 (94). HRMS (EI), calcd for C₂₆H₂₁NO₃ (M⁺), m/z = 379.15668, found 379.15633.

5-mesityl-2-methoxy-5H-benzo[b]carbazole-6,11-dione (11g)



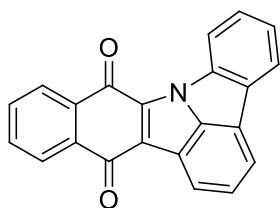
Following the general procedure, **11g** was obtained as an orange solid (51 %), mp = 239 – 240 °C. ¹H NMR (250 MHz, CDCl₃) δ 8.25 (dt, ³J = 6.2 Hz, ⁴J = 3.2 Hz, 1H, CH_{Ar}), 8.04 (dd, ³J = 7.5 Hz, ⁴J = 1.3 Hz, 1H, CH_{Ar}), 7.93 (d, ⁴J = 2.4 Hz, 1H, CH_{Ar}), 7.79 – 7.58 (m, 2H, CH_{Ar}), 7.11 – 6.98 (m, 3H, CH_{Ar}), 6.86 (d, ³J = 9.1 Hz, 1H, CH_{Ar}), 3.97 (s, 3H, OCH₃), 2.42 (s, 3H, CH₃), 1.86 (s, 6H, 2CH₃). ¹³C NMR (63 MHz, CDCl₃) δ 181.8, 177.5 (C=O), 158.3, 139.1, 135.6, 135.3, 135.0, 134.5 (C_{Ar}), 133.8 (CH_{Ar}), 133.7 (2C_{Ar}), 133.0 (C_{Ar}), 132.7 (CH_{Ar}), 129.5 (2CH_{Ar}), 126.8 (C_{Ar}), 126.6, 126.4 (CH_{Ar}), 125.0 (C_{Ar}), 120.0 (CH_{Ar}), 119.1 (C_{Ar}), 113.0, 103.1 (CH_{Ar}), 56.0 (OCH₃), 21.4 (CH₃), 17.5 (2CH₃). IR (ATR, cm⁻¹), $\tilde{\nu}$ = 2917 (m), 2850 (w), 2833 (w), 1652 (s), 1591 (s), 1511 (s), 1483 (s), 1459 (s), 1452 (s), 1434 (s), 1288 (s), 1259 (s), 1216 (s), 1178 (s), 1153 (s), 1122 (m), 1089 (m). MS (EI, 70 eV), m/z (%) = 397 (4), 396 (28), 395 (100), 380 (16), 366 (17), 336 (11), 262 (14), 119 (12). HRMS (EI), calcd for C₂₆H₂₁NO₃ (M⁺), m/z = 395.44984, found 395.44984

5-cyclohexyl-5H-benzo[b]carbazole-6,11-dione (11h)



Following the general procedure, **11h** was obtained as an orange solid (19 %), mp = 159 – 160 °C. ¹H NMR (300 MHz, CDCl₃) δ 8.55 – 8.51 (m, 1H, CH_{Ar}), 8.27 – 8.05 (m, 2H, CH_{Ar}), 7.80 – 7.59 (m, 3H, CH_{Ar}), 7.45 – 7.29 (m, 2H, CH_{Ar}), 5.74 (br-s, 1H, NCH), 2.53 – 1.33 (m, 10H). ¹³C NMR (75 MHz, CDCl₃) δ 181.5, 179.3, 138.8, 134.9, 134.7, 133.9 (C_{Ar}), 133.7, 132.9, 126.8, 126.7, 126.1 (CH_{Ar}), 125.1 (C_{Ar}), 124.3, 124.2 (CH_{Ar}), 119.5 (C_{Ar}), 114.3 (CH_{Ar}), 57.1 (CH), 31.1 (br, 2 CH₂), 26.4 (2CH₂), 25.5 (CH₂). IR (ATR, cm⁻¹), $\tilde{\nu}$ = 3070 (w), 2920 (m), 2856 (w), 1722 (m), 1645 (s), 1588 (s), 1552 (w), 1510 (s), 1494 (s), 1451 (s). MS (EI, 70 eV), m/z (%) = 329 (M⁺, 57), 300 (2), 286 (5), 247 (100), 219 (19), 190 (21), 163 (7), 105 (4), 77 (6), 55 (5). HRMS (EI), calcd for C₂₂H₁₉NO₂ (M⁺), m/z = 329.14103, found 329.14101

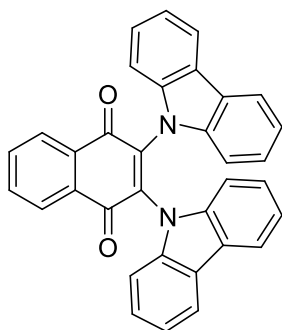
Benzo[b]indolo[3,2,1-jk]carbazole-9,14-dione (12a)



Starting from carbazole, following the general procedure, **12a** was obtained as a light red solid (28 %), mp = 251 – 253 °C. ¹H NMR (300 MHz, CDCl₃) δ = 8.64 (d, ³J = 8.1 Hz, 1H, CH_{Ar}), 8.27 – 8.15 (m, 3H, CH_{Ar}), 7.99 – 7.87 (m, 2H, CH_{Ar}), 7.81 – 7.70 (m, 2H, CH_{Ar}), 7.64 – 7.59 (m, 2H, CH_{Ar}), 7.44 – 7.35 (m, 1H, CH_{Ar}). ¹³C NMR (75 MHz, CDCl₃) δ = 181.7,

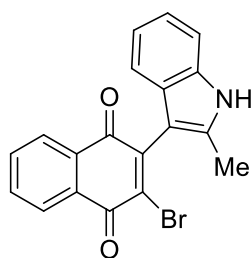
177.9 (C=O), 142.2, 139.4, 136.5 (C_{Ar}), 134.1 (CH_{Ar}), 133.8 (C_{Ar}), 133.3 (CH_{Ar}), 132.9, 131.6 (C_{Ar}), 128.4, 127.5, 126.9, 126.8 (CH_{Ar}), 126.3 (C_{Ar}), 125.3, 124.0, 123.3, 122.0 (CH_{Ar}), 120.9, 117.3 (C_{Ar}), 117.0 (CH_{Ar}). IR (ATR, cm⁻¹), $\tilde{\nu}$ = 3304 (w), 3286 (w), 3049 (w), 2920 (m), 2850 (m), 2679 (w), 1655 (s), 1593 (s), 1479 (s), 1263 (m), 1238 (s), 1223 (s), 1093 (m), 1063 (m), 1041 (m), 1012 (m). MS (EI, 70 eV), m/z (%) = 321 (M⁺, 100), 292 (18), 264 (17), 238 (3), 188 (3), 161 (3), 132 (11). HRMS (ESI-TOF), calcd for C₂₂H₁₁NO₂ ([M+H]⁺), m/z= 322.08626, found 322.08623; calcd for C₂₂H₁₁NaNO₂ ([M+Na]⁺), m/z= 344.0682, found 344.06811.

2,3-di (9H-carbazol-9-yl)naphthalene-1,4-dione (12b)



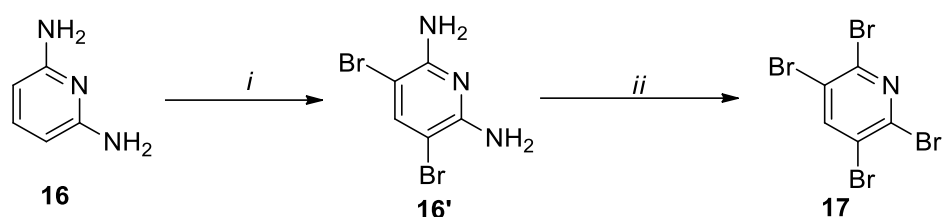
Starting from carbazole, following the general procedure, **13b** was obtained as a black-violet solid (32 %), mp = 103 – 105 °C. ¹H NMR (300 MHz, CDCl₃) δ = 8.40 – 8.33 (m, 2H, CH_{Ar}), 7.92 – 7.85 (m, 2H, CH_{Ar}), 7.75 – 7.67 (m, 4H, CH_{Ar}), 7.11 – 6.96 (m, 12H, CH_{Ar}). ¹³C NMR (75 MHz, CDCl₃) δ 180.0 (2C=O), 138.8 (4C_{Ar}), 136.7 (2C_{Ar}), 134.7 (2CH_{Ar}), 131.9 (2C_{Ar}), 127.6 (2CH_{Ar}), 125.7 (4CH_{Ar}), 124.8 (4C_{Ar}), 121.3 (4CH_{Ar}), 120.0 (4CH_{Ar}), 111.7 (4CH_{Ar}). IR (ATR, cm⁻¹), $\tilde{\nu}$ = 3045 (w), 3024 (w), 2924 (w), 1666 (m), 1624 (w), 1591 (m), 1489 (w), 1448 (m), 1441 (m), 1371 (m), 1331 (m), 1311 (m), 1263 (s), 1223 (s), 1180 (m), 1113 (m), 1101 (m), 1053 (w). MS (EI, 70 eV), m/z (%) = 490 (100), 489 ([M+H]⁺, 488 (15), 322 (9), 245 (8), 167 (18), 91 (7), 69 (13), 43 (19). HRMS (ESI-TOF), calcd for C₃₄H₂₀N₂O₂ ([M+H]⁺), m/z= 489.15975, found 489.16001.

2-bromo-3-(2-methyl-1H-indol-3-yl)naphthalene-1,4-dione (12c)



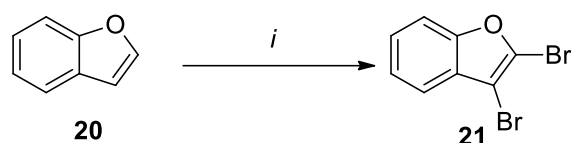
Starting from 2-methylindole, following the general procedure, **13c** was obtained as a black-violet solid (67 %), mp = 117 – 118 °C. ¹H NMR (250 MHz, CDCl₃) δ 8.40 (s, NH), 8.28 – 8.11 (m, 2H, CH_{Ar}), 7.86 – 7.70 (m, 2H,), 7.32 – 7.25 (m, 2H,), 7.25 – 7.00 (m, 2H,), 2.33 (s, 3H, CH₃). ¹³C NMR (75 MHz, CDCl₃) δ 181.5, 178.5 (C=O), 145.7, 139.2, 135.8, 135.4 (C_{Ar}), 134.1, 134.0 (CH_{Ar}), 132.0, 131.4 (C_{Ar}), 127.5 (2CH_{Ar}), 127.0 (C_{Ar}), 121.8, 120.5, 119.9, 110.9 (CH_{Ar}), 108.1 (C_{Ar}), 13.9 (CH₃). IR (ATR, cm⁻¹), $\tilde{\nu}$ = 3312 (m), 1643 (m), 1599 (s), 1548 (s), 1310 (m), 1239 (m), 1257 (m), 1194 (m), 1093 (s). MS (EI, 70 eV), m/z (%) = 369 (17), 368 (25), 367 (94), 366 (17), 365 (85), 286 (100), 269 (12), 258 (17), 230 (24), 143 (29). HRMS (ESI-TOF), calcd for C₁₉H₁₂BrNO₂ ([M+H]⁺), m/z= 366.01242, found 366.01256.

7.5. Supplement for Chapter 4



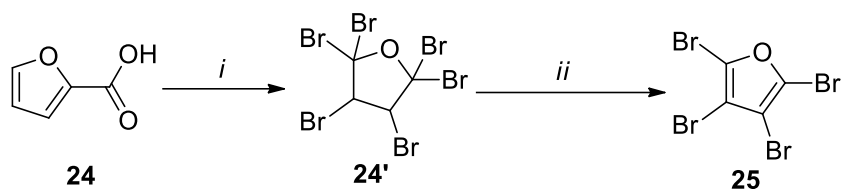
Scheme S7. Synthesis of 2,3,5,6-Tetrabromopyridine **17**

Procedure for starting compound 17: Bromine was dropped slowly into 200 ml glacial acetic acid solution of pyridine-2,6-diamine (10,9 g, 100 mmol). Then the reaction was stirred for 5 h at room temperature. The mixture worked up with Na₂SO₃ to remove all residual bromine, then was neutralized by NaOH to pH = 8-9. The brown solid was filtered, and washed with water. The obtained brown solid was dissolved in solution of HBr 48%. The solution was dropped into a saturated aqueous solution of NaNO₂ in -3 °C. The mixture was stirred for 3 h -3 °C and at room temperature for 2h. After neutralizing with NaOH, the mixture was extracted with ethyl acetate. The organic layers were dried over sodium sulfate and concentrated under vacuum. The crude material was purified by flash column chromatography (silica gel, heptane/ethylacetate).



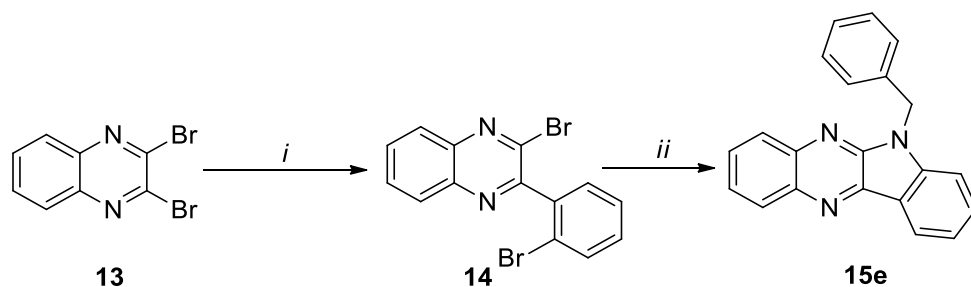
Scheme S8. 2,3-Dibromobenzofuran synthesis

Procedure for the starting compound 21: A solution of benzofuran (125 mmol) and AcOK (55.1 g, 562.5 mmol) in dichloromethane was dropped slowly into the solution of Br₂ in dichloromethane at 20 °C, then the mixture was reflux for 18 h. After removing the residual bromine by Na₂SO₃, the mixture was extracted with dichloromethane. The organic layers were dried over sodium sulfate and concentrated under vacuum. The crude material was purified by flash column chromatography (silica gel, heptane).

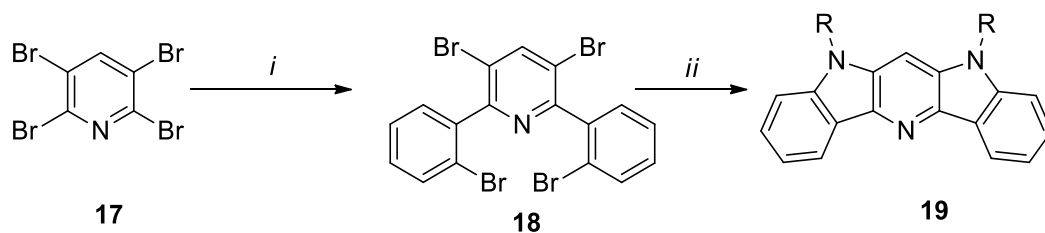


Scheme S9. 2,3,4,5-Tetrabromofuran synthesis

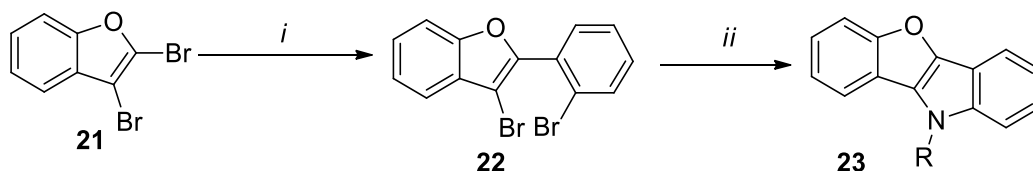
Procedure for the starting compound 25: Br₂ was dropped into the solution of furan-2-carboxylic acid (336 mg, 3 mmol) and KOH (168 mg, 3 mmol) under nitrogen atmosphere. The mixture was reflux for 6 h, then worked up with Na₂SO₃ and was extracted with dichloromethane. The organic layers were collected and dried by Na₂SO₄. The obtained solid was refluxed in MeOH in the presence of KOH for 12h. The solution was diluted with water, then extracted with ethyl acetate. The organic layer was collected, dried, then purified by flash column chromatography (silica gel, heptane).



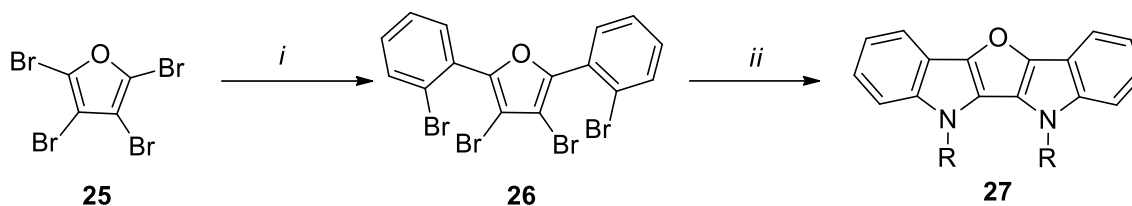
Scheme S10. Synthesis of indolo[2,3-*b*]quinoxalines **15e**.



Scheme S11. Synthesis of 5,7-disubstituted 5,7-dihydropyrido[3,2-*b*,5,6-*b'*]diindoles **19**.



Scheme 25. Synthesis of benzo[4,5]-furo[3,2-*b*]indoles **23**.



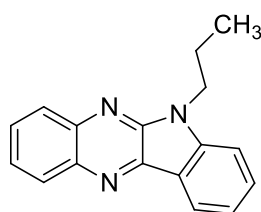
Scheme S12. Synthesis of furo[3,2-b,4,5-b']diindole **27**.

General procedure for Suzuki-Miyaura reaction. Brominated starting materials, 2-bromophenylboronic acid, Pd(PPh₃)₄ (5 mol%) and base were added to a 500 mL Schlenk flask under Argon atmosphere. To the mixture 70 mL of 1,4-dioxane and 10 mL of distilled water were added. The reaction was heated at desired temperature until the reaction was completed. The mixture was allowed to reach room temperature, was diluted with water and extracted with dichloromethane. The combined organic layers were dried over Na₂SO₄, filtered and the solvent was evaporated *in vacuo*. The brown residue was purified by column chromatography (silica gel, heptane/ethylacetate) to yield **14**, **18**, **22**, and **26**, respectively.

General procedure for double C-N cross-coupling

The corresponding amount of amine was added to a pressure tube charged with **14**, **18**, **22** or **26** and Pd₂(dba)₃ (5 mol%), ligand (10 mol%) and base under Argon. The mixture was dissolved in anhydrous toluene (10 mL). The tube was sealed with a Teflon valve and stirred at the designated temperature. After the reaction was completed, the mixture was allowed to reach room temperature, worked up with water and extracted with dichloromethane. The combined organic layers were dried over sodium sulfate and concentrated under vacuum. The crude material was purified by flash column chromatography (silica gel, heptane/ethylacetate) gel to yield compounds **15**, **19**, **23**, and **27**, respectively.

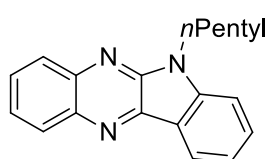
6-propyl-6H-indolo[2,3-b]quinoxaline (15a)



Following the general procedure to yield **15a** (80 %) as a yellow solid; m.p. 99 - 100 °C; ¹H NMR (300 MHz, CDCl₃) δ 8.50 (d, ³J = 7.7 Hz, 1H, CH_{Ar}), 8.31 (dd, ³J = 8.3 Hz, ⁴J = 1.3 Hz, 1H, CH_{Ar}), 8.14 (dd, ³J = 8.3 Hz, ⁴J = 1.1 Hz, 1H, CH_{Ar}), 7.82 – 7.60 (m, 3H, CH_{Ar}), 7.48 (d,

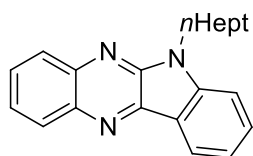
$^3J = 8.2$ Hz, 1H, CH_{Ar}), 7.44 – 7.33 (m, 1H, CH_{Ar}), 4.58 – 4.37 (m, 2H, CH₂), 2.13 – 1.90 (m, 2H, CH₂), 1.03 (t, $^3J = 7.4$ Hz, 3H, CH₃); ^{13}C NMR (63 MHz, CDCl₃) δ 145.8, 144.7, 140.8, 140.0, 139.2 (C_{Ar}), 131.0, 129.4, 128.8, 127.9, 126.0, 122.9, 120.9 (CH_{Ar}), 119.5 (C_{Ar}), 109.6 (CH_{Ar}), 43.2, 21.9 (CH₂), 11.7 (CH₃). IR (ATR, cm⁻¹), $\tilde{\nu} = 2970$ (m), 2951 (m), 2929 (w), 2870 (m), 1610 (m), 1581 (m), 1574 (m), 1487 (s), 1464 (s), 1435 (m), 1406 (s), 1394 (m), 1369 (m). MS (EI, 70 eV), m/z (%) = 261 (M⁺, 46), 232 (73), 219 (100), 102 (11), 90 (10), 77 (7); HRMS (ESI), calcd. for C₁₇H₁₆N₃ ([M+H]⁺), 262.13387; found, 262.13391.

6-Pentyl-6H-indolo[2,3-b]quinoxaline (15b)



Following the general procedure to yield **15b** (93 %) as a yellow solid; m.p. 90 - 91 °C; ^1H NMR (300 MHz, CDCl₃) δ 8.40 (d, $^3J = 7.6$ Hz, 1H, CH_{Ar}), 8.22 (dd, $^3J = 8.3$ Hz, $^4J = 1.3$ Hz, 1H, CH_{Ar}), 8.06 (dd, $^3J = 8.3$ Hz, $^4J = 1.2$ Hz, 1H, CH_{Ar}), 7.73 – 7.53 (m, 3H, CH_{Ar}), 7.39 (d, $^3J = 8.2$ Hz, 1H, CH_{Ar}), 7.35 – 7.25 (m, 1H, CH_{Ar}), 4.45 – 4.34 (m, 2H, CH₂), 1.94 – 1.77 (m, 2H, CH₂), 1.33 (m, 4H, 2CH₂), 0.81 (t, $^3J = 7.1$ Hz, 3H, CH₃); ^{13}C NMR (63 MHz, CDCl₃) δ 145.6, 144.4, 140.6, 140.0, 139.2 (C_{Ar}), 130.8, 129.3, 128.6, 127.8, 125.8, 122.7, 120.6 (CH_{Ar}), 119.4 (C_{Ar}), 109.4 (CH_{Ar}), 41.4, 29.1, 28.1, 22.3 (CH₂), 13.9 (CH₃); IR (ATR, cm⁻¹), $\tilde{\nu} = 2964$ (w), 2953 (w), 2931 (w), 2870 (w), 1608 (m), 1579 (m), 1491 (m), 1466 (s), 1441 (w), 1406 (s), 1379 (m), 1358 (m). MS (EI, 70 eV), m/z (%) = 289 (M⁺, 52), 260 (6), 246 (11), 2332 (80), 219 (100), 129 (11), 90 (10), 77 (9); HRMS (EI), calcd. for C₁₉H₁₉N₃ ([M]⁺), 289.15735; found, 289.15720.

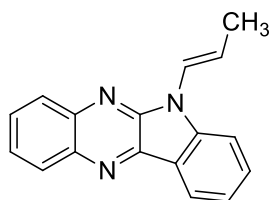
6-Heptyl-6H-indolo[2,3-b]quinoxaline (15c)



Following the general procedure to yield **15c** (85 %) as a yellow solid; m.p. 66 - 68 °C; ^1H NMR (300 MHz, CDCl₃) δ 8.50 (d, $^3J = 7.7$ Hz, 1H, CH_{Ar}), 8.32 (dd, $^3J = 8.3$ Hz, $^4J = 1.3$ Hz, 1H, CH_{Ar}), 8.15 (dd, $^3J = 8.3$ Hz, $^4J = 1.2$ Hz, 1H, CH_{Ar}), 7.81 – 7.64 (m, 3H, CH_{Ar}), 7.47 (d, $^3J = 8.2$ Hz, 1H, CH_{Ar}), 7.42 – 7.32 (m, 1H, CH_{Ar}), 4.58 – 4.40 (m, 2H, CH₂), 2.03 – 1.85 (m, 2H, CH₂), 1.51 – 1.16 (m, 8H, 4CH₂), 0.86 ($^3J = 6.8$ Hz, 3H, CH₃); ^{13}C NMR (75 MHz, CDCl₃) δ 145.8, 144.6, 140.7, 139.8, 139.0 (C_{Ar}), 131.1, 129.2, 128.8, 127.9, 126.1, 123.0, 120.9 (CH_{Ar}), 119.4 (C_{Ar}), 109.6 (CH_{Ar}), 41.6, 31.8, 29.1, 28.6, 27.1, 22.7 (CH₂), 14.1 (CH₃). IR (ATR, cm⁻¹), $\tilde{\nu} = 2951$ (m), 2922 (m), 2870 (m), 2850 (m), 1606 (m), 1581 (m), 1487 (s), 1464 (s), 1435 (m), 1408 (s), 1394 (m), 1369 (s),

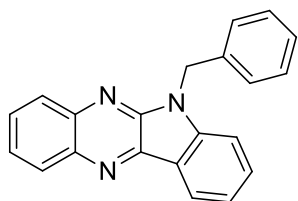
1358 (s). MS (EI, 70 eV), m/z (%) = 317 (M^+ , 41), 233 (100), 219 (96), 102 (6); HRMS (ESI), calcd. for $C_{21}H_{24}N_3$ ($[M+H]^+$), 318.19647; found, 318.19666.

6-(Prop-1-en-1-yl)-6H-indolo[2,3-b]quinoxaline (15d)



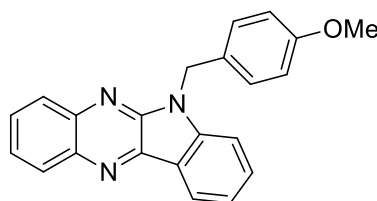
Following the general procedure to yield **15d** (73 %) as a yellow solid; m.p. 142 - 143 °C; 1H NMR (300 MHz, $CDCl_3$) δ 8.50 (d, $^3J = 7.6$ Hz, 1H, CH_{Ar}), 8.32 (dd, $^3J = 8.2$ Hz, $^4J = 1.4$ Hz, 1H, CH_{Ar}), 8.21 - 8.15 (m, 1H, CH_{Ar}), 7.83 - 7.63 (m, 3H, CH_{Ar}), 7.47 - 7.38 (m, 2H, CH_{Ar}), 6.92 - 6.79 (m, 1H, $CH=CH$), 6.27 - 6.07 (m, 1H, $CH=CH$), 1.76 (dd, $^3J = 7.0$ Hz, $^4J = 1.8$ Hz, 3H, CH_3); ^{13}C NMR (63MHz, $CDCl_3$) δ 144.2, 140.6, 140.2, 139.4 (C_{Ar}), 131.0, 129.2, 128.9, 128.2, 128.1, 126.4, 122.6, 121.6, 121.1 (CH_{Ar}), 119.8 (C), 110.8 (CH_{Ar}), 14.1 (CH_3) (one signal of C was missing). IR (ATR, cm^{-1}), $\tilde{\nu} = 3055$ (m), 3045 (m), 2978 (m), 2931 (m), 2912 (m), 2852 (m), 1662 (m), 1628 (m), 1606 (m), 1581 (m), 1574 (m), 1485 (s), 1462 (s), 1435 (m). MS (EI, 70 eV), m/z (%) = 259 (M^+ , 100), 244 (29), 232 (22), 219 (42); HRMS (ESI), calcd. for $C_{17}H_{14}N_3$ ($[M+H]^+$), 260.11822; found, 260.11817.

6-Benzyl-6H-indolo[2,3-b]quinoxaline (15e)



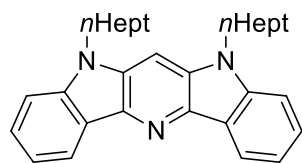
Following the general procedure to yield **15e** (94 %) as a yellow solid; m.p. 181 - 182 °C; 1H NMR (300 MHz, $CDCl_3$) δ 8.42 (d, $^3J = 7.5$ Hz, 1H, CH_{Ar}), 8.25 (dd, $^3J = 8.2$ Hz, $^4J = 1.3$ Hz, 1H, CH_{Ar}), 8.06 (dd, $^3J = 8.3$ Hz, $^4J = 1.2$ Hz, 1H, CH_{Ar}), 7.71 - 7.61 (m, 2H, CH_{Ar}), 7.57 - 7.47 (m, 1H, CH_{Ar}), 7.36 - 7.08 (m, 7H, CH_{Ar}), 5.63 (s, 2H, CH_2); ^{13}C NMR (75 MHz, $CDCl_3$) δ 145.9, 144.4, 140.8, 140.0, 139.5, 136.6 (C_{Ar}), 131.2, 129.3, 129.0 (CH_{Ar}), 128.9 (2 CH_{Ar}), 128.0, 127.8, 127.3 (2 CH_{Ar}), 126.3, 122.9 (CH_{Ar}), 121.3, 119.7 (C_{Ar}), 110.2 (CH_{Ar}), 45.1 (CH_2). IR (ATR, cm^{-1}), $\tilde{\nu} = 3059$ (m), 3026 (w), 1610 (m), 1581 (m), 1574 (m), 1485 (s), 1466 (s), 1452 (m), 1433 (m), 1406 (s). GC-MS (EI, 70 eV), m/z (%) = 309 (M^+ , 100), 266 (7), 251 (7), 232 (14), 207 (7), 91 (43), 84 (17), 66 (15), 49 (8); HRMS (ESI), calcd. for $C_{21}H_{16}N_3$ ($[M+H]^+$), 310.13387; found, 310.13398; calcd. for $C_{21}H_{16}N_3Na$ ($[M+Na]^+$), 332.11582; found, 332.11606.

6-(4-Methoxybenzyl)-6H-indolo[2,3-b]quinoxaline (15f)



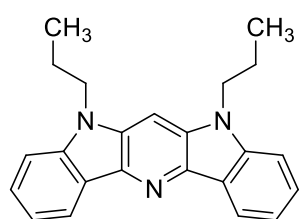
Following the general procedure to yield **15f** (92 %) as a yellow solid; m.p. 129 – 130 °C; ^1H NMR (300 MHz, CDCl_3) δ 8.41 (d, $^3J = 7.7$ Hz, 1H, CH_{Ar}), 8.25 (dd, $^3J = 8.3$ Hz, $^4J = 1.3$ Hz, 1H, CH_{Ar}), 8.08 (dd, $^3J = 8.3$ Hz, $^4J = 1.2$ Hz, 1H, CH_{Ar}), 7.77 – 7.49 (m, 3H, CH_{Ar}), 7.36 – 7.19 (m, 4H, CH_{Ar}), 6.78 – 6.71 (m, 2H, CH_{Ar}), 5.58 (s, 2H, CH_2), 3.67 (s, 3H, CH_3); ^{13}C NMR (63 MHz, CDCl_3) δ 159.1, 145.7, 144.2, 140.6, 140.0, 139.4 (C_{Ar}), 130.9, 129.3, 128.7 (CH_{Ar}), 128.6 (2 CH_{Ar}), 128.5 (C_{Ar}), 127.8, 126.0, 122.6, 121.0 (CH_{Ar}), 119.66 (C_{Ar}), 114.1 (2 CH_{Ar}), 110.1 (CH_{Ar}), 55.2 (OCH_3), 44.4 (CH_2). IR (ATR, cm^{-1}), $\tilde{\nu} = 2929$ (w), 1612 (w), 1583 (m), 1489 (m), 1470 (m), 1443 (w), 1410 (m), 1369 (m), 1360 (m). GC-MS (EI, 70 eV), m/z (%) = 339 (M^+ , 37), 121 (100), 90 (12); HRMS (ESI), calcd. for $\text{C}_{22}\text{H}_{18}\text{N}_3\text{O}_1$ ($[\text{M}+\text{H}]^+$), 340.14444; found, 340.14427.

5,7-diheptyl-5,7-dihydropyrido[3,2-b,5,6-b']diindole (19a)



Following the general procedure to yield **19a** (80 %) as a white solid; m.p. 162 - 164 °C; ^1H NMR (300 MHz, CDCl_3) δ 8.58 (d, $^3J = 7.6$ Hz, 2H, CH_{Ar}), 7.55 - 7.48 (m, 2H, CH_{Ar}), 7.42 – 7.30 (m, 5H, CH_{Ar}), 4.16 (t, $^3J = 7.1$ Hz, 4H, 2 CH_2), 1.91-1.76 (m, 4H, 2 CH_2), 1.50-1.15 (m, 16H, 8 CH_2), 0.86 (t, $^3J = 6.9$ Hz, 6H, 2 CH_3); ^{13}C NMR (63 MHz, CDCl_3) δ 141.5, 136.7, 133.7 (2 C_{Ar}), 126.4 (2 CH_{Ar}), 122.3 (2 C_{Ar}), 120.8, 119.4, 108.6 (2 CH_{Ar}), 94.2 (CH_{Heter}), 43.1, 31.8, 29.2, 28.9, 27.4, 22.7 (2 CH_2), 14.2 (2 CH_3). IR (ATR, cm^{-1}), $\tilde{\nu} = 3061$ (w), 3020(w), 2953(w), 2933(w), 2877(w), 2852(w), 1595(s), 1466(s), 1454(m), 1441(m), 1410(m). MS (EI, 70 eV), m/z (%) = 453 (M^+ , 100), 368 (40), 282 (12), 269 (25); HRMS (EI), calcd. for $\text{C}_{31}\text{H}_{39}\text{N}_3$ ($[\text{M}]^+$), 453.31385; found, 453.31353.

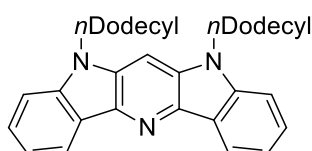
5,7-Dipropyl-5,7-dihydropyrido[3,2-b,5,6-b']diindole (19b)



Following the general procedure to yield **19b** (86 %) as a white solid; m.p. 168 - 170 °C; ^1H NMR (300 MHz, CDCl_3) δ 8.48 (d, $^3J = 7.7$ Hz, 2H, CH_{Ar}), 7.46 – 7.40 (m, 2H, CH_{Ar}), 7.32 – 7.20 (m, 5H, CH_{Ar}), 4.09 (t, $^3J = 7.1$ Hz, 4H, 2 CH_2), 1.90 – 1.73 (m, 4H, 2 CH_2), 0.88 (t, $^3J = 7.4$ Hz, 6H, 2 CH_3); ^{13}C NMR (63 MHz, CDCl_3) δ 141.5, 136.73, 133.7 (2 C_{Ar}), 126.2, 122.3 (2 CH_{Ar}), 120.6 (2 C_{Ar}), 119.3, 108.5 (2 CH_{Ar}), 94.1 (CH_{Heter}), 44.5,

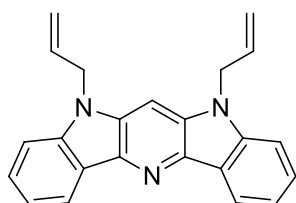
22.1 (2CH₂), 11.9 (2CH₃). IR (ATR, cm⁻¹), (= 2958(m), 2929(m), 2872(m), 1593(m), 1574(m), 1520(w), 1464(s), 1408(m), 1385(m), 1365(m), 1358(m). MS (EI, 70 eV), m/z (%) = 341 (M⁺, 100), 312 (89), 269 (39), 171 (6), 141 (20); HRMS (EI), calcd. for C₂₃H₂₃N₃ ([M]⁺), 341.18865; found, 341.18864.

5,7-Didodecyl-5,7-dihydropyrido[3,2-*b*,5,6-*b'*]diindole(19c)



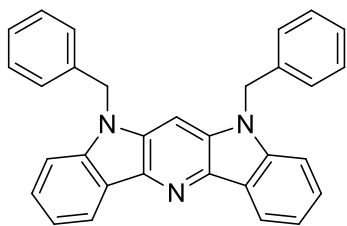
Following the general procedure to yield **19c** (71 %) as a white solid; m.p. 91 - 93 °C; ¹H NMR (300 MHz, CDCl₃) δ 8.57 (d, ³J = 7.5 Hz, 2H, CH_{Ar}), 7.55 - 7.49 (m, 2H, CH_{Ar}), 7.42 - 7.29 (m, 5H, CH_{Ar}), 4.43 - 4.15 (m, 4H, 2CH₂), 2.05 - 1.75 (m, 4H, 2CH₂), 1.56 - 1.07 (m, 36H, 18CH₂), 0.87 (t, ³J = 6.7 Hz, 6H, 2CH₃); ¹³C NMR (63 MHz, CDCl₃) δ 141.4, 136.8, 133.7 (2C_{Ar}), 126.3 (2CH_{Ar}), 122.3 (2C_{Ar}), 120.6, 119.3, 108.4 (2CH_{Ar}), 94.1 (CH_{Hetar}), 43.1, 31.9, 29.6 (2CH₂), 29.6 (4CH₂), 29.5, 29.4, 29.3, 28.7, 27.3, 22.6 (2CH₂), 14.0 (2CH₃). IR (ATR, cm⁻¹), $\tilde{\nu}$ = 2918 (s), 2848 (s), 1597 (m), 1466 (s), 1412 (m), 1350 (m), 1321 (s), 1257 (m), 1246 (m), 1209 (m), 1190 (m), 1117 (m). MS (EI, 70 eV), m/z (%) = 593 (M⁺, 100), 438 (45), 270 (16), 44 (21); HRMS (EI), calcd. for C₄₁H₅₉N₃ ([M]⁺), 593.47035; found, 593.47119.

5,7-Diallyl-5,7-dihydropyrido[3,2-*b*,5,6-*b'*]diindole(19d)



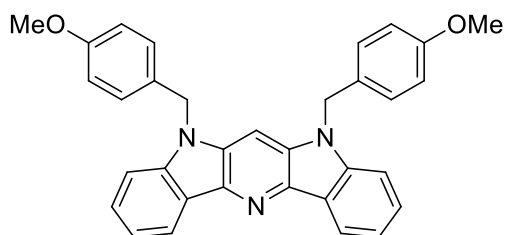
Following the general procedure to yield **19d** (84 %) as a white solid; m.p. 156 - 158 °C; ¹H NMR (300 MHz, CDCl₃) δ 8.49 (d, ³J = 7.2 Hz, 2H, CH_{Ar}), 7.44 (m, 2H, CH_{Ar}), 7.28 (m, 5H, CH_{Ar}), 6.02 - 5.86 (m, 2H, 2CH=CH₂), 5.04 (dd, ²J = 18.2 Hz, ³J = 13.7 Hz, 4H, 2CH=CH₂), 4.88 - 4.75 (m, 4H, 2CH₂); ¹³C NMR (63 MHz, CDCl₃) δ 141.4, 133.6, 133.6 (2C_{Ar}), 131.9 (2CH=CH₂), 126.5, 120.6, 119.6 (2CH_{Ar}), 117.0 (2CH=CH₂), 108.6 (2CH_{Ar}), 94.7 (C_{Hetar}), 45.3 (2CH₂) (one C signal was missing). IR (ATR, cm⁻¹), $\tilde{\nu}$ = 3057 (w), 2999 (w), 1616 (w), 1597 (m), 1514 (w), 1464 (s), 1435 (m), 1408 (m), 1385 (m), 1358 (m), 1336 (m), 1317 (s), 1284 (m), 1254 (s). GC-MS (EI, 70 eV), m/z (%) = 337 (M⁺, 100), 296 (70), 255 (28), 127 (16), 43 (37); HRMS (EI), calcd. for C₂₃H₁₉N₃ ([M]⁺), 337.15735; found, 337.15705.

5,7-Dibenzyl-5,7-dihydropyrido[3,2-b,5,6-b']diindole (19e)



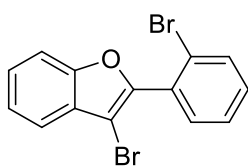
Following the general procedure to yield **19e** (70 %) as a white solid; m.p. 278 - 280 °C; ^1H NMR (300 MHz, CDCl_3) δ 8.51 (d, $^3J = 7.6$ Hz, 2H, CH_{Ar}), 7.42 – 6.94 (m, 17H, CH_{Ar}), 5.28 (s, 4H, 2 CH_2); ^{13}C NMR (75 MHz, CDCl_3) δ 141.9 (4 C_{Ar}), 136.5, 133.9 (2 C_{Ar}), 129.0 (2 CH_{Ar}), 129.0, 127.8, 126.6 (4 CH_{Ar}), 126.6 (2 CH_{Ar}), 120.1 (CH_{Heter}), 108.9 (2 CH_{Ar}), 46.2 (2 CH_2) (one signal of C is missing). IR (ATR, cm^{-1}), $\tilde{\nu} = 3028$ (w), 2922 (w), 2852 (w), 1616 (w), 1597 (m), 1510 (w), 1495 (m), 1483 (w), 1464 (s), 1450 (m), 1441 (m), 1408 (m). MS (EI, 70 eV), m/z (%) = 437 (M^+ , 100), 346 (61), 255 (12), 91 (60), 65 (8); HRMS (EI), calcd. for $\text{C}_{31}\text{H}_{23}\text{N}_3$ ($[\text{M}]^+$), 437.18865; found, 437.18850.

5,7-Bis(4-methoxybenzyl)-5,7-dihydropyrido[3,2-b,5,6-b']diindole(19f)



Following the general procedure to yield **19f** (60 %) as a white solid; m.p. 217 - 219 °C; ^1H NMR (250 MHz, CDCl_3) δ 8.53 (d, $^3J = 7.7$ Hz, 2H, CH_{Ar}), 7.44 – 7.36 (m, 2H, CH_{Ar}), 7.31 – 7.21 (m, 5H, CH_{Ar}), 7.01 – 6.88 (m, 4H, CH_{Ar}), 6.76 – 6.59 (m, 4H, CH_{Ar}), 5.23 (s, 4H, 2 CH_2), 3.64 (s, 6H, 2 CH_3); ^{13}C NMR (63 MHz, CDCl_3) δ 159.0 (2 C_{Ar}), 141.7 (4 C_{Ar}), 133.7, 128.5 (2 C_{Ar}), 127.8 (2 CH_{Ar}), 127.8 (4 CH_{Ar}), 119.7 (2 C_{Ar}), 114.2 (2 CH_{Ar}), 114.2, 108.7 (4 CH_{Ar}), 55.2 (2 OCH_3), 46.1 (2 CH_2) (one CH is missing); IR (ATR, cm^{-1}), $\tilde{\nu} = 2955$ (w), 2939 (w), 2839 (w), 1608 (m), 1595 (m), 1510 (s), 1464 (s), 1443 (m), 1408 (m), 1389 (m), 1352 (m). MS (EI, 70 eV), m/z (%) = 497 (M^+ , 81), 207 (8), 121 (100), 77 (11); HRMS (EI), calcd. for $\text{C}_{33}\text{H}_{27}\text{O}_2\text{N}_3$ ($[\text{M}]^+$), 497.20978; found, 497.20946.

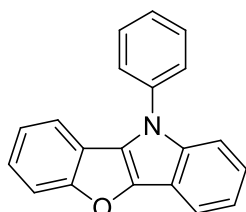
3-Bromo-2-(2-bromophenyl)benzofuran (22)



White solid, 84 %. ^1H NMR (250 MHz, CDCl_3) $\delta = 7.75$ (d, $^3J = 7.9$ Hz, 1H, CH_{Ar}), 7.65 – 7.50 (m, 3H, CH_{Ar}), 7.49 – 7.31 (m, 4H, CH_{Ar}). ^{13}C NMR (63 MHz, CDCl_3) $\delta = 154.0$, 151.4 (C_{Ar}), 133.6, 132.8, 131.5 (CH_{Ar}), 130.7, 128.5 (C_{Ar}), 127.3, 125.9 (CH_{Ar}), 124.0 (C_{Ar}), 123.7, 120.2, 111.8 (CH_{Ar}), 97.4 (C_{Ar}). IR (ATR, cm^{-1}), $\tilde{\nu} = 3055$ (w), 2953 (w), 1610 (w), 1591 (w), 1574 (w), 1562 (w), 1477

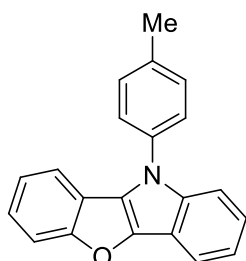
(w), 1460 (w), 1444 (s), 1344 (w). MS (EI, 70 eV), m/z (%) = 353 (M^+ , 100), 243 (32), 192 (12), 163 (57), 137 (9), 122 (8), 82 (11). HRMS (EI, 70 eV), $[C_{14}H_8OBr_2]$, 349.89364, found 349.89317, $[C_{14}H_8OBr^{81}Br]$, 351.89160, found 351.89126, $[C_{14}H_8O^{81}Br_2]$, 353.88955, found 353.88937.

10-Phenyl-10H-benzofuro[3,2-b]indole (23a)



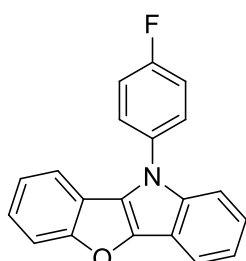
White solid, 63 %. M.p. 137 – 139 °C. 1H NMR (250 MHz, $CDCl_3$) δ 7.95 – 7.87 (m, 1H, CH_{Ar}), 7.75 – 7.58 (m, 6H, CH_{Ar}), 7.55 – 7.42 (m, 2H, CH_{Ar}), 7.38 – 7.28 (m, 3H, CH_{Ar}), 7.25 – 7.20 (m, 1H, CH_{Ar}). ^{13}C NMR (63 MHz, $CDCl_3$) δ 159.3, 143.7, 139.6, 138.4 (C_{Ar}), 129.8 ($2CH_{Ph}$), 126.8 (CH_{Ar}), 126.5 (C_{Ar}), 125.08 ($2CH_{Ph}$), 124.0, 123.2, 122.5, 120.7 (CH_{Ar}), 118.6(C_{Ar}), 118.4, 117.4 (CH_{Ar}), 114.6 (C_{Ar}), 112.7, 111.3 (CH_{Ar}). IR (ATR, cm^{-1}), $\tilde{\nu}$ = 3063 (w), 3045 (w), 2922 (w), 2850 (w), 1595 (w), 1547 (w), 1508 (m), 1498 (m), 1487 (m), 1450 (s), 1435 (m), 1417 (w). MS (EI, 70 eV), m/z (%) = 283 (M^+ , 100), 254 (44), 226 (4), 206 (5), 177 (7), 151 (8), 126 (3). HRMS (EI, 70 eV), m/z (%) $[C_{20}H_{13}ON]$, 283.09917, found 283.09843.

10-(*p*-tolyl)-10H-benzofuro[3,2-b]indole (23b)



White solid, 75 %.M.p., 134-135 °C. 1H NMR (300 MHz, $CDCl_3$) δ 7.93 – 7.86 (m, 1H, CH_{Ar}), 7.68 – 7.49 (m, 5H, CH_{Ar}), 7.45 – 7.40 (m, 2H, CH_{Ar}), 7.37 – 7.26 (m, 3H, CH_{Ar}), 7.25 – 7.20 (m, 1H, CH_{Ar}), 2.51 (s, 3H, CH_3). ^{13}C NMR (63 MHz, $CDCl_3$) δ 159.5, 143.6, 139.8, 136.8, 135.9 (C_{Ar}), 130.5 ($2CH_{Ar}$), 126.8 (C_{Ar}), 125.1 ($2CH_{Ar}$), 124.0, 123.2, 122.6, 120.7 (CH_{Ar}), 118.8(C_{Ar}), 118.6, 117.5 (CH_{Ar}), 114.6 (C_{Ar}), 112.8, 111.4 (CH_{Ar}), 21.3 (CH_3). IR (ATR, cm^{-1}), $\tilde{\nu}$ = 3051 (w), 3034 (w), 2918 (w), 1614 (w), 1549 (w), 1520 (s), 1485 (w), 1454 (s), 1441 (m). MS (EI, 70 eV), m/z (%) =, 297 (M^+ , 100), 282 (31), 268 (12), 254 (22), 226 (2), 206 (4), 190 (2), 177 (5), 165 (4), 149 (7). HRMS (EI, 70 eV) $[C_{21}H_{15}ON]$, 297.11482, found 297.11421.

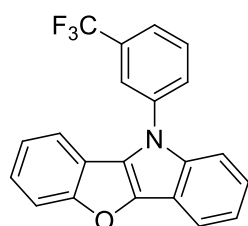
10-(4-Fluorophenyl)-10H-benzofuro[3,2-b]indole (23c)



White solid, 79 %.M.p., 167 – 168 °C. 1H NMR (300 MHz, $CDCl_3$) δ 7.94 – 7.84 (m, 1H, CH_{Ar}), 7.68 – 7.60 (m, 3H, CH_{Ar}), 7.59 – 7.52 (m, 1H, CH_{Ar}), 7.47 – 7.40 (m, 1H, CH_{Ar}), 7.37 – 7.27 (m, 5H, CH_{Ar}), 7.26 – 7.20 (m, 1H, CH_{Ar}). ^{19}F NMR (282 MHz, $CDCl_3$) δ -114.58. ^{13}C NMR (63 MHz, $CDCl_3$) δ 163.2 (d, $^1J = 248.3$ Hz, CF), 159.3, 143.6,

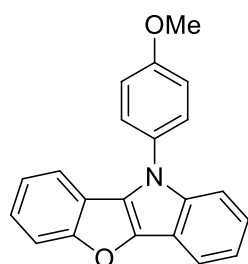
139.8 (C_{Ar}), 134.4 (d, ⁴J = 3.0 Hz, C_{Ar}), 126.9 (d, ³J = 8.5 Hz, 2CH_{Ar}), 126.6 (C_{Ar}), 124.1, 123.3, 122.6, 120.8 (CH_{Ar}), 118.5 (C_{Ar}), 118.1, 117.5 (CH_{Ar}), 116.7 (d, ²J = 22.7 Hz, 2CH_{Ar}), 114.5 (C_{Ar}), 112.8, 111.0 (CH_{Ar}). IR (ATR, cm⁻¹), $\tilde{\nu}$ = 3063 (m), 1911 (w), 1874 (w), 1837 (w), 1549 (w), 1513 (s), 1498 (s), 1453 (s), 1441 (m), 1413 (w). MS (EI, 70 eV), m/z (%) =, 301 (M⁺, 100), 272 (45), 251 (7), 224 (2), 196 (3), 177 (4), 150 (11). HRMS (EI, 70 eV)[C₂₀H₁₂ONF], 301.08974, found 301.08924.

10-(3-(Trifluoromethyl)phenyl)-10H-benzofuro[3,2-b]indole (23d)



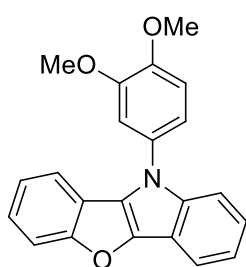
White solid, 81 %. M.p. 178 - 179 °C. ¹H NMR (300 MHz, CDCl₃) δ 7.96 (s, 1H, CH_{Ar}), 7.92 – 7.84 (m, 2H, CH_{Ar}), 7.79 – 7.57 (m, 4H, CH_{Ar}), 7.47 – 7.40 (m, 1H, CH_{Ar}), 7.35 – 7.27 (m, 3H, CH_{Ar}), 7.25 – 7.20 (m, 1H, CH_{Ar}). ¹⁹F NMR (282 MHz, CDCl₃) δ -62.67. ¹³C NMR (75 MHz, CDCl₃) δ 159.3, 144.2, 139.4, 139.1 (C_{Ar}), 132.5 (q, ²J = 32.9 Hz, CCF₃), 130.5 (CH_{Ar}), 128.0 (q, ⁴J = 1.0 Hz, CH_{Ar}), 126.1 (C_{Ar}), 124.3, 124.0 (CH_{Ar}), 123.7 (q, ¹J = 274.4 Hz, CF₃), 123.3 (q, ³J = 3.8 Hz, CH_{Ar}), 122.8 (CH_{Ar}), 121.8 (q, ³J = 3.8 Hz, CH_{Ar}), 121.4 (CH_{Ar}), 118.4 (C_{Ar}), 118.1, 117.7 (CH_{Ar}), 115.1 (C_{Ar}), 112.9, 110.9 (CH_{Ar}). IR (ATR, cm⁻¹), $\tilde{\nu}$ = 3061 (w), 1612 (w), 1593 (w), 1576 (w), 1512 (m), 1495 (m), 1483 (w), 1456 (S), 1439 (m), 1417 (w). MS (EI, 70 eV), m/z (%) = 351 (M⁺, 100), 332 (4), 322 (18), 302 (3), 282 (13), 254 (27), 226 (3), 206 (3), 175 (9), 151 (6). HRMS (EI, 70 eV)[C₂₁H₁₂ONF₃], 351.08655, found 351.08586.

10-(4-Methoxyphenyl)-10H-benzofuro[3,2-b]indole (23e)



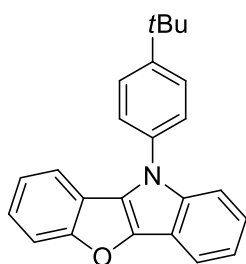
White solid, 65 %. M.p., 139 - 141 °C. ¹H NMR (300 MHz, CDCl₃) δ 7.91 – 7.82 (m, 1H, CH_{Ar}), 7.61 (d, ³J = 8.2 Hz, 1H, CH_{Ar}), 7.58 – 7.49 (m, 3H, CH_{Ar}), 7.46 – 7.40 (m, 1H, CH_{Ar}), 7.33 – 7.27 (m, 1H, CH_{Ar}), 7.26 – 7.16 (m, 3H, CH_{Ar}), 7.13 – 7.06 (m, 2H, CH_{Ar}), 3.89 (s, 3H, OCH₃). ¹³C NMR (75 MHz, CDCl₃) δ 159.42, 158.62, 143.37, 140.12, 131.30, 127.03 (C_{Ar}), 126.7 (2CH_{Ar}), 124.0, 123.1, 122.6, 120.6 (CH_{Ar}), 118.8 (C_{Ar}), 118.4, 117.4 (CH_{Ar}), 115.1 (2CH_{Ar}), 114.4 (C_{Ar}), 112.8, 111.3 (CH_{Ar}), 55.7 (CH₃). IR (ATR, cm⁻¹), $\tilde{\nu}$ = 3005 (m), 2951 (m), 2924 (m), 2872 (m), 2850 (m), 2831 (m), 1514 (s), 1504 (s), 1452 (s), 1435 (m). MS (EI, 70 eV), m/z (%) = 313 (M⁺, 100), 298 (13), 282 (8), 270 (21), 254 (10), 241 (14), 157 (7), 121 (7). HRMS (EI, 70 eV)[C₂₁H₁₅O₂N], 313.10973, found 313.10934.

10-(3,4-Dimethoxyphenyl)-10H-benzofuro[3,2-b]indole (23f)



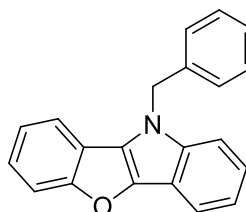
White solid, 51 %. M.p., 175 - 176 °C. ^1H NMR (300 MHz, CDCl_3) δ 7.85 – 7.77 (m, 1H, CH_{Ar}), 7.61 – 7.48 (m, 2H, CH_{Ar}), 7.45 – 7.39 (m, 1H, CH_{Ar}), 7.28 – 7.18 (m, 3H, CH_{Ar}), 7.17 – 7.12 (m, 2H, CH_{Ar}), 7.09 (d, $J = 2.4$ Hz, 1H, CH_{Ar}), 7.00 (d, $^3J = 8.5$ Hz, 1H, CH_{Ar}), 3.93 (s, 3H, OCH_3), 3.85 (s, 3H, OCH_3). ^{13}C NMR (75 MHz, CDCl_3) δ 159.5, 149.9, 148.2, 143.4, 140.1, 131.5, 127.01 (C_{Ar}), 124.1, 123.2, 122.7, 120.6 (CH_{Ar}), 118.8 (C_{Ar}), 118.3, 117.7, 117.5 (CH_{Ar}), 114.4 (C_{Ar}), 112.9, 111.8, 111.4, 109.4 (CH_{Ar}), 56.4, 56.3 (OCH_3). IR (ATR, cm^{-1}), $\tilde{\nu} = 3063$ (w), 3003 (w), 2951 (w), 2928 (w), 2850 (w), 2833 (w), 1595 (m), 1574 (w), 1547 (w), 1514 (s), 1450 (s), 1439 (s), 1417 (m). MS (EI, 70 eV), m/z (%) = 343 (M^+ , 100), 328 (14), 312 (10), 256 (14), 228 (8), 206 (9), 177 (6), 151 (6), 120 (4). HRMS (EI, 70 eV), $[\text{C}_{22}\text{H}_{17}\text{O}_3\text{N}]$, 343.12029, found 343.12067.

10-(4-(*Tert*-butyl)phenyl)-10H-benzofuro[3,2-*b*]indole (23g)



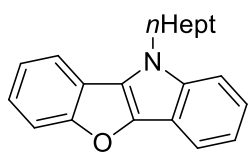
White solid, 84 %. M.p., 195 - 197 °C. ^1H NMR (300 MHz, CDCl_3) δ 7.94 – 7.86 (m, 1H, CH_{Ar}), 7.72 – 7.59 (m, 6H, CH_{Ar}), 7.58 – 7.53 (m, 1H, CH_{Ar}), 7.37 – 7.26 (m, 3H, CH_{Ar}), 7.26 – 7.21 (m, 1H, CH_{Ar}), 1.45 (s, 9H, 3 CH_3). ^{13}C NMR (63 MHz, CDCl_3) δ 159.5, 150.0, 143.7, 139.8, 135.8 (C_{Ar}), 126.7, 124.7 (2 CH_{Ar}), 124.0, 123.2, 122.6, 120.7 (CH_{Ar}), 118.9 (C_{Ar}), 118.7, 117.5 (CH_{Ar}), 114.6 (C_{Ar}), 112.8, 111.6 (CH_{Ar}), 34.9 ($\text{C}(\text{CH}_3)_3$), 31.6 (3 CH_3) (one signal of C could not be detected). IR (ATR, cm^{-1}), $\tilde{\nu} = 3059$ (w), 2958 (m), 2901 (w), 2864 (w), 1605 (w), 1547 (w), 1520 (m), 1504 (m), 1479 (w), 1454 (s), 1439 (m). MS (EI, 70 eV), m/z (%) = 339 (M^+ , 100), 324 (36), 309 (8), 282 (20), 254 (10), 206 (8), 177 (3), 162 (4), 148 (14). HRMS (EI, 70 eV), $[\text{C}_{24}\text{H}_{21}\text{ON}]$, 339.16177, found 339.16142.

10-Benzyl-10H-benzofuro[3,2-*b*]indole (23h)



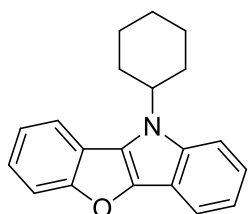
White solid, 67 %. M.p., 136 – 137 °C. ^1H NMR (250 MHz, CDCl_3) δ 7.89 – 7.81 (m, 1H, CH_{Ar}), 7.62 – 7.54 (m, 1H, CH_{Ar}), 7.44 – 7.32 (m, 2H, CH_{Ar}), 7.30 – 7.26 (m, 1H, CH_{Ar}), 7.25 – 7.13 (m, 8H, CH_{Ar}), 5.56 (s, 2H, CH_2). ^{13}C NMR (63 MHz, CDCl_3) δ 159.3, 142.7, 140.2, 137.5 (C_{Ar}), 129.1 (2 CH_{Ar}), 127.9 (CH_{Ar}), 127.3 (C_{Ar}), 126.8 (2 CH_{Ar}), 123.9, 122.7, 122.7, 119.9 (CH_{Ar}), 118.9 (C_{Ar}), 117.9, 117.5 (CH_{Ar}), 114.0 (C_{Ar}), 112.8, 110.5 (CH_{Ar}), 49.0 (CH_2). IR (ATR, cm^{-1}), $\tilde{\nu} = 3057$ (w), 1516 (w), 1495 (w), 1456 (s), 1441 (m), 1417 (w), 1394 (m), 1354 (m). MS (EI, 70 eV), m/z (%) = 297 (M^+ , 100), 268 (4), 220 (8), 206 (81), 190 (1), 177 (19), 151 (21). HRMS (EI, 70 eV), $[\text{C}_{21}\text{H}_{15}\text{ON}]$, 297.11482, found 297.11421.

10-Heptyl-10H-benzofuro[3,2-b]indole (23i)



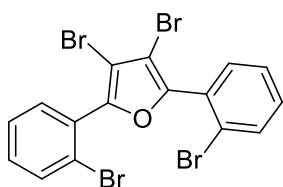
White solid, 53 %. M.p., 54 - 55 °C. ^1H NMR (300 MHz, CDCl_3) δ 7.85 (d, $^3J = 7.8$ Hz, 1H, CH_{Ar}), 7.78 – 7.71 (m, 1H, CH_{Ar}), 7.68 – 7.60 (m, 1H, CH_{Ar}), 7.46 (d, $^3J = 8.3$ Hz, 1H, CH_{Ar}), 7.38 – 7.27 (m, 3H, CH_{Ar}), 7.25 – 7.18 (m, 1H, CH_{Ar}), 4.43 (t, $^3J = 7.1$ Hz, 2H, CH_2), 2.08 – 1.85 (m, 2H, CH_2), 1.47 – 1.14 (m, 8H, 4 CH_2), 0.85 (t, $^3J = 6.8$ Hz, 3H, CH_3). ^{13}C NMR (63 MHz, CDCl_3) δ 159.4, 142.4, 139.7, 127.0 (C_{Ar}), 123.8, 122.7, 122.3, 119.4 (CH_{Ar}), 119.0 (C_{Ar}), 117.8, 117.4 (CH_{Ar}), 113.6 (C_{Ar}), 112.9, 110.3 (CH_{Ar}), 45.6, 31.8, 30.7, 29.2, 27.2, 22.7 (CH_2), 14.2 (CH_3). IR (ATR, cm^{-1}), $\tilde{\nu} = 3064$ (w), 3053 (w), 2949 (m), 2937 (m), 2918 (m), 2868 (w), 2850 (m), 1543 (w), 1514 (w), 1456 (s), 1441 (m). MS (EI, 70 eV), m/z (%) = 305 (M^+ , 100), 276 (2), 220 (86), 206 (10), 190 (5), 165 (12), 151 (7). HRMS (EI, 70 eV), $[\text{C}_{21}\text{H}_{23}\text{ON}]$, 305.17741, found 305.17746.

10-Cyclohexyl-10H-benzofuro[3,2-b]indole (23j)



White solid, 57 % .M.p., 163 - 164 °C. ^1H NMR (300 MHz, CDCl_3) δ 7.90 – 7.75 (m, 2H, CH_{Ar}), 7.63 – 7.55 (m, 1H, CH_{Ar}), 7.49 (d, $^3J = 8.5$ Hz, 1H, CH_{Ar}), 7.34 – 7.27 (m, 2H, CH_{Ar}), 7.24 – 7.10 (m, 2H, CH_{Ar}), 4.56 – 4.37 (m, 1H, C_6H_{11}), 2.21 – 1.82 (m, 7H, C_6H_{11}), 1.65 – 1.40 (m, 3H, C_6H_{11}). ^{13}C NMR (63 MHz, CDCl_3) δ 159.4, 143.3, 139.2, 125.3 (C_{Ar}), 123.7, 122.6, 122.4, 119.7 (CH_{Ar}), 119.3 (C_{Ar}), 119.2, 117.4, 112.9, 110.5 (CH_{Ar}), 54.8 (CH), 33.0, 26.2 (2 CH_2), 25.7 (CH_2) (one C_{Ar} -signal could not be detected). IR (ATR, cm^{-1}), $\tilde{\nu} = 3064$ (w), 3053 (w), 2949 (m), 2937 (m), 2918 (m), 2868 (w), 2850 (m), 1543 (w), 1514 (w), 1456 (s), 1441 (m). 3064 (w), 2935 (m), 2920 (m), 2852 (m), 1504 (w), 1454 (s), 1417 (w), MS (EI, 70 eV), m/z (%) = 289 (M^+ , 92), 207 (100), 177 (13), 151 (15). HRMS (EI, 70 eV)[$\text{C}_{20}\text{H}_{19}\text{ON}$], 289.14612, found 289.14568.

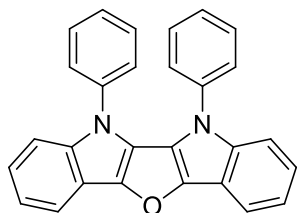
3,4-Dibromo-2,5-bis(2-bromophenyl)furan (26)



White solid, 78 %. M.p., 64 – 65 °C. ^1H NMR (300 MHz, CDCl_3) δ 7.70 (dd, $^3J = 8.0$ Hz, $^4J = 1.2$ Hz, 2H, CH_{Ar}), 7.56 (dd, $^3J = 7.7$ Hz, $^4J = 1.7$ Hz, 2H, CH_{Ar}), 7.47 – 7.38 (m, 2H, CH_{Ar}), 7.36 – 7.28 (m, 2H, CH_{Ar}). ^{13}C NMR (63 MHz, CDCl_3) δ 149.8(2 C_{Ar}), 133.6, 132.7, 131.4(2 CH_{Ar}), 130.3(2 C_{Ar}), 127.3(2 CH_{Ar}), 123.8, 104.3(2 C_{Ar}). IR (ATR, cm^{-1}), $\tilde{\nu} = 3064$ (w), 3053 (w), 2949 (m), 2937 (m), 2918 (m), 2868 (w), 2850 (m), 1543 (w), 1514 (w), 1456 (s), 1441 (m). 2953 (w), 2920 (m), 2850 (m), 1574 (w), 1558 (w), 1464 (m), 1456 (m), 1423 (m). MS (EI, 70 eV), m/z (%) = 536(100), 531 (M^+ , 75),

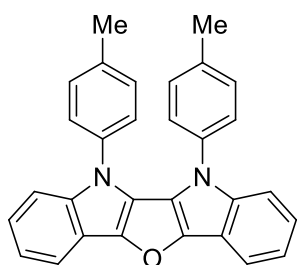
429(12),376(7),351(10),297(7),267(21),185(40),155(27),112(8).HRMS (EI, 70 eV)[C₁₆H₈OBr₄], 531.73032,found531.73071.

5,6-Diphenyl-5,6-dihydrofuro[3,2-b,4,5-b']diindole (27a)



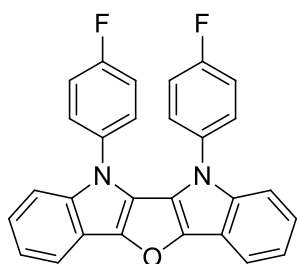
Green solid, 51 %. M.p., 220 – 222 °C. ¹H NMR (500 MHz, C₆D₆) δ 8.01 – 7.95 (m, 2H, CH_{Ar}), 7.39 (m,2H, CH_{Ar}), 7.24 – 7.18 (m, 2H, CH_{Ar}), 7.13 – 7.08 (m, 2H, CH_{Ar}), 6.90 – 6.84 (m, 4H, CH_{Ar}), 6.78 – 6.66 (m, 6H, CH_{Ar}). ¹³C NMR (126 MHz, C₆D₆) δ 146.5, 139.5, 139.1(2C_{Ar}), 128.9 (4CH_{Ar}), 126.4 (2CH_{Ar}), 125.8 (4CH_{Ar}), 122.6 (2CH_{Ar}), 121.8 (2C_{Ar}), 121.4, 116.8 (2CH_{Ar}), 116.4 (2C_{Ar}), 111.4 (2CH_{Ar}). IR (ATR, cm⁻¹), $\tilde{\nu}$ = 3064 (w), 3053 (w), 2949 (m), 2937 (m), 2918 (m), 2868 (w), 2850 (m), 1543 (w), 1514 (w), 1456 (s), 1441 (m). 3053 (w), 3036 (w), 2953 (w), 2918 (w), 2848 (w), 1595 (m), 1576 (m), 1564 (w), 1558 (w), 1506 (w), 1495 (s), 1462 (m), 1456 (s), 1446 (m), 1423 (s), 1404 (m). MS (EI, 70 eV), m/z (%) = 399 (29), 398 (M⁺, 100), 397 (38), 369 (11), 292 (6), 264 (3), 199 (9). HRMS (EI, 70 eV) [C₂₈H₁₈ON₂], 398.14136, found 398.14080.

5,6-Di-*p*-tolyl-5,6-dihydrofuro[3,2-b,4,5-b']diindole (27b)



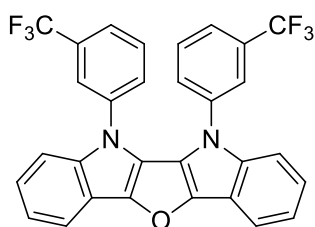
Green solid, 65 %. M.p., 221 - 223 °C. ¹H NMR (300 MHz, CDCl₃) δ 7.87 (d, *J* = 7.6 Hz, 2H, CH_{Ar}), 7.43 (d, ³*J* = 8.5 Hz, 2H, CH_{Ar}), 7.29 – 7.15 (m, 4H, CH_{Ar}), 7.13 – 7.07 (m, 4H, CH_{Ar}), 6.88 (d, ³*J* = 8.1 Hz, 4H, CH_{Ar}), 2.35 (s, 6H, 2CH₃). ¹³C NMR (75 MHz, CDCl₃) δ 145.7, 138.9, 136.4, 136.1 (2C_{Ar}), 129.5, 125.6 (4CH_{Ar}), 122.0 (2CH_{Ar}), 121.6 (2C_{Ar}), 120.7, 116.4 (2CH_{Ar}), 115.5, 111.2 (2CH_{Ar}), 21.2 (2CH₃).IR (ATR, cm⁻¹), $\tilde{\nu}$ = 2949 (m), 2937 (m), 2918 (m), 2850 (m), 1456 (s), 1441 (m). 2920 (m), 1606 (m), 1581 (m), 1514 (s), 1462 (s), 1446 (m), 1429 (s), 1410 (m).MS (EI, 70 eV), m/z (%) = 426 (M⁺, 100), 411 (13), 305 (3), 213 (10), 190 (3), 152 (1). HRMS (EI, 70 eV) [C₃₀H₂₂ON₂], 426.17266, found 426.17206

5,6-Bis(4-fluorophenyl)-5,6-dihydrofuro[3,2-b,4,5-b']diindole (27c)



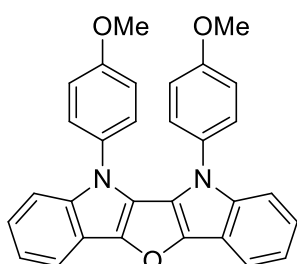
Green solid, 59 %. M.p., 224 - 225 °C. ^1H NMR (300 MHz, C_6D_6) δ 8.17 – 7.97 (m, 2H, CH_{Ar}), 7.37 – 7.30 (m, 4H, CH_{Ar}), 7.27 – 7.21 (m, 2H, CH_{Ar}), 6.75 – 6.59 (m, 4H, CH_{Ar}), 6.59 – 6.30 (m, 4H, CH_{Ar}). ^{19}F NMR (282 MHz, C_6D_6) δ -115.22. ^{13}C NMR (63 MHz, C_6D_6) δ 161.5 (d, $^1J = 246.7$ Hz, 2CF), 146.2, 139.5 (2 C_{Ar}), 134.8 (d, $^4J = 2.9$ Hz, 2 C_{Ar}), 127.6 (d, $^3J = 8.5$ Hz, 4 CH_{Ar}), 122.7 (2 CH_{Ar}), 121.7 (2 C_{Ar}), 121.5, 116.8 (2 CH_{Ar}), 116.2, (2 C_{Ar}), 115.7 (d, $^2J = 22.9$ Hz, 4 CH_{Ar}), 111.1 (2 CH_{Ar}). IR (ATR, cm^{-1}), $\tilde{\nu} = 3053$ (w), 2916 (w), 2874 (w), 1608 (m), 1581 (m), 1568 (m), 1504 (s), 1485 (s), 1462 (s), 1429 (s), 1410 (m). MS (EI, 70 eV), m/z (%) = 434 (M^+ , 100), 405 (11), 385 (3), 338 (2), 310 (3), 283 (2), 217 (8). HRMS (EI, 70 eV) [$\text{C}_{28}\text{H}_{16}\text{ON}_2\text{F}_2$], 434.12252, found 434.12178.

5,6-Bis(3-(trifluoromethyl)phenyl)-5,6-dihydrofuro[3,2-b,4,5-b']diindole (27d)



Green solid, 66 %. M.p., 205 – 207 °C. ^1H NMR (300 MHz, CDCl_3) δ 7.87 (d, $^3J = 7.7$ Hz, 2H, CH_{Ar}), 7.53 (s, 2H, CH_{Ar}), 7.44 (m, 4H, CH_{Ar}), 7.37 – 7.27 (m, 4H, CH_{Ar}), 7.26 – 7.15 (m, 4H, CH_{Ar}). ^{19}F NMR (282 MHz, CDCl_3) δ -62.63. ^{13}C NMR (75 MHz, CDCl_3) δ 146.5, 139.3, 139.0 (2 C_{Ar}), 131.9 (q, $^2J = 33.1$ Hz, 2 CCF_3), 129.7 (2 CH_{Ar}), 128.6 (q, $^3J = 3.8$ Hz, 2 CH_{Ar}), 123.4 (q, $^4J = 1.5$ Hz, 2 CH_{Ar}), 123.3 (q, $^1J = 272.5$ Hz, 2 CF_3), 122.9 (2 CH_{Ar}), 122.2 (q, $^3J = 3.8$ Hz, 2 CH_{Ar}), 121.6 (2 CH_{Ar}), 120.6 (2 C_{Ar}), 116.8 (2 CH_{Ar}), 116.0 (2 C_{Ar}), 110.7 (2 CH_{Ar}). IR (ATR, cm^{-1}), $\tilde{\nu} = 3078$ (w), 1614 (w), 1595 (m), 1579 (w), 1568 (w), 1495 (m), 1464 (s), 1456 (s), 1443 (m), 1427 (m), 1404 (w). MS (EI, 70 eV) m/z (%) = 534 (M^+ , 100), 505 (7), 437 (3), 388 (2), 290 (3), 267 (12), 232 (2), 145 (8). HRMS (EI, 70 eV) [$\text{C}_{30}\text{H}_{16}\text{ON}_2\text{F}_6$], 534.11613, found 534.11547

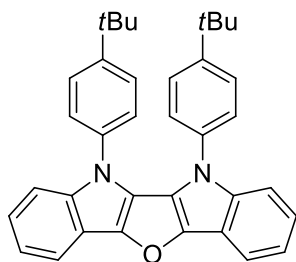
5,6-Bis(4-methoxyphenyl)-5,6-dihydrofuro[3,2-b,4,5-b']diindole (27e)



Green solid, 53 % .M.p., 250-252 °C. ^1H NMR (500 MHz, C_6D_6) δ 8.03 – 7.97 (m, 2H, CH_{Ar}), 7.41 – 7.36 (m, 2H, CH_{Ar}), 7.25 – 7.21 (m, 2H, CH_{Ar}), 7.15 – 7.12 (m, 2H, CH_{Ar}), 6.81 – 6.75 (m, 4H, CH_{Ar}), 6.35 – 6.26 (m, 4H, CH_{Ar}), 3.31 (s, 6H, OCH_3). ^{13}C NMR (126 MHz, C_6D_6) δ 158.4, 146.1, 139.8, 131.8 (2 C_{Ar}), 127.4 (4 CH_{Ar}), 122.4 (2 C_{Ar}), 122.4, 121.1, 116.8 (2 CH_{Ar}), 116.1 (2 C_{Ar}), 114.3 (4 CH_{Ar}), 111.3 (2 CH_{Ar}), 54.8 (2 OCH_3). IR (ATR, cm^{-1}), $\tilde{\nu} = 3063$ (w), 2955 (m), 2922 (m), 2850 (m), 2837 (m), 1581 (m), 1568 (m), 1504 (S), 1470 (m), 1454 (s), 1427 (s). MS (EI, 70 eV), m/z (%) = 458 (M^+ , 100),

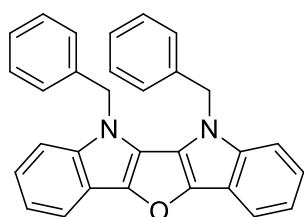
443 (5), 371 (5), 229 (13), 207 (1), 151 (3). HRMS (EI, 70 eV) [C₃₀H₂₂O₃N₂], 458.16249, found 458.16239

5,6-Bis(4-(*tert*-butyl)phenyl)-5,6-dihydrofuro[3,2-*b*,4,5-*b'*]diindole (27f)



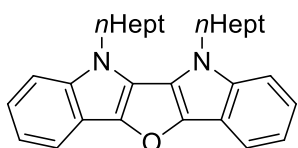
Green solid, 86 %. M.p., 230 - 232 °C. ¹H NMR (300 MHz, CDCl₃) δ 7.85 (d, ³J = 7.7 Hz, 2H, CH_{Ar}), 7.40 (d, ³J = 8.2 Hz, 2H, CH_{Ar}), 7.25 – 7.10 (m, 12H, CH_{Ar}), 1.29 (s, 18H, 6CH₃). ¹³C NMR (75 MHz, CDCl₃) δ 149.6, 146.0, 140.0, 136.2 (2C_{Ar}), 125.8, 125.3 (4CH_{Ar}), 122.1 (2CH_{Ar}), 121.5 (2C_{Ar}), 120.9, 116.3 (2CH_{Ar}), 115.7 (2C_{Ar}), 111.7 (2CH_{Ar}), 34.6 (2C_{Ar}), 31.6(6CH₃). IR (ATR, cm⁻¹), $\tilde{\nu}$ = 3057 (w), 3041 (w), 2962 (m), 1608 (w), 1576 (w), 1514 (m), 1487 (w), 1462 (s), 1446 (m), 1427 (m), 1404 (m), MS (EI, 70 eV), m/z (%) = 510 (M⁺, 100), 437 (7), 409 (2), 320 (4), 292 (1), 248 (4), 213 (5). HRMS (EI, 70 eV) [C₃₆H₃₄ON₂], 510.26657, found 510.26635.

5,6-Dibenzyl-5,6-dihydrofuro[3,2-*b*,4,5-*b'*]diindole (27g)



Green solid, 53 %. M.p., 230 – 232 °C. ¹H NMR (250 MHz, CDCl₃) δ 7.82 – 7.74 (m, 2H, CH_{Ar}), 7.24 – 7.05 (m, 12H, CH_{Ar}), 6.92 – 6.82 (m, 4H, CH_{Ar}), 5.21 (s, 4H, CH₂). ¹³C NMR (63 MHz, CDCl₃) δ 144.79, 138.8, 137.2 (2C_{Ar}), 128.9 (4CH_{Ar}), 127.52 (2CH_{Ar}), 125.6 (4CH_{Ar}), 121.6 (2CH_{Ar}), 121.4 (2C_{Ar}), 119.9, 116.3 (2CH_{Ar}), 114.9 (2C_{Ar}), 110.0 (2CH_{Ar}), 48.8 (2CH₂). IR (ATR, cm⁻¹), $\tilde{\nu}$ = 2920 (w), 1732 (w), 1699 (w), 1576 (m), 1556 (w), 1495 (m), 1464 (m), 1452 (s), 1427 (s), 1408 (m). MS (EI, 70 eV), m/z (%) = 426 (M⁺, 100), 335 (39), 306 (12), 91 (24), 73 (5), 60 (7), 43 (8). HRMS (EI, 70 eV)[C₃₀H₂₂ON₂], 426.17266, found 426.17337.

5,6-Diheptyl-5,6-dihydrofuro[3,2-*b*,4,5-*b'*]diindole (27h)



Green solid, 46 %. M.p., 109 – 111 °C. ¹H NMR (300 MHz, Acetone) δ 7.85 – 7.68 (m, 2H, CH_{Ar}), 7.65 – 7.52 (m, 2H, CH_{Ar}), 7.30 – 7.10 (m, 4H, CH_{Ar}), 4.69 – 4.39 (m, 4H, 2CH₂), 2.02 – 1.88 (m, 4H, 2CH₂), 1.50 – 1.25 (m, 16H, 8CH₂), 0.84 (t, ³J = 6.8 Hz, 6H, 2CH₃). ¹³C NMR (75 MHz, Acetone) δ 145.0, 139.4 (2C_{Ar}), 122.2 (2CH_{Ar}), 122.1 (2C_{Ar}), 120.4, 116.6 (2CH_{Ar}), 115.5 (2C_{Ar}), 111.5 (2CH_{Ar}), 47.2, 32.5, 31.5, 29.9, 27.8, 23.2 (2CH₂), 14.3 (2CH₃). IR (ATR, cm⁻¹), $\tilde{\nu}$ = 2951 (m), 2924 (m), 2854 (m), 1645 (w), 1620 (w), 1578 (m), 1485(w), 1464(s), 1429 (s), 1408 (w). MS (EI, 70 eV), m/z (%) = 442 (M⁺, 100), 357 (3), 314 (1), 259 (8), 137 (3), 96 (1), 76 (1), 43 (4). HRMS (EI, 70 eV) [C₃₀H₃₈ON₂], 442.29787, found 442.29764.

